Molecular Tweezers: Studies Directed Towards the Preparation of Effective Charge Transport Materials

Khushabu Thakur
Marquette University

MOLECULAR TWEEZERS: STUDIES DIRECTED TOWARDS THE PREPARATION OF EFFECTIVE CHARGE TRANSPORT MATERIALS

by

Khushabu Thakur, B.Sc., M.Sc.

A Dissertation submitted to the Faculty of the Graduate School,
Marquette University,
in Partial Fulfillment of the Requirements for
the Degree of Doctor of Philosophy

Milwaukee, Wisconsin

May 2013

ABSTRACT

MOLECULAR TWEEZERS: STUDIES DIRECTED TOWARDS THE PREPARATION OF EFFECTIVE CHARGE TRANSPORT MATERIALS

Khushabu Thakur, B.Sc, M.Sc.

Marquette University, May 2013

An important focus of the modern areas of photovoltaics and molecular electronics is to identify molecules or molecular assemblies that can promote effective charge/exciton transport over long distances. In order to be able to exert control and establish necessary structural parameters for reproducible production of self-assembled structures for long-distance charge transport, our laboratory has been actively engaged towards the preparation of a variety of well-defined, cofacially-arrayed polybenzenoid nanostructures in which aromatic donors are cofacially stacked.

Herein, we undertake the design and synthesis of tweezer-like molecules for their usage for the preparation of long-range charge transport assemblies. We have successfully developed an efficient synthesis of molecular tweezers with different pincers using a common doubly-annulated *m*-terphenyl platform. The ready availability of these tweezers with different pincers allows us to demonstrate that they bind a variety of electron acceptors as guests via electron donor-acceptor or charge-transfer interactions. Moreover, the tweezers with electron-rich pincers [e.g. trimethylpyrene (**TMP**) pincers] undergo a ready self-assembly into cofacially-arrayed polybenzenoid nanostructures when prompted by 1-electron oxidation. The effectiveness of the functionality of various tweezers and the rigidity of the tweezer platforms was evaluated by comparison of the EDA complexation binding constants with the tweezers derived from completely rigid (**CRP**) and non-annulated platforms (**NAP**) and that of doubly-annulated platform (**DAP**). These studies established that rigidification of the tweezer platform does not contribute, in any significant way, to the functionality of the tweezers. Moreover, a comparative study of electron transfer prompted self-assembly of the **NAP-TMP** and **DAP-TMP** tweezers established that they both undergo ready self-association with comparable efficiency.

We have also synthesized a triptycene scaffold and carefully evaluated its optoelectronic properties. This triptycene scaffold and its derivatives are expected to form two-dimensional self-assemblies which are potentially useful as long-range charge-transport materials in modern photovoltaic devices.

ACKNOWLEDGEMENTS

Khushabu Thakur, B.Sc., M.Sc.

I would like to sincerely thank Prof. Rajendra Rathore for his assistance and guidance in getting my graduate career started on the right foot and providing me the opportunity to work in his lab. His pursuit for the science and his enthusiasm for the research have made deep impression on me. I would also like to thank my committee members Prof. Scott Reid and Prof. James Gardinier for taking time to read my thesis and suggest corrections. I would like to express my gratitude to all the Professors in the Chemistry department who directly or indirectly contributed to my academic progress at Marquette University. I would also like to thank Mrs. Nandini Pai, my M.Sc. advisor, for motivating me to pursue doctoral studies.

I would like to thank Matthew Modjewski for teaching me lab skills and helping me start my research in this lab. Thanks to Dr. Vijay Vyas, Dr. Tushar Navale, Dr. Shriya Wadumethridge, and Dr. Ruchi Shukla for their support in academic discussions, synthetic problems and data interpretation. I would like to thank my current group members Anitha, Mosharraf, Dr. Majher Sarker, Tasnuva, Dr. Marat Talipov, Joe, and Marek for their help and support.

I would like to acknowledge the funding sources – Marquette University, Department of Chemistry and National Science Foundation.

Thanks to Dr. Sergey V. Lindeman for single crystal X-ray crystallography and helpful discussions. Also thanks to Dr. Sheng Cai for the help with NMR experiments, Mark

Bartelt for his prompt help in fixing instrumental glitches, extremely helpful office assistant Linda Davis and business manager Paul Dion. I would also like to extend my thanks to the Marquette University staff that was always available for help.

Finally, I wish to thank all my family and friends whose continuous support and encouragement constantly motivated me to undertake and finish this endeavor. I would specially like to thank my parents and my sisters Bhupali and Dhanashree for their support during all these years of my doctoral research.

TABLE OF CONTENTS

LIST OF TABLES

LIST OF FIGURES

LIST OF CHARTS

LIST OF SCHEMES

CHAPTER 1
BACKGROUND AND PROBLEM STATEMENT

Over the last couple of decades, considerable efforts have been made to identify conducting organic materials for modern photovoltaic applications.[1-13] Toward this end, most attention has been focused on various pi-conjugated organic polymers such as poly-p-phenylenes,[1,2] polythiophenes,[3-7] polyphenylvinylenes,[8,9] and polyfluorenes.[10-13]

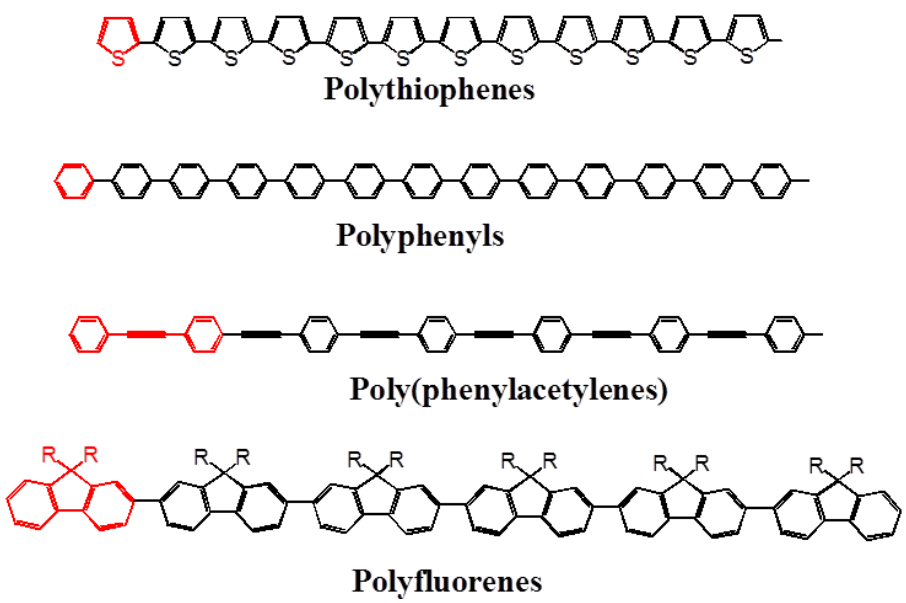

Figure 1.1 Structures of various pi conjugated organic polymers.[1-13]

When such pi-conjugated materials are employed in photovoltaic devices, their assembly in charge transport layers is expected to be randomized and the efficiency of charge transport (CT) is expected to be governed by both *intramolecular* and *intermolecular* mechanisms, i.e. Figure 1.2.[14-1]

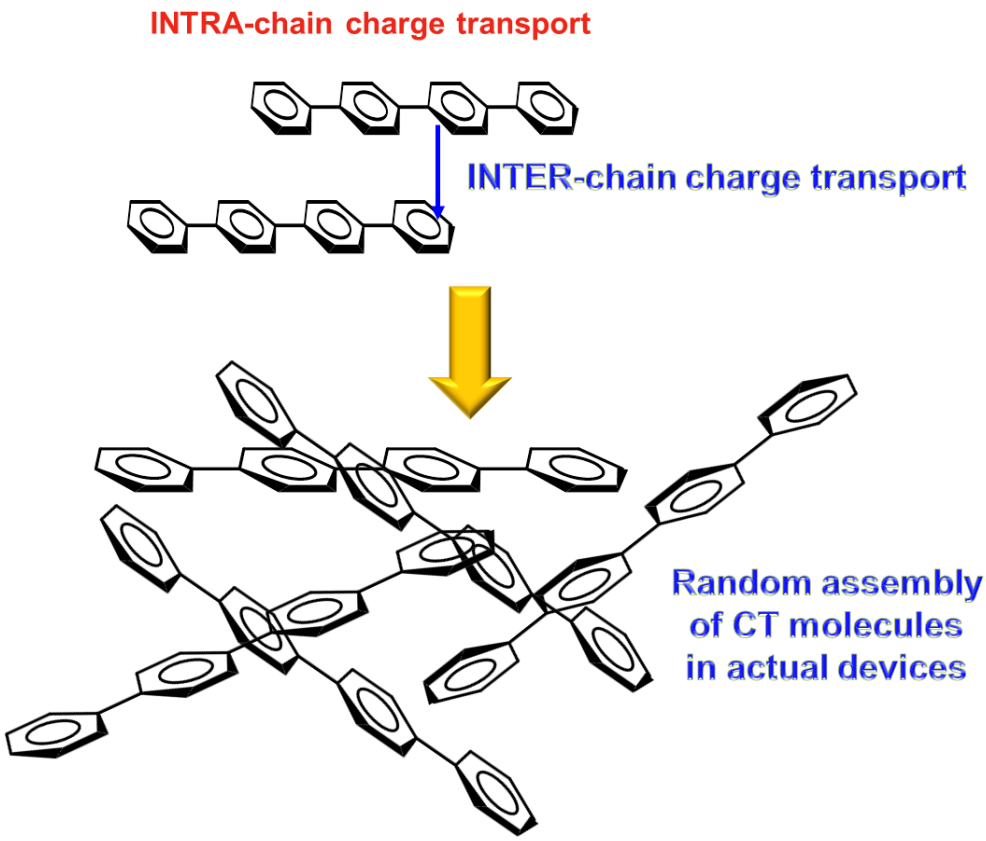

Figure 1.2 Cartoon diagram showing the intra-chain versus inter-chain charge transport (CT) in poly-*p*-phenylene wires and their randomized assembly in amorphous bulk material.[14-17]

The next generation of conductive organic materials for photovoltaic applications should therefore consider the fundamental question of intra- and inter-chain charge transport when designing functional materials for both electron and hole transport for applications in modern photovoltaic devices. In our laboratory, we have synthesized and studied cofacially arrayed polyfluorenes molecules in order to seek insight into the mechanism of charge transport in pi-stacked structures (Figure 1.3).[18-20]

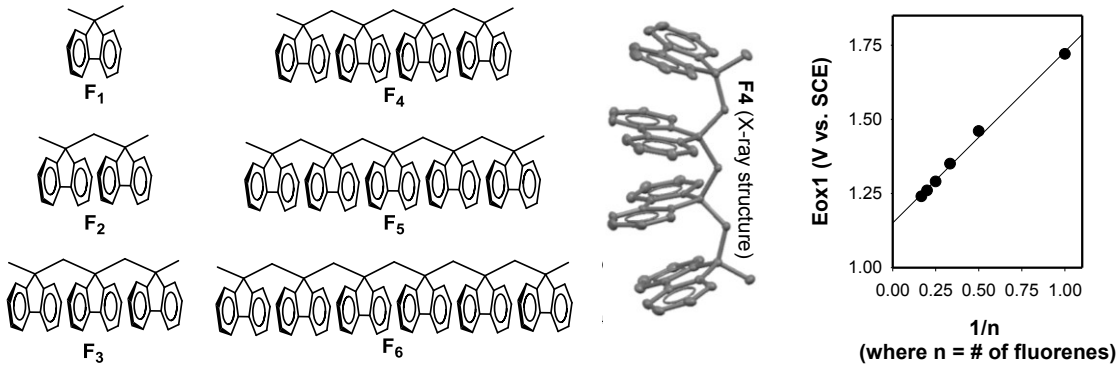

Figure 1.3 Showing the molecular structures of cofacially arrayed polyfluorenes F1-F6 (left), X-ray crystal structure of F4 (middle), and a plot of E_{ox1} vs 1/n (right), where n is the number of fluorene moieties.[18-20]

The cofacial pi-stacking of these fluorenes moieties in F2-F6 provides effective electronic coupling between the subunits and thereby facilitates electron and energy transfer.[21] The electronic coupling in F2-F6 can be easily gauged by electrochemical method where the first oxidation potential (E_{ox1}) decreases with the increasing number of fluorene moieties and decrease in the E_{ox1} values follows a 1/n relationship, where n is number of fluorene moieties in polyfluorenes (Figure 1.3, right).[18-21]

An important focus of the modern areas of photovoltaics and molecular electronics is to identify molecules or molecular assemblies that can promote effective charge/energy transport over long distances. One of the important goals of the research program in our laboratory is to design and synthesize novel molecules that can be self-assembled and allow an effective charge delocalization over long distances. For example, we recently described that three cofacially juxtaposed phenylene rings in triptycene are electronically coupled and a single charge in triptycene is stabilized by delocalization onto three benzenoid rings.[22] The stabilization of cationic charge by

triptycene can be gauged by the decrease in its first oxidation potential, when compared to a model compound, as well as the appearance of an intervalence NIR transition in the spectrum of its cation radical. With the aid of X-ray crystallography, it was also shown that triptycene derivatives produce solid-state assemblies that are amenable for long-range charge transport owing to effective intermolecular pi-pi stacking (Figure 1.4).[22]

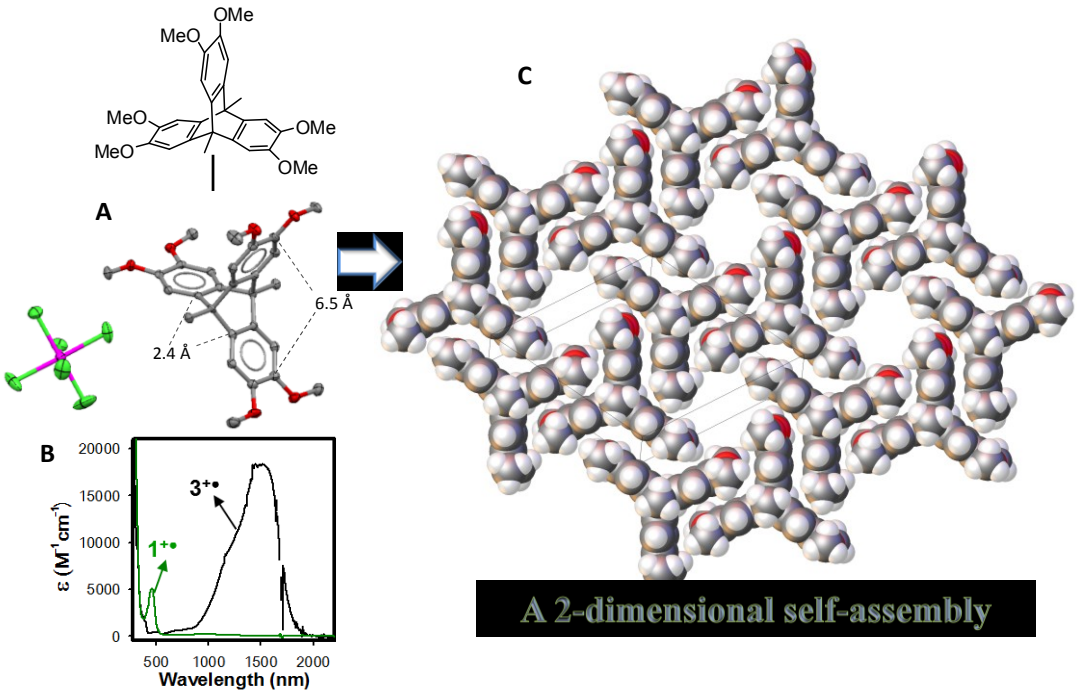

Figure 1.4 **(**A) X-ray structure of cation radical of hexamethoxy-triptycene. (B) Absorption spectra of cation radical of hexamethoxy-triptycene in CH_2Cl_2 at 22 ^{o}C. (C) Ultimate 2D electronically coupled solid-state assembly of hexamethoxytriptycene cation radical (SbCl6-) as determined by X-ray crystallography.[22]

Problem Statement. Based on the background presented above and successful preparation of assemblies with triptycene derivatives, this study aims to identify and synthesize versatile tweezer-like molecular scaffolds that can self-assemble into materials which can allow long-distance charge-transport and may have potential for applications in photovoltaics and molecular electronics. We believe that the unique structural features embodied in tweezers (vide infra) makes them ideal candidates for the preparation of non-covalent self-assemblies that may allow long-distance charge-transport. Herein we describe briefly the state of art understanding of various tweezer-like structure reported in the literature as follows.

Definition of Molecular Tweezer. The molecules with an open cavity capable of binding guest molecule are called tweezers. The molecular structure of a tweezer can be divided into a molecular platform and a pair of pincers, i.e. Figure 1.5.

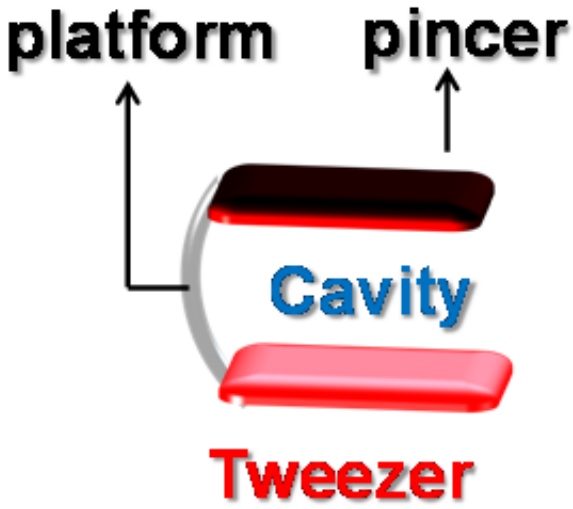

Figure 1.5 Naming of the components of a molecular tweezer.

The guests bind in the cavity of a molecular tweezer by various non-covalent weak molecular forces such as van der Waals forces, π-π interactions, hydrophobic forces, hydrogen bonding, metal coordination and electrostatic effects, etc., (eq 1).

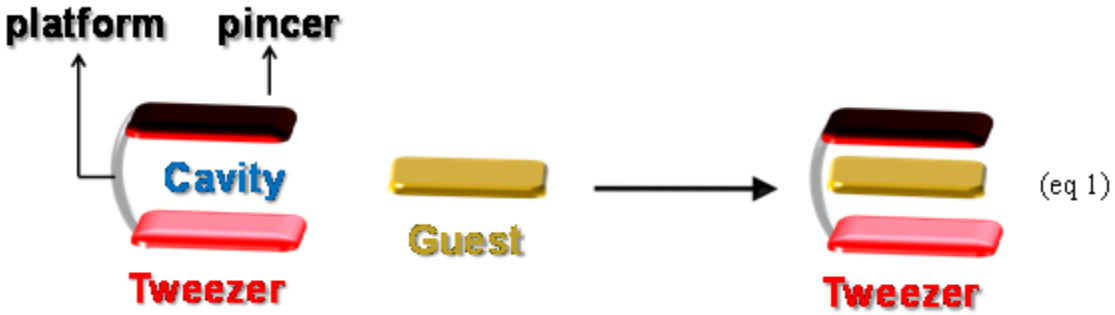

The planar aromatic pincers are generally connected to the platform in such a way that they are held at a distance of ~7 Å. A separation of ~7 Å between the cofacially-held aromatic pincers allows an effective π-π-interaction between the guest and pincers as they lay at a distance which approximates the van der Waal's contact, (eq 2).

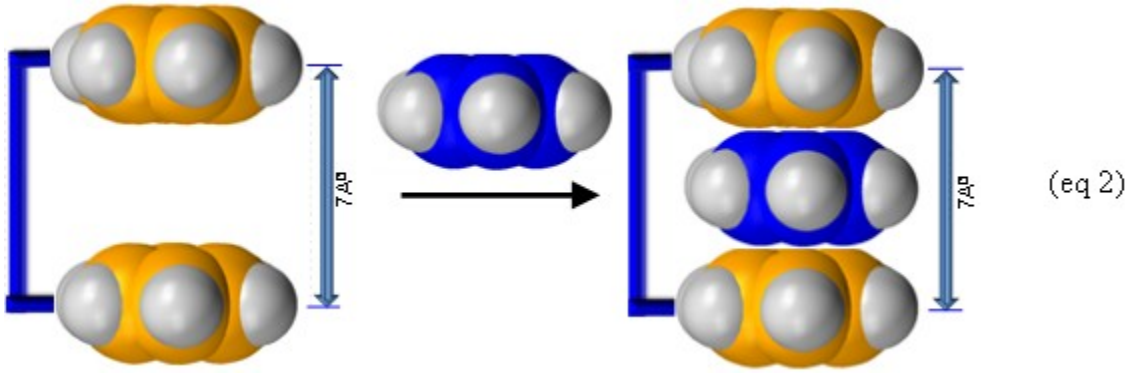

First Molecular Tweezer. The concept of "molecular tweezers" was introduced by Whitlock[23] and coworkers in early 1960s and such molecules at present are also referred to as "molecular clips",[24] i.e. Figure 1.6.

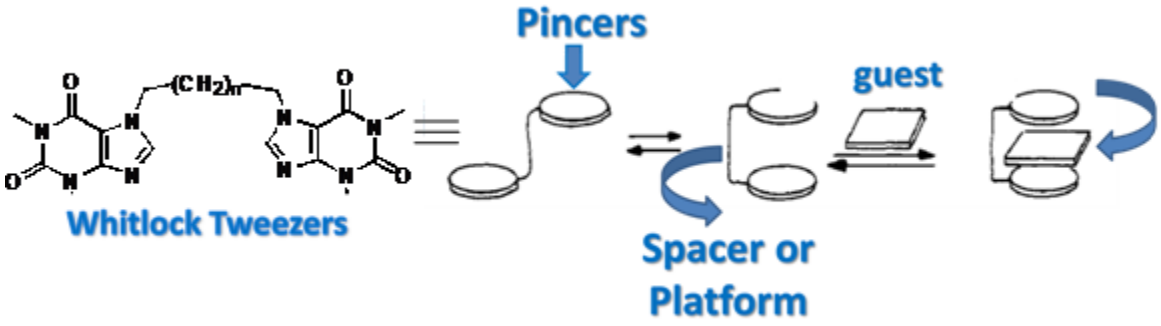

Figure 1.6 Structure of Whitlock molecular tweezer.[23]

Tweezer-like structures are widespread in nature. The tweezer phenomenon is highly prevalent in nature and plays an important role in many functional biological systems. For example, proteins can very selectively and preferentially bind a number of substrates by tweezer-like action. However, unlike tweezers in proteins substrates are not permanently bound and therefore this phenomenon is not as obvious in proteins.

The concept of "intercalation" in DNA bears direct resemblance to the functional molecular tweezers. For example, the π-bases in DNA are cofacially sacked and thus allow an extensive π,π-interaction between the bases, see Figure 1.7.[25]

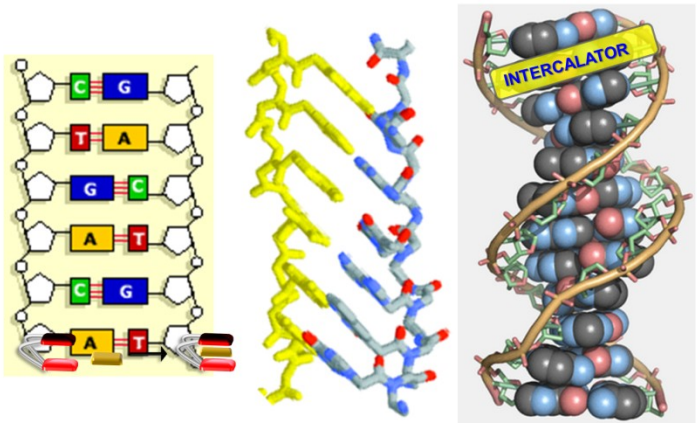

Figure 1.7 Structure of DNA showing that an aromatic intercalator functions as a guest molecule between a pair of bases in DNA.[25]

Thus, intercalation occurs when an aromatic ligand of an appropriate size and chemical nature fit itself in between base pairs of DNA (Figure 1.7, right) and thus bears direct conceptual similarities to the functioning of molecular tweezers. The intercalation in DNA has been exploited for the study electron transport through stacked pi-bases by Barton and coworkers.[25] For example they demonstrated with the aid of emission spectroscopy that a ruthenium complex containing a flat highly-emissive aromatic ligand readily intercalates between the bases of DNA, i.e. Figure 1.8.[25]

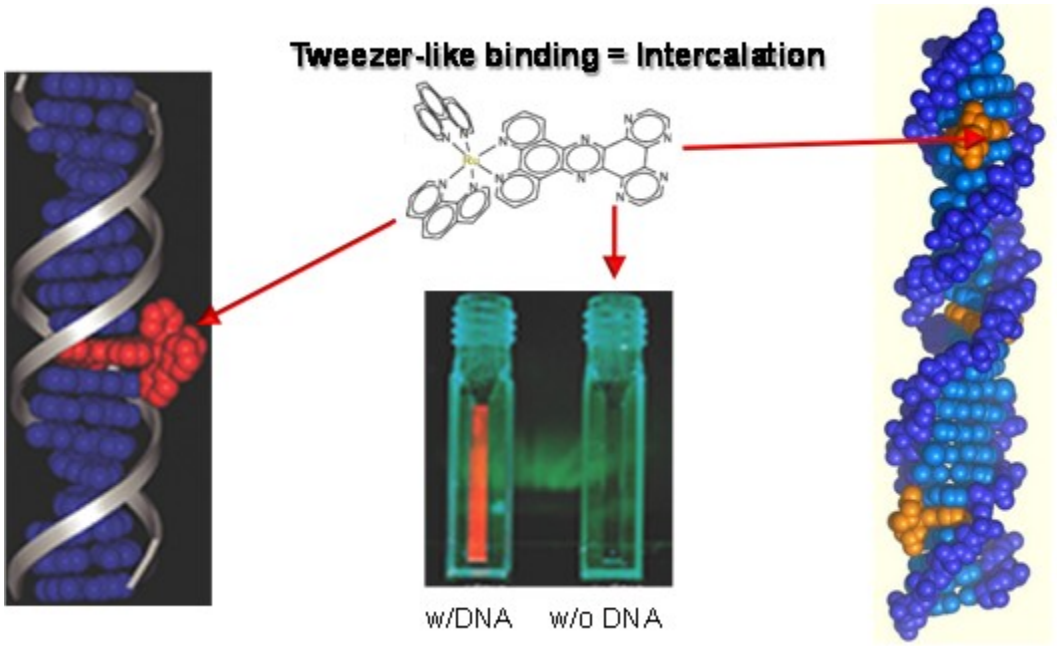

Figure 1.8 Intercalation of a ruthenium complex containing a flat highly-emissive aromatic ligand in between a pair of bases in DNA.[25]

A variety of modern drugs for treatment of aggressive cancers are being designed based on the intercalation of flat aromatic systems in between a pair of bases in DNA. For example, *anthracyclines* (or *anthracycline* antibiotics) are a class of drugs that are used in cancer chemotherapy and their function can be traced to an intercalation mechanism, i.e. Figure 1.9, left.[26]

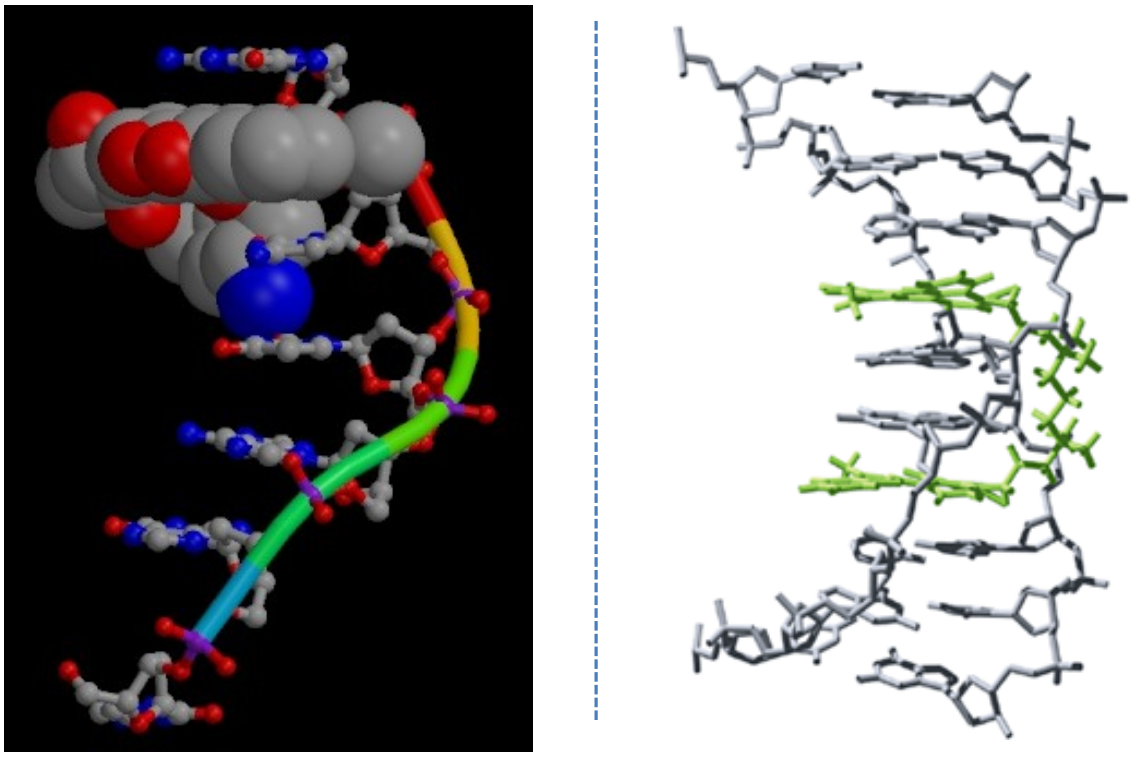

Figure 1.9 Left: Intercalation of an anthracycline drug in DNA. Right: A new and highly effective tweezer-like drug (green) functions by double intercalation in DNA.[26]

Glioblastoma, with an average survival rate of only five years, is the most common and aggressive type of brain tumor. Recently, a high performance tweezer-like drug which kills 50% of glioblastoma cells at its lowest dosages was discovered. The high cytotoxicity of this new tweezer-like drug on cancerous cells arises due to the dual binding (or intercalation) of the drug in DNA molecules (see Figure 1.9, right).[26]

The intercalation phenomenon is extensively utilized for the synthesis of functional materials based on protein-DNA composites for variety of materials applications, e.g. see Figure 1.10.[27]

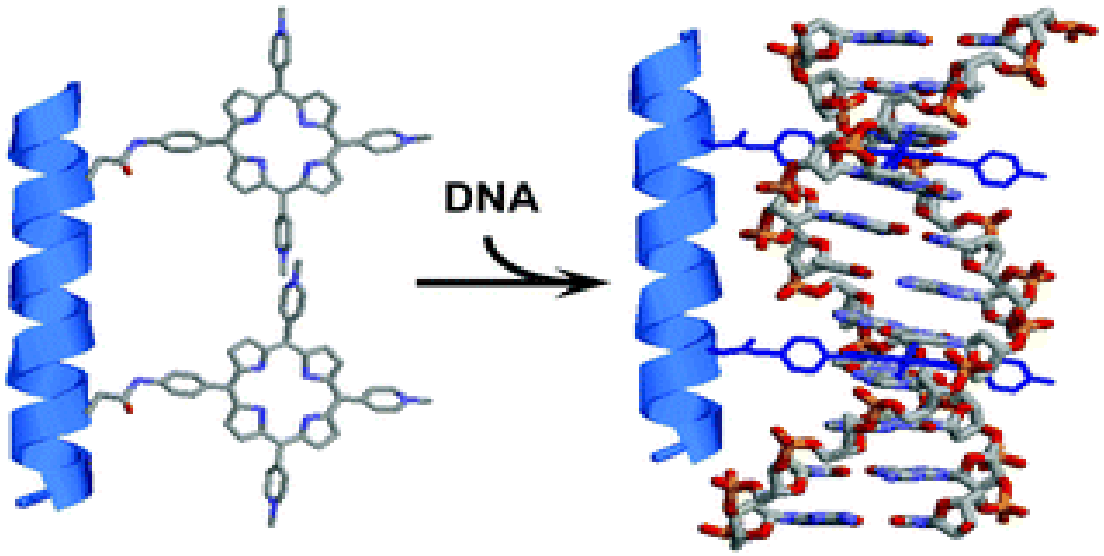

Figure 1.10 The preparation of protein-DNA composites for materials applications.[27]

Various molecular scaffolds for tweezers. Recognition of planer molecules based on non-covalent interaction is of current interest in host guest chemistry. Molecular tweezers have found widespread use in studies of important processes such as electron donor-acceptor interactions, electron/energy transfer reactions, drug-DNA interaction and host-guest complaxation. Accordingly, herein we undertake a brief survey of different molecular scaffolds utilized for the preparation of synthetic molecular tweezers as follows.

Zimmerman and coworkers in 1987 introduced the concept of rigid tweezers using a U-shaped acridine as a platform for the preparation of tweezers (see structure below).[28]

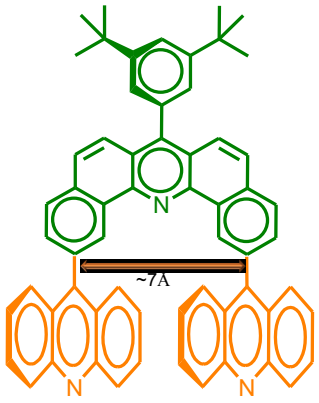

Zimmerman and coworkers also synthesized tweezers containing functional group imbedded deep within their cavities for binding of biological guests by added hydrogen bonding interactions (see structures below).[28]

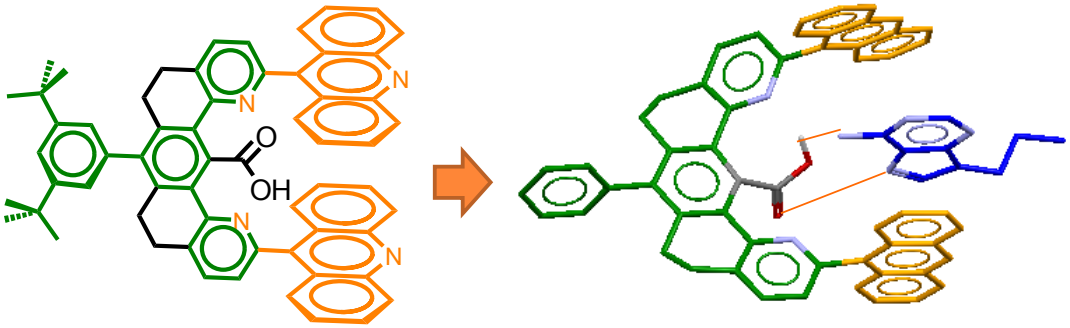

Amongst the know tweezers, the Zimmerman tweezer are most popular but their synthesis are rather cumbersome. A number of simpler tweezer platforms have been identified as follows.

For example, Fukazawa and coworkers introduced the dioxa-o-cyclophane moiety which can be readily synthesized from tetrakisbromomethylbenzene and 1,2-dihydroxybenzenes.[29] Upon carefully controlling the ratio of two reactants they can also synthesize both symmetrical and unsymmetrical tweezers (see structures below).

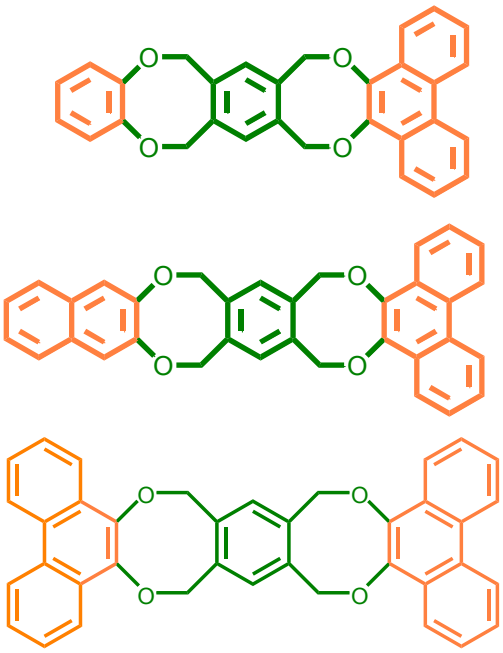

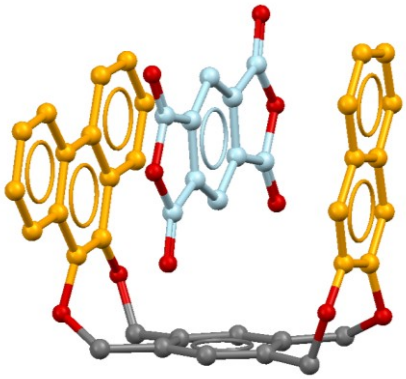

These conformationally flexible tweezers bind a variety of electron poor guests rather poorly due to the extensive conformational mobility.

A number of tweezers based on Kagan's ether[30] and Toger's base[31] have been synthesized and they show somewhat limited binding abilities. However, a number of EDA complexes of these tweezers have been characterized by X-ray crystallography (see structures below).

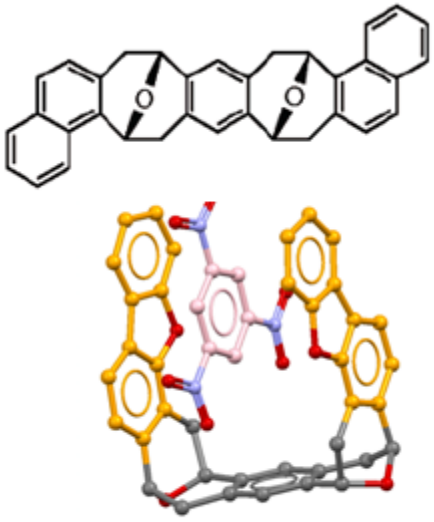

Tweezers based on *Kagan's ethers*

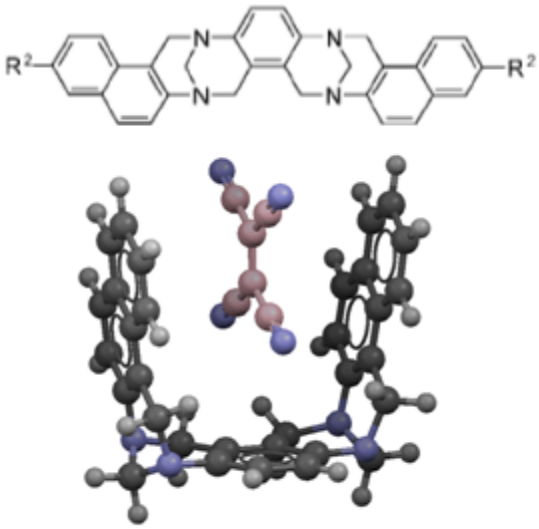

Tweezers based on *Tröger's base*

Tweezers based on bowl-shaped hydrocarbons pincers are being exploited for the binding/separation of fullerenes and related molecules with curved structures. For example, Sygula and co-workers made use of the dibenzo-cyclooctane platform to make molecular tweezers containing curved corannulene as pincers for the binding of C60 and it was termed a "buckycatcher" (see structures below).[32] Complexation of C60 with the buckycatcher was confirmed by NMR titrations and by X-ray crystallography of an isolated C60-buckycatcher complex (see structure below). These results provide evidence for the importance of concave-convex pi-pi interactions in the supramolecular chemistry of fullerene carbon cages and the curbed bowl-like polycyclic aromatic hydrocarbons. The complexation studies of C60 with the buckycatcher by NMR titration method showed that it binds C60 with the binding constant of 8600 ± 500 M^{-1}.[32]

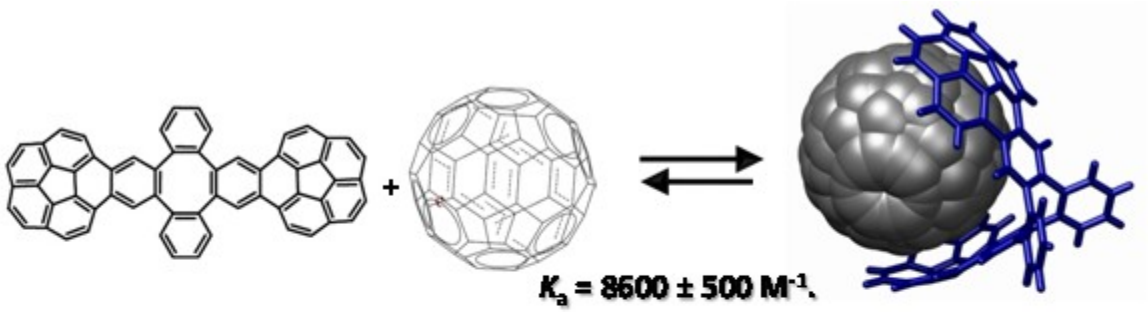

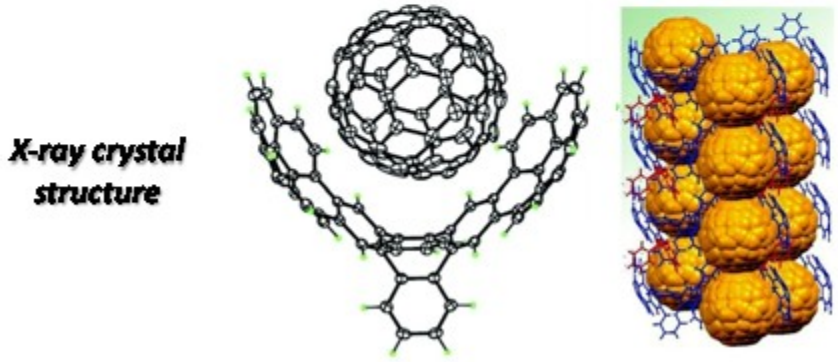

A number of porphyrin-based tweezers have also been identified for the cocrystallization of C60 and C70 (see structures below).[33] Note that the distance between two porphyrin pincers was found to be approximately 12 Å which is well-suited for the binding of spherical C60 as demonstrated by molecular modeling (see structure below).

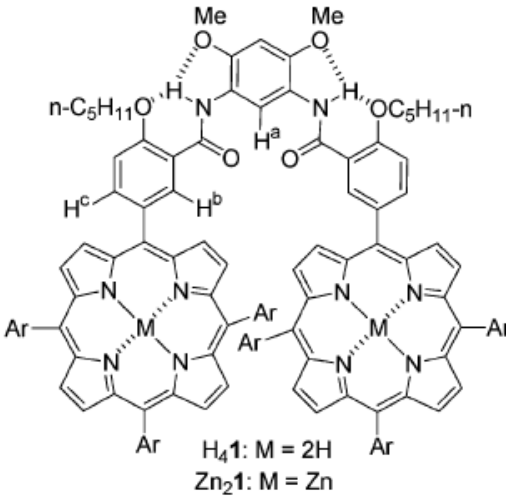

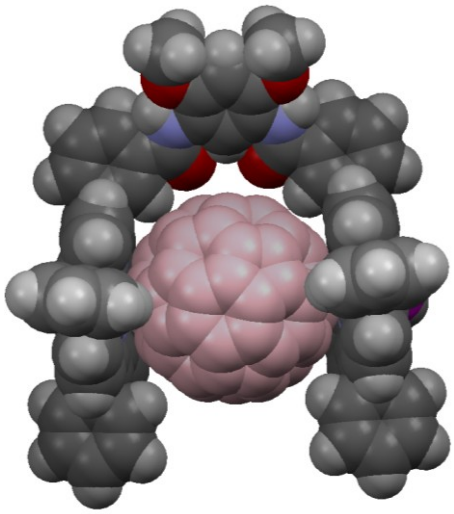

The survey provided above pertaining to the literature of tweezer is rather brief and is only intended to familiarize the readers with the wide applicability of the molecular tweezers.

Our Tweezer Platform. In this study, we have identified a doubly-annulated *m*-terphenyl and a non-annulated *m*-terphenyl derivative which can serve as versatile platforms for the preparation of variety of tweezers and tweezer-like molecules. The availability of these platforms allows us demonstrate that tweezers hold potential to be utilized for the preparation of self-assembled materials for long-range charge-transport (see Figure 1.11).

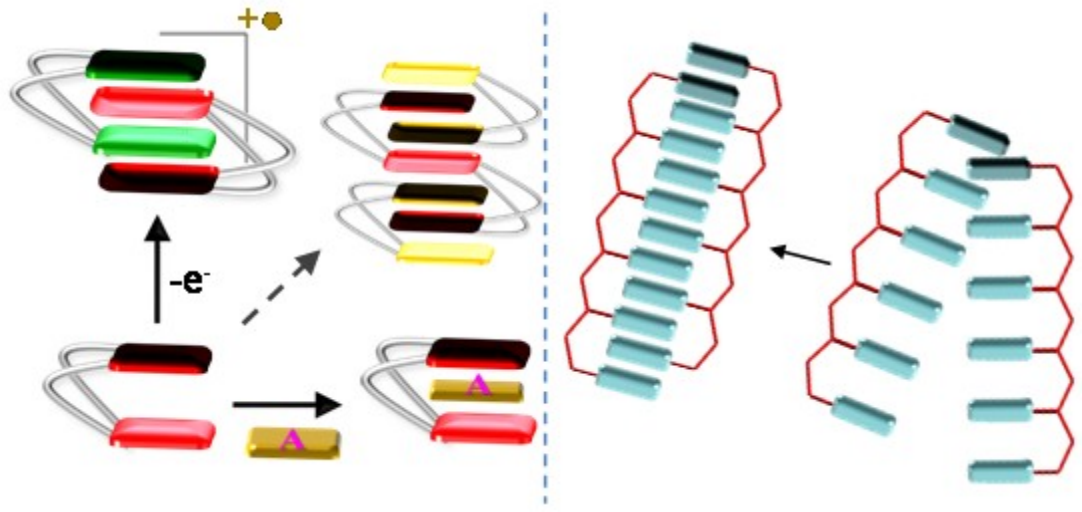

Figure 1.11 Cartoon diagram showing self-assemblies of molecular tweezers.

Accordingly, this thesis consists of 4 chapters which delineate the progress made to date:

Chapter 2 describes the synthesis of a new tweezer platform which allows the ready preparation of a variety of tweezers with different pincers in a single synthetic step. The

functioning of these tweezers is demonstrated by quantitative binding studies with a variety of electron acceptors as guests. Furthermore, we delineated with a proof of concept experiment that tweezers can be self-assembled into 1-dimensional cofacially-arrayed molecular wires when prompted by 1-electron oxidation.

Chapter 3 describes the successful search of tweezer platforms which can allow the ready preparation of multi-pincer tweezers or comb-like structures for the preparation of 1-dimensional wire or two-dimensional charge-transport assemblies.

Chapter 4 includes a highly relevant study to the theme discussed above and includes the probing of the dynamics of cofacial stacking in a conformationally mobile bichromophoric donor when prompted by 1-electron oxidation.

Chapter 5 describes synthesis and study of a versatile triptycene-based scaffold which may prove quite useful for the preparation of long-range charge transport assemblies/ materials.

CHAPTER 2
STUDIES OF GUEST BINDING AND ELECTRON-TRANSFER INDUCED SELF-ASSEMBLY OF A NEW CLASS OF ADAPTABLE MOLECULAR TWEEZERS

INTRODUCTION

Molecular tweezers are the macromolecules with an open cavity that allows the binding of guest molecules. The term "molecular tweezers" was coined by Whitlock[1] in early 1960s and such molecules are also referred to as "molecular clips".[2] Binding of the guests in the cavity of molecular tweezers is governed by various non-covalent weak molecular forces such as van der Waals forces, π-π interactions, hydrophobic forces, hydrogen bonding and electrostatic effects. Molecular tweezers are of the considerable interest in the recognition/sensing of a variety of guests including a number of explosives such as trinitrotoluene.[3] Due to the potential applications of tweezers for the detection of a variety of synthetic as well as biological guest molecules, tremendous synthetic effort is devoted towards the preparation of a variety of tweezer platforms. A brief survey of the literature pertaining to molecular tweezers is summarized in the previous chapter.

Zimmerman's tweezer[4] (see Figure 2.1) is the most recognized tweezer amongst all known tweezer-like scaffolds.

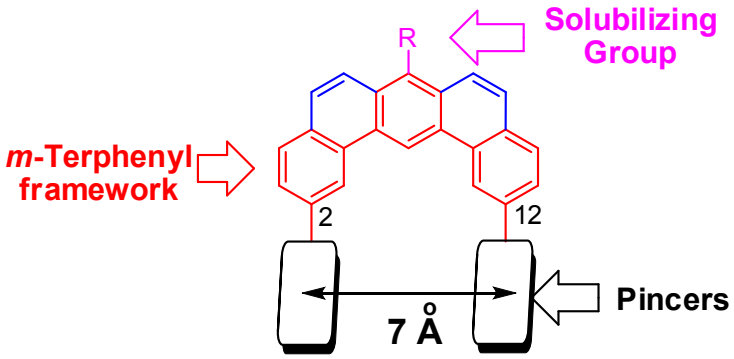

Figure 2.1 The molecular structure and various design features of the Zimmerman's tweezers.[4]

The structural features of Zimmerman's tweezers (**ZT**) include a doubly annulated *m*-terphenyl framework in which the pincers are connected at 2- and 12-positions of terphenyl and they are held at a distance of ~7 Å. A separation of ~7 Å between cofacially-held pincers allows effective π-π interactions with the sandwiched guest molecule. Despite the effectiveness for binding a variety of guest molecules by Zimmerman's tweezers,[4] the main drawback lies in the fact that their syntheses are rather tedious (e.g. see Scheme 2.1) and the platform holding the pincers is highly electro-active. As apparent from the partial synthetic scheme shown below, the pincers are attached in the very beginning of the synthesis of **ZT**s. Therefore, the synthesis of each tweezer with different pincers requires one to go through the entire synthesis from the beginning. Furthermore, the synthetic scheme for **ZT**s has a number of steps which are rather time consuming and give low product yield.[4]

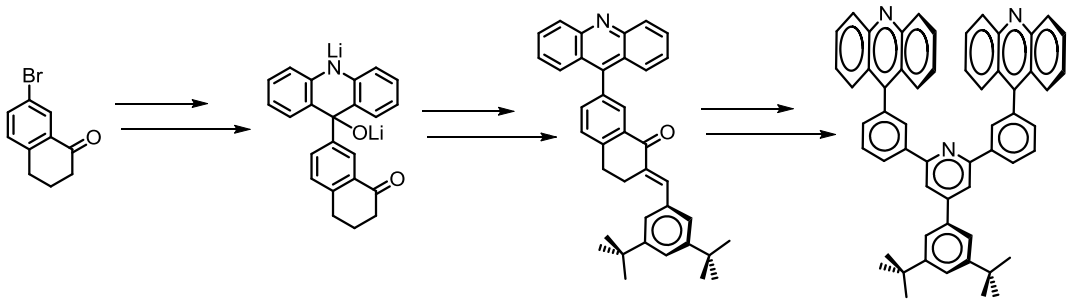

Scheme 2.1 A partial synthetic scheme for the preparation of a Zimmerman's tweezer.[4]

Accordingly, we consider the preparation of a common doubly-annulated *m*-terphenyl platform, with appropriate functional groups, which will allow a ready attachment of pincers in one synthetic step. In this context, we note a recent report by Rathore and coworkers[5] where they described a versatile synthesis for the efficient preparation of doubly annulated *p*-terphenyls, e.g. Scheme 2.2.

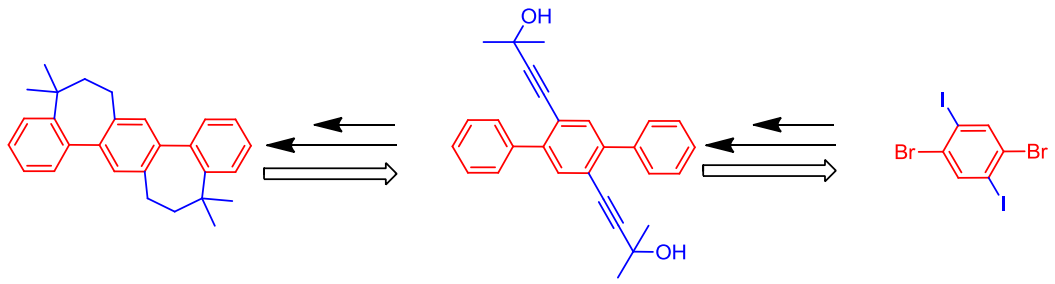

Scheme 2.2 An efficient strategy for the preparation of doubly annulated *p*-terphenyls.[5]

It can be readily envisioned by an inspection of Scheme 2.2 that if a similar double annulation is performed onto a *m*-terphenyl derivative, the resultant doubly-annulated derivative with appropriate substitutions at 2- and 14-positions will serve as a

versatile platform for the ready construction of a variety of tweezers with different pincers (i.e. Scheme 2.3).

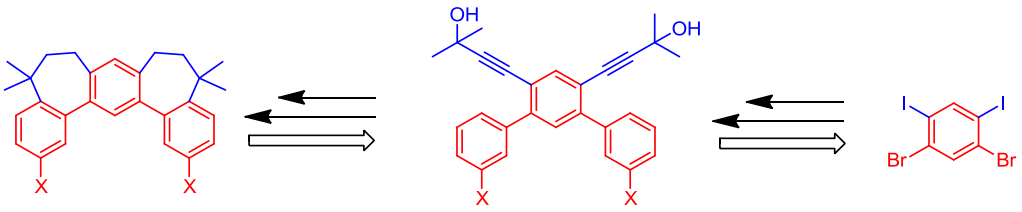

Scheme 2.3 A double annulation strategy for the construction a *m*-terphenyl-based platform for the synthesis of various tweezers.

Our proposed doubly-annulated *m*-terphenyl (**TP**) platform for the preparation of tweezers holds a number of advantages when compared to the platform utilized for the preparation of Zimmerman's tweezers (see Figure 2.2), as detailed below:

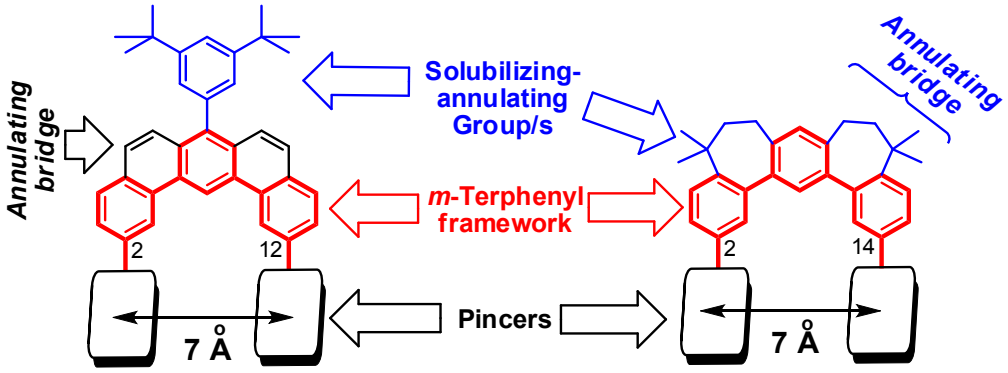

Figure 2.2 Comparison of Zimmerman's tweezer platform (left) with our proposed doubly-annulated *m*-terphenyl (TP) platform (right).

(1) Unlike the syntheses of Zimmerman's tweezers (see Scheme 2.1), the synthesis of the proposed new class of tweezers will employ a common doubly-annulated *m*-

terphenyl (**TP**) platform which can be transformed to a variety of tweezers with different pincers in one synthetic step.

(2) The conformation flexibility of the annulating bridges in **TP**-based tweezers will allow the pincers to adapt to a guest molecule for an efficient binding.

(3) Unlike the Zimmerman's tweezer platform which requires the installation of a solubilizing group (see Figure 2.2), the annulating bridges in **TP**-based tweezers also serve as solubilizing groups.

(4) In addition, the platform is oxidized at a relatively high potential (~1.7 V vs SCE) and also the electronic coupling between the pincers and the platform is minimized due to *meta* connections.[6]

Accordingly, in this chapter we will describe the successful preparation of a doubly-annulated *m*-terphenyl (**TP**) platform, containing trifluoromethane-sulfonate (or triflate, -OTf) groups at 2- and 14-positions for ready installation of various pincers via a facile and high-yielding Suzuki coupling reaction.[7] Moreover, the successful preparation of a number of tweezers based on **TP**-platform with different pincers varying from monobenzenoid to polybenzenoid electron donors (such as tetramethylbenzene, naphthalene, pyrene, trimethylpyrene) to large graphite fragment such as HBCs as pincers (see Chart 2.1) will be described.

Chart 2.1 Structures of different pincers used in various tweezers.

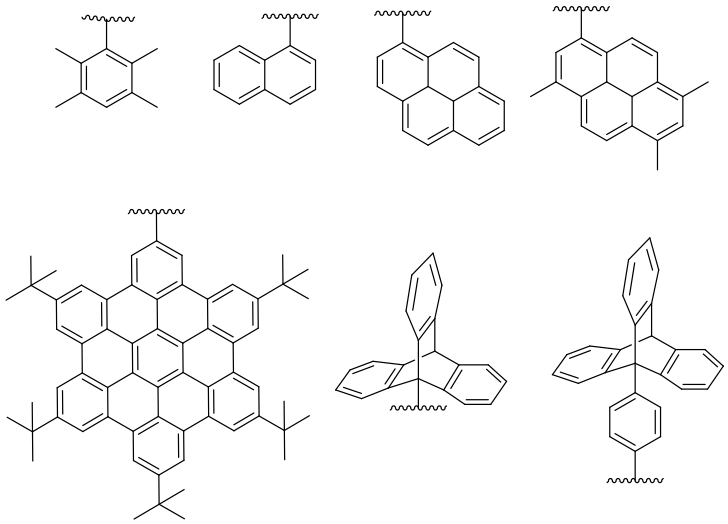

The ready availability of variety of tweezers with different pincers allows us not only to demonstrate that they bind a variety of electron acceptors as guests but also show that one of the tweezers with electron-rich pincers (i.e. trimethylpyrene pincers) undergoes a ready self-assembly when prompted by 1-electron oxidation. The development of a versatile synthesis of various tweezers using doubly-annulated *m*-terphenyl (**TP**) platform also allows ready preparation of tweezers containing triptycene and 9-phenyltriptycene as pincers (see Chart 1.1); and these new tweezers are expected to show gear like functioning. The details of these findings are described herein.

Results and Discussion

1. Synthesis of the doubly-annulated *m*-terphenyl as a common platform for the preparation of various tweezers.

The synthesis of the doubly-annulated *m*-terphenyl platform (**TP** or **1g**) begins with commercially-available 1,5-dibromo-2,4-diodobenzene **1a** which can also be synthesized in excellent yields in 50-100 gram quantities by an iodination of *m*-

dibromobenzene in concentrated sulfuric acid (see Scheme 2.4). Thus, an efficient palladium-catalyzed Sonogashira coupling[8] of the commercially available and inexpensive 1,1-dimethyl-2-propyne-1-ol with **1a** leads to a quantitative formation of **1b** where the more reactive iodo substituents are selectively substituted by acetylenic alcohols. A standard Suzuki coupling of the dibromo-diacetylenic derivative **1b** with 3-methoxybenzeneboronic acid in the presence of a Pd(0) catalyst afforded the desired terphenyl **1c** in good overall yield. The resulting diacetylenic-*m*-terphenyl **1c** was then subjected to catalytic hydrogenation in ethyl acetate in the presence of 10% palladium on activated carbon as the catalyst. The resulting reduced terphenyl **1d** was sufficiently pure and thus was treated directly with methanesulfonic acid in dichloromethane at room temperature to afford the doubly-bridged *m*-terphenyl **1e** via two facile intramolecular Friedel-Crafts cyclizations[5] (Scheme 2.2).

Scheme 2.4 Synthesis of the doubly-annulated *m*-terphenyl platform for the preparation of various tweezers.

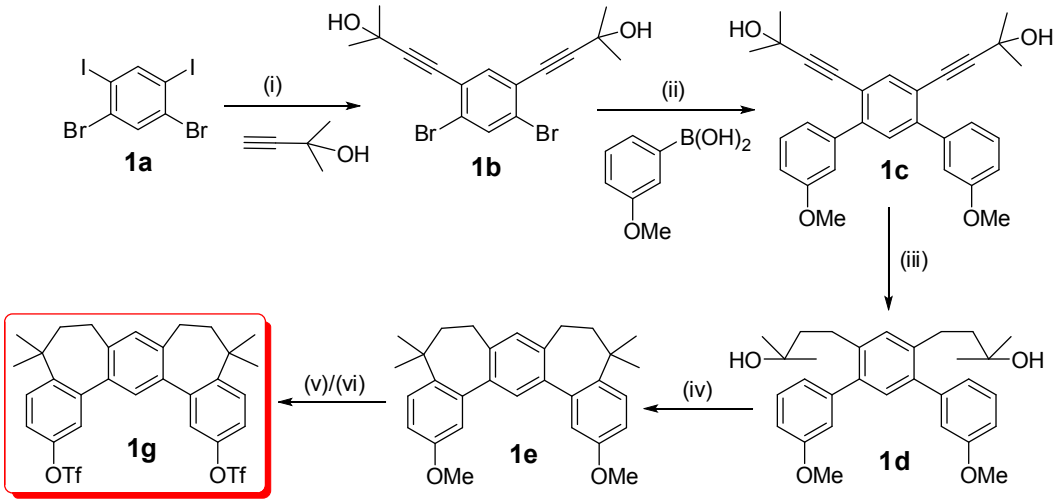

(i) $PdCl_2(PPh_3)_2$/CuI/(^{i}Pr)$_2$NH/Benzene; (ii) $Pd(PPh_3)_4$ (2 mol%)/2M Na_2CO_3/DME/reflux, 16h; (iii) Pd/C/H_2/ EtOAc; (iv) $MeSO_3H/CH_2Cl_2$; (v) BBr_3/CH_2Cl_2/-10 ^oC; (vi) Triflic anhydride/pyridine/CH_2Cl_2.

The conversion of the 2,14-methoxy substituents of **1e** to the corresponding trifluoromethanesulfonates (i.e. **1e** → **1g**) was easily accomplished by a demethylation reaction[9] using BBr_3 followed by a reaction[10] with triflic anhydride in a mixture of pyridine and dichloromethane in an excellent yield.

2. Synthesis of various tweezers using the doubly-annulated *m*-terphenyl as a common precursor.

Synthesis of various tweezers (see structures below) containing duryl (**T-Dur**), naphthyl (**T-Nap**) and pyrenyl (**T-Py**) groups as pincers was readily accomplished by a standard Suzuki coupling of the doubly-annulated *m*-terphenyl-ditriflate **1g** with various boronic acids (i.e. durylboronic acid or 2-naphthylboronic acid or 2-pyrenylboronic acid) in the presence of a Pd(0) catalyst, i.e. (eq 1).

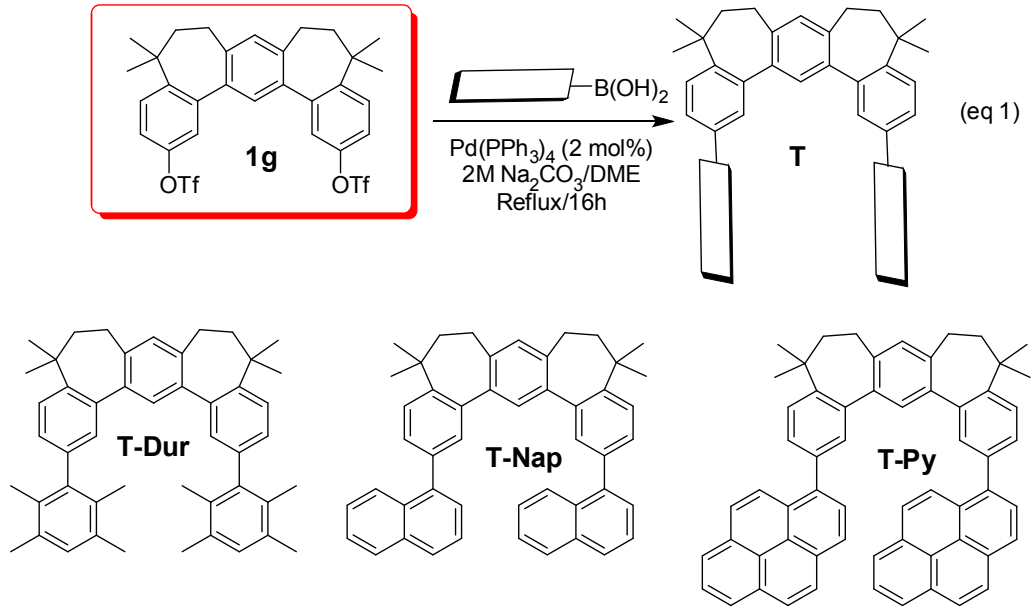

Encouraged by the successful synthesis of the first three tweezers in eq 1, we next undertook the preparation of a tweezer containing large graphitic fragments (e.g. hexabenzocoronene, HBC) as pincers because HBC pincers are known to undergo reversible 1-electron oxidation[11] and it is expected that such a tweezer (i.e. **T-HBC**) may self-assemble when subjected to 1-electron oxidation. The required mono-bromo-HBC derivative [or 1-bromo-5,8,11,14,17-pentakis(1,1-dimethylethyl)hexabenzocoronene, **Br-HBC**] for the synthesis of **T-HBC** was obtained by oxidative cyclodehydrogenation of known *pentakis*(4-*tert*-butylphenyl)-4-bromophenylbenzene[12] using DDQ as an oxidant in a mixture of methansulfonic acid in dichloromethane (see Scheme 2.5).[13]

Scheme 2.5 Synthetic scheme for the preparation of tweezer T-HBC.

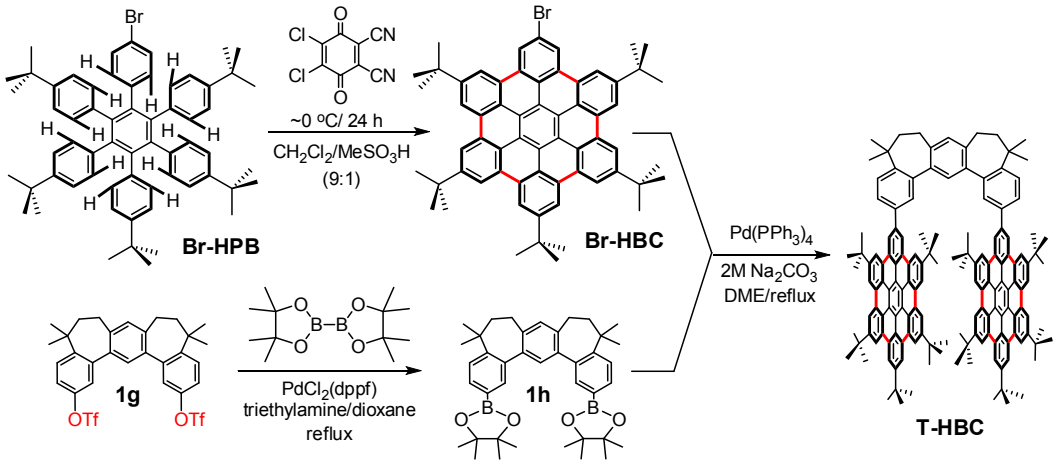

Initial attempts to prepare a boronic acid or boronic ester of **Br-HBC** were met with difficulty. However, the search of the literature revealed that benzenetriflates can be directly converted to the corresponding boronic esters by a simple 1-step transformation using *bis(*pinacoloto)diboron and a palladium catalyst.[14] Accordingly, a simple conversion of ditriflate **1g** to diboronic ester **1h** using *bis*(pinacoloto)diboron and $PdCl_2$(dppf) in dioxane followed by a standard Suzuki coupling with two equivalents of **Br-HBC** afforded **T-HBC** in good yield. Although, the MALDI mass spectrometry of sparingly soluble **T-HBC** confirmed its successful synthesis (see Figure 2.3), the further studies, unfortunately, were hampered due to its poor solubility in common organic solvents.

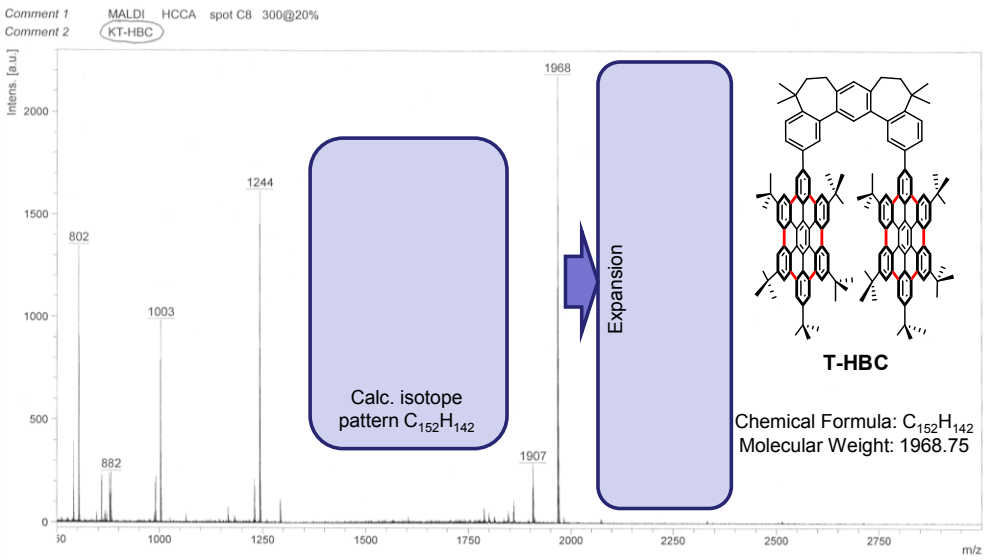

Figure 2.3 Positive ion MALDI-TOF MS spectrum of tweezer T-HBC (structure in the right) using Dithranol as the matrix. The spectrum represents the summation of scans from >100 laser shots collected by rastering various positions of the sample. (Inset, Right) Expanded MS spectrum showing the observed isotopic pattern for $C_{152}H_{142}$. (Inset, Left) Calculated isotopic pattern for $C_{152}H_{142}$.

We believe the poor solubility of **T-HBC** may arise, in part, due to the self-aggregation of tweezers. Three different views of the calculated structure of a dimeric aggregate of **T-HBC** are shown in Figure 2.4.

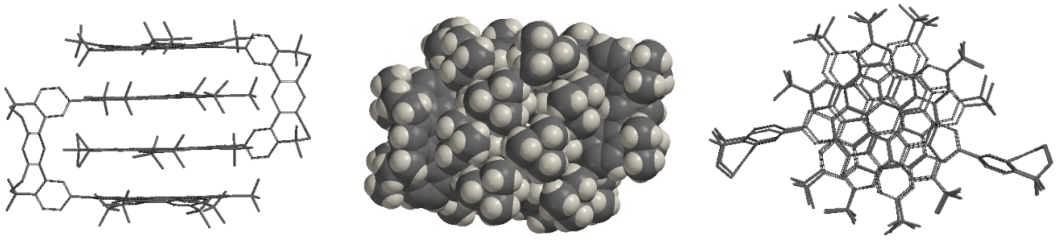

Figure 2.4 AM1-optimized structure of a dimeric aggregate of **T-HBC.**

Owing to the poor solubility of tweezer with HBC pincers, possibly due to self-aggregation, prompted us to synthesize a tweezer with the 1,3,6-trimethylpyrene as pincers because 1,3,6,8-tetrasubstituted-pyrenes are known to undergo highly reversible oxidation to form stable cation radicals at ambient temperatures.[15] Indeed, using a strategy similar to the synthesis of **T-HBC** (i.e. Scheme 2.5), allowed a successful preparation of **T-TMP**, i.e. eq 2.

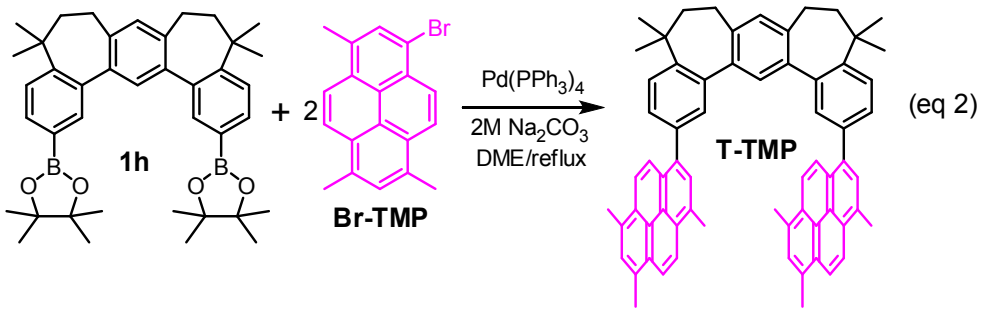

The 1-bromo-3,6,8-trimethylpyrene (**Br-TMP**), required for the synthesis of **T-TMP** in eq 2, was in turn obtained in excellent yield from pyrene by a recently-developed procedure from our laboratory and is shown in Scheme 2.6.

Scheme 2.6 Synthetic scheme for the preparation of 1-bromo-3,6,8-trimethylpyrene (Br-TMP).

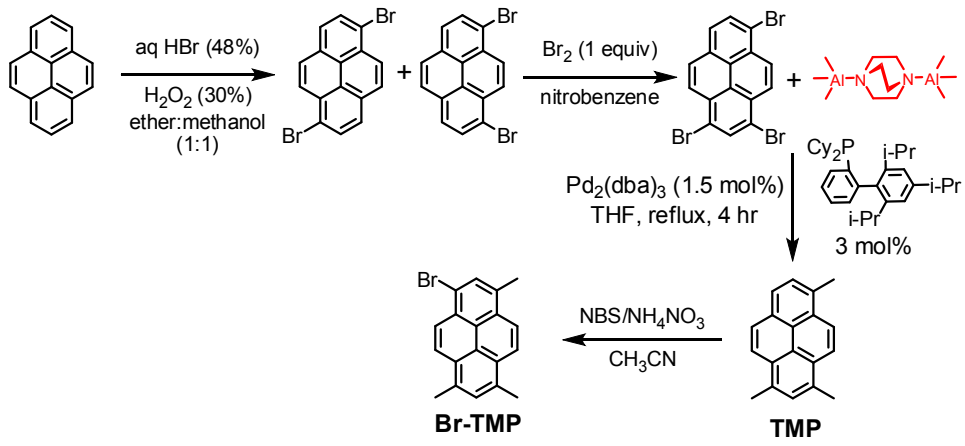

Thus, a mixture of pyrene and aqueous hydrobromic acid (48%) in a 1:1 mixture of methanol and ether was treated dropwise with aqueous hydrogenperoxide (30%) and the resulting mixture was stirred at 22 ^{o}C for 24 h to afford a nearly quantitative yield of an isomeric mixture of dibromopyrenes[16] (Scheme 2.6). The mixture of dibromopyrenes was then treated with 1 equivalent of bromine in nitrobenzene at 22 ^{o}C to afford a good yield of tribromopyrene[17] after a couple of crystallizations from toluene. It is noted that the use of more than 1 equivalent of bromine leads to formation of tetrabromopyrene which cannot be easily separated from the tribromopyrene. Tribromopyrene was quantitatively converted to the corresponding trimethylpyrene (**TMP**) by a palladium catalyzed methylation reaction using trimethylaluminum-DABCO complex as a methylating agent[18] (see Scheme 1.6). Finally, the bromotrimethylpyrene (**Br-TMP**) was obtained by a reaction of TMP with NBS in acetonitrile in the presence of ammonium nitrate as the catalyst[19] (Scheme 2.6).

3. Study of the conformational flexibility of the doubly-annulated TP-based tweezers.

Molecular modeling studies showed that the doubly annulated *m*-terphenyl (**TP**) platform for the preparation of tweezers exists in two different conformations which are almost isoenergetic. DFT calculations at B3LYP/6-31G* level indicated that *anti*-conformer was only 0.26 kcal/mol more stable than *syn* conformer, i.e. Figure 2.5.

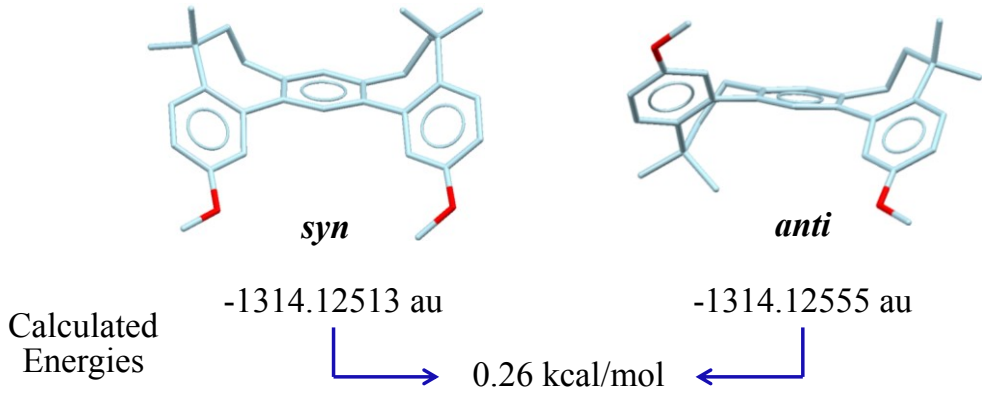

Figure 2.5 Structures of the two (almost) isoenergetic atropisomers of the doubly bridged *m*-terphenyl 1e as obtained by DFT calculations at the B3LYP/6-31G* level.

The interconversion between the (isoenergetic) *syn* and *anti*-conformers of **1e** was apparent by the presence of broadened methyl signals in its ^{1}H NMR spectrum at ambient temperatures (see Figure 2.6). Variable-temperature ^{1}H NMR spectroscopy of a representative doubly-bridged *m*-terphenyl **1e** in $CDCl_3$ over a temperature range of +20 to -60 °C showed that the interchange between the two isoenergetic conformers can be frozen at ~-60 °C.

The activation energy for the interchange between *syn* and *anti*-conformers was estimated by the line-shape analysis of the signals in the variable-temperature ^{1}H NMR spectra in Figure 2.6. The line shape analysis is a process where all the data was

processed using 'Nuts' software and values of rate of interconversion (k) at each indicated temperature were obtained from the WinDNMR software. The temperature dependence on the rate constants was used to calculate the activation energy for the conformational change in **1e** by treating the data with the linearized Arrhenius equation, i.e. eq 3.

$$\ln k = -E_a / R\ (1/T) + \ln A \qquad \text{(eq 3)}$$

Where E_a is activation energy, R is gas constant, and T is temperature in Kelvin. Plotting the ln k verses 1/T yields a straight line, whose slope (m = $-E_a/R$) can be used to determine E_a for the conformational exchange of **1e** (see Figure 2.7). The activation energy E_a for the exchange of two conformers of **1e** was found to be 11.5 kcal/mol.

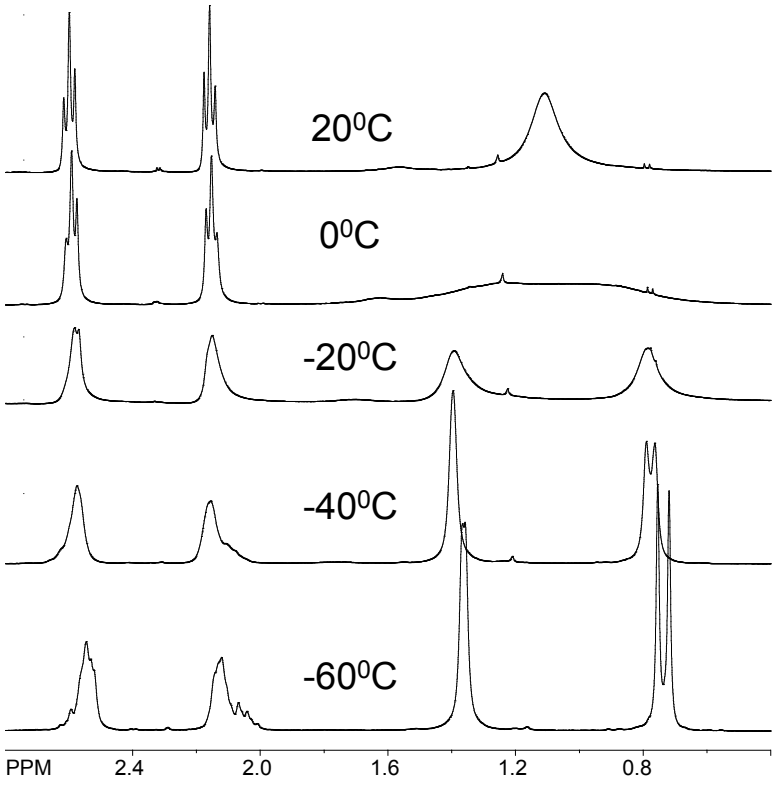

Figure 2.6 ^{1}H NMR spectra of the aliphatic region of the doubly annulated *m*-terphenyl 1e which show that the broadened signal at ~1.1 ppm due to the four methyl groups split into two sets of signals at ~-60 °C.

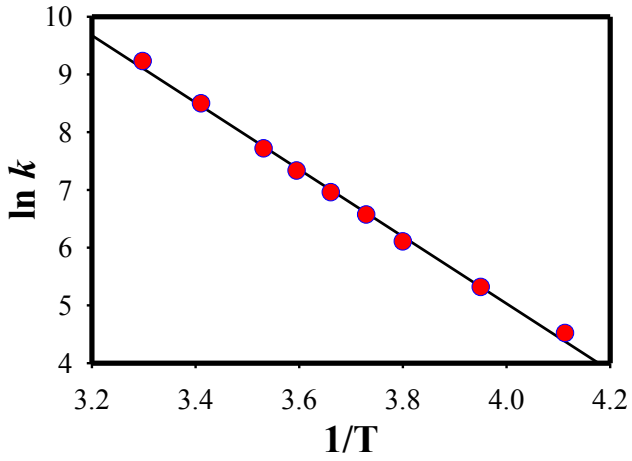

Figure 2.7 Arrhenius plot for the calculation of activation energy E_a for the conformational exchange of **1e**.

An X-ray crystallographic analysis of the doubly annulated *m*-terphenyl **1e** showed that it exists in the solid state in the relatively more stable *anti*-conformation (see Figure 2.8).

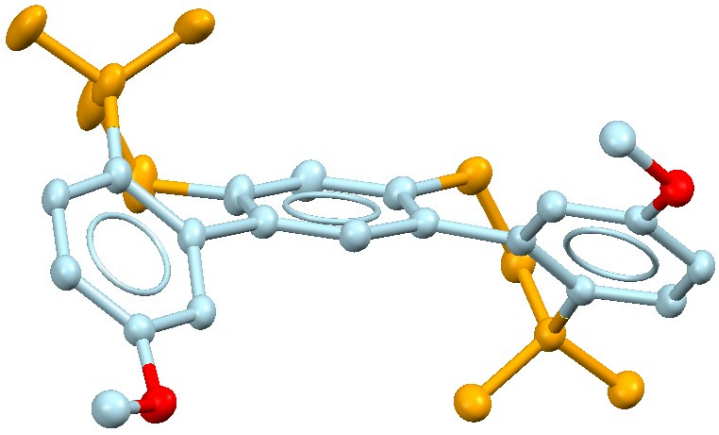

Figure 2.8 An ORTEP diagram of the molecular structure of the doubly annulated terphenyl **1e**.

DFT calculations with various TP-based tweezers showed that the energy difference between *syn*- and *anti*-conformations varied only between 0.2-0.3 kcal/mol. The selected variable temperature ^{1}H NMR spectra of **T-Py** are presented in Figure 2.9 and they showed that the broadened methyl peaks at room temperature split upon cooling to -60 °C and the observed temperature dependence for **T-Py** was similar to that observed for **1e** in Figure 2.6.

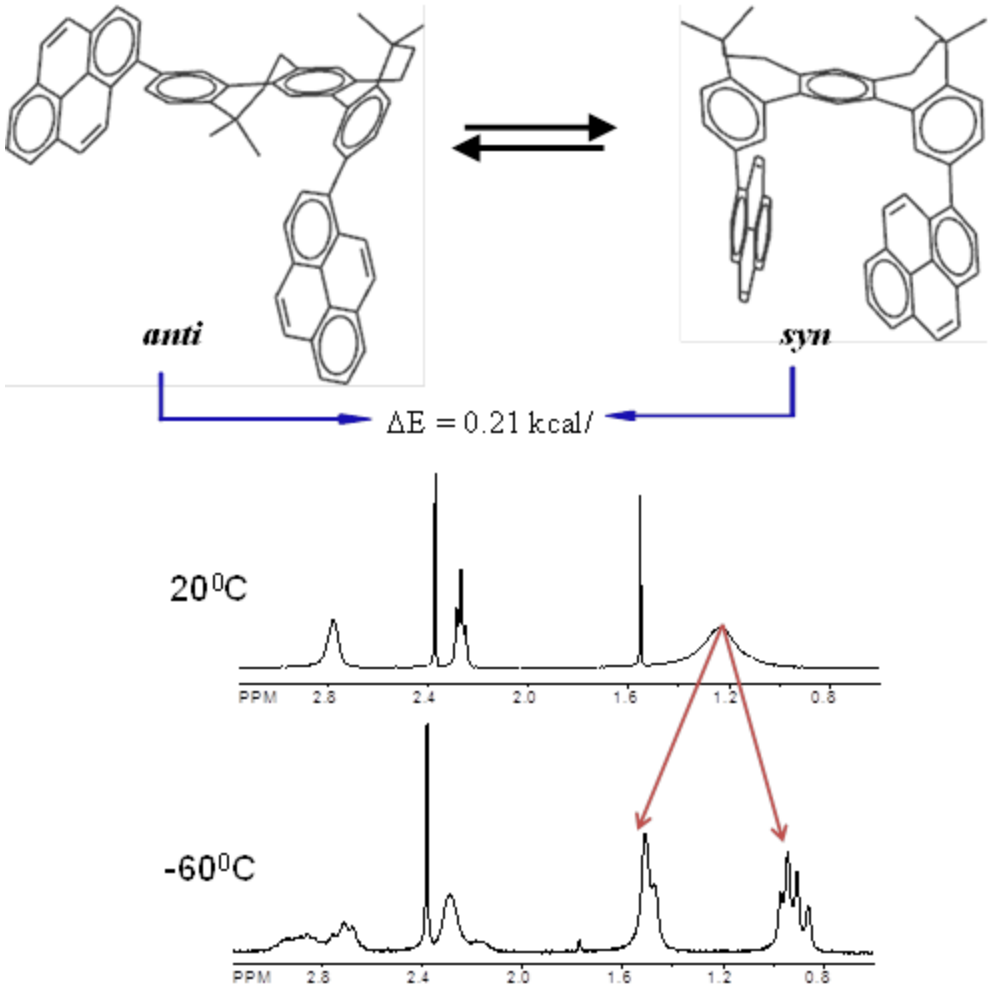

Figure 2.9 ^{1}H NMR spectra of the aliphatic region of T-Py which show that the broadened signal at ~1.2 ppm due to the four methyl groups split into two sets of signals at ~-60 °C.

4. Binding of electron acceptors as guests to various tweezers via electron donor-acceptor or charge transfer interactions

Various tweezers (i.e. **T-Dur**, **T-Nap**, and **T-Py**), obtained above, were subjected to electron donor-acceptor or charge transfer interactions with a selected set of electron acceptors (see Chart 2.2) as follows.

Chart 2.2 Various guests as electron acceptors and tweezers as electron donors used for the donor-acceptor studies.

Tweezers as electron donors

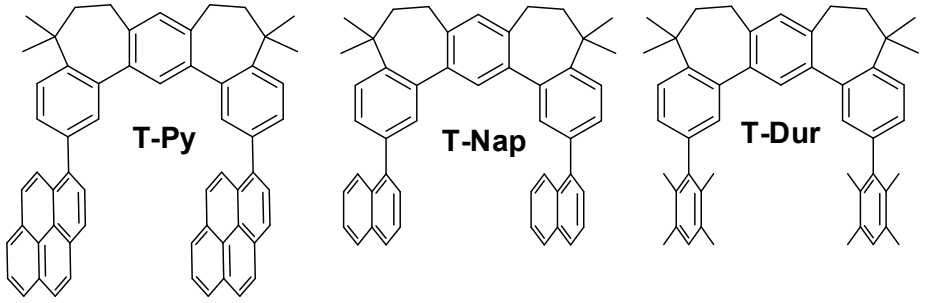

Guests as electron acceptors

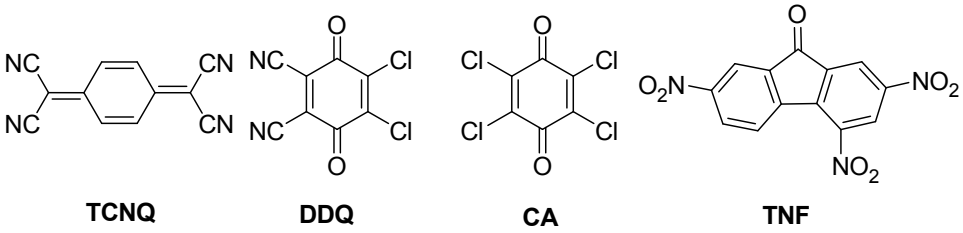

Of the various measures available for the quantitative evaluation of intermolecular interactions in molecular recognition and self-assembly of supramolecular host-guest chemistry in solution, the appearance of new spectral bands (or colors) arising from the charge-transfer (CT) transitions between electron donors and electron acceptors is especially useful and easy to probe.[20] Indeed, the CT absorptions are diagnostic of a very wide spectrum of intermolecular electron donor-acceptor (EDA) interactions arising in

extremely stable, isolable complexes on one hand, to highly transient complexes (with collisional lifetimes) at the other extremum. From a structural point of view, we have earlier established[20] that the critical donor-acceptor distance for effective charge-transfer interactions require that donor and acceptor must lie at a van der Waal's contact (i.e. ~3.5 Å for the systems discussed in Chart 2.1).

The quantitative intermolecular association was evaluated in the form of the K_{DA} and ε_{CT} values for the formation and visualization, respectively, of various tweezer/acceptor complexes; and the quantitative analysis of the spectrophotometric absorption changes was treated by the Benesi-Hilderbrand method,[21] (eq 4).

$$\frac{[\mathbf{A}]}{A_{CT}} = \frac{1}{\varepsilon_{CT}} + \frac{1}{K_{DA}\varepsilon_{CT}} \frac{1}{[\mathbf{D}]} \qquad \text{(eq 4)}$$

Where A_{CT} is the molar absorbance and ε_{CT} is the extinction coefficient of the charge transfer band at the monitoring wavelength. The concentration of the electron acceptor was kept at least 10 times greater than that of tweezer donors,[21a] and a plot of [**A**]/A_{CT} versus the reciprocal donor concentration was found to be linear in all tweezer/acceptor complexation measurements. From the slope $[K_{DA}\varepsilon_{CT}]^{-1}$ and the intercept $[\varepsilon_{CT}]^{-1}$, the values of association constant (K_{DA}) and extinction coefficient (ε_{CT}) were readily calculated.

For example, the UV-vis spectral changes in Figure 2.10 typically show the monotonic growth of the diagnostic charge-transfer absorbance with its visible maximum at λ_{CT} = 899 nm upon the incremental addition of tweezer **T-Py** to a solution of 2,3-dichloro-5,6-dicyano-*p*-benzoquinone (**DDQ**) in dichloromethane at 22 °C.

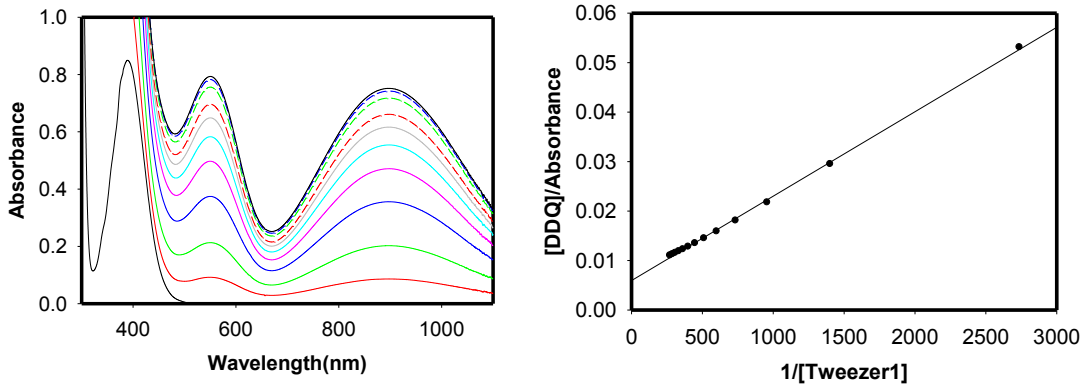

Figure 2.10 Left: Spectral changes attendant upon the incremental addition of a solution of tweezer **T-Py** (0.00374 M) to a solution of DDQ (0.022 M) in dichloromethane. Right: The Benesi-Hildebrand plot.

The well-resolved (featureless) absorption band in Figure 2.10 was ascribed to the intermolecular donor-acceptor association, as originally formulated by Mulliken,[22] *i.e.* eq 5.

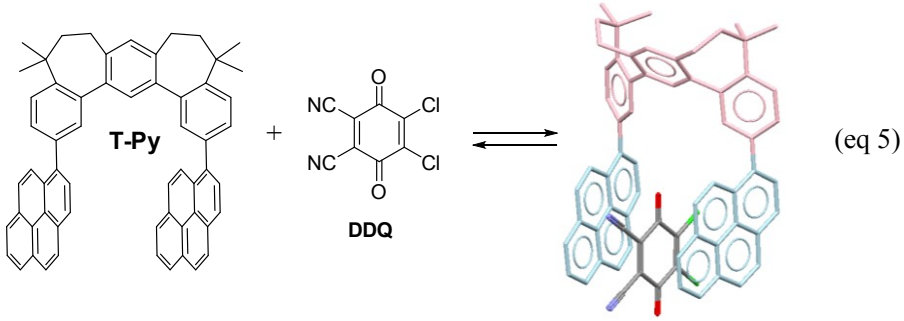

(eq 5)

For the quantitative analysis of the [**T-Py**, DDQ] association in solution, the spectrophotometric absorbance changes in Figure 2.10 were treated by the Benesi-Hildebrand procedure and a plot of [**DDQ**]/A_{CT} versus the reciprocal donor concentration (1/[**T-Py**]) was found to be linear (see Figure 2.10, right), and the least-squares fit produced a correlation coefficient of greater than 0.99. From the slope $[K_{DA}\varepsilon_{CT}]^{-1}$ and the

intercept $[\varepsilon_{CT}]^{-1}$, the values of the association constant and the extinction coefficient were readily extracted as $K_{DA} = 415\ M^{-1}$ and $\varepsilon_{899\ nm} \sim 70\ M^{-1}\ cm^{-1}$, respectively.

In order to determine if **T-Py** functions like a tweezer, i.e. DDQ binds between a pair of pyrene moieties, as shown by the calculated structure of [**T-Py**, DDQ] in eq 5, a comparison of the binding of DDQ with model donor (i.e. 1-phenylpyrene) was compared as follows. Thus, an exposure of a solution of 1-phenylpyrene with a solution of DDQ in dichloromethane produced a red- colored solution with a diagnostic charge-transfer absorption band at λ_{CT} = 909 nm. The quantitative comparison of the binding energies of **T-Py** and 1-phenylpyrene with DDQ in Figure 2.11 confirmed that the model 1-phenylpyrene (K_{DA} = 23 M^{-1} and $\varepsilon_{909\ nm} \sim 147\ M^{-1}\ cm^{-1}$) binds DDQ less efficiently then the tweezer **T-Py** ($K_{DA} = 415\ M^{-1}$ and $\varepsilon_{899\ nm} \sim 70\ M^{-1}\ cm^{-1}$).

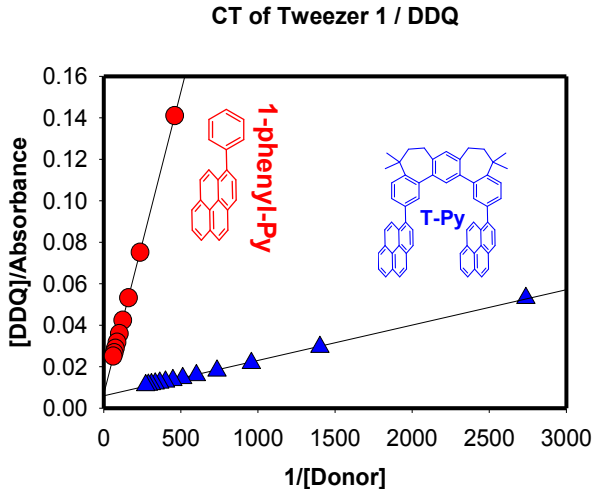

Figure 2.11 Graphical comparison of binding efficiencies of T-Py and 1-phenylpyrene with DDQ using Benesi-Hildebrand plots.

Isolation and X-ray crystallographic characterization of [**T-Py**, DDQ] **complex.**

A relatively strong association of DDQ with tweezer (i.e. **T-Py**) in comparison to the model compound (i.e. 1-phenylpyrene) together with modeling studies (see eq. 5) suggests that DDQ is sandwiched between pyrene moieties in **T-Py** tweezer. Such a structural assignment was further verified by the isolation of dark-colored crystals of the 1:1 complex from an equimolar solution of **T-Py** and DDQ in a mixture of dichloromethane and acetonitrile, simply by a very slow evaporation of the solution at ambient temperatures. X-ray crystallography of a single crystal of the electron donor-acceptor (or charge-transfer) complex of [**T-Py**, DDQ] revealed that DDQ is indeed sandwiched between a pair of pyrenyl donors with an interplanar separation of $d \sim 3.2$ Å, as illustrated in the top and side perspectives in Figure 2.12**.**

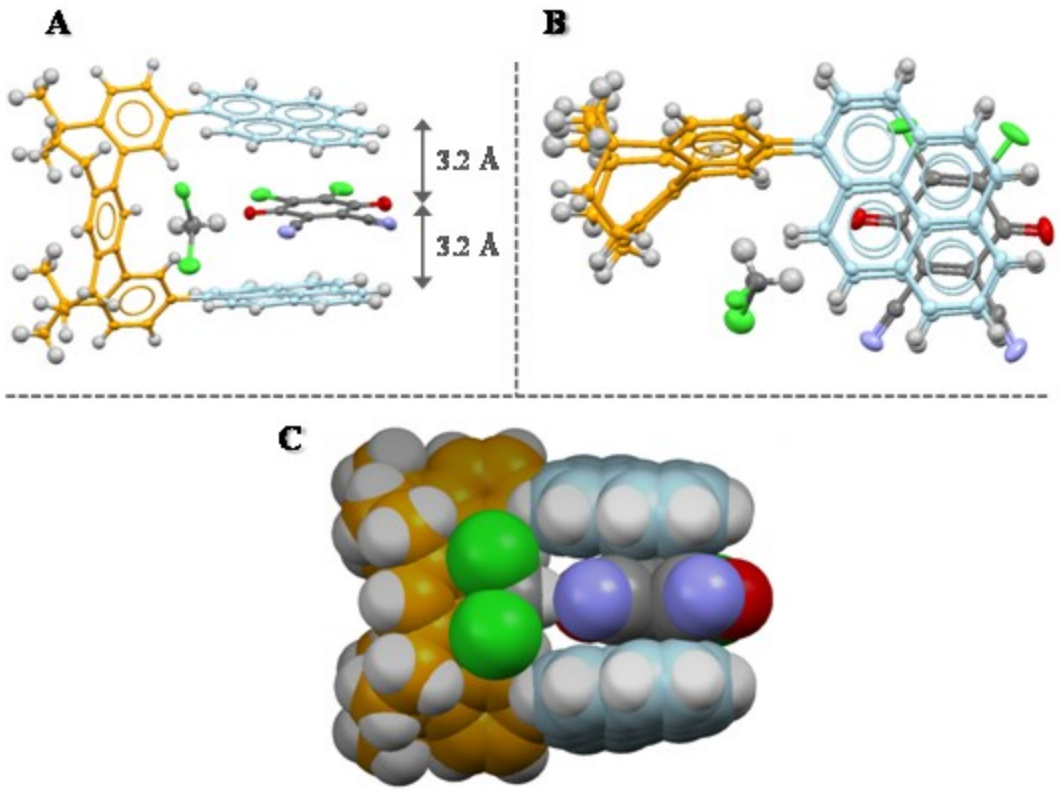

Figure 2.12 Showing the side and top views (A/B) and a space-filling representation (C) of the X-ray structures of 1:1 D···A complex of [T-Py, DDQ] together with a solvent molecule (i.e. CH_2Cl_2).

The additional features of the X-ray structure of [**T-Py**, DDQ] complex are described as follows. For example, the entire complex contains a local symmetry plane, i.e. the *m*-terphenyl platform of the **T-Py** tweezer adopts an achiral *syn* conformation (compare Figures 2.8 and 2.12B). The pyrene pincers are oriented almost parallel to each other (within 13.2 deg) and DDQ is sandwiched exactly between them and the two interplanar distances are identical at 3.2 Å. The remaining empty space near the central benzene ring of the *m*-terphenyl platform in [**T-Py**, DDQ] complex is filled by a solvent (i.e. CH_2Cl_2) molecule which also makes C-H···π and C-H···O contacts[23] providing the weak intermolecular forces for the solid state assembly (see Figure 2.13).

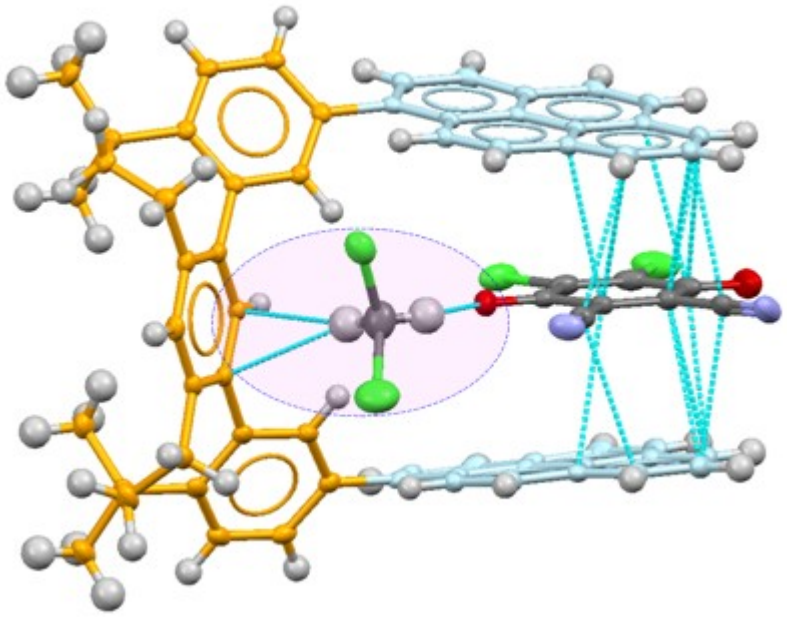

Figure 2.13 Showing the C-H···π and C-H···O contacts (highlighted by a circle) of the dichloromethane molecule in the crystal structure of [T-Py, DDQ] complex.

The molecular packing diagram (see Figure 2.14) provides a closer look at the interaction amongst the [**T-Py**, DDQ] D···A complexes. The D···A units in the crystal structure form ···[D···A···D]···[D···A···D]···[D···A···D]··· stacks along the crystallographic [101] direction. The interplanar distances between the pyrene moieties of a pair of D···A complexes (i.e. D]···[D) vary between 3.38 and 3.50 Å, which are closer to a standard van-der-Waals separation (3.4 Å).

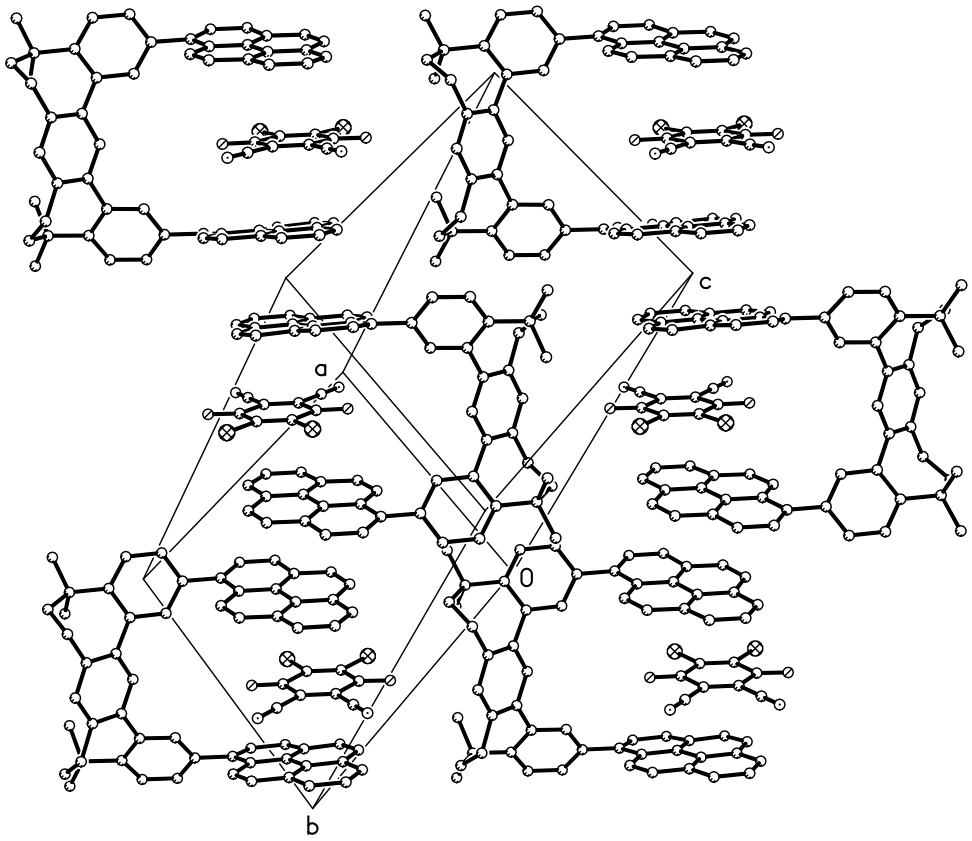

Figure 2.14 Packing diagram of [T-Py, DDQ] complex in its X-ray crystal structure.

Comparison of the binding of DDQ with the tweezers containing pincers of different size and electron donacity.

The availability of the three tweezers (Chart 2.3) containing pyrene (E_{ox} ~ 1.36 V), naphthalene (E_{ox} ~ 1.4 V) and durene (E_{ox} ~ 1.8 V) as pincers (or electron donors) allowed us to examine the effect of the size and electron donacity of the pincers on the binding strengths of the tweezer/electron acceptor complexes with DDQ as a common electron acceptor. As noted in literature, the size complementarity between donor and acceptor and the electron donacity of the pincers plays a critical role in controlling the binding strength of tweezer/guest complexes.

Chart 2.3 Showing the structures of various tweezers and their model compounds as electron donors used for the donor-acceptor studies.

Tweezers as electron donors

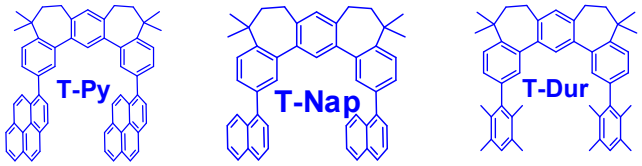

Model electron donors

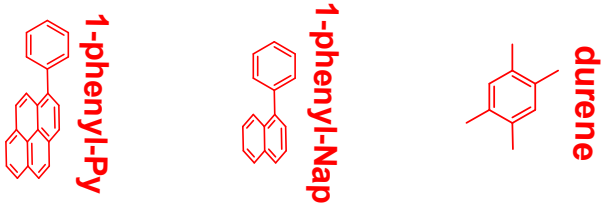

Accordingly, the quantitative analysis of the binding of DDQ with various tweezers and their model compound (Chart 2.3) in solution was carried out by spectrophotometric analyses (see Figures 2.S1 and 2.S6 in the experimental section) and the absorbance data were treated according to the Benesi-Hildebrand procedure. The Benesi-Hildebrand plots of [**DDQ**]/Absorbance$_{CT}$ versus the reciprocal donor concentration (1/[**D**]) for various donors in Chart 1.3 are compiled in Figure 2.15. Also, the Table 2.1 compares the values of association constants (K), extinction coefficient (ε_{CT}), and the "effective absorbance" ($K_{DA}\varepsilon_{CT}$) of the EDA complexes.

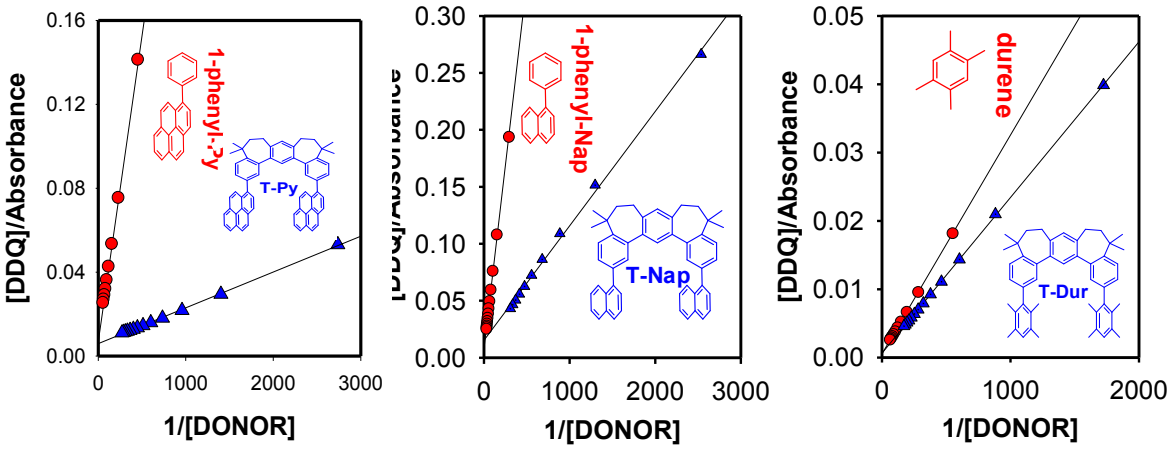

Figure 2.15 Graphical comparison of binding efficiencies of tweezers with different pincers and their model compounds with DDQ using Benesi-Hildebrand plots.

Table 2.1 Compilation of association constants (K), extinction coefficient (ε_{CT}), and the "effective absorbance" ($K_{DA}\varepsilon_{CT}$) of the EDA complexes T-Py, T-Nap, T-Dur and their model compounds with DDQ.

Tweezer/ model compound	λ_{CT} (nm)	K_{DA} (M^{-1})	ε_{CT} ($M^{-1}cm^{-1}$)	$K_{DA}\varepsilon_{CT}$
T-Py	899	415	70	29,095
Ph-Py	909	23	147	3,432
T-Nap	684	196	52	10,179
Ph-Nap	683	15	109	1,576
T-Dur	611	26	1,667	43,821
Dur	591	16	1,994	31,133

Comparison of both association constants (K) and "effective absorbance" ($K_{DA}\varepsilon_{CT}$) of various EDA complexes in Table 2.1 clearly indicates that various tweezers bind DDQ with greater efficiency than the corresponding model compounds.

Furthermore, the efficiency of the EDA association of DDQ with both tweezers and the corresponding model compounds increases with increasing donor strength of the pincers. Unfortunately, the increasing size of the pincers in various tweezers also correspond to their decreasing oxidation potentials and therefore any conclusion with regard to the size complementarity between donor and acceptor cannot be conclusively drawn with this set of molecules.

Comparison of the binding of a TP-tweezer containing pyrenes as pincers (T-Py) with electron acceptors of varying strength

As demonstrated above that the increasing donor strength of the pincers in various tweezers leads to increased efficiency of the EDA association (see Table2.1). Accordingly, herein we examine the effect of the electron acceptor strength of on the EDA association using a series of electron acceptors as guests (see Chart 2.4) with a common tweezer (i.e. T-Py).

Chart 2.4 Various electron acceptor guests used for the D-A complexation with tweezer T-Py.

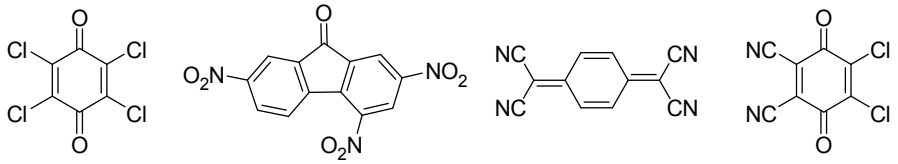

	CA	**TNF**	**TCNQ**	**DDQ**
E_{red} (V vs SCE)	0.02	0.10	0.23	0.56

The quantitative analysis of the binding of **T-Py** with various electron acceptors (see Chart 2.3) as guests in solution was carried out by spectrophotometric analyses (see Figures 2.S7 and 2.S15 in the experimental section) and the absorbance data were treated according to the Benesi-Hildebrand procedure. The Table 2.1 compares the values of

association constants (K), extinction coefficient (ε_{CT}), and the "effective absorbance" ($K_{DA}\varepsilon_{CT}$) of the EDA complexes of T-Py with various acceptors.

Table 2.2 Compilation of association constants (K), extinction coefficient (ε_{CT}), and "effective absorbance" ($K_{DA}\varepsilon_{CT}$) of the EDA complexes of CA, TNF, TCNQ, and DDQ with tweezer T-Py.

Acceptor	E_{red} in V (vs. SCE)	Tweezer/ model	λ_{CT} (nm)	K_{DA} (M^{-1})	ε_{CT} ($M^{-1}cm^{-1}$)	$K_{DA}\varepsilon_{CT}$
CA	0.02	**T-Py**	632	54	95	5160
		1-Ph-Py	638	6	163	971
TNF	0.10	**T-Py**	536	12	4,533	55,648
		1-Ph-Py	536	2	2508	4,728
TCNQ	0.27	**T-Py**	777	26	3,087	79,936
		1-Ph-Py	-n/a-	-n/a-	-n/a-	-n/a-
DDQ	0.56	**T-Py**	899	415	70	29,095
		1-Ph-Py	909	23	147	3,432

Comparison of both association constants (K) and "effective absorbance" ($K_{DA}\varepsilon_{CT}$) of various EDA complexes in Table 2.2 suggested that binding efficiencies of electron acceptor of similar size (i.e. CA and DDQ) with tweezer **T-Py** increases with the increasing acceptor strength of the guests. Unfortunately, the non-planarity of TNF and different size of TCNQ as compared to DDQ and chloranil did not correspond to the predicted trend.

5. Electron transfer induced self-assembly of a molecular tweezer containing trimethylpyrene as pincers.

The motivation for developing new platforms for synthesis of tweezers was driven by the fact that they hold potential to be assembled into dimeric structures when prompted by 1-e^- oxidation, i.e. Scheme 2.7.

Scheme 2.7 Proposed electron-transfer induced self-assembly of molecular tweezers.

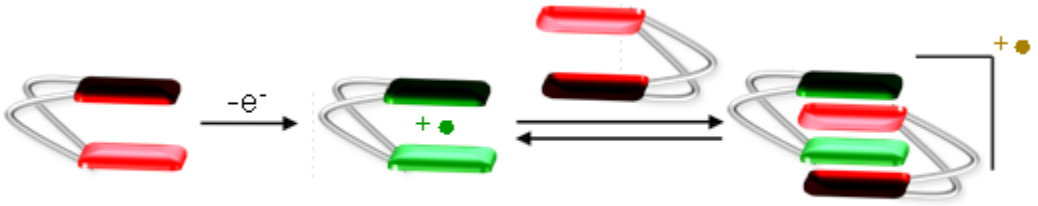

The conjecture in Scheme 2.7 is largely compelled by the fact that a variety of planar aromatic cation radicals undergo dimerization when exposed to their neutral counterparts; and the resulting dimeric cation radicals can be characterized by the observation of an intense intervalence transition in the near-IR region of their electronic spectra in solution or by X-ray crystallography in solid state.[24] The association constants for the formation of dimeric cation radicals (i.e. $D_2^{+\bullet}$) in solution are generally small[24] and the higher order aggregate (i.e. $D_3^{+\bullet}$ or $D_4^{+\bullet}$) in solution are rarely observed, i.e. Scheme 2.8.

Scheme 2.8 Formation of a dimeric cation radical from planar aromatic hydrocarbons.

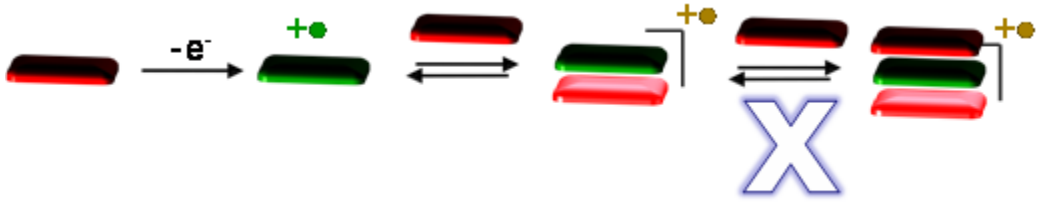

It is further noted that we have earlier characterized the cation radicals of a class of cofacially stacked polyfluorenes[25] where a single charge is delocalized over 2-6 fluorene moieties and the characteristic near-IR transition showed a dramatic red-shift with the increasing number of fluorene moieties, i.e. Figure 2.16.

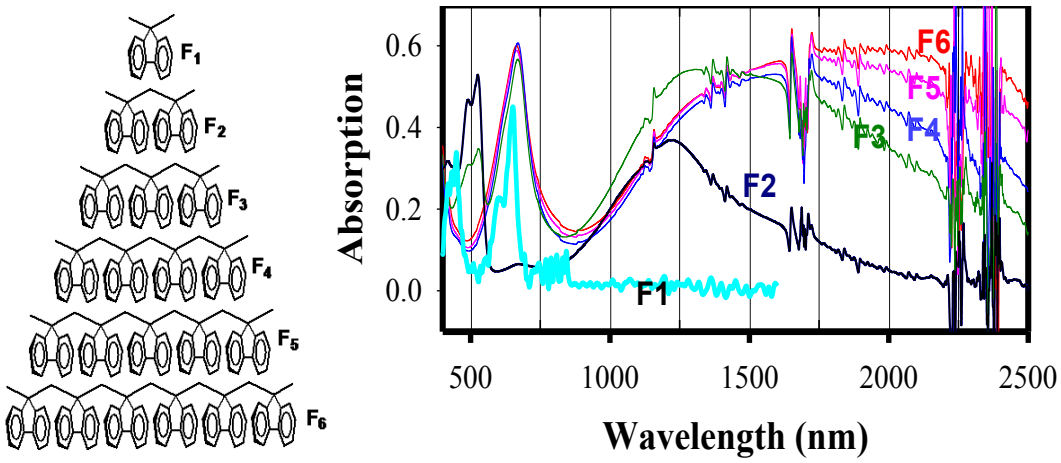

Figure 2.16 Electronic spectra of F1-F6 cation radicals. Note that $F1^{+\bullet}$ does not show a NIR transition while the intense NIR transition is observed F2-F6 cation radicals which shifts red with increasing number of fluorene moieties.

Accordingly, herein we will demonstrate with the aid of tetramethylpyrene (**TMP**) as the model compound that a doubly annulated terphenyl-based tweezer, containing trimethylpyrene as pincers (i.e. **T-TMP**), undergoes an efficient dimerization when prompted by 1-electron oxidation as follows.

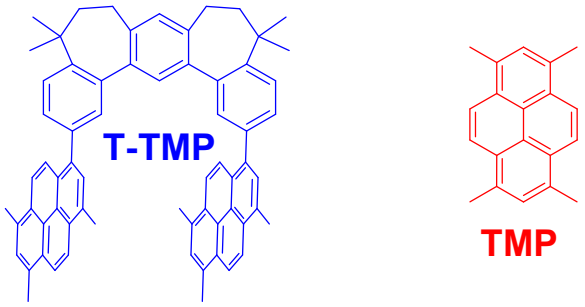

The electron donor strength and the initial indication of the cation radical stability of the tweezer **T-TMP** and its model compound **TMP** were evaluated by electrochemical oxidation at a platinum electrode as a 2 x 10^{-3} M solution in dichloromethane containing 0.1 M *n*-Bu_4NPF_6 as the supporting electrolyte. The cyclic voltammograms of **T-TMP** and **TMP** (Figure 2.17) consistently met the reversibility criteria at various scan rates of 50-500 mV/s, as they all showed cathodic/anodic peak current ratios of i_a/i_c = 1.0 (theoretical). The reversible oxidation potential of model **TMP** (E_{ox} = 1.00 V vs. SCE) was calibrated with added ferrocene (E_{ox} = 0.45 V vs SCE) as an internal standard. It is noted that under these conditions, model **TMP** does not undergo a second electrochemical oxidation (see Figure 2.17, top and/or eq 6) in the readily accessible potential range (i.e. <1.7 V vs SCE).

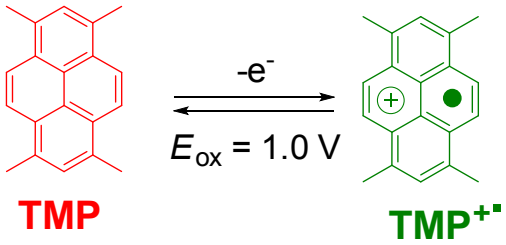

(eq 6)

The cyclic voltammogram of tweezer **T-TMP** (in Figure 2.17, bottom) shows two closely spaced reversible oxidation waves which correspond to the two oxidation events occurring at oxidation potentials of 0.95 and 1.11 V vs. SCE was when calibrated with added ferrocene as an internal standard.

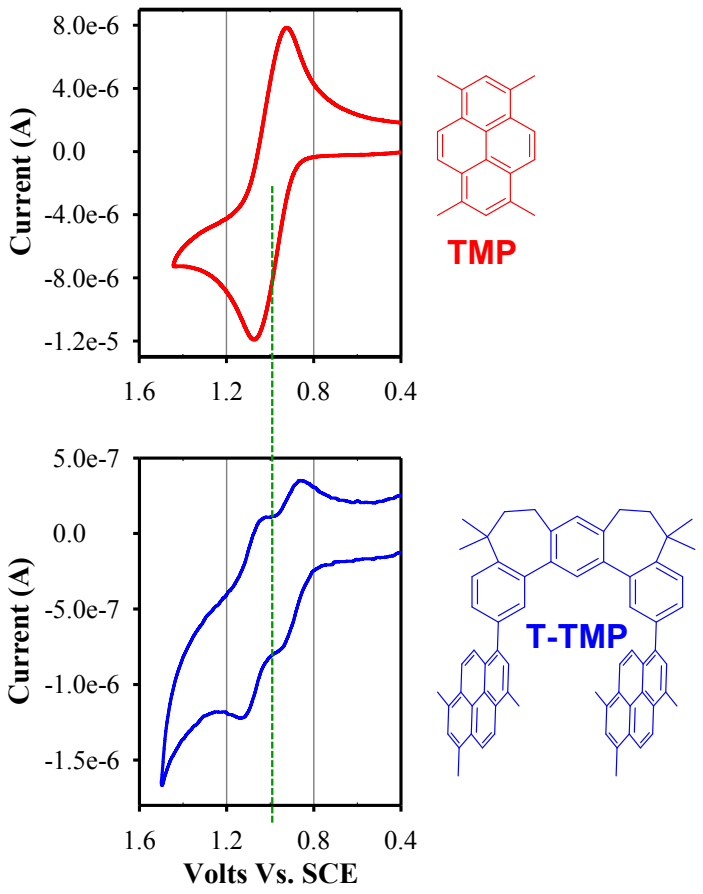

Figure 2.17 Cyclic voltammograms of 2 mM tetramethylpyrene (TMP) and tweezer T-TMP and in CH_2Cl_2 containing 0.1 M *n*-Bu_4NPF_6 at scan rate of 100 mV s^{-1} at 22 °C.

The oxidation events in the cyclic voltammogram of tweezer **T-TMP** (in Figure 2.17, bottom) are summarized in eq 7.

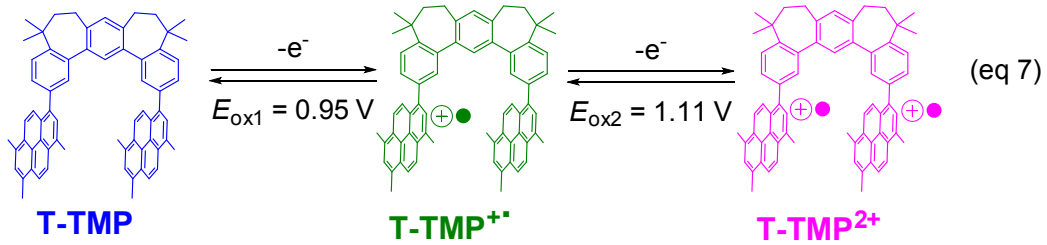

(eq 7)

It is interesting to note that although the trimethylpyrene pincers lie far away from each other for the cofacial interaction (i.e. with an interplanar separation of ~7 Å), the loss of second electron occurs at a relatively higher potential (by ~160 mV). As such this observation suggests that oxidation of **T-TMP**$^{+\bullet}$ to **T-TMP**$^{+2}$ must introduce a significant amount of Columbic repulsion between the oxidized trimethylpyrene pincers.

The electrochemical reversibility and low oxidation potential of both **TMP** and **T-TMP** allowed the us generate their cation radicals by chemical oxidation using the stable aromatic cation radical salt $MA^{+\bullet}$ $SbCl_6^-$ (E_{red} = 1.1 V vs. SCE) as a 1-electron oxidant.[26] As sown in Figure 2.18 (top), the addition of excess neutral **T-TMP** to a solution of its cation radicals (i.e. **T-TMP**$^{+\bullet}$) showed the appearance of a new transition in the NIR region in its electronic spectrum. Furthermore, the NIR transition grew in intensity up to the addition of 1 equiv. of tweezer **T-TMP**. Note that a similar spectra titration of **TMP**$^{+\bullet}$ with neutral **TMP** also produced a characteristic new NIR transition due to the formation of a dimeric cation radical (Figure 2.18, bottom), however, a large excess of neutral **TMP** (~30 equiv.) was needed in order to reach a maximum concentration of its dimeric cation radical.

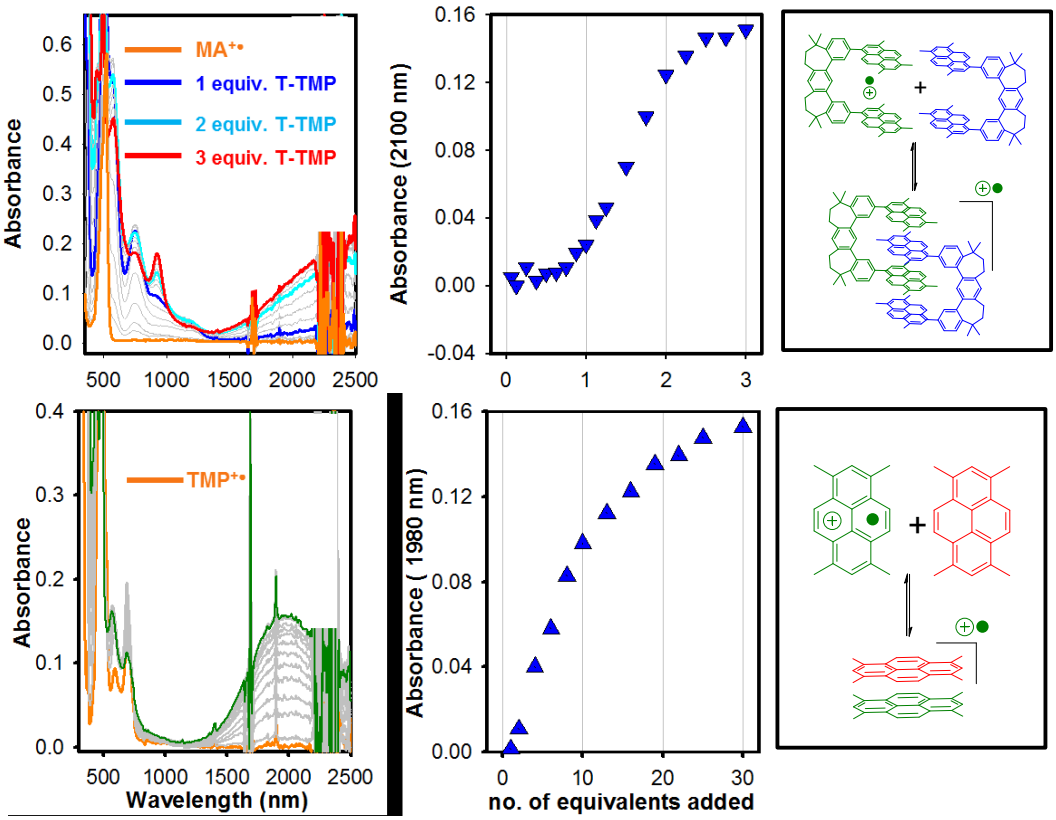

Figure 2.18 Top (left). Spectral changes upon the reduction of 1.1 x 10^{-4} M $MA^{+\bullet}$ by an incremental addition of **T-TMP**. ***Top (middle)***. A plot of changes in absorbance at 2100 nm against the added equivalents of neutral **T-TMP.** ***Bottom (left).*** Spectral changes upon the incremental addition of neutral **TMP** to a solution of $\mathbf{TMP^{+\bullet}}$. ***Bottom (middle).*** A plot of changes in absorbance at 1980 nm against the added equivalents of neutral**TMP.**

A spectral comparison of dimeric cation radicals of the tweezer and model **TMP** showed that NIR transition in $\mathbf{(T\text{-}TMP)_2^{+\bullet}}$ is red-shifted as compared to model $\mathbf{(TMP)_2^{+\bullet}}$. Such a red shift of the NIR transition in $\mathbf{(T\text{-}TMP)_2^{+\bullet}}$ is understandable by the fact that a single charge is delocalized over four cofacially arrayed pyrenyl moieties as compared to only two in model $\mathbf{(TMP)_2^{+\bullet}}$ (compare Figures 2.18 and 2.16). The calculated molecular structure of dimeric $\mathbf{(T\text{-}TMP)_2^{+\bullet}}$ is shown in Figure 2.19. We are

actively pursuing the crystallographic characterization of dimeric self-assembly of (**T-TMP)$_2^{+\bullet}$**.

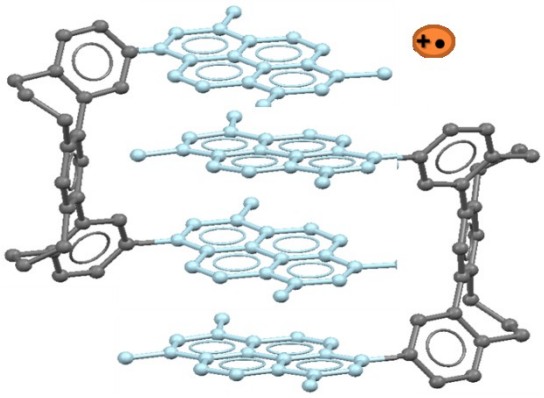

Figure 2.19 Structure of dimeric self-assembly of (T-TMP)$_2^{+\bullet}$ obtained by DFT calculation at B3LYP/6-31G* level.

Conclusions

We have successfully developed an efficient synthesis of tweezers using a common doubly-annulated *m*-terphenyl platform. The ready availability of these tweezers with different pincers allows us to demonstrate that they bind a variety of electron acceptors as guests via electron donor-acceptor or charge-transfer interactions. We have also shown that a tweezer with electron-rich pincers (i.e. trimethylpyrene pincers) undergoes a ready self-assembly when prompted by 1-electron oxidation to a stabilized dimeric cation radical. The development of a versatile synthesis of various tweezers also allowed us to synthesize tweezers containing triptycene and 9-phenyltriptycene as pincers (see Chart 2.1 and the Experimental section) and study of their gear-like functioning is under investigation.

Experimental section

General Experimental Methods and Materials. All reactions were performed under argon atmosphere unless otherwise noted. All commercial reagents were used without further purification unless otherwise noted. Dichloromethane (Aldrich) was repeatedly stirred with fresh aliquots of concentrated sulfuric acid (~10 % by volume) until the acid layer remained colorless. After separation it was washed successively with water, aqueous sodium bicarbonate, water, and aqueous sodium chloride and dried over anhydrous calcium chloride. The dichloromethane was distilled twice from P_2O_5 under an argon atmosphere and stored in a Schlenk flask equipped with a Teflon valve fitted with Viton O-rings. The hexanes and toluene were distilled from P_2O_5 under an argon atmosphere and then refluxed over calcium hydride (~12 h). After distillation from CaH_2, the solvents were stored in Schlenk flasks under an argon atmosphere. Tetrahydrofuran (THF) was dried initially by distilling over lithium aluminum hydride under an argon atmosphere. The THF was further refluxed over metallic sodium in the presence of benzophenone until a persistent blue color was obtained and then it was distilled under an argon atmosphere and stored in a Schlenk flask equipped with a Teflon valve fitted with Viton O-rings. NMR spectra were recorded on Varian 300 and 400 MHz NMR spectrometers. GC-MS spectra were obtained on a Fisons 8000 trio instrument at an ionization potential of 70 eV.

Cyclic Voltammetry (CV). The CV cell was of an air-tight design with high vacuum Teflon valves and Viton O-ring seals to allow an inert atmosphere to be maintained without contamination by grease. The working electrode consisted of an adjustable platinum disk embedded in a glass seal to allow periodic polishing (with a fine emery

cloth) without changing the surface area (~1 mm2) significantly. The reference SCE electrode (saturated calomel electrode) and its salt bridge were separated from the catholyte by a sintered glass frit. The counter electrode consisted of platinum gauze that was separated from the working electrode by ~3 mm. The CV measurements were carried out in a solution of 0.2 M supporting electrolyte (tetra-*n*-butylammonium hexafluorophosphate, TBAH) and 2-5 x 10^{-3} M substrate in dry dichloromethane under an argon atmosphere. All the cyclic voltammograms were recorded at a sweep rate of 200 mV sec^{-1}, unless otherwise specified and were IR compensated. The oxidation potentials ($E_{1/2}$) were referenced to SCE, which was calibrated with added (equimolar) ferrocene ($E_{1/2}$ = 0.450 V *vs*. SCE). The $E_{1/2}$ values were calculated by taking the average of anodic and cathodic peak potentials in the reversible cyclic voltammograms.

Preparation of various intermediates for syntheses of doubly annulated tweezers

1, 5-Dibromo-2,4-diiodobenzene (1a).

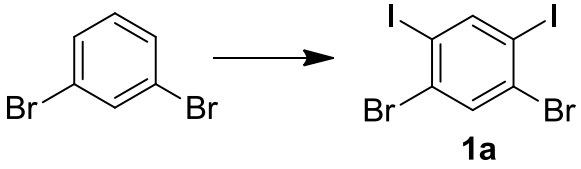

1a

In a 500 mL 3-neck flask with a thermometer adapter and condensor, 1, 4-dibromobenzene (19.5 g, 82.7 mmol) was dissolved in 250 mL concentrated sulfuric acid while heating. Elemental iodine (46.2 g, 181.9 mmol) was added to the solution portion wise during heating. The resulting purple solution was stirred at 125-135 °C for 2 days. The sublimated iodine deposited on the walls of the flask was redissolved into the solution by occasional shaking of the flask. The solution was cooled to room temperature

and poured into ice water (300 mL), and extracted with dichloromethane (3 x 30 mL). The dichloromethane layer was then stirred with dilute sodium hydroxide (300 mL) to remove any excess iodine. The dichloromethane layer was extracted once more, dried over anhydrous magnesium sulfate, evaporated, and dried under vacuum. A large portion of the product remained as a solid mass which was broken up, stirred with dilute sodium hydroxide solution (300 mL), and filtered. Both portions combined gave a yellow solid which was recrystallized from a dichloromethane/methanol mixture (39.77 g, 98.68%); mp 164-166 ^{o}C ^{1}H NMR ($CDCl_3$) δ: 8.27 (1H, s), 7.82 (1H, s).

Preparation of 1b:

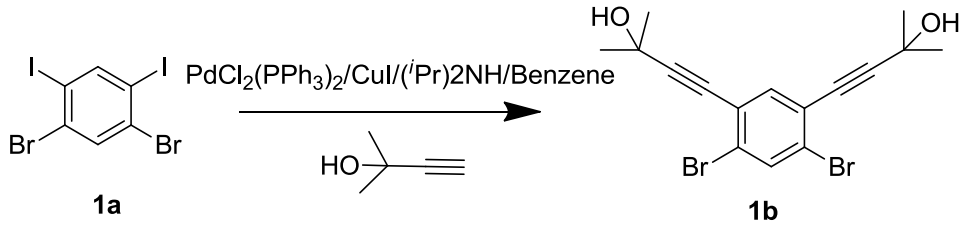

In a Shlenk flask, 1, 5-dibromo-2, 4-diiodobenzene (2.00 g, 4.10 mmol), dry benzene (20 mL) and diisopropylamine (12 mL) were added under an argon atmosphere. The solution was degassed. Then CuI (120 mg) was added along with dichloro-bis(triphenylphosphine)palladium (100 mg). The solution was again degassed. Finally 3-methyl-2-butene-2-ol was added. The mixture was stirred overnight at room temperature. The reaction was then quenched with addition of 50 mL of water, and extracted with ether. Organic layer was collected and washed with water and dried over $MgSO_4$. The crude product was obtained by removal of ether under reduced pressure. The product was then purified by column chromatography using hexanes/ethyl acetate (1.00 g, 61%). mp

110-112 ^{o}C 1H NMR ($CDCl_3$) δ: 7.78 (1H, s), 7.48 (1H, s), 2.23 (2H, s). ^{13}C NMR ($CDCl_3$) δ: 31.44, 79.62, 100.15, 124.39, 125.73, 135.80, 136.89.

Preparation of 1c:

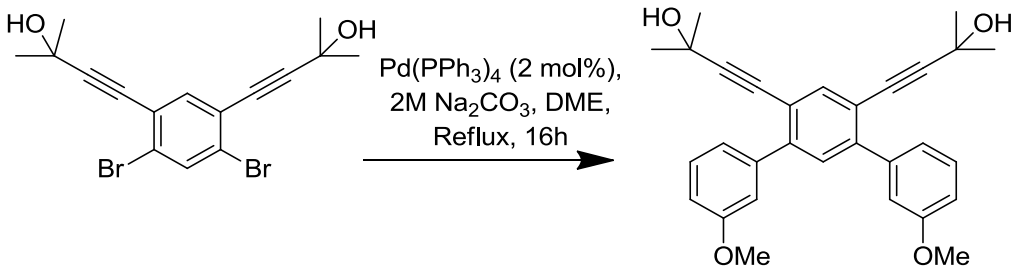

1b **1c**

Diacetylene compound (0.9 g, 2.5 mmol) and the corresponding *m*-methoxybenzo boronic acid (3 equiv, 0.95 g, 6.25 mmol) were dissolved in anhydrous 1,2-dimethoxyethane (DME) (30 mL) in an oven dried Schlenk flask under an argon atmosphere and the flask was evacuated and filled with argon (3x). In another oven dried Schlenk flask a solution of anhydrous sodium carbonate (5.0 g) in water (20 mL) was prepared under an argon atmosphere and the flask was also evacuated and filled with argon (3x). To the DME solution, $Pd(PPh_3)_4$ (50 mg) and the salt solution were added sequentially under a strict argon atmosphere followed by evacuation and filling the flask with argon (3x) after each addition. The flask was covered with aluminum foil and the solution was allowed to reflux overnight. The resulting solution was cooled to room temperature, quenched with water (50 mL) and extracted with dichloromethane (3 x 20 mL). The organic layer was dried over anhydrous magnesium sulfate, evaporated and dried under vacuum. The crude product was then purified by column chromatography using a hexanes/ethyl mixture to give the pure product (0.8 g, 80%); mp 104-106 ^{o}C ^{1}H

NMR ($CDCl_3$) δ : 7.68 (1H, s), 7.42 (1H, s), 7.32 (2H, t, *J* = 7.60 Hz), 7.18 (2H, d, *J* = 7.04 Hz), 7.17 (2H, s), 6.91 (2H, d, *J* = 8.45 Hz), 3.84 (6H, s), 2.11 (2H, s), 1.49 (12H, s). ^{13}C NMR ($CDCl_3$) δ: 31.26, 55.51, 65.75, 81.12, 113.42, 115.2, 120.20, 121.85, 129.13, 130.49, 137.59, 141.10, 143.65, 159.32.

Preparation of 1d:

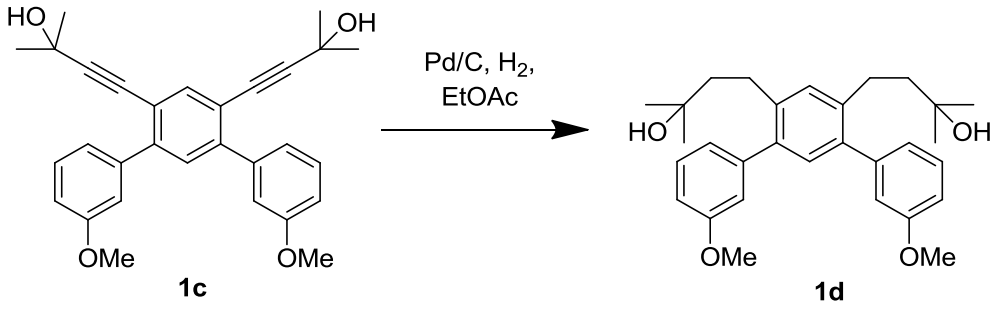

The diacetylene **1c** (0.8 g, 1.76 mmol) was placed into a Parr apparatus along with a stir bar and dissolved in ethyl acetate (26 mL). To the solution, 10 % Palladium on activated carbon catalyst (100 mg) was added. The vessel was then put under hydrogen pressure (3 bar) for 24 hours after which time the solution was filtered over a short pad of silica gel. The silica gel was washed with ethyl acetate (2 x 20 mL), the solvent was evaporated and the product was dried under vacuum and used without further purification. (0.7 g, 86%) ^1H NMR ($CDCl_3$) δ : 7.30 (2H, t, *J* = 7.66 Hz), 7.20 (1H, s), 7.11 (1H, s), 6.93 (2H, d, *J* = 7.50 Hz), 6.88 (2H, s), 6.87 (2H, d, *J* = 8.13 Hz), 3.81 (6H, s), 2.70 (4H, m), 1.67 (4H, m), 1.12 (12H, s).

Preparation of 1e:

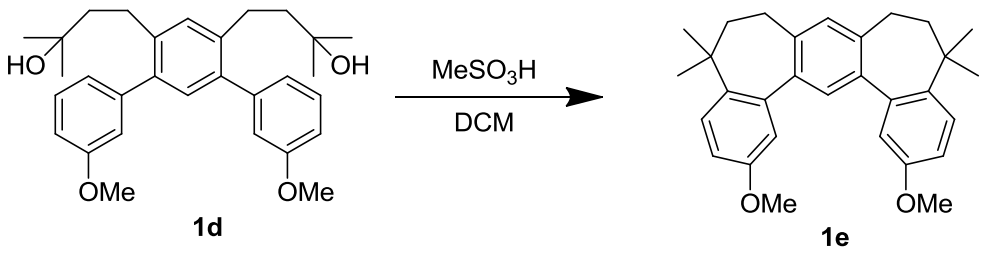

To a stirred solution of **1d** (0.7 g, 0.155 mmol) in dichloromethane (30 mL) at room temperature was added methanesulfonic acid (2 mL). The reaction progress was monitored by ^{1}H NMR, and upon completion, the solution was quenched with aqueous sodium bicarbonate (100mL) and extracted with dichloromethane (3 x 20 mL). The combined organic extracts were dried over anhydrous magnesium sulfate, evaporated and dried under vacuum. The solid was purified by recrystallization from a dichloromethane/methanol mixture to give the product **1e** (0.58g, 87.87%); mp 168-170 ^{o}C ^{1}H NMR ($CDCl_3$) δ : 7.38 (1H ,s), 7.36 (2H, d, *J* = 2.61 Hz), 7.04 (1H, s), 6.99 (2H, d, *J* = 2.61 Hz), 6.85 (2H, dd, *J* = 8.78 Hz, 2.61 Hz), 3.85 (6H, s), 2.58 (4H, t, *J* = 7.122 Hz), 2.09 (4H, t, *J* = 7.122 Hz), 1.09 (12H, broad s) . ^{13}C NMR ($CDCl_3$) δ :32.37, 37.24, 48.62, 55.46, 111.86, 116.23, 126.59, 127.48, 138.51, 138.96, 141.51, 141.81, 158.03.

Preparation of 1f:

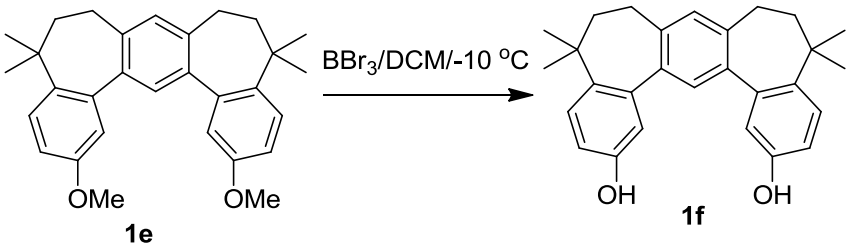

The solution of diether (0.46 g, 1.086 mmol) in DCM was cooled to -10 ^{o}C under argon atmosphere using ice-acetone bath. The solution of BBr_3 (0.615 mL, 6.516 mmol) in 10 mL DCM was added to the above cooled solution drop wise over the period of 30 min. The mixture was gradually warmed to room temperature and stirred for 2 hrs. The reaction was quenched with water (50 mL) and extracted with dichloromethane (3 x 20 mL). The organic layer was dried over anhydrous magnesium sulfate, evaporated and dried under vacuum**.** The product formed (0.4g, 93.24%) was immediately subjected to the next step without any purification. ^{1}H NMR ($CDCl_3$) δ: 7.32 (1H, s), 7.30 (2H, d, *J* = 4.58Hz), 7.02 (1H, s), 6.94 (2H, d, *J* = 2.75Hz), 6.78 (2H, dd, *J* = 8.48Hz, 2.75Hz), 4.23 (2H, broad), 2.57 (4H, t, *J* = 6.77Hz), 2.08 (4H, t, *J* = 6.77Hz), 1.06 (12H, s).

Preparation of 1g:

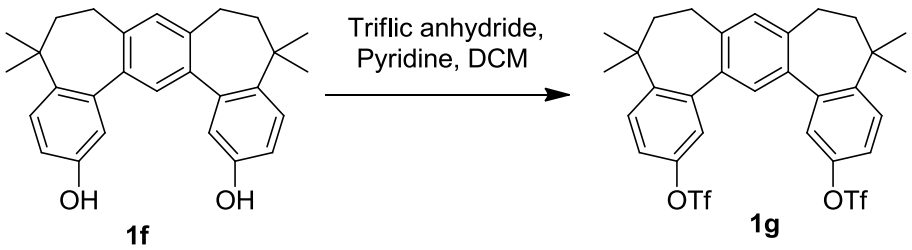

In a Schlenk flask under an argon atmosphere, **(1f)** (0.4g, 1.003mmol) and pyridine (0.24 mL, 3.010 mmol) were dissolved in dry DCM (40 ml). The solution was cooled at -10 ^{0}C with ice-acetone bath. In a dropping funnel, a solution of triflic anhydride (0.7 mL, 3.96 mmol) in DCM (10 mL) was taken and was added to the above cooled solution over 10 min. under argon. The reaction mixture was stirred for 6 hrs at 0 ^{0}C. The reaction mixture was concentrated on rotary evaporator. The residual brown oil was diluted with ethyl

acetate .Washed with 5% HCl followed by sat.NaCl and sodium bicarbonate .Organic layer was dried over anhydrous magnesium sulfate, evaporated and dried under vacuum**.** The product formed (0.6 g, 90.22 %) was purified with column chromatography using hexanes/ethyl acetate. mp 170-172 ^{o}C ^{1}H NMR ($CDCl_3$) δ : 7.54 (2H ,d, J = 8.67Hz), 7.30 (2H, s), 7.23(3H, m), 7.11(2H, s), 2.60 (4H, t, J = 6.65 Hz), 2.17 (4H, t, J = 6.65 Hz), 1.12 (12H, broad s) . ^{13}C NMR ($CDCl_3$) δ : 31.64, 32.19, 38.04, 48.58, 119.73, 122.71, 127.59, 127.71, 128.09, 139.81, 140.34, 142.79, 146.75, 148.35 .

Preparation of T-Py:

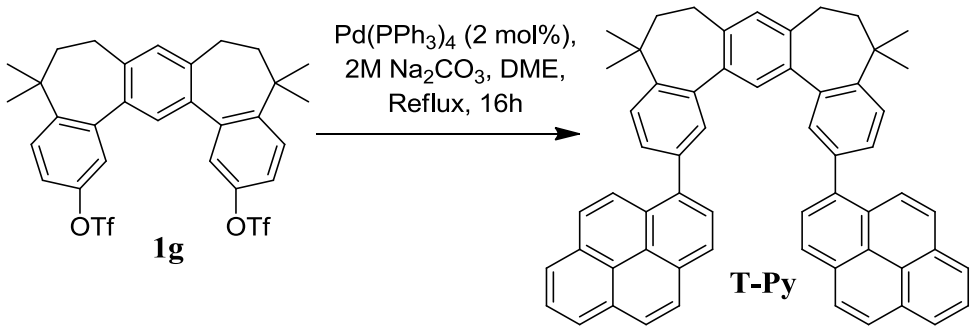

Ditriflate compound **1g** (0.6 g,0.90 mmol) and 1-pyreneboronicacid (3 equiv, 0.66 g, 2.71 mmol) were dissolved in anhydrous toluene (30 mL) in an oven dried Schlenk flask under an argon atmosphere and the flask was evacuated and filled with argon (3x). In another oven dried Schlenk flask a solution of anhydrous sodium carbonate (5.0 g) in water (20 mL) was prepared under an argon atmosphere and the flask was also evacuated and filled with argon (3x). To the dioxane solution, $Pd(PPh_3)_4$ (50 mg) and the salt solution were added sequentially under a strict argon atmosphere followed by evacuation and filling the flask with argon (3x) after each addition. The flask was covered with foil

and the solution was allowed to reflux overnight. The resulting solution was cooled to room temperature, quenched with water (50 mL) and extracted with dichloromethane (3 x 20 mL). The organic layer was dried over anhydrous magnesium sulfate, evaporated and dried under vacuum. The product was further purified by column chromatography using a hexanes/ethyl mixture to give the pure product (0.5 g, 72 %) m.p. 340 ^{o}C ^{1}H NMR ($CDCl_3$) δ : 8.24 (2H, d, *J* = 9.02 Hz), 8.12 (4H, t, *J* = 8.45 Hz), 8.01(6H, m), 7.90 (6H, m), 7.68 (2H, d, *J* = 1.74 Hz), 7.62 (2H, d, *J* = 7.71 Hz), 7.55 (2H, dd, *J* = 8.20, 1.74 Hz), 7.52 (1H, s), 7.17 (1H,s), 2.76 (4H, Broad), 2.26 (4H, t, *J* = 6.71 Hz), 1.24 (12H, Broad). ^{13}C NMR ($CDCl_3$) δ :31.86, 32.55, 37.99, 48.94, 124.81, 124.89, 125.05, 125.07, 125.10, 125.62, 125.69, 126.03, 127.41, 127.49, 127.56, 127.62, 127.83, 128.42, 128.67, 129.39, 130.60, 131.09, 131.60, 132.57, 137.62, 139.14, 139.38, 140.72, 141.77, 145.21.

Preparation of T-Nap

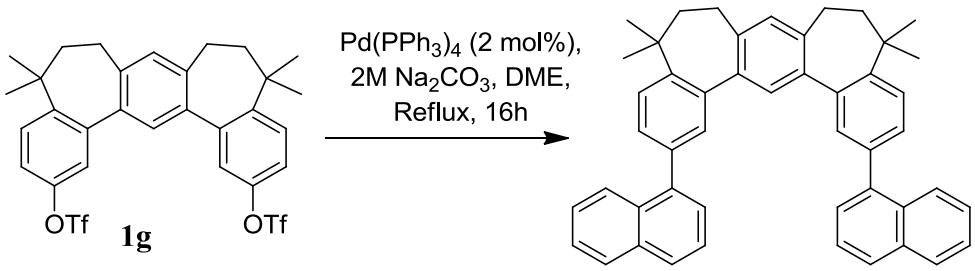

1g **T-Nap**

Ditriflate compound **1g** (0.2 g,0.30 mmol) and 1-naphthaleneboronicacid (3 equiv,0.156 g, 0.90 mmol) were dissolved in anhydrous toluene (30 mL) in an oven dried Schlenk flask under an argon atmosphere and the flask was evacuated and filled with argon (3x). In another oven dried Schlenk flask a solution of anhydrous sodium carbonate (2.5 g) in

water (10 mL) was prepared under an argon atmosphere and the flask was also evacuated and filled with argon (3x). To the dioxane solution, $Pd(PPh_3)_4$ (50 mg) and the salt solution were added sequentially under a strict argon atmosphere followed by evacuation and filling the flask with argon (3x) after each addition. The flask was covered with foil and the solution was allowed to reflux overnight. The resulting solution was cooled to room temperature, quenched with water (50 mL) and extracted with dichloromethane (3 x 20 mL). The organic layer was dried over anhydrous magnesium sulfate, evaporated and dried under vacuum. The product was further purified by column chromatography using a hexanes/ethyl mixture to give the pure product (0.1 g, 53.4 %); ^{1}H NMR ($CDCl_3$) δ : 7.95 (2H, d, *J* = 8.37 Hz), 7.85 (2H, d, *J* = 7.67 Hz), 7.809 (2H, d, *J* = 7.67 Hz), 7.55 (2H, d, *J* = 8.14 Hz), 7.51 (2H, d, *J* = 1.86 Hz), 7.47 (1H, s), 7.42 (8H, m), 7.34 (2H, d, *J* = 8.37 Hz), 7.12 (1H, s), 2.70 (4H, t, *J* = 6.51 Hz), 2.21 (4H, t, *J* = 6.51 Hz), 1.17 (12H, Broad)

Preparation of T-Dur:

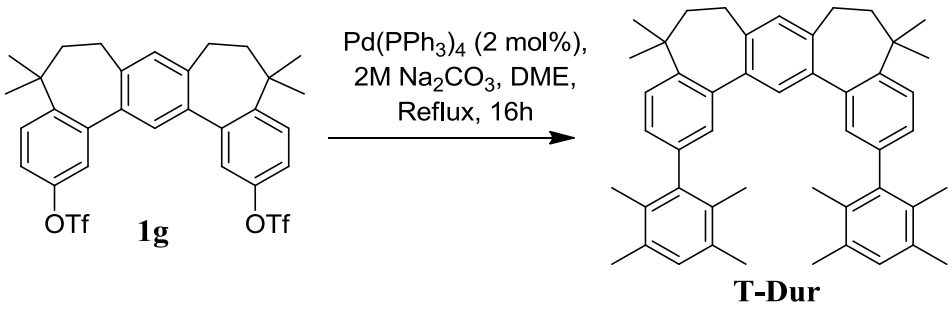

1g **T-Dur**

Ditriflate compound **1g** (0.2 g,0.30 mmol) and 1-naphthaleneboronicacid (3 equiv, 0.16 g, 0.90 mmol) were dissolved in anhydrous toluene (30 mL) in an oven dried Schlenk flask under an argon atmosphere and the flask was evacuated and filled with argon (3x).

In another oven dried Schlenk flask a solution of anhydrous sodium carbonate (2.5 g) in water (10 mL) was prepared under an argon atmosphere and the flask was also evacuated and filled with argon (3x). To the dioxane solution, $Pd(PPh_3)_4$ (50 mg) and the salt solution were added sequentially under a strict argon atmosphere followed by evacuation and filling the flask with argon (3x) after each addition. The flask was covered with foil and the solution was allowed to reflux overnight. The resulting solution was cooled to room temperature, quenched with water (50 mL) and extracted with dichloromethane (3 x 20 mL). The organic layer was dried over anhydrous magnesium sulfate, evaporated and dried under vacuum. The product was further purified by column chromatography using a hexanes/ethyl mixture to give the pure product (0.12 g, 63.2%); ^{1}H NMR ($CDCl_3$) δ : 7.48 (2H, d, *J* = 7.89 Hz), 7.28 (1H, s), 7.16 (2H, s), 7.08 (1H, s), 7.05 (2H, d, *J* = 7.89 Hz), 6.98 (2H, s), 2.66 (4H, Broad), 2.26 (12H, s), 2.19 (4H, t, *J* = 6.99 Hz), 1.93 (12H, s), 1.15 (12H, Broad). ^{13}C NMR ($CDCl_3$) δ: 1.26, 17.62, 20.44, 32.66, 37.85, 48.90, 125.49, 127.40, 128.08, 128.10, 130.58, 131.61, 132.41, 133.74, 138.79, 140.41, 140.53, 141.92, 142.00, 141.18.

Preparation of Br-HBC

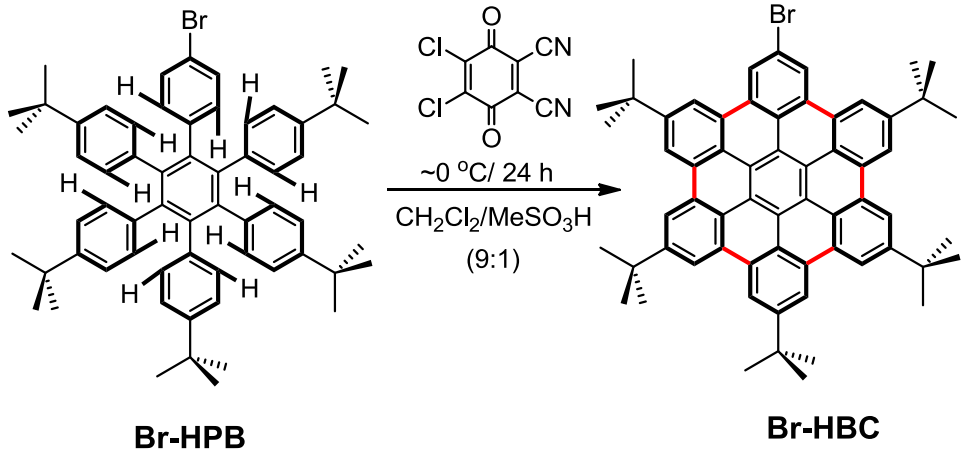

Br-HPB (0.45 g, 0.51 mmol) was dissolved in the dichloromethane (30 mL) and cooled to 0 ^{o}C. Methanesulfonic acid (3 mL) and DDQ (0.85 g, 3.62 mmol) were added to and the reaction mixture was stirred for 24 hrs. It was then quenched with water and extracted with dichloromethane (3 x 20 mL). Solvent was evaporated on the rotary evaporator and dried under vaccume. The product thus formed was passed through a short pad of silica gel to get pure Br-HBC (0.42 g, 94.8%) ^{1}H NMR ($CDCl_3$) δ: 9.18 (2H, s), 9.12 (2H, s), 9.05 (2H, s), 8.94 (2H, s), 8.69 (2H, s), 8.66 (2H, s), 1.92(9H, s), 1.88(18H, s), 1.79(18H, s).

Preparation of T-HBC

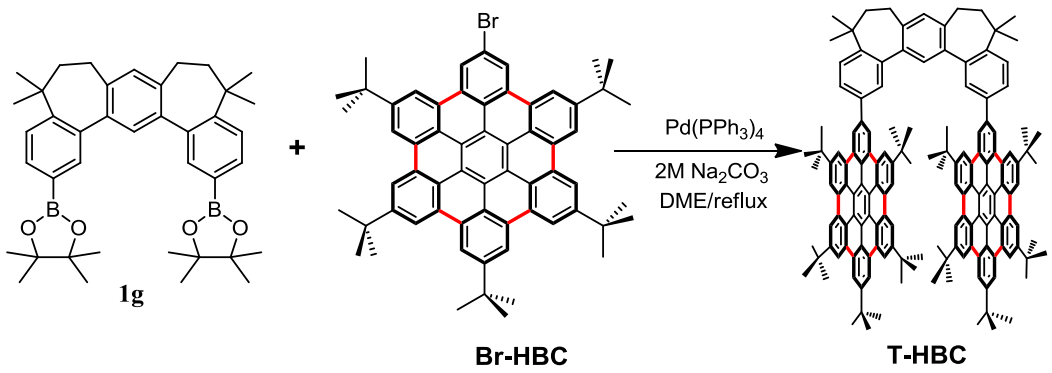

Diboronic ester **1g** (0.16 g, 0.26 mmol) and the trimethylbromopyrene (2 equiv, 0. 46 g, 52 mmol) were dissolved in anhydrous 1,2-dimethoxyethane (DME) (20 mL) in an oven dried Schlenk flask under an argon atmosphere and the flask was evacuated and filled with argon (3x). In another oven dried Schlenk flask a solution of anhydrous sodium carbonate (2.5 g) in water (10 mL) was prepared under an argon atmosphere and the flask was also evacuated and filled with argon (3x). To the DME solution, $Pd(PPh_3)_4$ (50 mg) and the salt solution were added sequentially under a strict argon atmosphere followed by evacuation and filling the flask with argon (3x) after each addition. The flask was covered with foil and the solution was allowed to reflux overnight. The resulting solution was cooled to room temperature, quenched with water (50 mL) and extracted with dichloromethane (3 x 20mL). The organic layer was dried over anhydrous magnesium sulfate, evaporated and dried under vacuum (0.3 g crude).

Preparation of dibromopyrene:

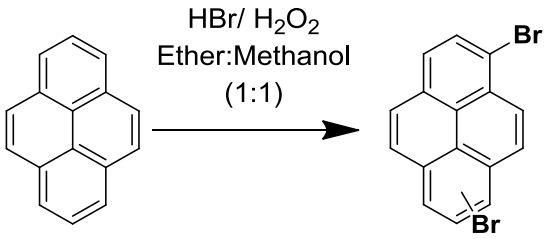

The isomeric mixture of dibromopyrenes was prepared by closely following a literature procedure[**] as detailed below. To a solution of pyrene (6.0 g, 29.7 mmol) in a mixture of ether (120 mL) and methanol (120 mL) aqueous HBr (48%, 7.4 mL) was added. To the resulting mixture, 30% aqueous solution of H_2O_2 (6.1 mL) was added dropwise over 20 min and it was allowed to stir at 22 ^oC. After 24 hrs of stirring a voluminous precipitate was formed. The precipitate was filtered and washed with hot ethanol (2 × 20 mL). Product was dried under vacuum (8.00g, 74%)

Preparation of tribromopyrene:

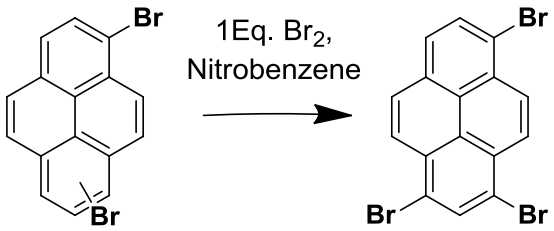

Mixture of 1, 6 and 1, 8-dibromopyrene (2 g, 5.55 mmol) was dissolved in nitrobenzene (100 mL). Br_2 solution (0.9 g, 5.55 mmol) was added to it drop wise. Mixture was stirred at room temp overnight. Product was filtered and recrystallized from hot toluene to yield tribromopyrene (2.00 g, 80%) ^1H NMR (300 MHz, $CDCl_3$, δ) 8.58 (d, J = 9.6 Hz, 1H),

8.56 (s, 1H), 8.50 (d, *J* = 9.6 Hz, 1H), 8.43 (d, *J* = 9.2 Hz, 1H), 8.31 (d, *J* = 8.2 Hz, 1H), 8.15 (d, *J* = 9.2 Hz, 1H), 8.10 (d, *J* = 8.2 Hz, 1H).

Preparation of 1,3,6-trimethylpyrene:

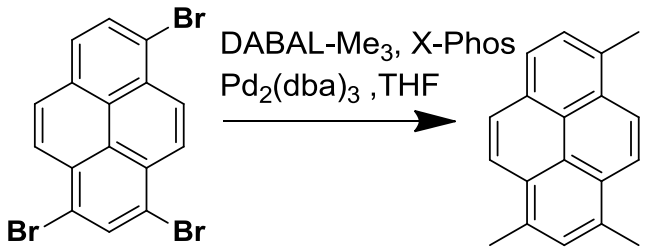

TMP

To a suspension of 1, 3, 6-tribromopyrene (500 mg, 1.13 mmol) in THF (50 mL) under Argon, was added XPhos (20 mg, 0.04 mmol), $Pd_2(dba)_3$ (20 mg, 0.02 mmol) and DABAL-Me_3 (875 mg, 3.41 mmol). The flask was covered with aluminum foil and the solution was refluxed for 6 hours. The flask was then cooled to room temperature and the contents were poured slowly upon 5 % HCl solution (50 mL). The organic layer was extracted using dichloromethane. The organic layer was dried over anhydrous $MgSO_4$ and removed *in vacuo*. Column chromatography (silica gel/hexanes) afforded 1, 3, 6-trimethylpyrene as colorless shiny solid. Yield (236 mg, 85 %). mp 174-176 °C, ^{1}H NMR (300 MHz, $CDCl_3$, δ) 8.25 (d, *J* = 9.5 Hz, 1H), 8.20 (d, *J* = 9.5 Hz, 1H) 8.14 (d, *J* = 9.2 Hz, 1H), 8.05 (d, *J* = 7.7 Hz, 1H), 7.99 (d, *J* = 9.2 Hz, 1H), 7.83 (d, *J* = 7.7 Hz, 1H), 7.73 (s, 1H), 2.98 (s, 3H), 2.95 (s, 3H), 2.94 (s, 3H); ^{13}C NMR (75 MHz, $CDCl_3$, δ) 131.86, 131.74, 131.64, 130.21, 130.05, 129.44, 128.16, 127.86, 127.76, 126.46, 125.44, 125.35, 124.48, 123.62, 122.92, 122.52, 20.13, 20.01, 19.87.

Preparation of 1-bromo-3,6,8-trimethylpyrene:

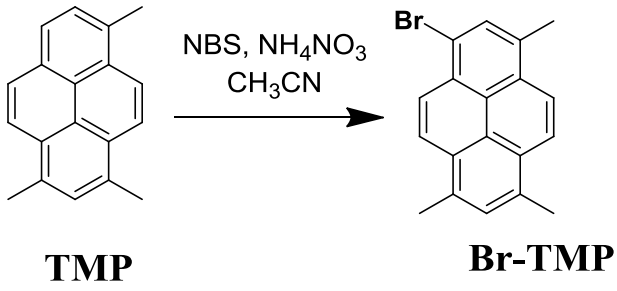

To a solution of 1,3,6-trimethylpyrene (1.0g, 4.09 mmol) in acetonitrile (250 mL) was added *N*-bromosuccinimide (0.72 g, 4.09 mmol) and NH_4NO_3 (32 mg, 0.40 mmol). The mixture was stirred overnight at room temperature and thereafter filtered and washed with water (10 mL × 3) and methanol (10 mL × 2) to yield the crude product which was used as such in the next step. Yield (1.17g, 88 %). mp <400 °C, ^{1}H NMR (300 MHz, $CDCl_3$, δ) 8.36 (d, *J* = 9.5 Hz, 1H), 8.25 (m, 3H), 8.15 (d, *J* = 9.5 Hz, 1H), 8.11 (s, 1H), 7.77 (s, 1H), 2.95 (s, 6H), 2.94 (s, 3H); ^{13}C NMR (75 MHz, $CDCl_3$, δ) 132.80, 132.62, 132.53, 131.84, 130.92, 129.13, 128.45, 128.05, 127.96, 126.65, 124.95, 124.56, 123.97, 122.66, 122.38, 119.40, 20.05, 20.03, 19.88.

Preparation of 2e:

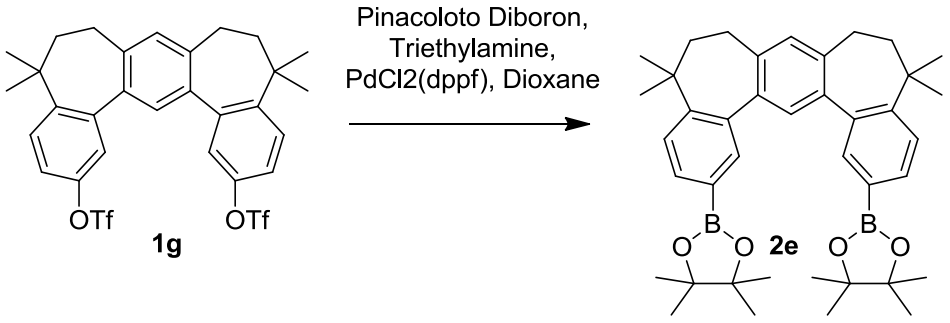

To a Schlenk flask under argon atmosphere, a mixture of triflate **1g** (2.0 g, 3.01 mmol) and $PdCl_2$ (100 mg) were added to a solution of dioxane (60 mL) and trimethylamine (1.34 mL, 9.05 mmol). The mixture was stirred and then Bis(Pinacoloto)Diboron (2.3 g, 9.05 mmol) was added. The reaction mixture was heated to reflux overnight, which gives monoboronic ester and subjected again to the same procedure to get diboronic ester **2e** (1.3 g, 72.2%) ^{1}H NMR ($CDCl_3$) δ : 7.85 (2H, S,), 7.77 (2H, dd, *J* = 7.81 Hz, 1.45 Hz), 7.51 (1H, S,), 7.49 (2h, d, *J* = 3.60 Hz), 7.00 (1H, S,), 2.55 (4h, t, *J* = 6.30 Hz), 2.12 (4H, t, *J* = 6.79 Hz), 1.33 (24H, S,), 1.12 (12H, Broad)

Preparation of T-TMP:

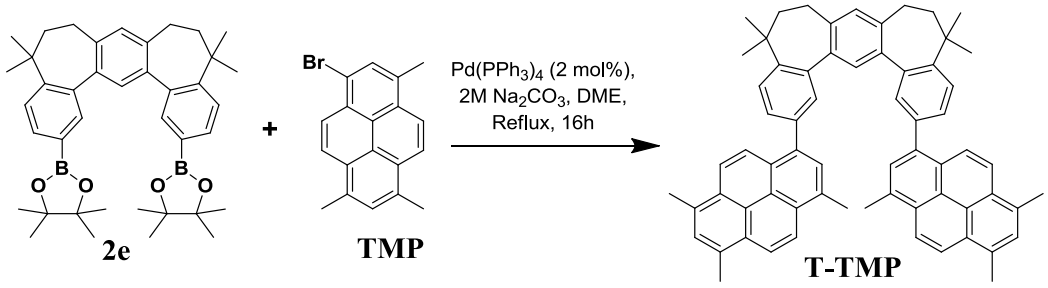

Diboronic ester **2e** (0.3 g, 0.48 mmol) and the bromo-trimethylbromopyrene **Br-TMP** (3 equiv, 0. 5 g, 1.55 mmol) were dissolved in anhydrous 1,2-dimethoxyethane (DME) (40 mL) in an oven dried Schlenk flask under an argon atmosphere and the flask was evacuated and filled with argon (3x). In another oven dried Schlenk flask a solution of anhydrous sodium carbonate (2.5 g) in water (10 mL) was prepared under an argon atmosphere and the flask was also evacuated and filled with argon (3x). To the DME solution, $Pd(PPh_3)_4$ (50 mg) and the salt solution were added sequentially under a strict argon atmosphere followed by evacuation and filling the flask with argon (3x) after each addition. The flask was covered with foil and the solution was allowed to reflux

overnight. The resulting solution was cooled to room temperature, quenched with water (50 mL) and extracted with dichloromethane (3 x 20mL). The organic layer was dried over anhydrous magnesium sulfate, evaporated and dried under vacuum. Purified by column chromatography using a hexanes/ethyl mixture to give the pure product (0.8 g, 80%); m.p. above 400 ^{o}C ^{1}H NMR ($CDCl_3$) δ : 8.12 (6H, m), 7.97 (2H, d, *J* = 9.78 Hz), 7.80 (2H, s), 7.64 (4H, d, *J* = 2.07 Hz), 7.59 (2H, d, *J* = 8.023 Hz), 7.50 (3H, d, *J* = 7.95 Hz), 7.16 (1H, s), 2.89 (6H, s), 2.87 (6H, s), 2.79 (6H, s), 2.75 (4H, Broad), 2.24 (4H, t, *J* = 6.51 Hz), 1.20 (12h, Broad) ^{13}C NMR (75 MHz, $CDCl_3$, δ) 19.90, 19.97, 20.06, 31.17, 32.60, 37.96, 48.98, 122.40, 122.82, 123.41, 124.39, 125.49, 125.61, 127.40, 127.60, 127.94, 127.99, 128.20, 128.82, 129.41, 129.74, 130.22, 131.30, 131.42, 131.52, 132.48, 136.78, 139.08, 139.75, 140.70, 141.82, 145.01.

^{1}H NMR spectrum of 1b

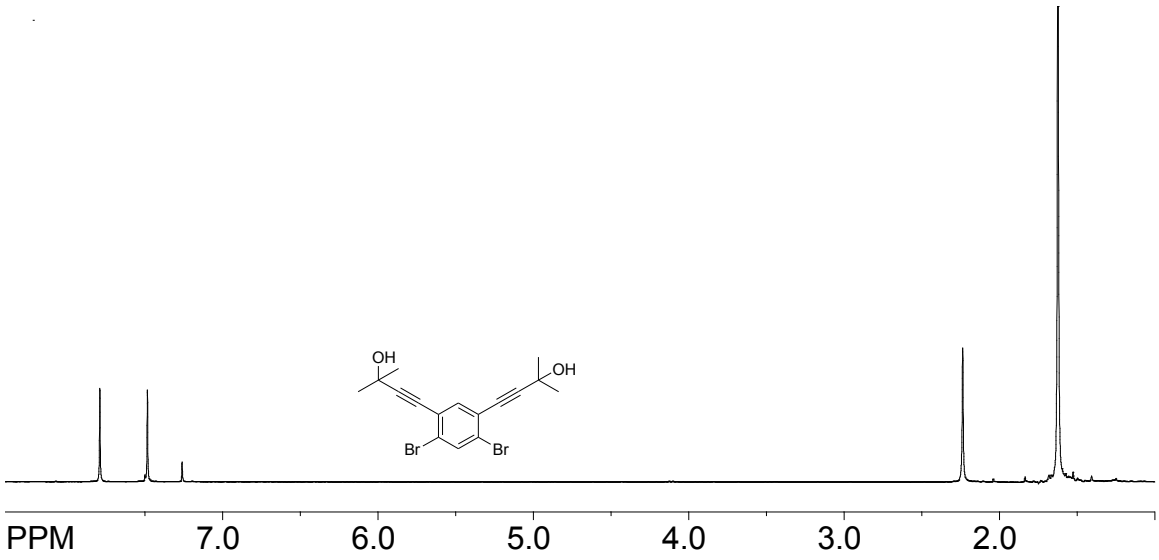

^{13}C NMR spectrum of 1b

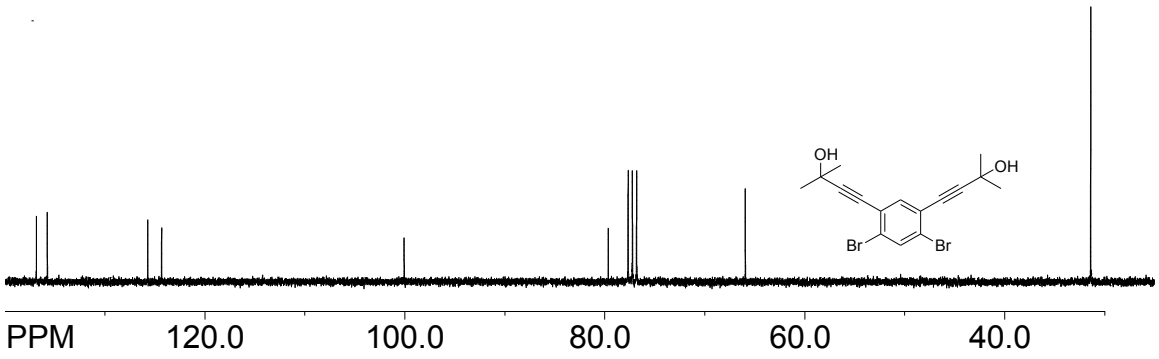

^{1}H NMR spectrum of 1c

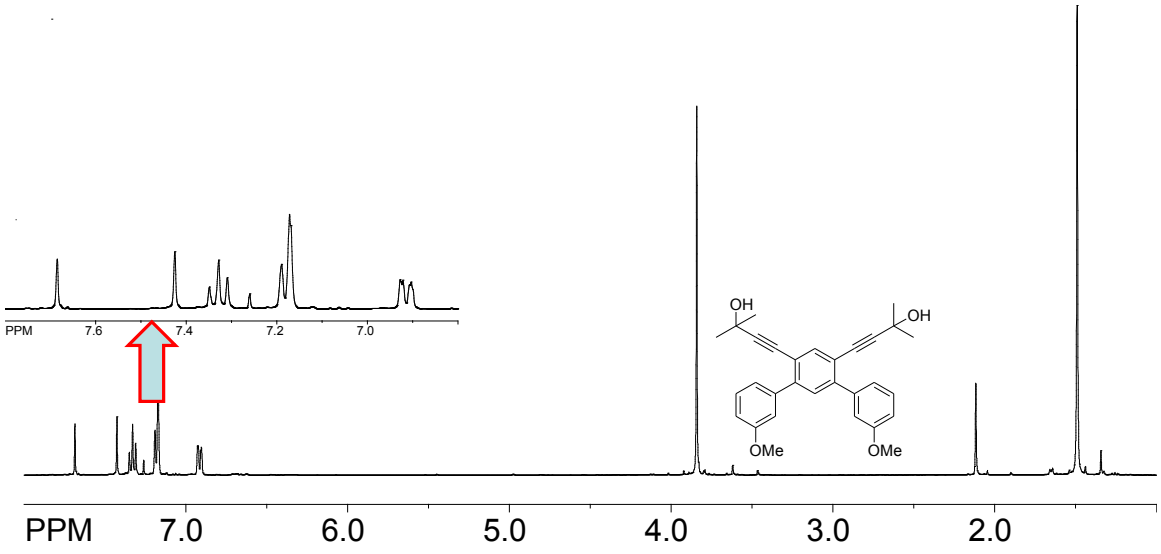

^{13}C NMR spectrum of 1c

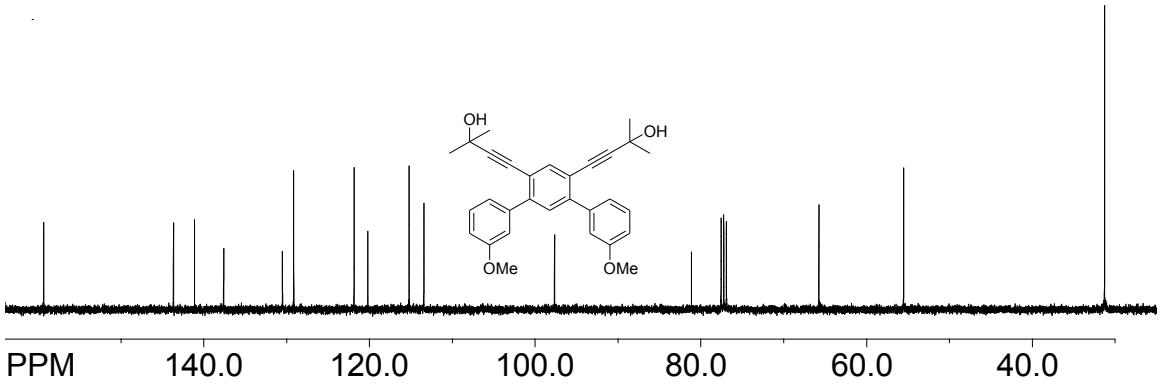

^{1}H NMR spectrum of 1d

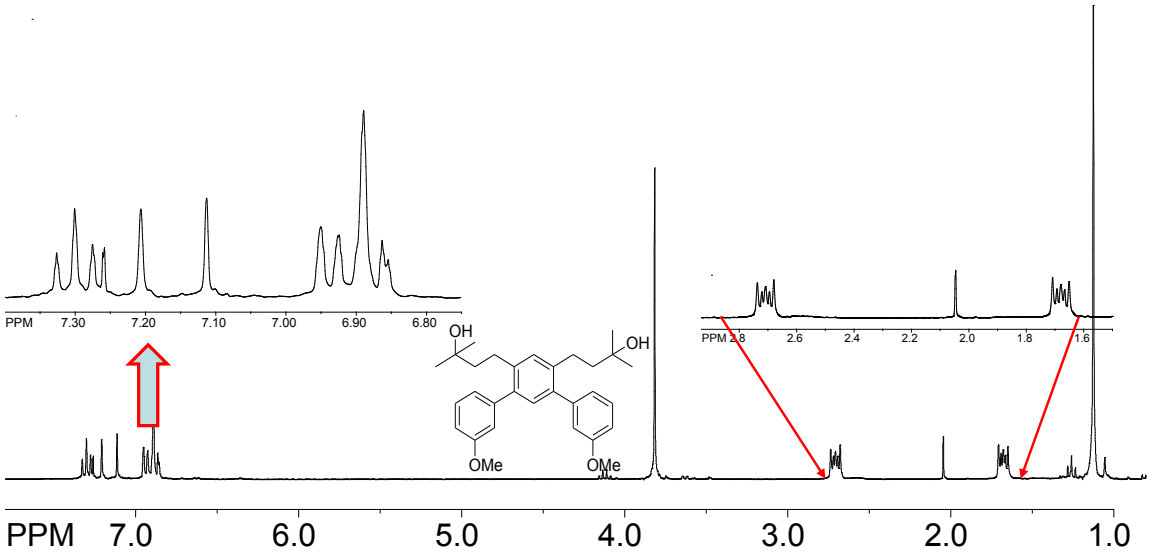

^{1}H NMR spectrum of 1e

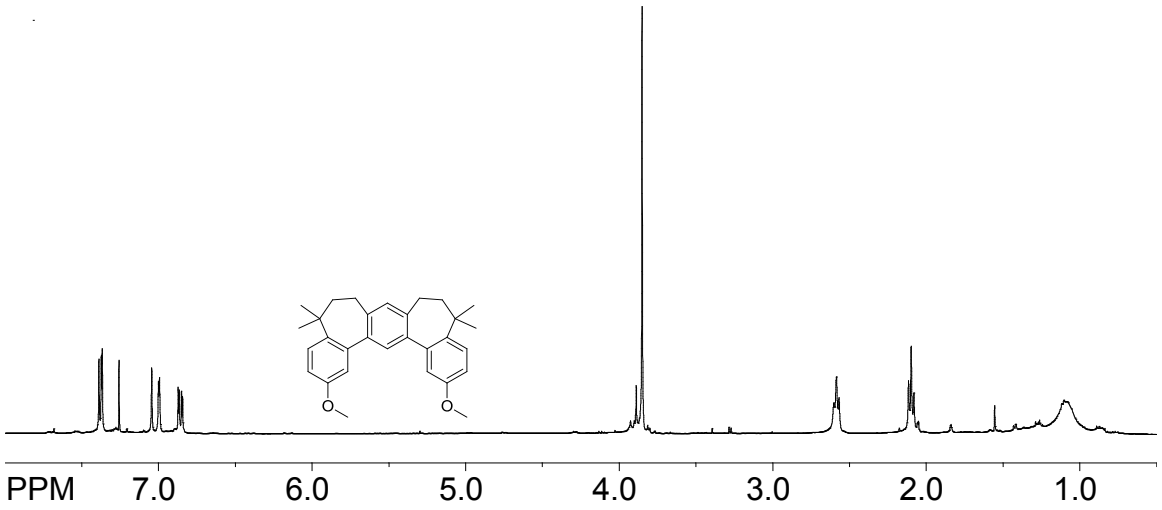

^{13}C NMR spectrum of 1e

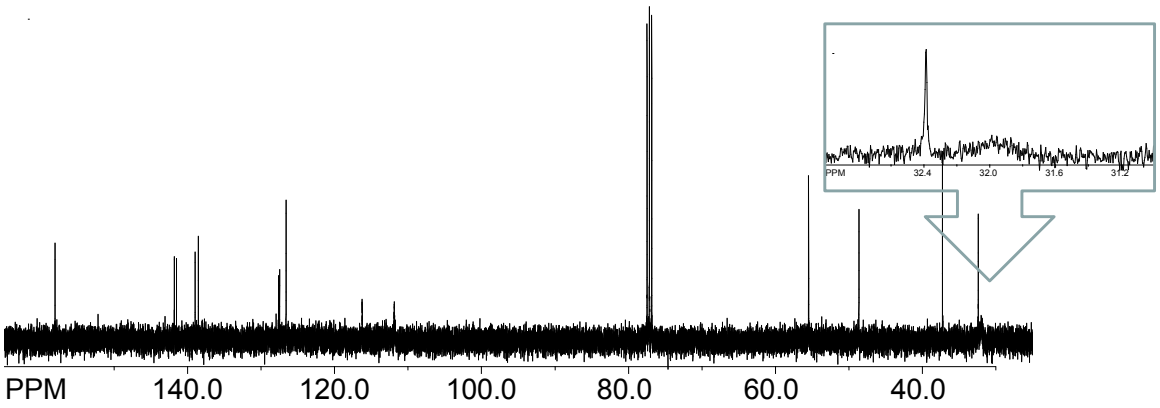

^{1}H NMR spectrum of 1f

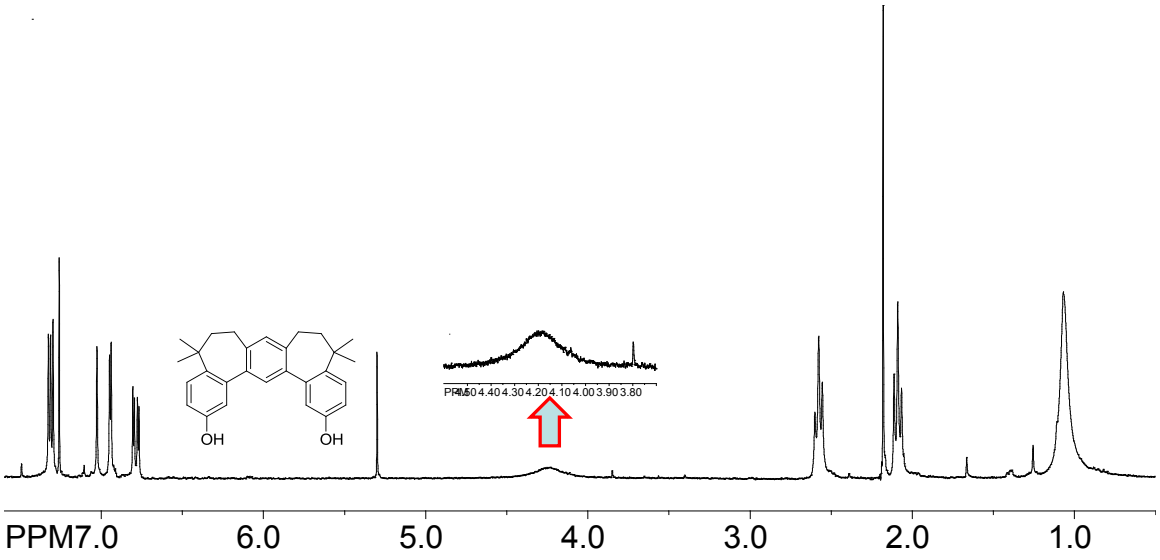

^{1}H NMR spectrum of 1g

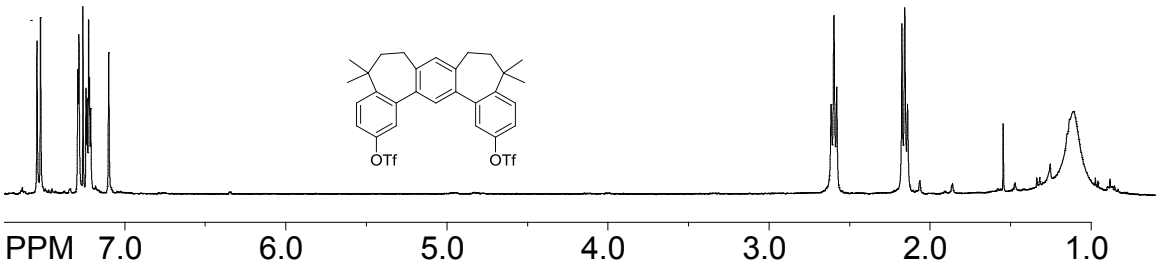

^{13}C NMR spectrum of 1g

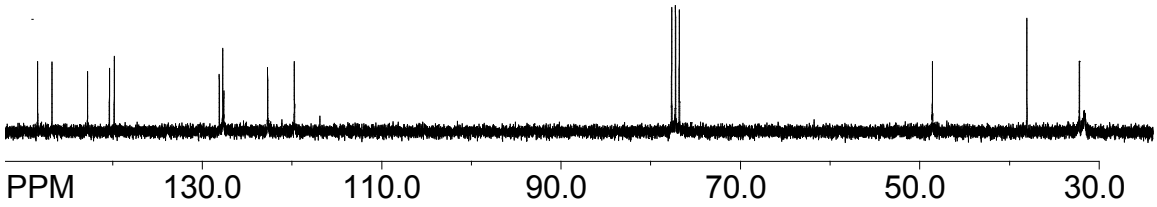

^{1}H NMR spectrum of T-Py

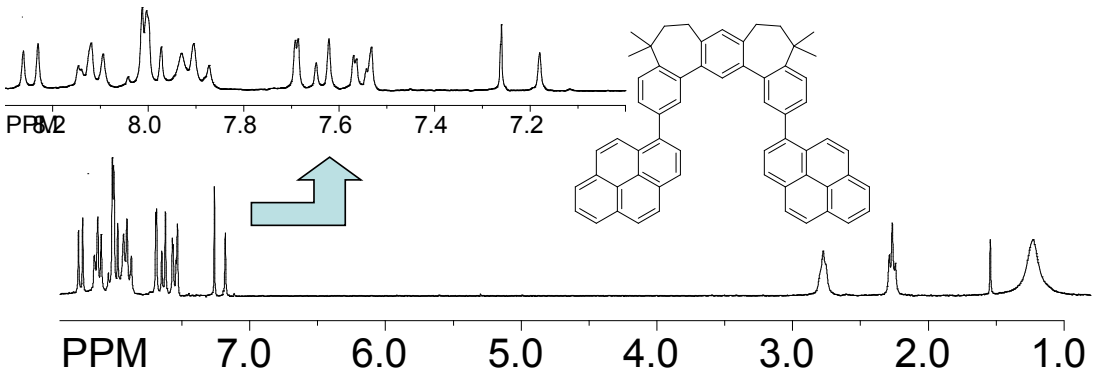

^{13}C NMR spectrum of T-Py

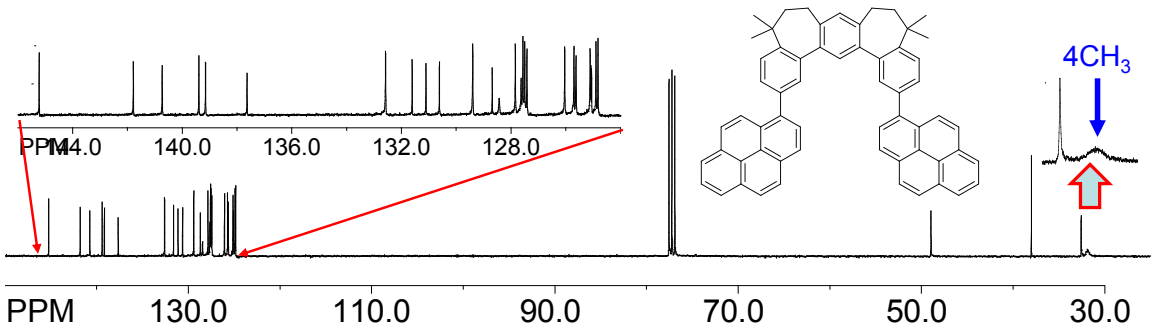

^{1}H NMR spectrum of T-Nap

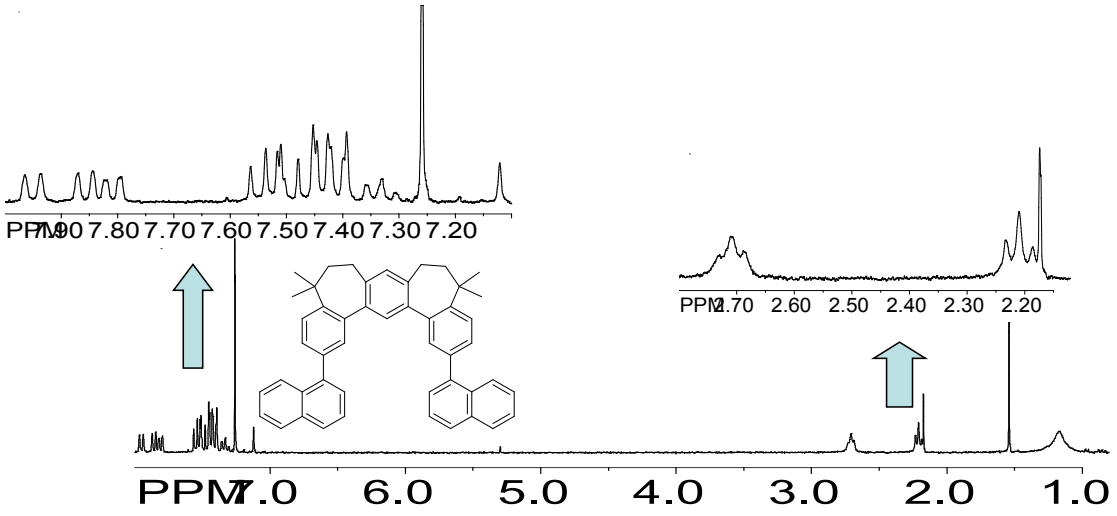

^{13}C NMR spectrum of T-Nap

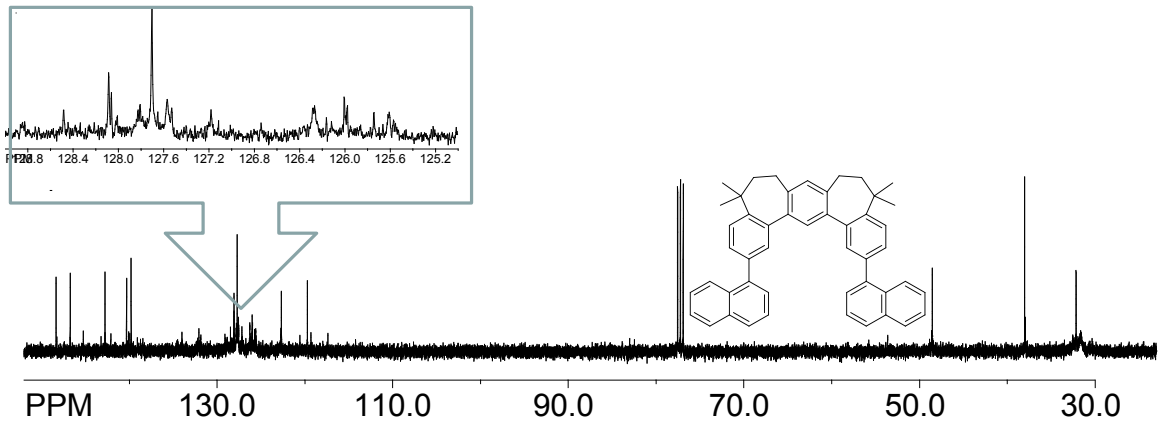

^{1}H NMR spectrum of T-Dur

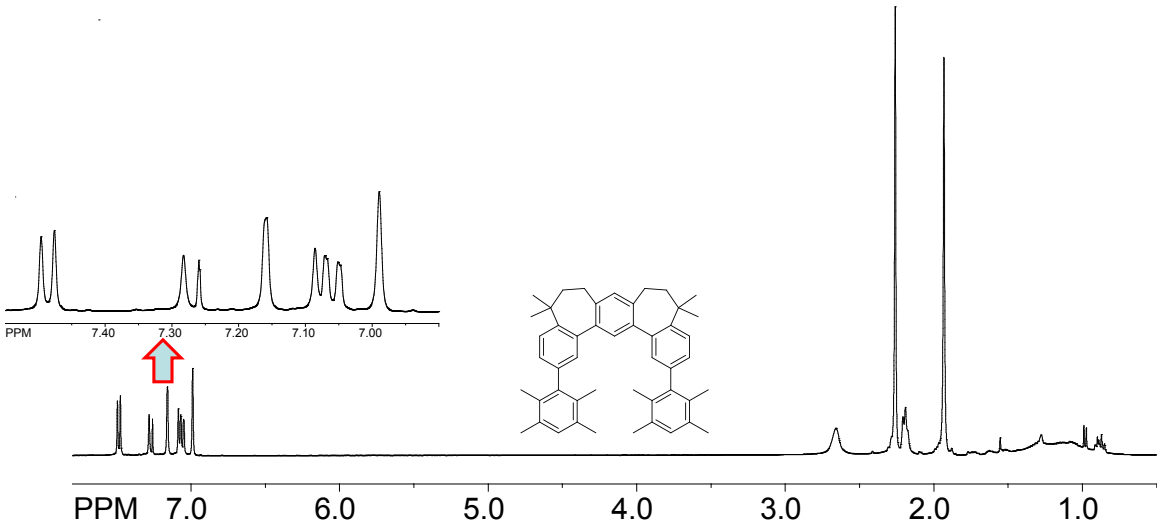

^{13}C NMR spectrum of T-Nap

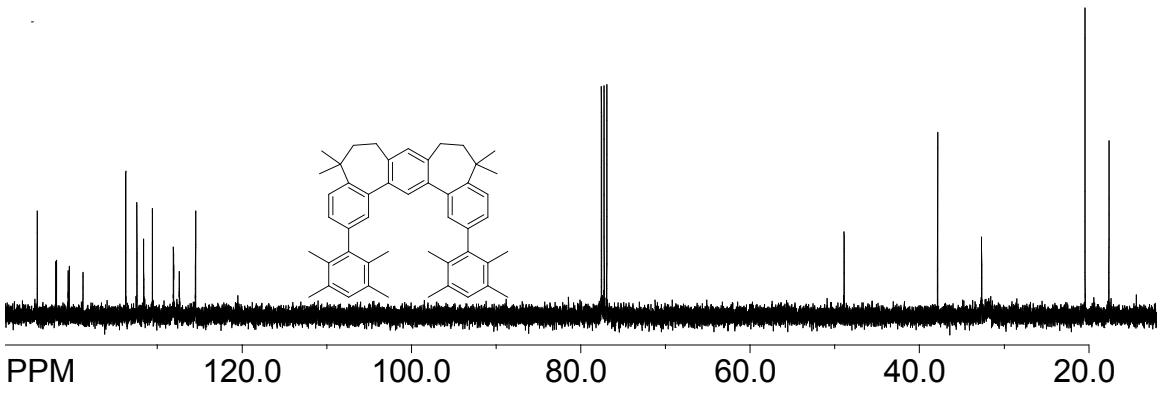

^{1}H NMR spectrum of Br-HBC

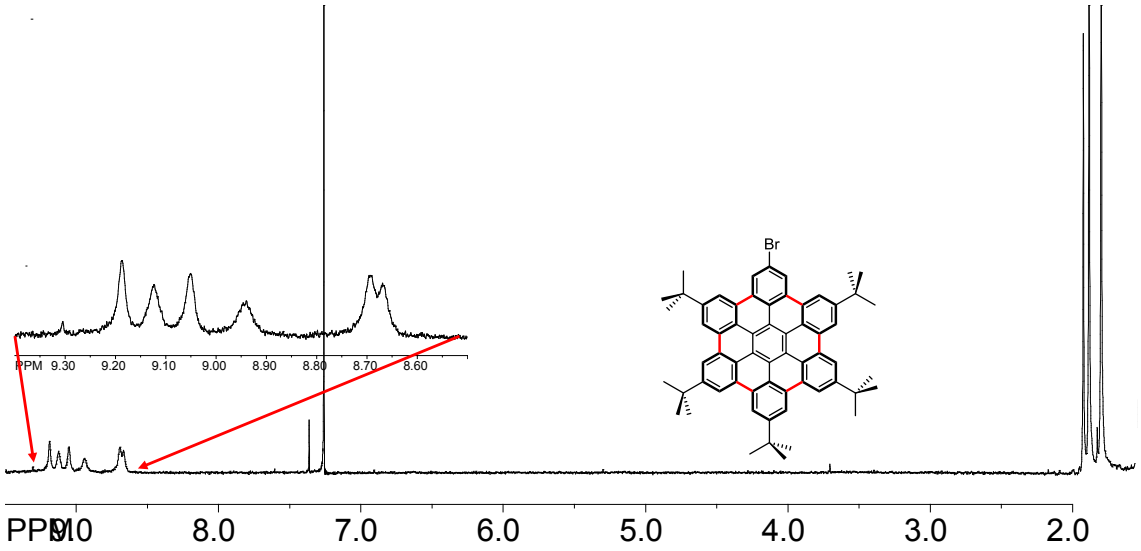

^{1}H NMR spectrum of tribromopyrene

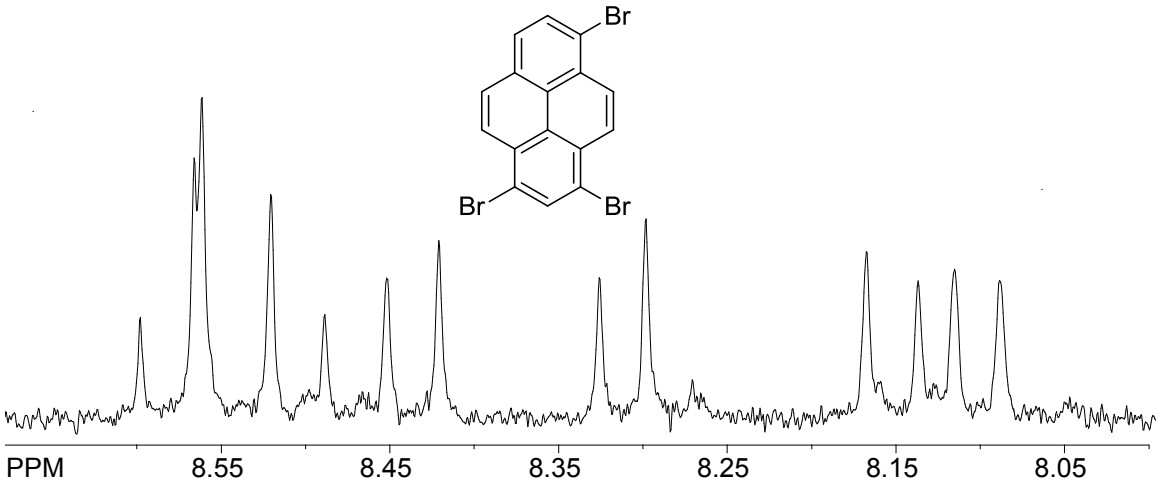

^{1}H NMR spectrum of TMP

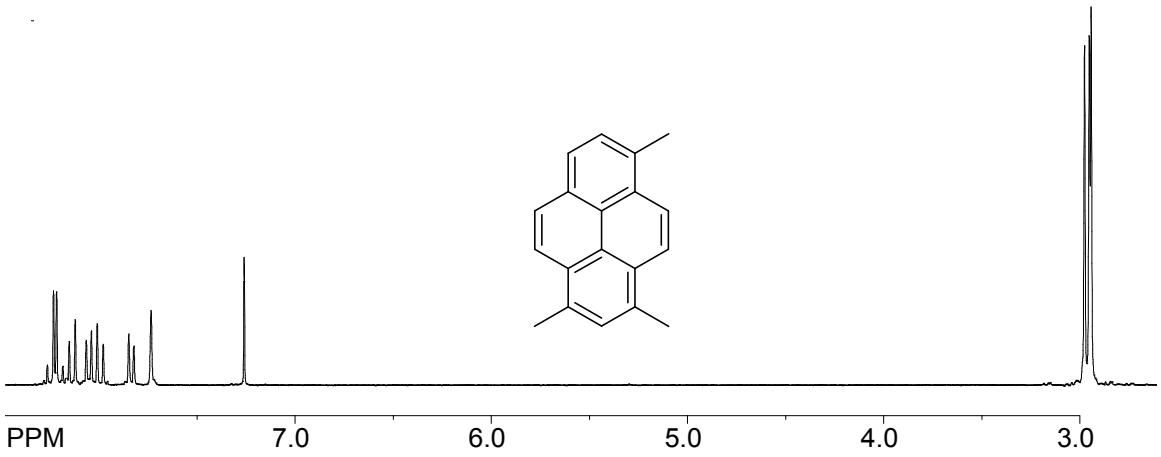

^{13}C NMR spectrum of TMP

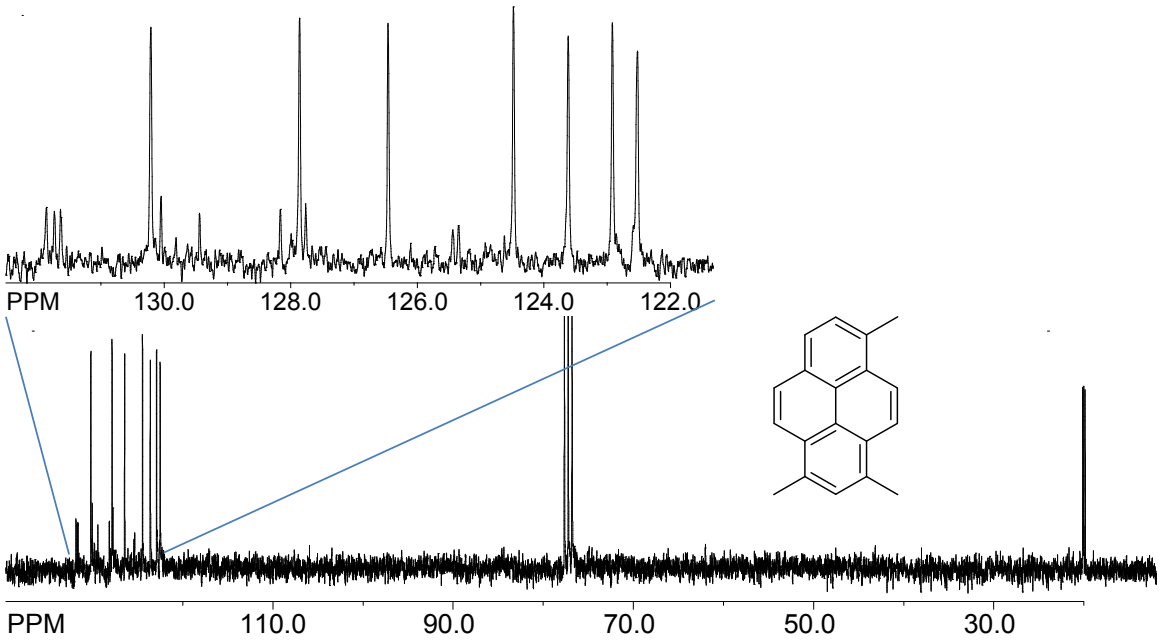

^{1}H NMR spectrum of Br-TMP

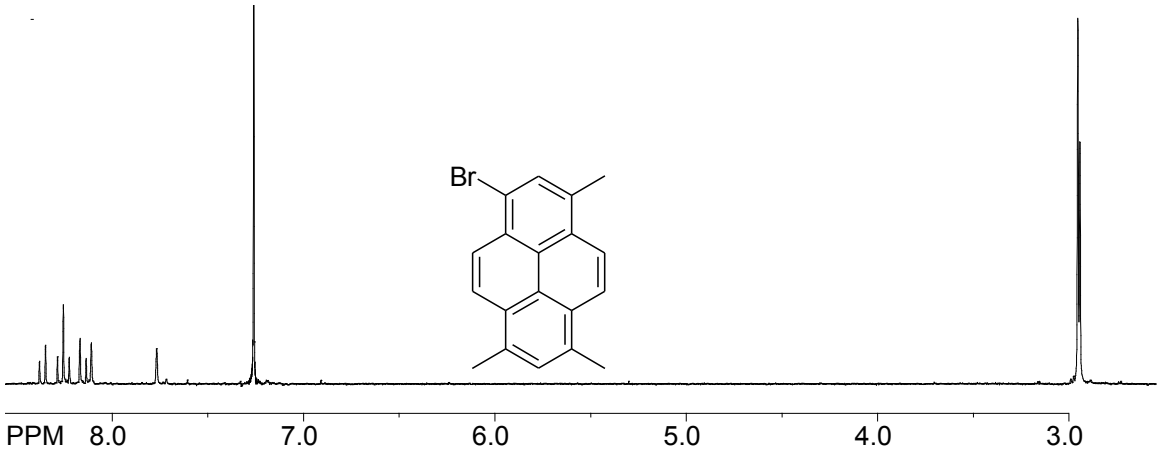

^{13}C NMR spectrum of Br-TMP

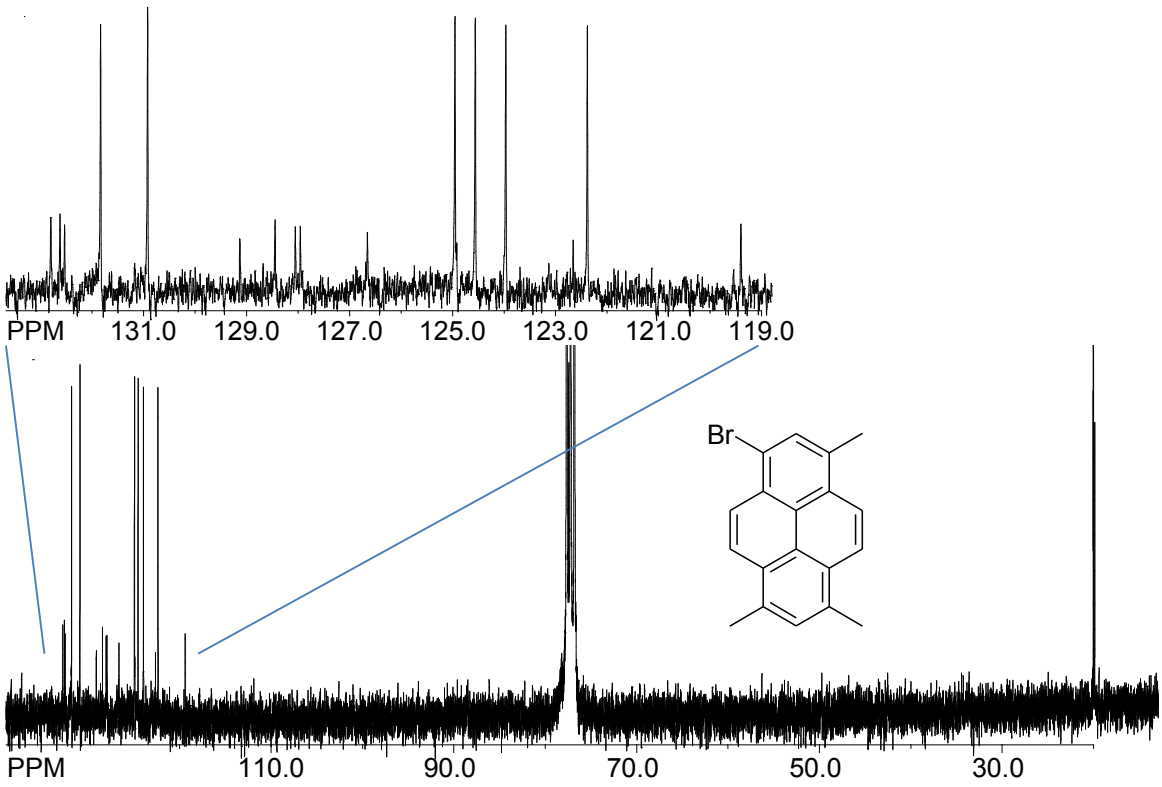

^{1}H NMR spectrum of T-TMP

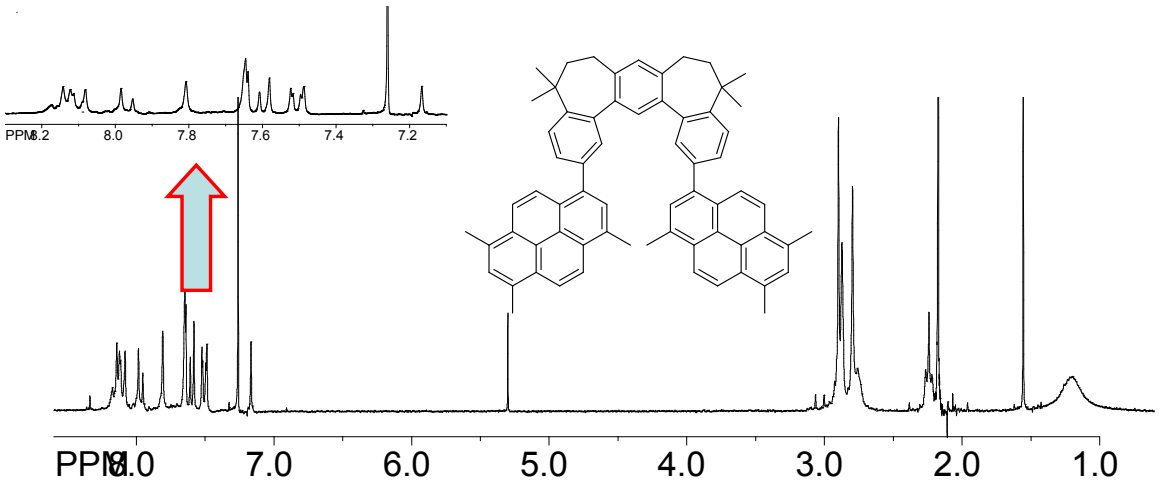

^{13}C NMR spectrum of T-TMP

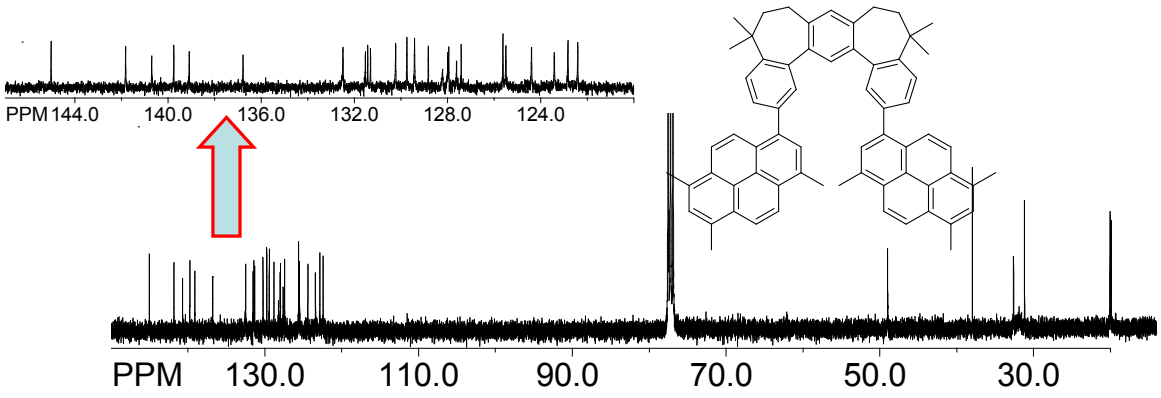

Crystal data and structure refinement for raj15l

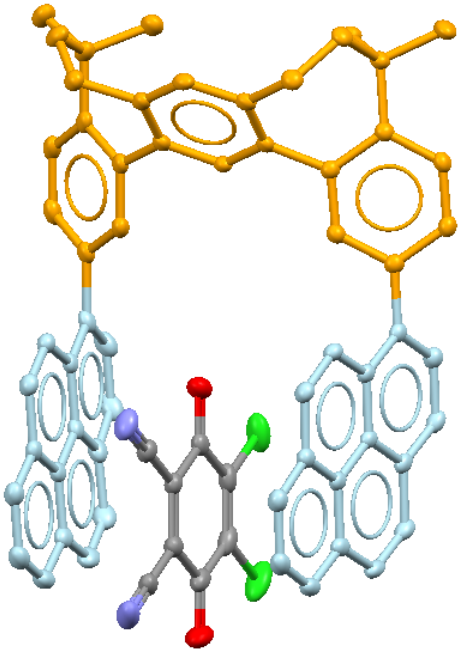

Identification code	raj15l	
Empirical formula	C69 H48 Cl4 N2 O2	
Formula weight	1078.89	
Temperature	100(2) K	
Wavelength	1.54178 Å	
Crystal system	Triclinic	
Space group	P -1	
Unit cell dimensions	a = 13.1071(4) Å	α= 111.1770(10)°.
	b = 13.8434(4) Å	β= 93.5480(10)°.
	c = 16.9161(5) Å	γ = 110.5820(10)°.
Volume	2615.93(13) $Å^3$	
Z	2	
Density (calculated)	1.370 Mg/m^3	
Absorption coefficient	2.458 mm^{-1}	
F(000)	1120	
Crystal size	0.42 x 0.38 x 0.35 mm^3	
Theta range for data collection	2.87 to 67.52°.	
Index ranges	-15<=h<=15, -16<=k<=15, 0<=l<=19	

Reflections collected	20885
Independent reflections	8793 [R(int) = 0.0184]
Completeness to theta = 67.52°	98.0 %
Absorption correction	Semi-empirical from equivalents
Max. and min. transmission	0.4800 and 0.4250
Refinement method	Full-matrix least-squares on F^2
Data / restraints / parameters	8793 / 0 / 699
Goodness-of-fit on F^2	1.023
Final R indices [I>2sigma(I)]	R1 = 0.0482, wR2 = 0.1331
R indices (all data)	R1 = 0.0513, wR2 = 0.1362
Extinction coefficient	0.00026(8)
Largest diff. peak and hole	0.663 and -0.792 e.$Å^{-3}$

Charge transfer studies of various tweezers with different guests.

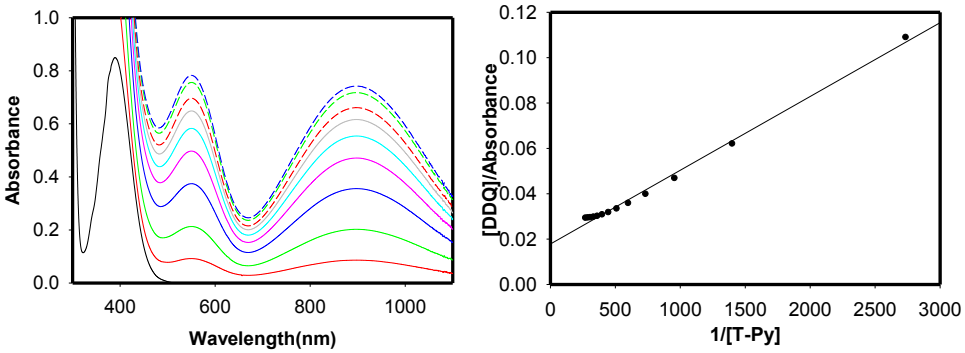

Figure 2.S.1 Spectral changes attendant upon the incremental addition of tweezer **T-Py** to DDQ in DCM (left) and Benesi-Hildebrand plot (right).

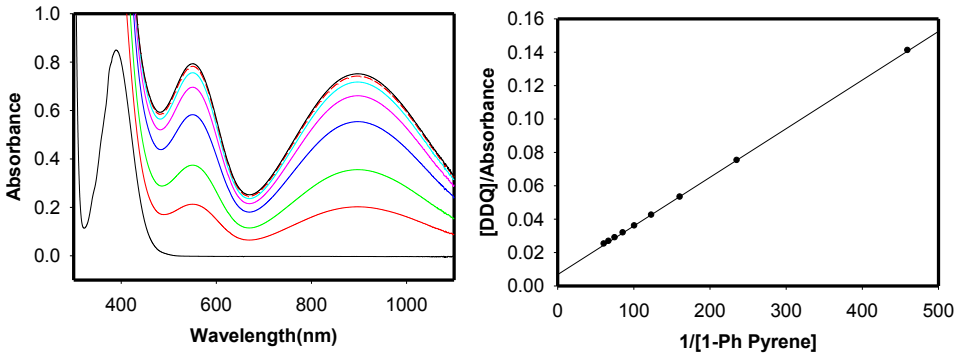

Figure 2.S.2 Spectral changes attendant upon the incremental addition of tweezer **1-Phpy** to DDQ in DCM (left) and Benesi-Hildebrand plot (right).

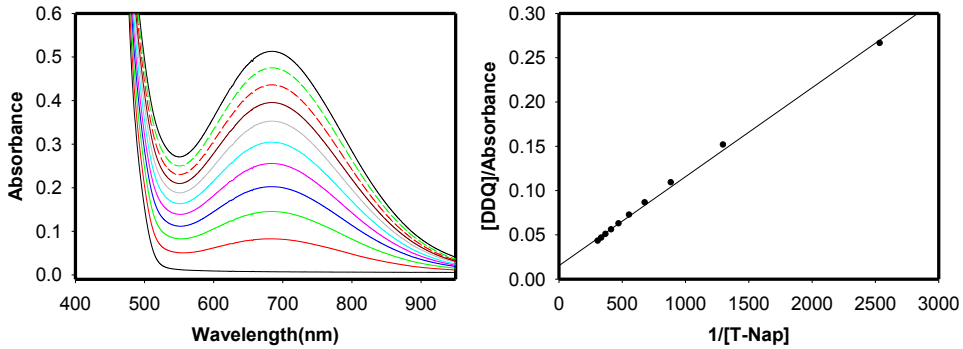

Figure 2.S.3 Spectral changes attendant upon the incremental addition of tweezer **T-Nap** to DDQ in DCM (left) and Benesi-Hildebrand plot (right).

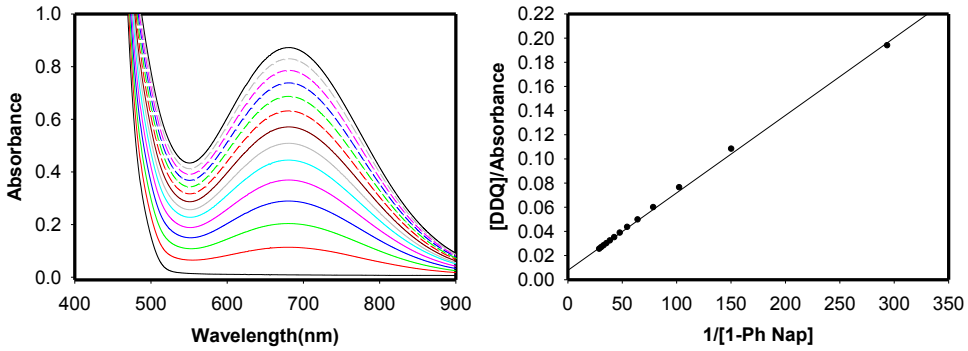

Figure 2.S.4 Spectral changes attendant upon the incremental addition of tweezer **1-PhNap** to DDQ in DCM (left) and Benesi-Hildebrand plot (right).

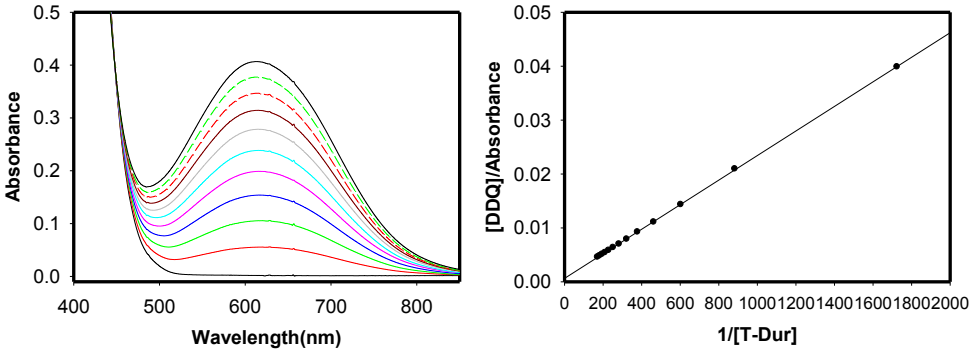

Figure 2.S.5 Spectral changes attendant upon the incremental addition of tweezer **T-Dur** to DDQ in DCM (left) and Benesi-Hildebrand plot (right).

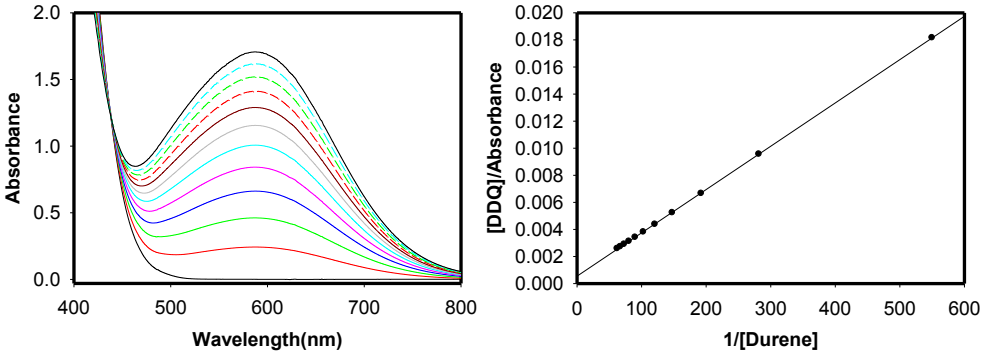

Figure 2.S.6 Spectral changes attendant upon the incremental addition of tweezer **Durene** to DDQ in DCM (left) and Benesi-Hildebrand plot (right).

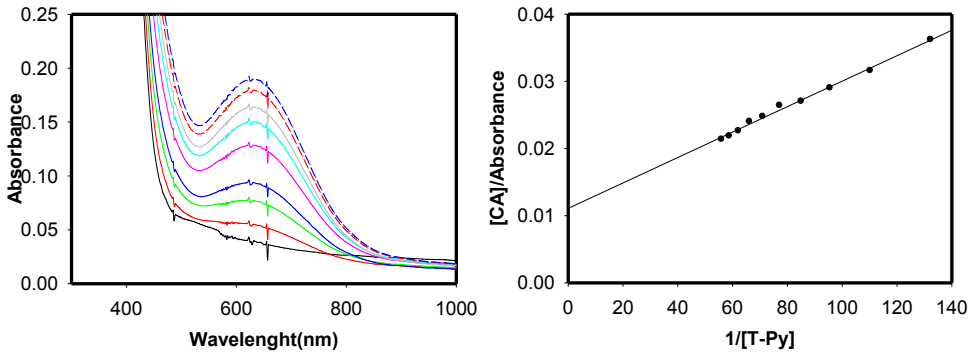

Figure 2.S.7 Spectral changes attendant upon the incremental addition of tweezer **T-Py** to CA in DCM (left) and Benesi-Hildebrand plot (right).

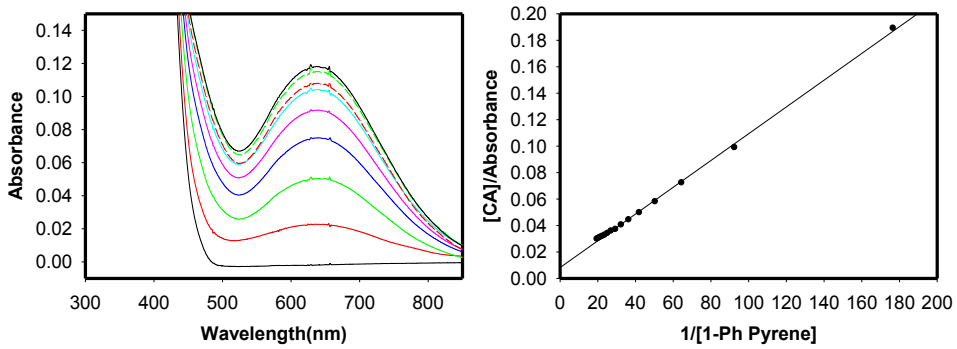

Figure 2.S.8 Spectral changes attendant upon the incremental addition of tweezer **1-Phpy** to CA in DCM (left) and Benesi-Hildebrand plot (right).

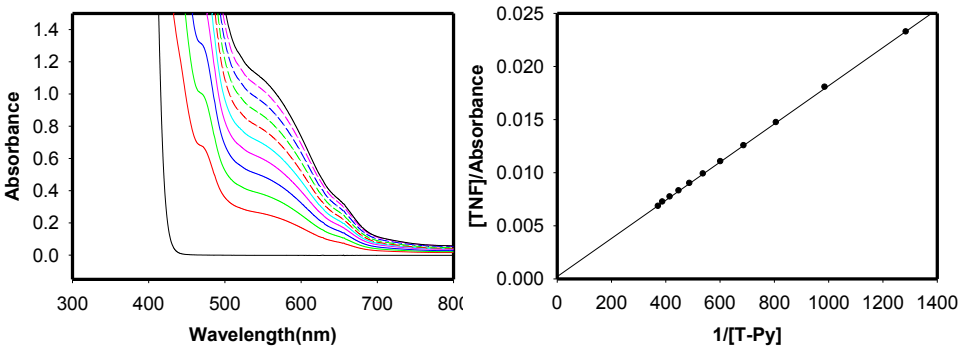

Figure 2.S.9 Spectral changes attendant upon the incremental addition of tweezer **T-Py** to TNF in DCM (left) and Benesi-Hildebrand plot (right).

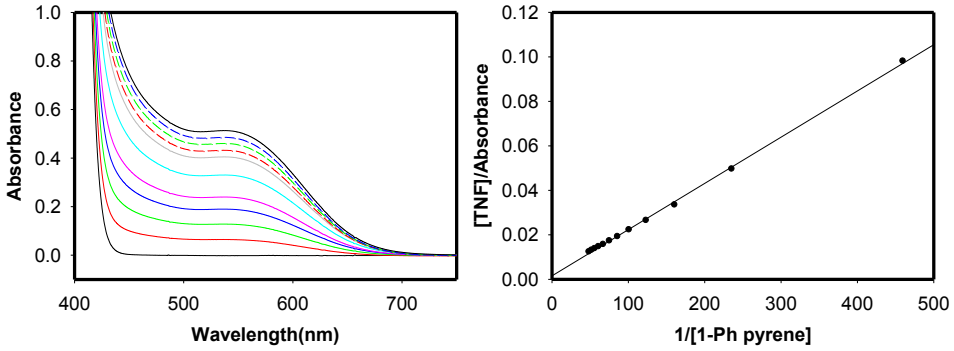

Figure 2.S.10 Spectral changes attendant upon the incremental addition of tweezer **1-Phpy** to TNF in DCM (left) and Benesi-Hildebrand plot (right).

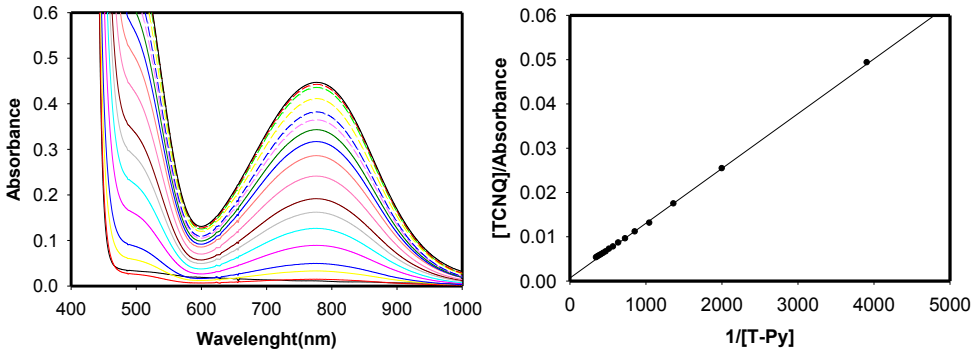

Figure 2.S.11 Spectral changes attendant upon the incremental addition of tweezer **T-Py** to TCNQ in DCM (left) and Benesi-Hildebrand plot (right).

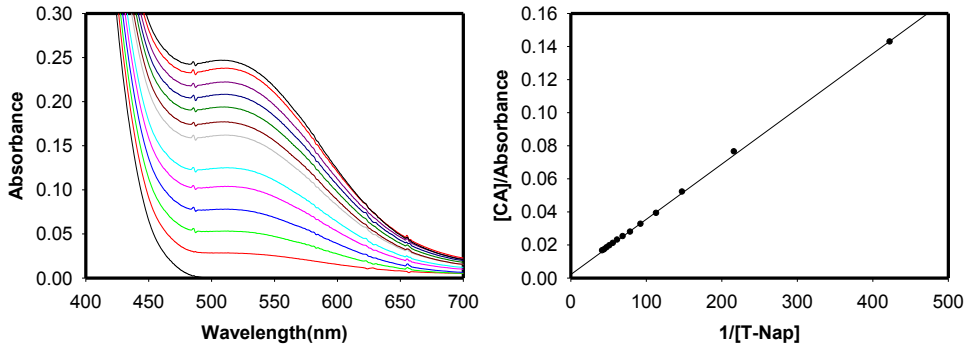

Figure 2.S.12 Spectral changes attendant upon the incremental addition of tweezer **T-Nap** to CA in DCM (left) and Benesi-Hildebrand plot (right).

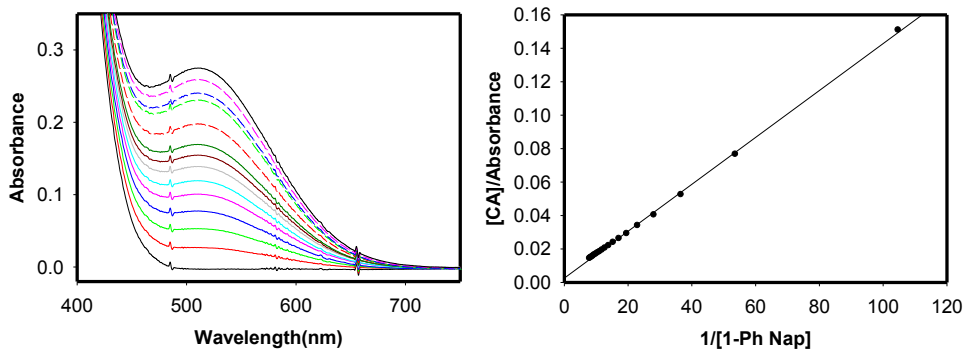

Figure 2.S.13 Spectral changes attendant upon the incremental addition of tweezer **1-PhNap** to CA in DCM (left) and Benesi-Hildebrand plot (right).

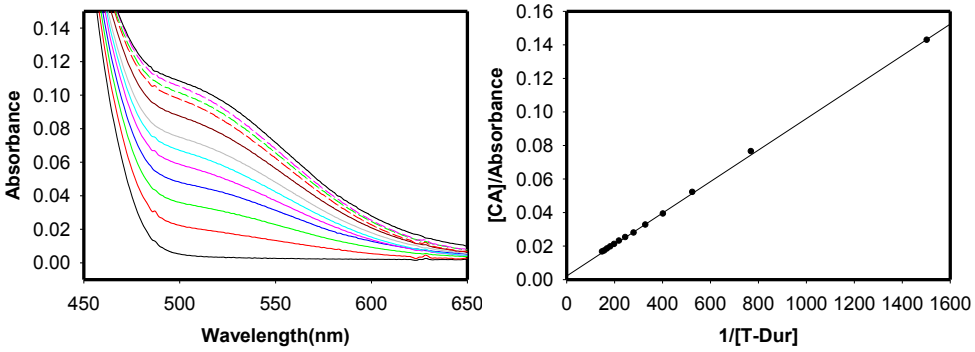

Figure 2.S.14 Spectral changes attendant upon the incremental addition of tweezer **T-Dur** to CA in DCM (left) and Benesi-Hildebrand plot (right).

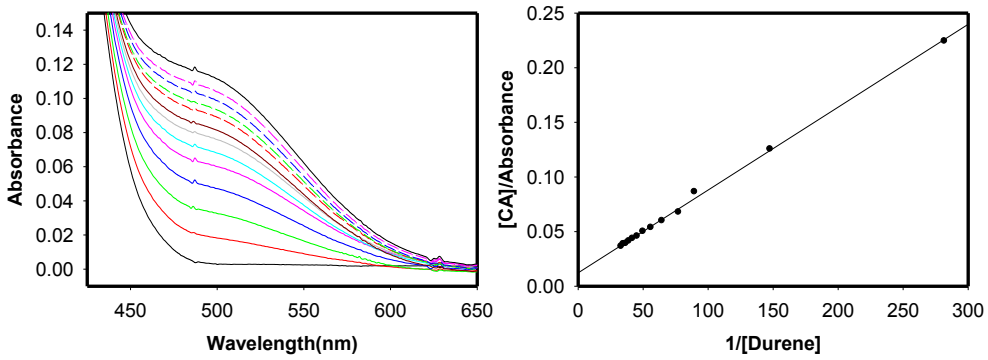

Figure 2.S.15 Spectral changes attendant upon the incremental addition of tweezer **Durene** to CA in DCM (left) and Benesi-Hildebrand plot (right).

The preparation of gear-like TP- tweezers with triptycene and 9-phenyltriptycene as pincers

Many gear like molecules have been popularized by Kelly and coworkers.[27] These authors have also demonstrated that riptycene-based molecules hold potential for the construction of chemically-powered molecular motors.[28]

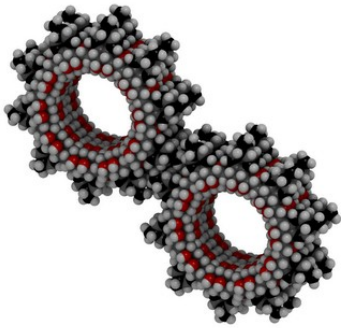

Herein, our initial effort towards preparation of gear-like molecules includes the synthesis of two TP- tweezers with triptycene and 9-phenyltriptycene as pincers, i.e. Figure 1.S16.

Figure 2.S.16 Showing the shape-similarity of a TP-tweezer with triptycene as pincers with a cake mixer.

The completed syntheses of TP-tweezers with triptycene and 9-phenyltriptycene as pincers are detailed in Scheme 1.9 and 1.10 below.

Scheme1.S.1 Synthesis of a TP-tweezer with triptycene as pincers.

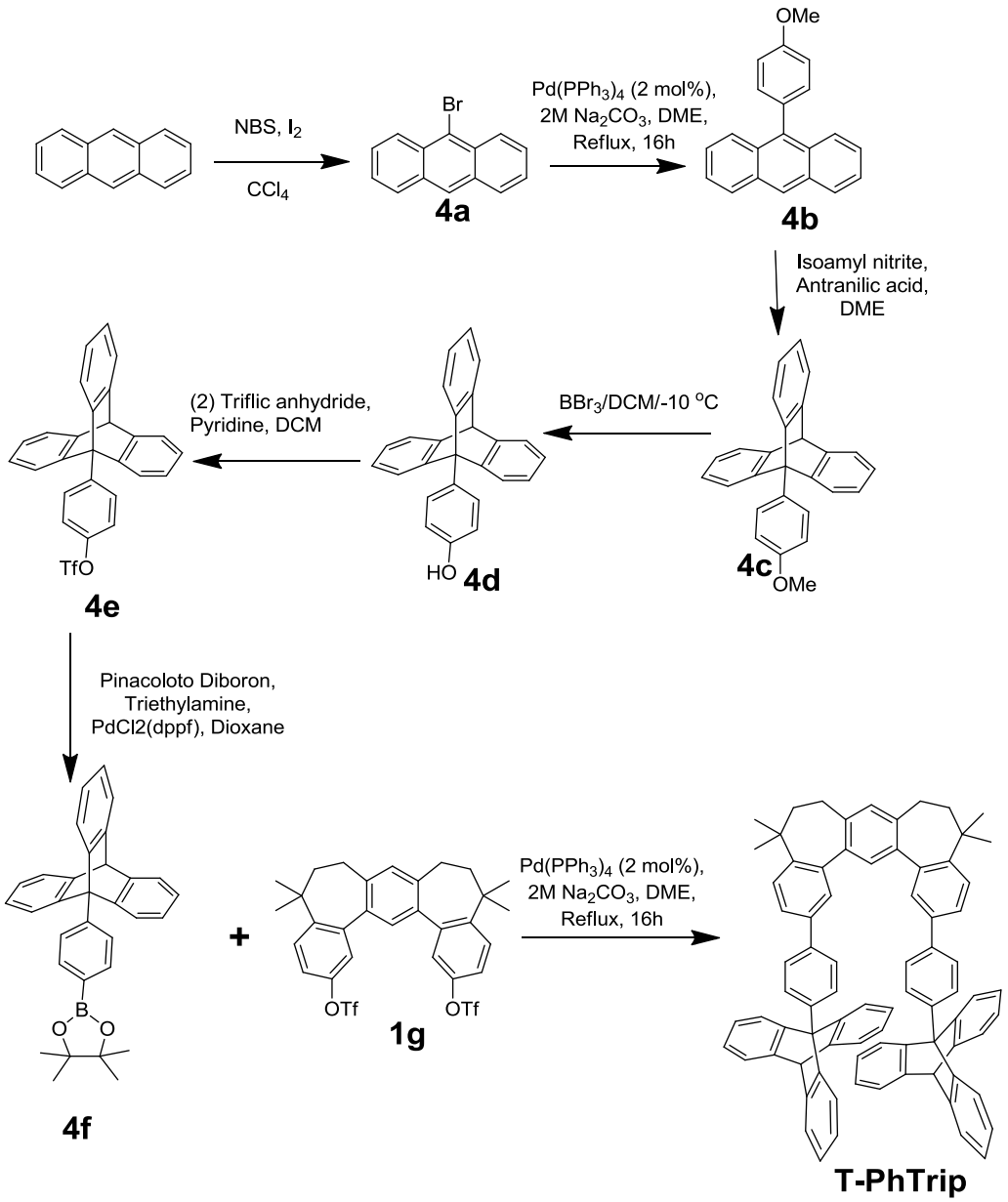

Scheme1.S.2 Synthesis of a TP-tweezer with 9-phenyltriptycene as pincers.

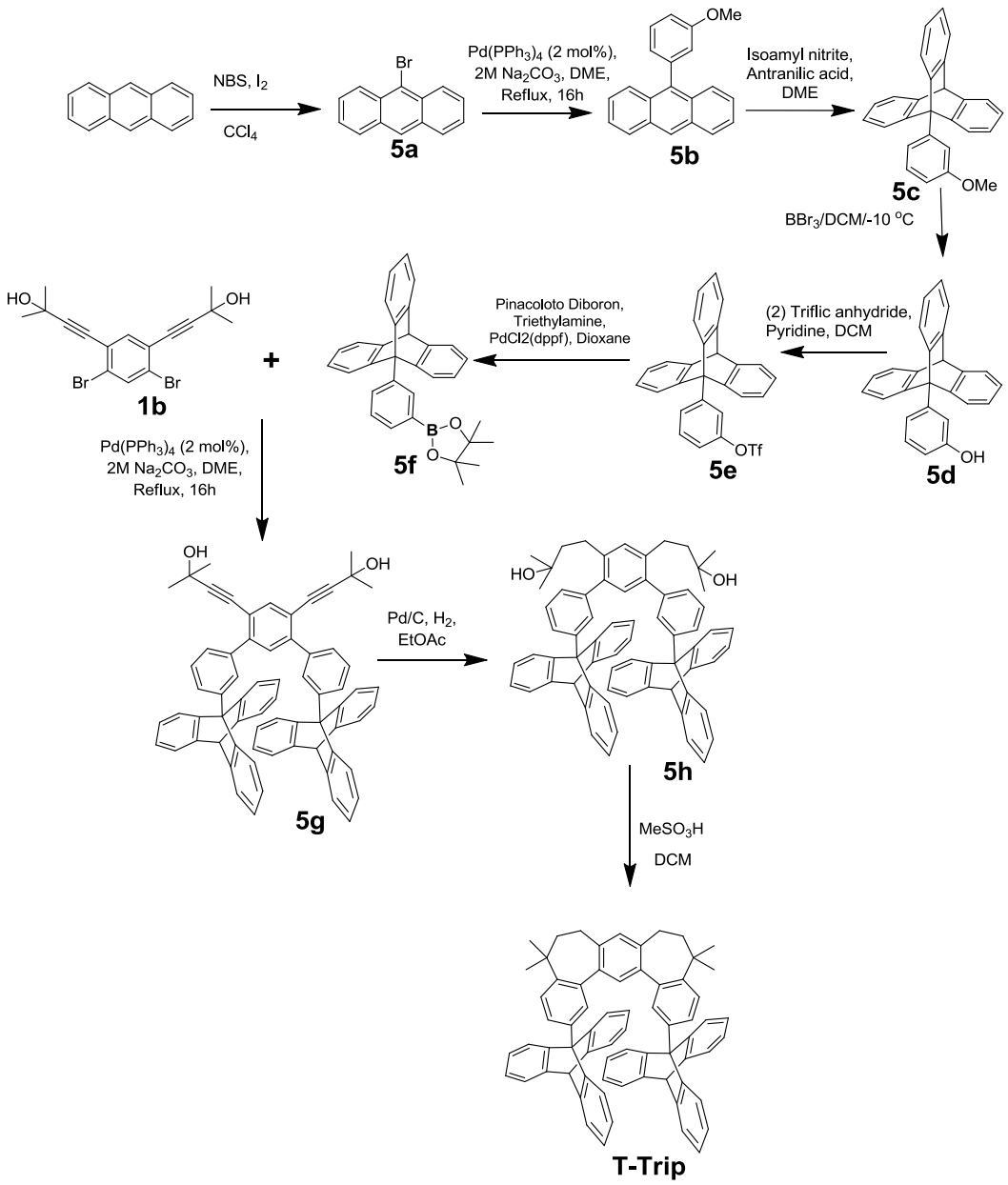

The structures of both TP- tweezers with triptycene and 9-phenyltriptycene as pincers were established by X-ray crystallography. Studies are under progress to demonstrate their gear-like functioning.

Preparation of 5a:

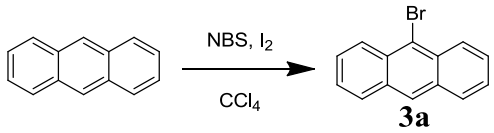

To the mixture of anthracene (2.0 g, 11.24 mmol) and NBS (2.0 g, 11.24 mmol) in CCl_4 (16 mL), was added solution of I_2 in CCl_4 (6-8 drops). The reaction mixture was refluxed for 1 hr after which turned brown and crystals of succicimide appeared at the surface of the reaction. The solution was filtered warm and washed with cyclohexane. The filtrate was concentrated and dried in vacuum to afford the crude product that was recrystallized from DCM and methanol.(2.23 g, 77.4 %). m.p. 88-90 ^oC ^1H NMR ($CDCl_3$) δ: 8.52 (2H, dd, J = 8.84 Hz, 0.87 Hz), 8.41 (1H, s), 7.98 (2H, dt, J = 8.46 Hz, 0.66 Hz), 7.60 (2H, m), 7.49 (2H, m) ^{13}C NMR (75 MHz, $CDCl_3$, δ) 122.51, 125.81, 127.28, 127.37, 127.78, 128.77, 130.74, 132.31.

Preparation of 5b:

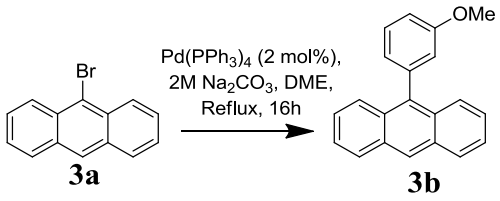

9-Bromoanthracene (2.0 g, 7.78 mmol) and the corresponding *m*-methoxy boronic acid (1.42 g, 9.33 mmol) were dissolved in anhydrous 1,2-dimethoxyethane (DME) (60 mL) in an oven dried Schlenk flask under an argon atmosphere and the flask was evacuated and filled with argon (3x). In another oven dried Schlenk flask a solution of anhydrous

sodium carbonate (5.0 g) in water (20 mL) was prepared under an argon atmosphere and the flask was also evacuated and filled with argon (3x). To the DME solution, $Pd(PPh_3)_4$ (50 mg) and the salt solution were added sequentially under a strict argon atmosphere followed by evacuation and filling the flask with argon (3x) after each addition. The flask was covered with foil and the solution was allowed to reflux overnight. The resulting solution was cooled to room temperature, quenched with water (50 mL) and extracted with dichloromethane (3 x 20mL). The organic layer was dried over anhydrous magnesium sulfate, evaporated and dried under vacuum. Purified by column chromatography using a hexanes/ethyl mixture to give the pure product (1.56 g, 70.5%) m.p. 142-144 ^{o}C 1H NMR ($CDCl_3$) δ:8.62 (1H, s), 8.18 (2H, d, *J* = 8.14 Hz), 8.0 (2H, d, *J* = 8.60 Hz), 7.61 (5H, m), 7.28 (1H, t, *J* =1.64 Hz), 7.26 (2H, s), 3.97 (3H, s) ^{13}C NMR (75 MHz, $CDCl_3$, δ) 55.29, 113.35, 116.72, 123.83, 125.25, 125.54, 126.75, 126.98, 128.47, 129.54, 130.24, 130.25, 131.47, 136.98, 140.35, 140.34, 159.75.

Preparation of 5c:

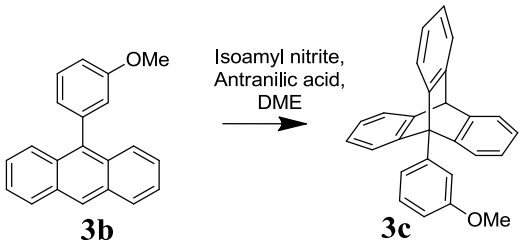

3b **3c**

In a schelnk **3b** (1.80 g, 6.33 mmol) and isoamylnitrite (2 mL, 17.09 mmol) were dissolved in DME (40 mL) with short reflux condenser over it. And the mixture was heated to boil. Half of the Anthracitic acid (2 g in 20 mL DME) was added portion wise in the reaction mixture from the top of the condenser for 20 min (it was leached into the

reaction mixture with DME). Reaction mixture was heated to reflux. The heating mental was removed and isoamilnitrite (2 mL, 17.09 mmol) was added again. The remaining anthranilic acid (2 g) in DME (20 mL) was then added for about 20 min. The reaction mixture was refluxed for 10 min and then 95 % ethanol and sat. solution of NaOH were added and the precipitated product was filtered. The precipitate was washed with cold methanol : water (4:1) mixture to give pure product (1 g, 44 %). m.p. 102-104 ^{o}C 1H NMR ($CDCl_3$) δ:7.72 (2H, m), 7.58 (1H, t, *J* = 8.12 Hz), 7.43 (3H, dd, *J* = 6.99 Hz, 1.55 Hz), 7.32 (3H, dd „*J* = 6.99 Hz, 1.55 Hz), 7.09 (1H, dt, *J* = 8.055 Hz, 1.83 Hz), 6.98 (6H, m), 5.42 (1H, s), 3.91 (3H, s) ^{13}C NMR (75 MHz, $CDCl_3$, δ) 55.35, 55.60, 60.48, 112.55, 117.92, 123.79, 124.15, 124.76, 124.80, 125.30, 129.61, 138.08, 146.80, 146.93, 159.97.

Preparation of 5d:

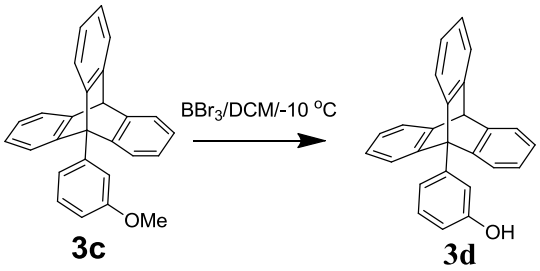

3c **3d**

The solution of ether (1 g, 2.7 mmol) in DCM (30 mL) was cooled to -10 ^{o}C under argone atmosphere using ice-acetone bath. The solution of BBr_3 (0.8 mL, 8.31 mmol) in 10 mL DCM was added to the above cooled solution drop wise over the period of 30 min. The mixture was gradually warmed to room temperature and stirred for 2 hrs. The reaction was quenched with water (50 mL) and extracted with dichloromethane (3 x 20 mL). The organic layer was dried over anhydrous magnesium sulfate, evaporated and dried under vacuum**.** The product formed (0.84 g, 87.4%) was immediately subjected to

the next step without any purification. ^{1}H NMR ($CDCl_3$) δ: 7.66 (1H, d, *J* = 7.86 Hz), 7.59 (1H, t, *J* = 2.12 Hz), 7.49 (1H, t, *J* = 7.95 Hz), 7.39 (3H, dd, *J* = 7.06 Hz, 1.32 Hz), 7.28 (3H, d, *J* = 7.6 Hz), 6.95 (7H, m), 5.42 (1H, s), 5.33 (1H, broad).

Preparation of 5e:

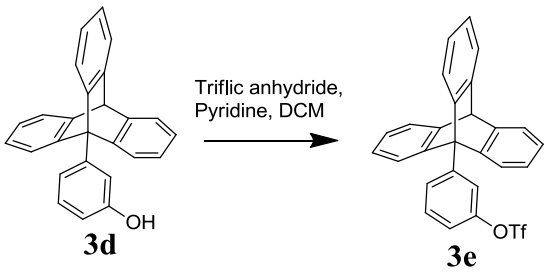

3d **3e**

In Shlenk fask under an argon atmosphere , **(3d)** (0.84 g, 2.42 mmol) and pyridine (0.6 mL, 7.26 mmol) were dissolved in dry DCM (40 mL). The solution was cooled at -10 ^{o}C with ice-acetone bath. In a dropping funnel about 10ml of DCM was taken and triflic anhydride (0.6 mL, 3.5 mmol) was added to it under Ar. The reaction mixture was stirred for 6 hrs at 0 ^{o}C and then concentrated on rotary evaporator. The residual brown oil was diluted with ethyl acetate .Washed with 5% HCl followed by sat.NaCl and sodium bicarbonate. Organic layer was dried over anhydrous magnesium sulfate, evaporated and dried under vacuum**.** The product formed (1.12g, 99%) was purified with column chromatography. m.p. 152-154 ^{o}C ^{1}H NMR ($CDCl_3$) δ: 8.20 (1H, d, *J* = 7.82 Hz), 8.05 (1H, s), 7.76 (1H, t, *J* = 7.82 Hz), 7.50 (1H, s), 7.46 (3H, d, *J* = 7.45 Hz), 7.17 (3H, d, *J* = 7.45 Hz), 7.01 (6H, m), 5.45 (1H, s) ^{13}C NMR (75 MHz, $CDCl_3$, δ) 55.21, 60.11, 120.40, 124.06, 124.08, 125.00, 125.68, 130.44, 131.53, 139.88, 145.95, 146.73, 150.06.

Preparation of 5f:

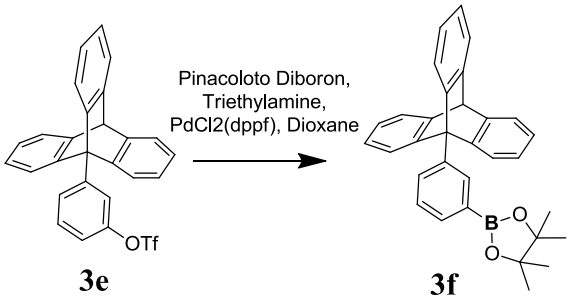

3e **3f**

In an oven dried Shlenk flask, under argon atmosphere, the mixture of $PdCl_2$ (100 mg) in dioxane (70 mL) triflate **3e** (3.5 g, 7.32 mmol) and triethylamine (3.1 mL, 21.96 mmol) were added. The mixture was stirred. bis-(pinacoloto)diboron (3.71 g, 14.64 mmol) was added to mixture. Reaction was heated to reflux for overnight. Reaction was quenched with water and extracted with DCM to give yellowish solid product (2.54 g, 76.2 %). ^{1}H NMR ($CDCl_3$) δ: 8.61 (1H, s), 8.18 (1H, d, *J* = 8.00 Hz), 7.97 (1H, d, *J* = 7.25 Hz), 7.65 (1H, t, *J* = 7.75 Hz), 7.42 (3H, dd, *J* = 6.86 Hz, 1.66 Hz), 7.27 (3H, d, *J* = 7.42 Hz), 6.97 (6H, m), 5.41 (1H, s), 1.36 (12H, s) ^{13}C NMR (75 MHz, $CDCl_3$, δ) 25.14, 55.38, 60.39, 84.06, 123.70, 124.80, 124.84, 125.20, 128.00, 133.74, 134.76, 135.81, 137.90, 146.92, 146.94.

Preparation of 5g:

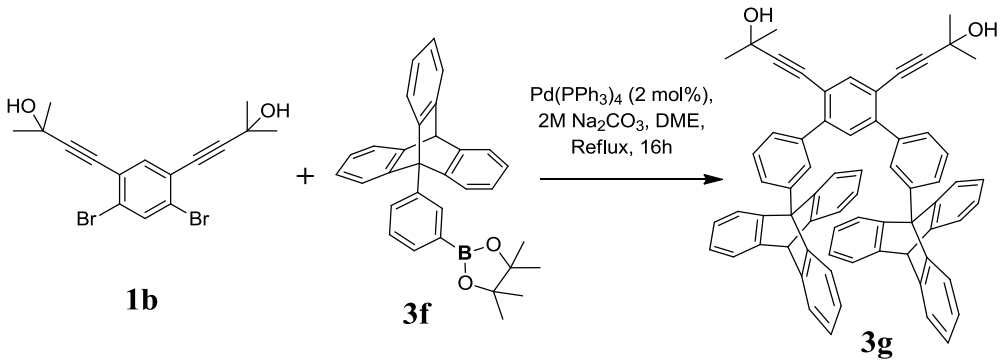

1b **3f** **3g**

Dibromodiacetylene (0.17 g, 0.44 mmol) and the corresponding triptycene boronic acid (0.6 g, 1.31 mmol) were dissolved in anhydrous 1,2-dimethoxyethane (DME) (30 mL) in an oven dried Schlenk flask under an argon atmosphere and the flask was evacuated and filled with argon (3x). In another oven dried Schlenk flask a solution of anhydrous sodium carbonate (2.5 g) in water (10 mL) was prepared under an argon atmosphere and the flask was also evacuated and filled with argon (3x). To the DME solution, $Pd(PPh_3)_4$ (50 mg) and the salt solution were added sequentially under a strict argon atmosphere followed by evacuation and filling the flask with argon (3x) after each addition. The flask was covered with foil and the solution was allowed to reflux overnight. The resulting solution was cooled to room temperature, quenched with water (50 mL) and extracted with dichloromethane (3 x 20 mL). The organic layer was dried over anhydrous magnesium sulfate, evaporated and dried under vacuum. Purified by column chromatography using a hexanes/ethyl mixture to give the pure product (0.25 g, 63.4%) m.p. 110-112 ^{o}C 1H NMR ($CDCl_3$) δ: 8.66 (2H, s), 8.08 (2H, d, J = 8.18 Hz), 7.78 (6H, m), 7.44 (6H, d, J = 6.96 Hz), 7.34 (6H, d, J = 7.43 Hz), 7.00 (6H, d, J = 7.20 Hz), 6.92 (6H, t, J = 7.43 Hz), 5.44 (2H, s), 1.63 (2H, Broad), 1.21 (12H, s) ^{13}C NMR (75 MHz, $CDCl_3$, δ) 25.05, 25.81, 30.87, 55.33, 60.45, 65.55, 80.99, 98.22, 120.41, 123.89, 124.66, 124.82, 125.41, 128.26, 128.37, 131.56, 131.63, 136.47, 140.14, 143.48, 146.79, 146.97.

Preparation of 5h:

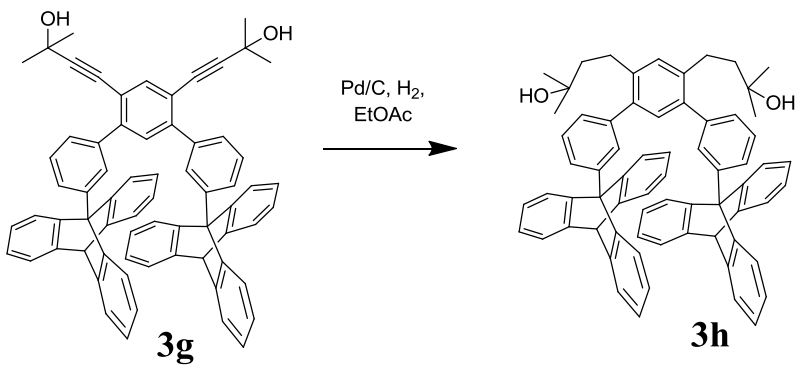

The diacetylene (0.24 g, 0.68 mmol) from above was placed into a Parr apparatus along with a stir bar and dissolved in ethyl acetate (26 mL). To the solution, 10% Palladium on activated Carbon catalyst (100 mg) was added. The vessel was then put under hydrogen pressure (3bar) for 24 hours after which time the solution was filtered over a short pad of silica gel. The silica gel was washed with ethyl acetate (2 x 20 mL), the solvent was evaporated and the product was dried under vacuum and used without further purification. (0.21 g, 96.6%); ^{1}H NMR ($CDCl_3$) δ: 8.17 (2H, s), 8.08 (2H, d, *J* = 7.95 Hz), 7.70 (2H, t, *J* = 7.59 Hz), 7.58 (2H, d, *J* = 7.59 Hz), 7.42 (6H, d, *J* = 7.24 Hz), 7.34 (4H, d, *J* = 11.38 Hz), 7.27 (4H, d, *J* = 11.38 Hz), 6.97 (6H, t, *J* = 7.21 Hz), 6.87 (6h, t, *J* = 7.61 Hz), 5.42 (2H, s), 2.85 (4H, m), 1.75 (4H, m), 1.11 (12H, s) ^{13}C NMR (75 MHz, $CDCl_3$, δ) 25.67, 26.00, 29.27, 46.03, 55.35, 60.43, 70.98, 123.80, 124.65, 124.80, 125.30, 128.40, 128.49, 130.40, 130.67, 132.46, 136.55, 139.43, 139.70, 141.87, 146.84, 146.93.

Preparation of T-Trip:

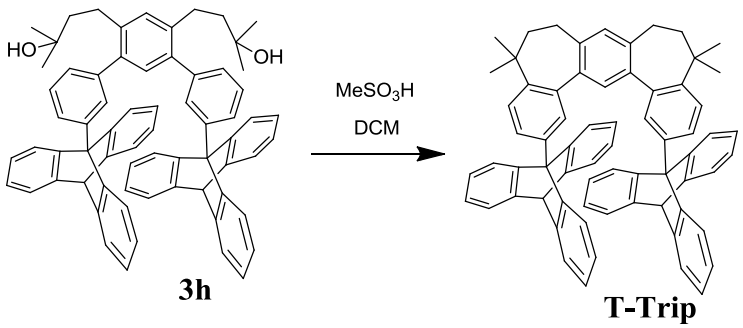

To a stirred solution of **3h** (1.4 g, 1.54 mmol) in dichloromethane (30 mL) at room temperature was added methanesulfonic acid (2 mL). The reaction progress was monitored by ^{1}H NMR, and when it was deemed complete, the solution was quenched with aqueous sodium bicarbonate (100 mL) and extracted with dichloromethane (3 x 20 mL). The combined organic extracts were dried over anhydrous magnesium sulfate, evaporated and dried under vacuum. The solid was purified by recrystallization from a dichloromethane/methanol mixture to give the product (1.34 g, 99%); ^{1}H NMR ($CDCl_3$) δ: 8.22 (2H, s), 8.12 (2H, d, *J* = 8.24 Hz), 7.80 (2H, d, *J* = 8.5 Hz), 7.55 (1H, s), 7.44 (6H, d, *J* = 7.17 Hz), 7.35 (6H, d, *J* = 7.67 Hz), 7.27 (1H, s), 6.89 (6H, t, *J* = 7.10 Hz), 6.66 (6H, Broad), 5.46 (2H, s), 2.87 (4H, s), 2.37 (4H, t, *J* = 6.63 Hz), 1.33 (12H, s) ^{13}C NMR (75 MHz, $CDCl_3$, δ) 32.67, 32.68, 37.92, 48.97, 53.62, 55.33, 60.06, 123.59, 124.56, 124.69, 125.20, 125.83, 124.60, 130.47, 133.34, 134.50, 139.17, 140.73, 142.11, 145.10, 146.79, 146.84.

Preparation of 4b:

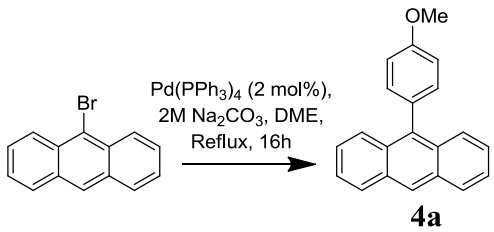

4a

9-Bromoanthracene (2.0 g, 7.78 mmol) and the corresponding *p*-methoxy boronic acid (1.42 g, 9.33 mmol) were dissolved in anhydrous 1,2-dimethoxyethane (DME) (60 mL) in an oven dried Schlenk flask under an argon atmosphere and the flask was evacuated and filled with argon (3x). In another oven dried Schlenk flask a solution of anhydrous sodium carbonate (5.0 g) in water (20 mL) was prepared under an argon atmosphere and the flask was also evacuated and filled with argon (3x). To the DME solution, $Pd(PPh_3)_4$ (50 mg) and the salt solution were added sequentially under a strict argon atmosphere followed by evacuation and filling the flask with argon (3x) after each addition. The flask was covered with foil and the solution was allowed to reflux overnight. The resulting solution was cooled to room temperature, quenched with water (50 mL) and extracted with dichloromethane (3 x 20 mL). The organic layer was dried over anhydrous magnesium sulfate, evaporated and dried under vacuum. Purified by column chromatography using a hexanes/ethyl mixture to give the pure product (2.0 g, 90%) m.p. 158-160 ^{o}C 1H NMR ($CDCl_3$) δ: 8.49 (1H, s), 8.04 (2H, d, J = 8.49 Hz), 7.73 (2H, d, J = 8.66 Hz), 7.46 (2H, t, J = 6.49 Hz), 7.36 (4H, m), 7.13 (2H, d, J = 8.66 Hz), 3.95 (3H, s) ^{13}C NMR (400 MHz, $CDCl_3$, δ) 55.61, 114.04, 125.29, 125.46, 126.61, 127.15, 128.56, 130.76, 131.03, 131.63, 132.53, 137.05, 159.22.

Preparation of 4c:

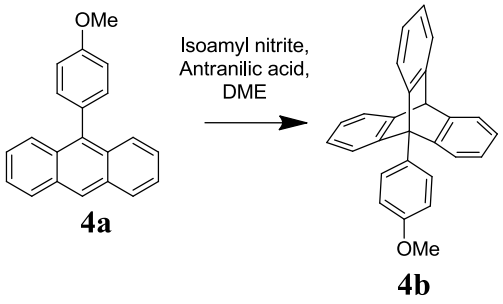

4a **4b**

In a Schelnk **4b** (2.0 g, 7.03 mmol) and isoamylnitrite (2 mL, 17.09 mmol) were dissolved in DME (40 mL) with short reflux condenser over it. And the mixture was heated to boil. Half of the anthracitic acid (2 g in 20 mL DME) was added portion wise in the reaction mixture from the top of the condenser for 20 min (it was leached into the reaction mixture with DME). Reaction mixture was heated to reflux.heating mental was removed and isoamilnitrite (2 mL, 17.09 mmol) was added again. The remaining anthranilic acid (2 g) in DME (20 mL) was then added for about 20 min. The reaction mixture was refluxed for 10 min. and then 95 % ethanol and sat. solution of NaOH were added and the precipitated product was filtered. The precipitate was washed with cold methanol : water (4:1) mixture to give pure product (1.31 g, 52 %). m.p. 212-214 ^{o}C ^{1}H NMR ($CDCl_3$) δ: 8.06 (2H, d, *J* = 8.92 Hz), 7.44 (3H, d, *J* = 8.92 Hz), 7.29 (3H, d, *J* = 6.81 Hz), 7.20 (2H, d, *J* = 8.92 Hz), 6.98 (6H, m), 5.43 (1H, s), 3.98 (3H, s) ^{13}C NMR (400 MHz, $CDCl_3$, δ) 55.32, 55.57, 59.82, 113.93, 123.76, 124.63, 124.75, 125.23, 128.44, 132.92, 146.91, 147.18, 158.58.

Preparation of 4d:

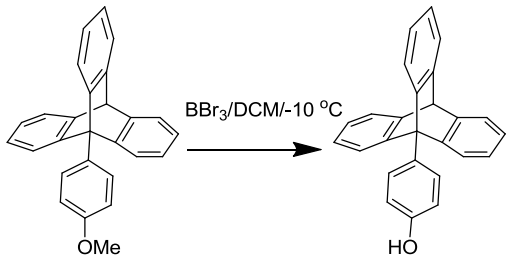

4b **4c**

The solution of ether **4b** (1.36 g, 3.77 mmol) in DCM (30 mL) was cooled to -10 ^{o}C under argon atmosphere using ice-acetone bath. The solution of BBr_3 (1.1 mL, 11.32mmol) in 10 mL DCM was added to the above cooled solution dropwise over the period of 30 min. The mixture was gradually warmed to room temperature and stirred for 2 hrs. The reaction was quenched with water (50 mL) and extracted with dichloromethane (3 x 20 mL). The organic layer was dried over anhydrous magnesium sulfate, evaporated and dried under vacuum**.** The product formed (1.25 g, 96.1%) was immediately subjected to the next step without any purification. ^{1}H NMR ($CDCl_3$) δ: 7.99 (2H, d, *J* = 8.84 Hz), 7.42 (3H, d, *J* = 7.095 Hz), 7.27 (3H, d, *J* = 7.82 Hz), 7.11 (2H, d, *J* = 8.84 Hz), 6.97 (6H, m), 5.41 (1H, s).

Preparation of 4e:

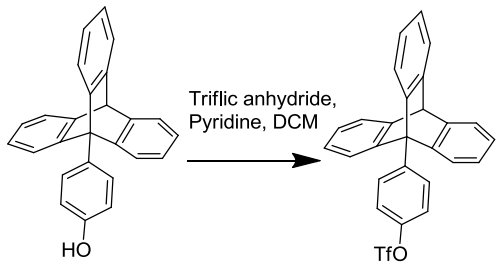

4c **4d**

In Shlenk flask under an argon atmosphere, **(4c)** (1.25 g, 3.61 mmol) and pyridine (0.9 mL, 10.83 mmol) were dissolved in dry DCM (40 mL). The solution was cooled at -10 ^{o}C with ice-acetone bath. In a dropping funnel, was taken a solution of triflic anhydride (0.82 mL, 5.05 mmol) in DCM (10 mL) and kept under argon. This was added to the above cooled solution over a period of 10 min. The reaction mixture was stirred for 6 hours at 0 ^{0}C. It was then concentrated on rotary evaporator and the residual brown oil was diluted with ethyl acetate, washed with 5% HCl followed by sat.NaCl and sodium bicarbonate. Organic layer was dried over anhydrous magnesium sulfate, evaporated and dried under vacuum**.** The product formed (1.52 g, 88.3%) was purified with Column chromatography. m.p. 300-302 ^{o}C ^{1}H NMR ($CDCl_3$) δ: 8.23 (2H, d, *J* = 9.01 Hz), 7.58 (2H, d, *J* = 9.01Hz), 7.45 (3H, d, *J* = 6.84 Hz), 7.16 (3H, d, *J* = 7.54 Hz), 6.99 (6H, m), 5.44 (1H, s) ^{13}C NMR (400 MHz, $CDCl_3$, δ) 55.25, 59.99, 121.51, 124.06, 124.16, 124.94, 125.63, 133.62, 137.43, 146.17, 146.17, 146.78, 148.61.

Preparation of 4f:

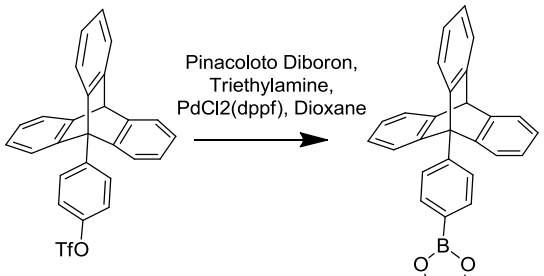

4d **4e**

To a Schlenk flask under argon atmosphere, a mixture of triflate **4d** (1 g, 2.1 mmol) and $PdCl_2$ (100 mg) were added to a solution of dioxane (40 mL) and trimethylamine (1.0

mL, 6.3 mmol). The mixture was stirred. Bis-(pinacoloto)diboron (1.1 g, 4.2 mmol) was added to mixture. Reaction was heated to reflux overnight. Reaction was quenched with water and extracted with DCM to give yellow colored solid product (0.89 g, 95.6%). m.p. 240-242 ^{o}C1H NMR ($CDCl_3$) δ: 8.16 (2H, d, *J* = 8.40 Hz), 8.11 (2H, d, *J* = 8.40 Hz), 7.44 (3H, d, *J* = 7.22 Hz), 7.29 (1H, s), 7.26 (2H, s), 6.98 (6H, m), 5.43 (1H, s), 1.45 (12H, s) ^{13}C NMR (400 MHz, $CDCl_3$, δ) 25.19, 55.35, 60.58, 84.20, 123.79, 124.76, 124.80, 125.31, 131.10, 135.03, 139.78, 146.72, 146.92.

Preparation of T-PhTrip:

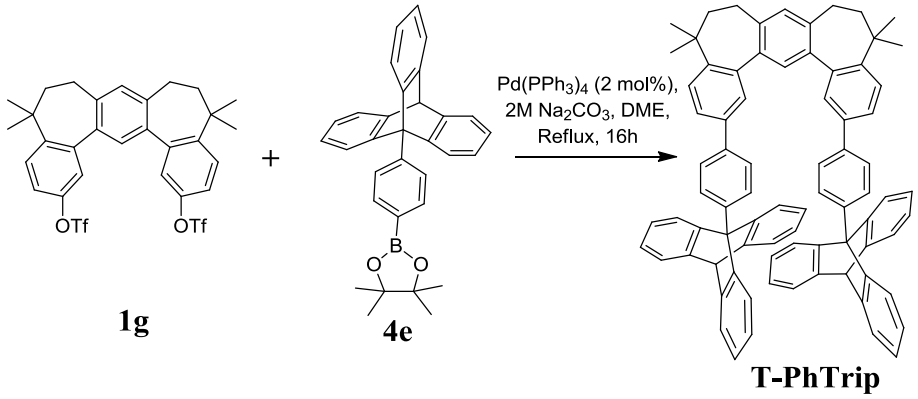

1g **4e** **T-PhTrip**

DiTriflate compound **1g** (0.43 g, 0.65 mmol) and triptycene boronic ester **4e** (3 equiv,0.89 g, 1.95 mmol) were dissolved in anhydrous Toluene (30 mL) in an oven dried Schlenk flask under an argon atmosphere and the flask was evacuated and filled with argon (3x). In another oven dried Schlenk flask a solution of anhydrous sodium carbonate (2.5 g) in water (10 mL) was prepared under an argon atmosphere and the flask was also evacuated and filled with argon (3x). To the toluene solution, $Pd(PPh_3)_4$ (50 mg) and the salt solution were added sequentially under a strict argon atmosphere followed by evacuation and filling the flask with argon (3x) after each addition. The flask was

covered with foil and the solution was allowed to reflux overnight. The resulting solution was cooled to room temperature, quenched with water (50 mL) and extracted with dichloromethane (3 x 20 mL). The organic layer was dried over anhydrous magnesium sulfate, evaporated and dried under vacuum. The product was further purified by column chromatography using a hexanes/ethyl mixture to give the pure product (0.4 g, 59.9%) m.p. Above 400 ^{o}C1H NMR ($CDCl_3$) δ: 8.17 (4H, d, *J* = 8.45 Hz), 7.95 (4H, d, *J* = 8.45 Hz), 7.88 (2H, s), 7.75 (2H, dd, *J* = 8.19 Hz, 2.09 Hz), 7.67 (1H, s), 7.65 (2H, d, *J* = 8.19 Hz), 7.40 (6H, d, *J* = 7.31 Hz), 7.29 (6H, d, *J* = 7.31 Hz), 7.16 (1H, s), 6.91 (12H, m), 5.40 (2H, s), 2.72 (4H, Broad), 2.23 (4H, t, *J* = 6.57 Hz), 1.24 (12H, Broad) ^{13}C NMR (400 MHz, $CDCl_3$, δ) 32.54, 38.00, 48.90, 55.32, 60.20, 123.74, 124.70, 124.79, 125.25, 125.90, 126.49, 127.14, 127.72, 127.99, 129.35, 132.12, 135.44, 138.85, 139.12, 139.57, 141.32, 141.83, 145.71, 146.84, 146.87.

^{1}H NMR spectrum of 5a

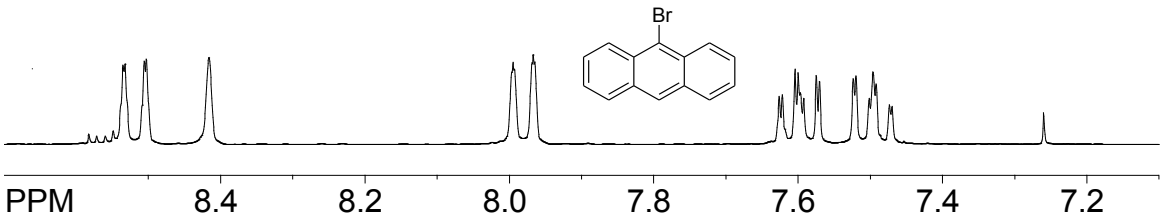

^{13}C NMR spectrum of 5a

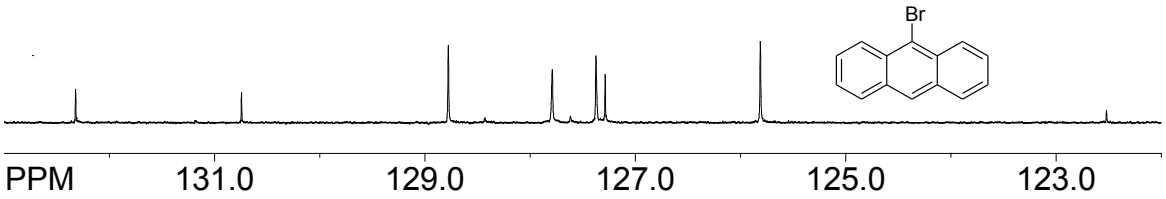

^{1}H NMR spectrum of 5b

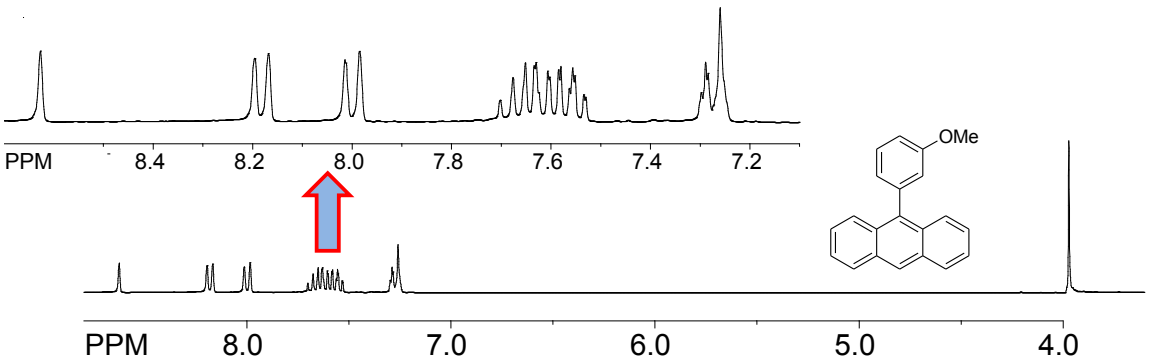

^{13}C NMR spectrum of 5b

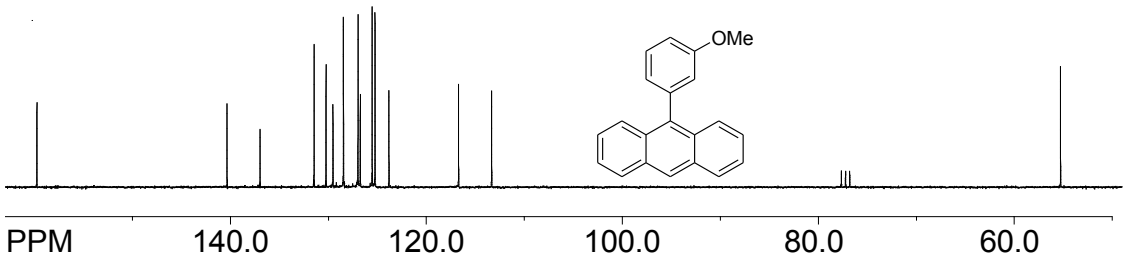

^{1}H NMR spectrum of 5c

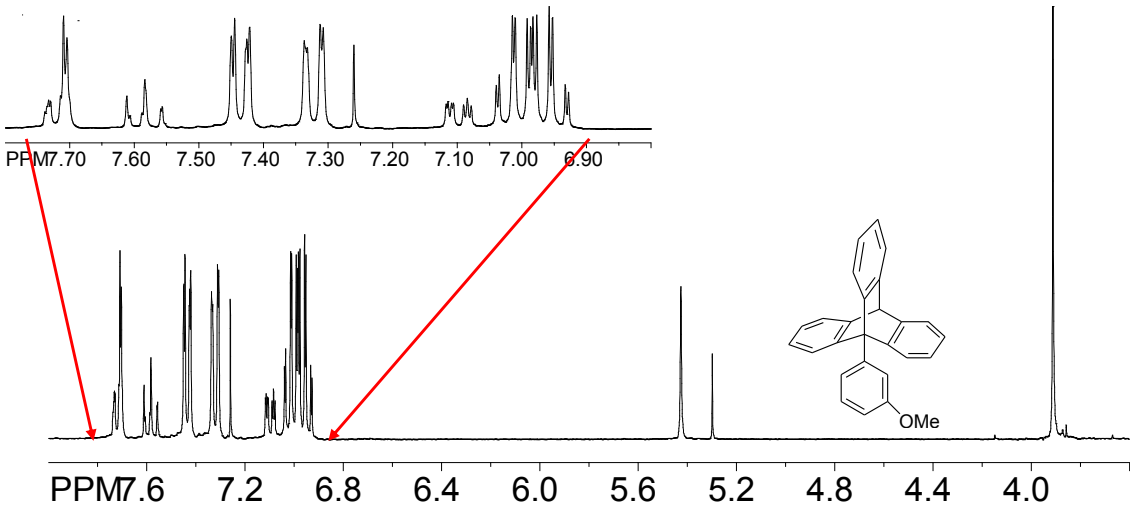

^{13}C NMR spectrum of 5c

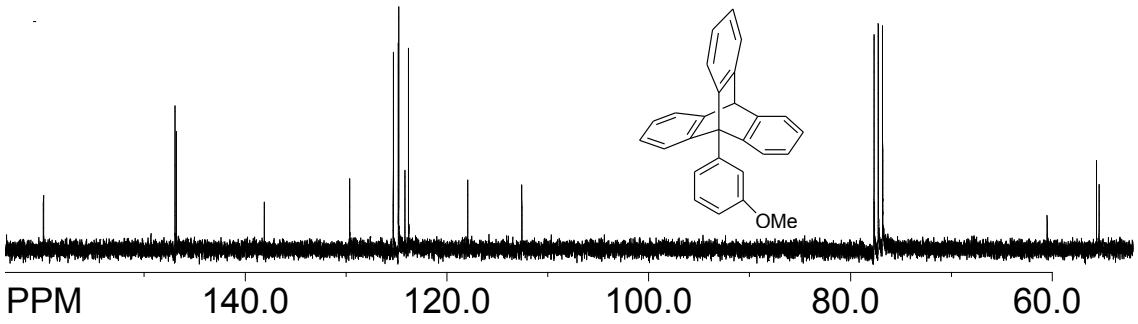

^{1}H NMR spectrum of 5d

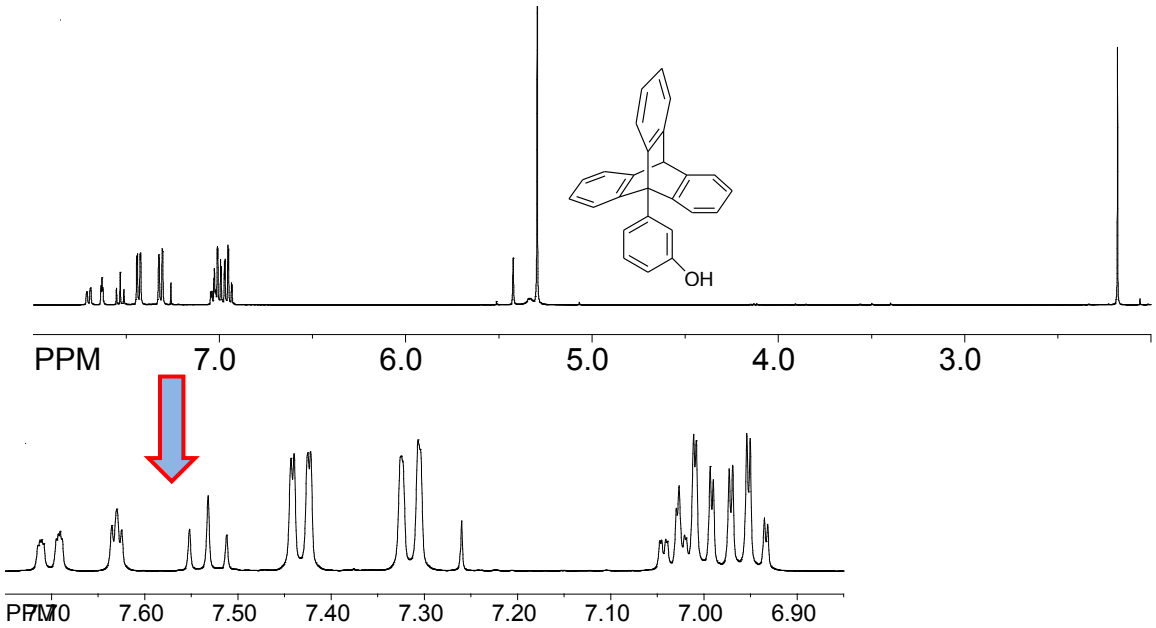

^{1}H NMR spectrum of 5e

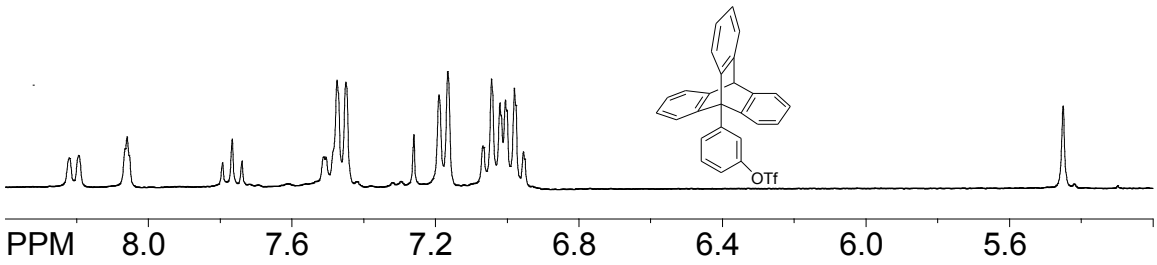

^{13}C NMR spectrum of 5e

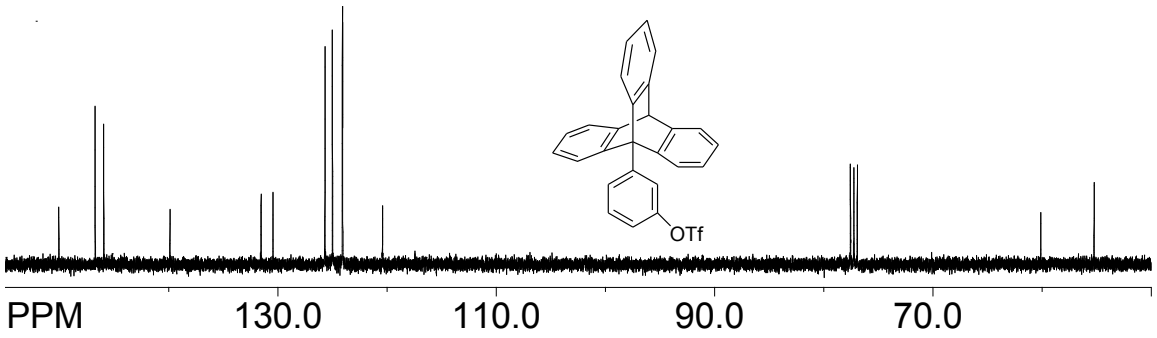

^{1}H NMR spectrum of 5f

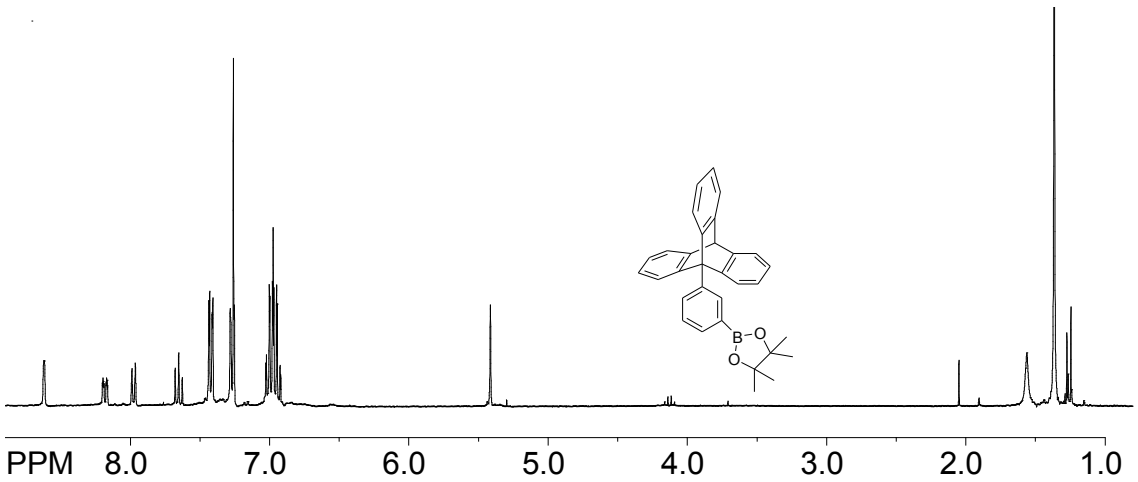

^{13}C NMR spectrum of 5f

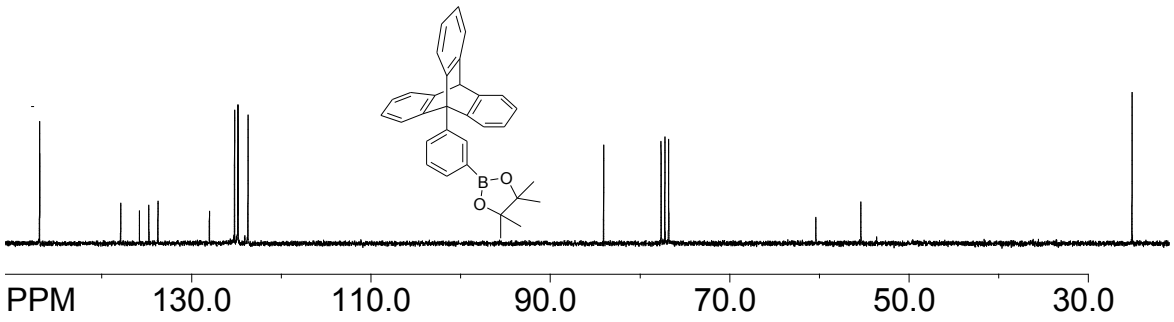

^{1}H NMR spectrum of 5g

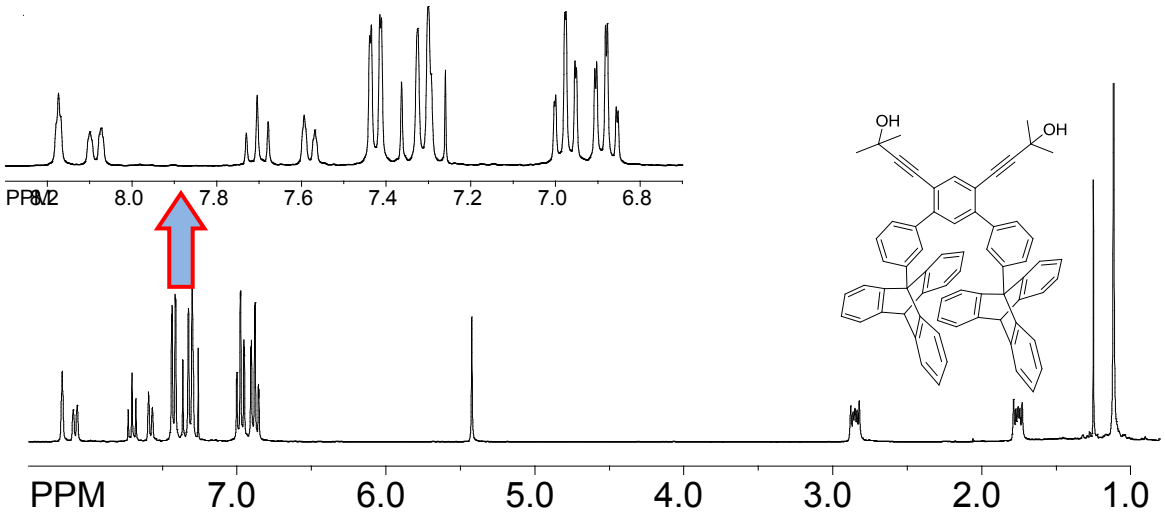

^{13}C NMR spectrum of 5g

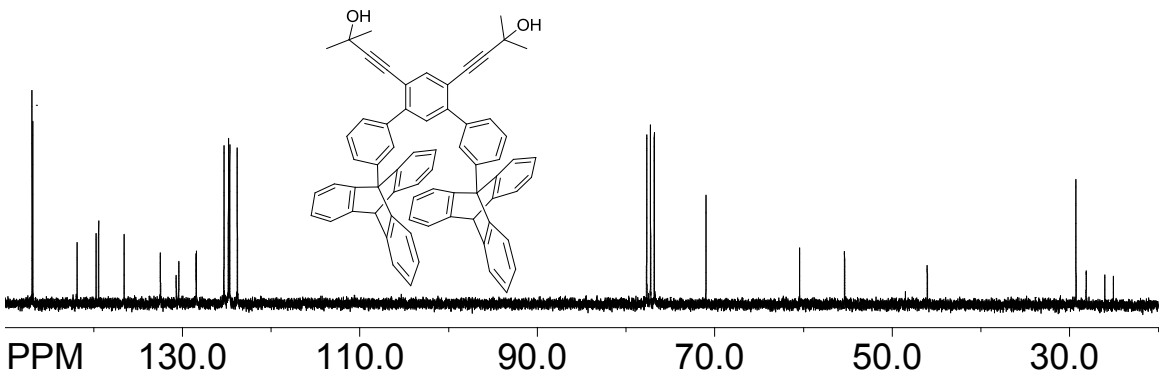

^{1}H NMR spectrum of 5f

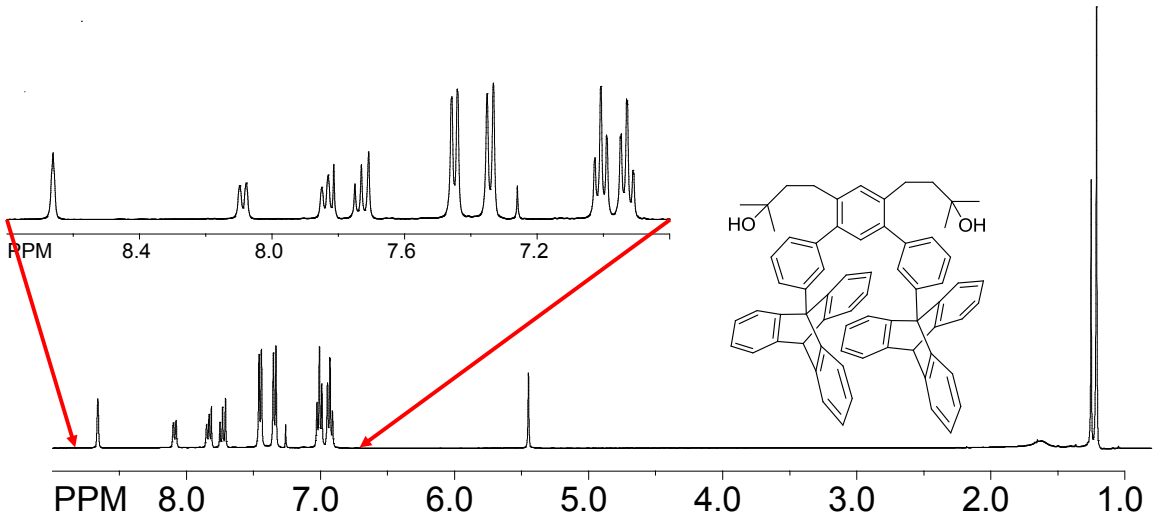

^{13}C NMR spectrum of 5f

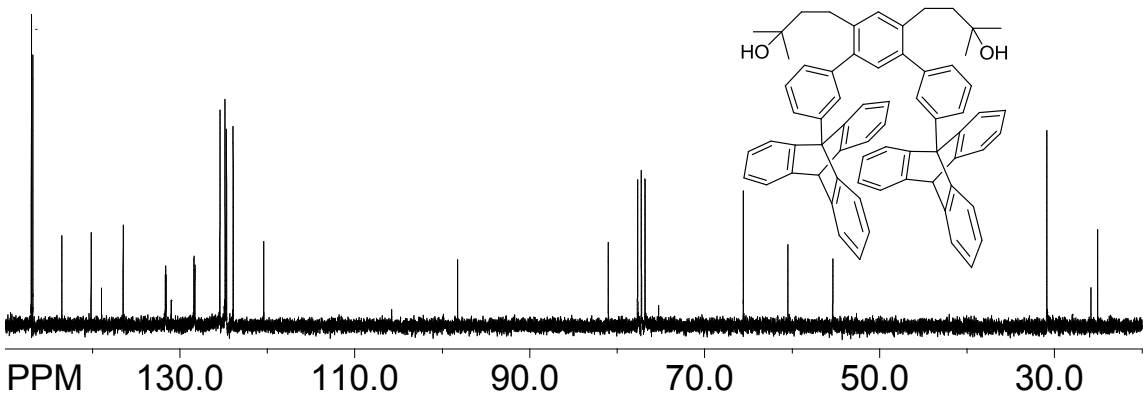

^{1}H NMR spectrum of T-Trip

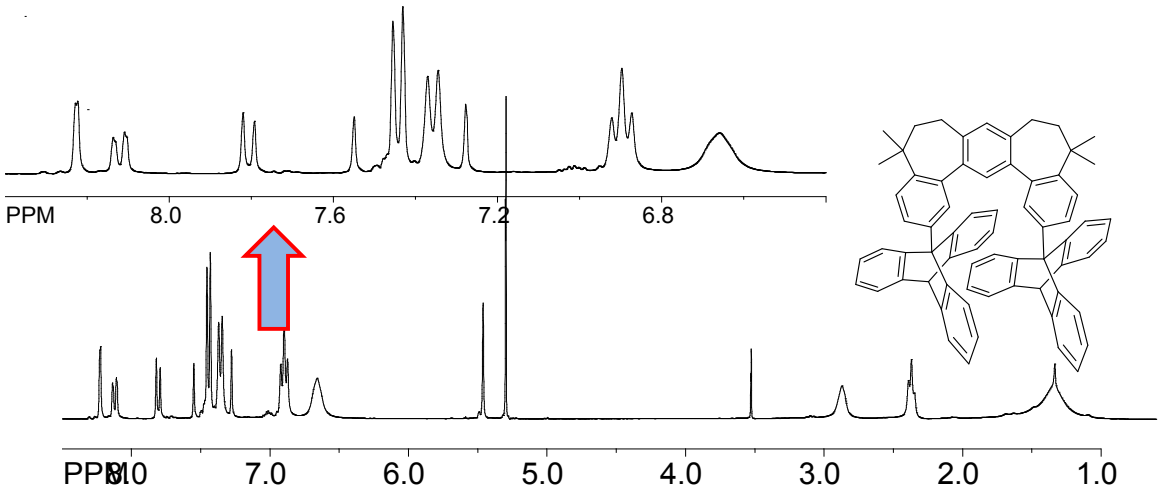

^{13}C NMR spectrum of T-Trip

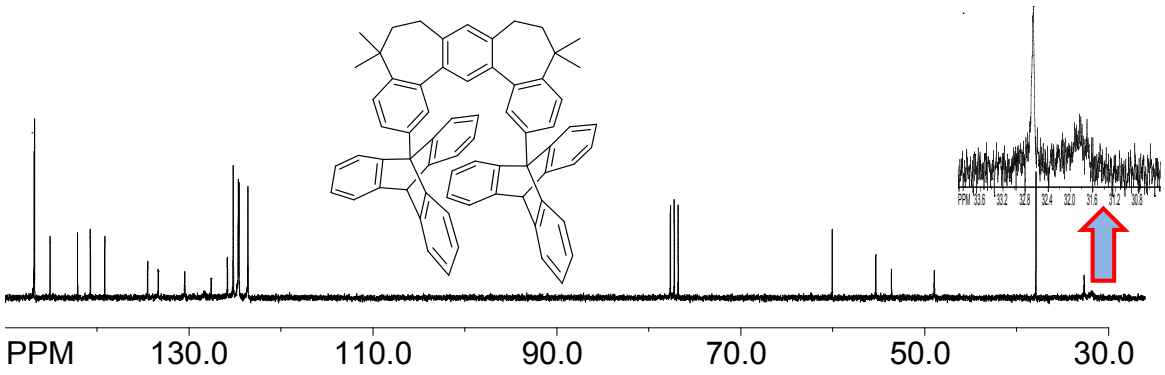

^{1}H NMR spectrum of 4b

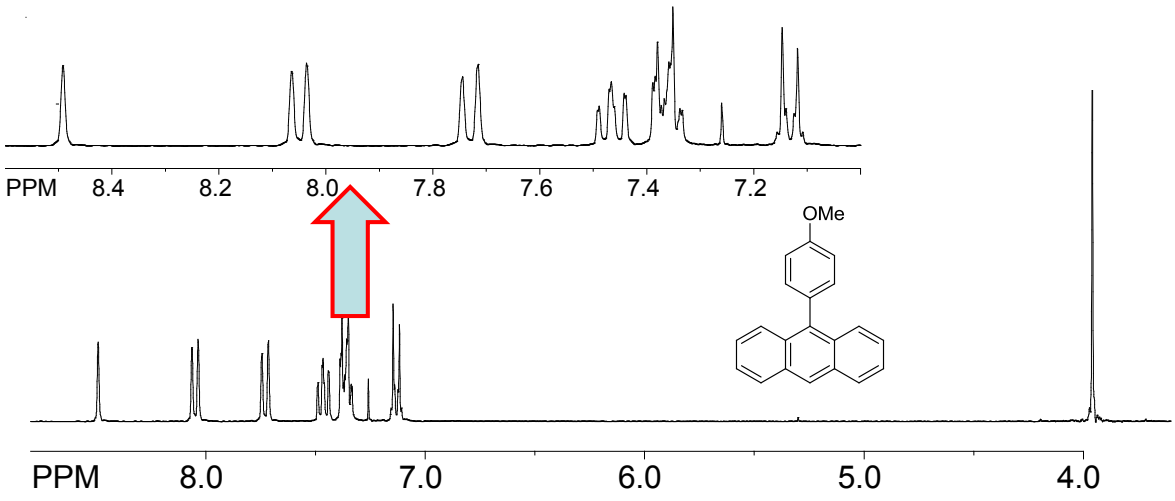

^{13}C NMR spectrum of 4b

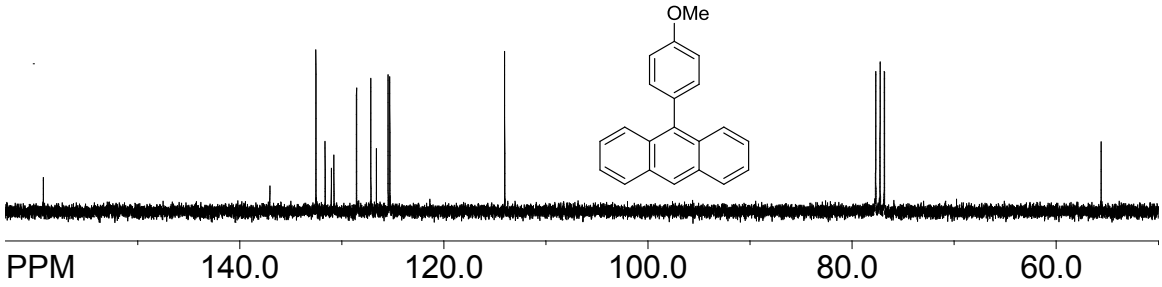

^{1}H NMR spectrum of 4c

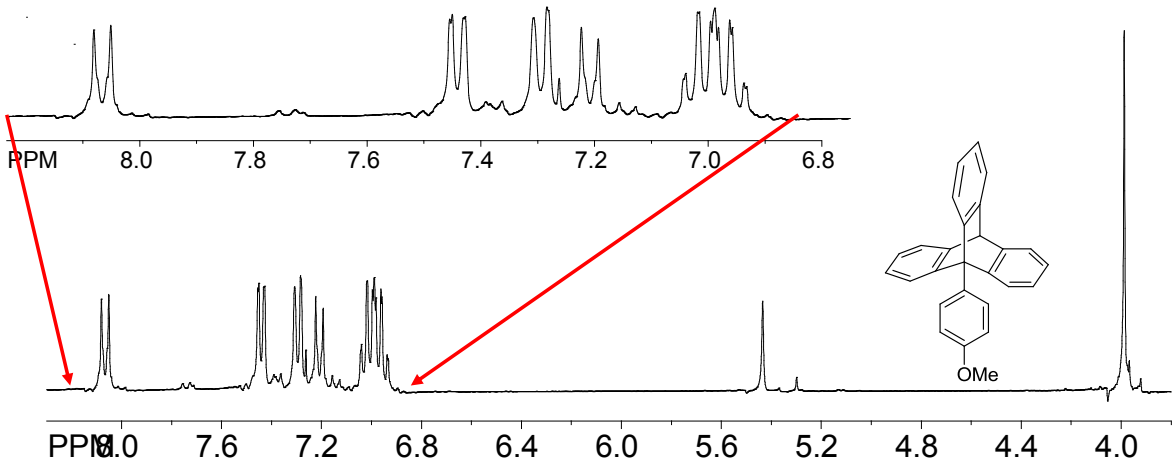

^{13}C NMR spectrum of 4c

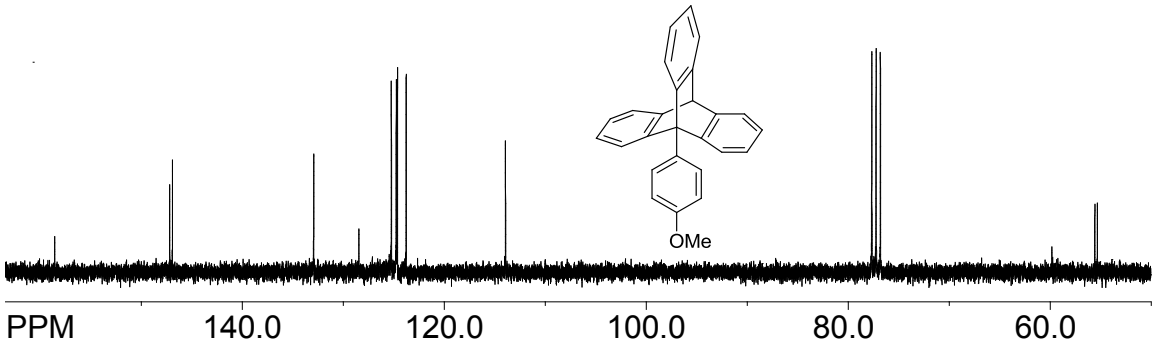

^{1}H NMR spectrum of 4d

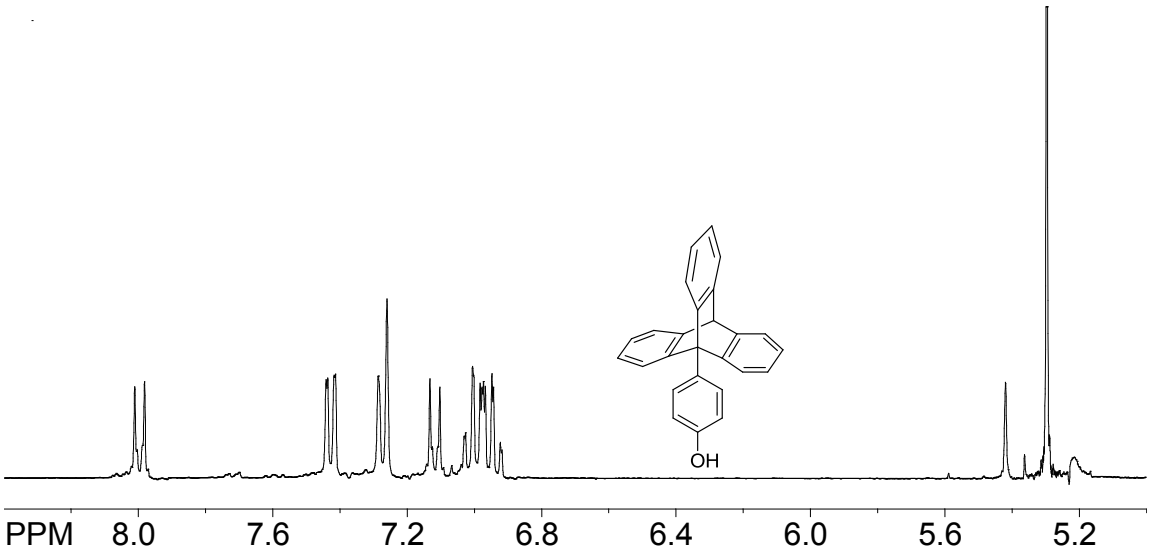

^{1}H NMR spectrum of 4e

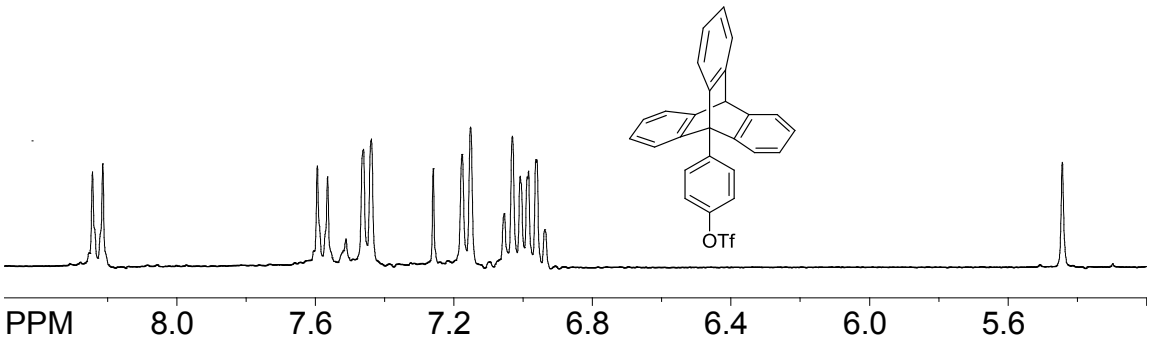

^{13}C NMR spectrum of 4e

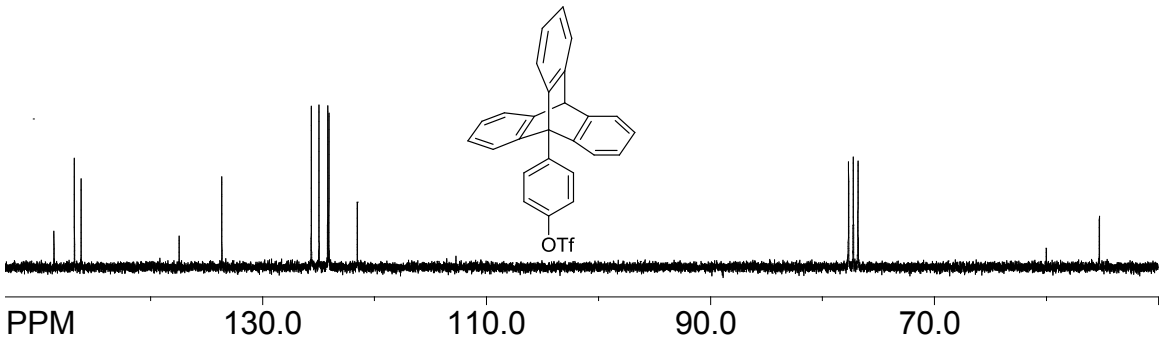

^{1}H NMR spectrum of 4f

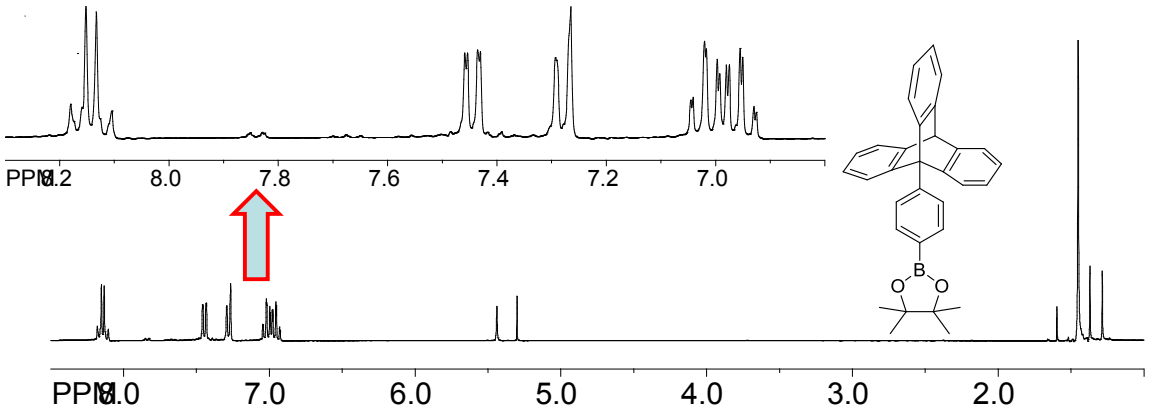

^{13}C NMR spectrum of 4f

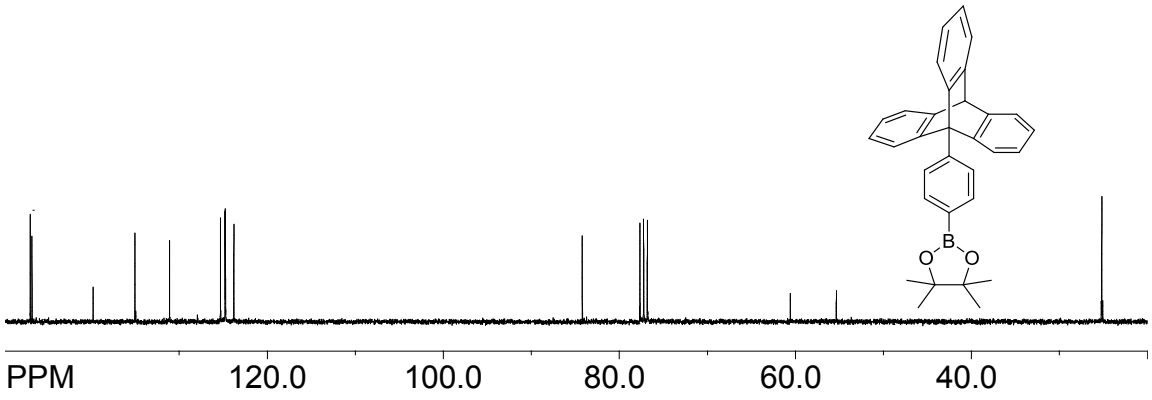

^{1}H NMR spectrum of T-PhTrip

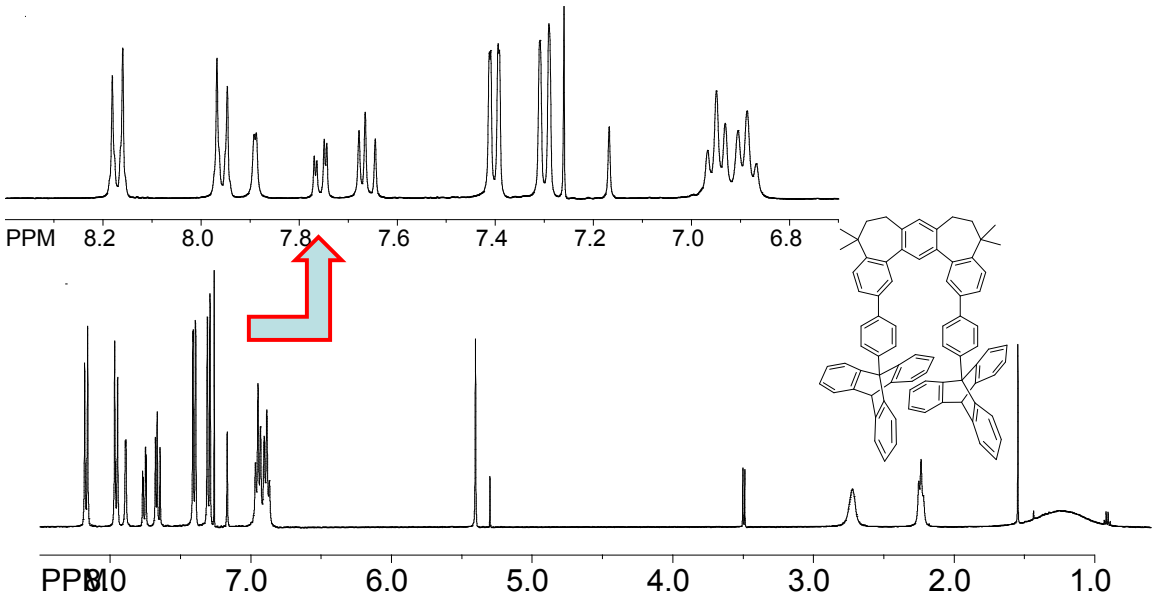

^{13}C NMR spectrum of T-PhTrip

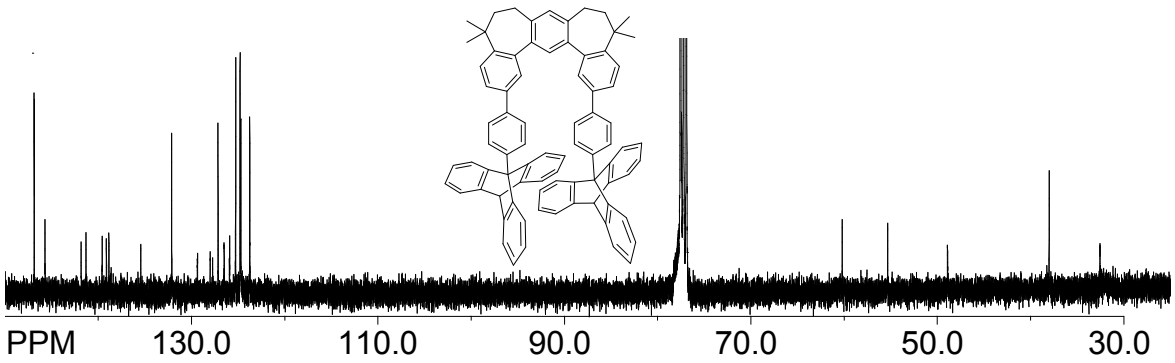

Crystal data and structure refinement for raj16n

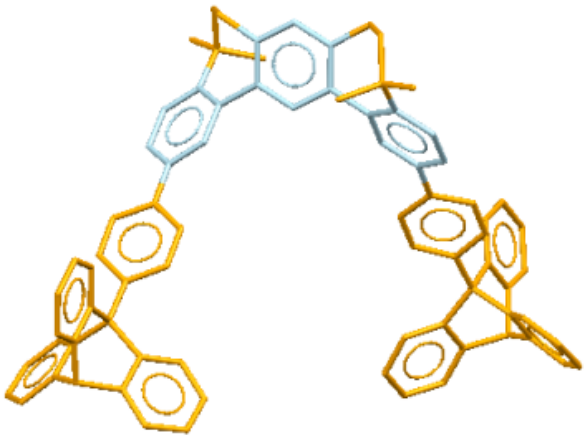

Identification code	raj16n
Empirical formula	C81.21 H64.42 Cl3.94
Formula weight	1179.76
Temperature	100(2) K
Wavelength	1.54178 Å
Crystal system	Triclinic
Space group	P -1
Unit cell dimensions	a = 13.8361(5) Å α= 80.801(2)°.
	b = 15.4369(5) Å β= 89.090(2)°.
	c = 16.9141(6) Å γ = 64.392(2)°.
Volume	3210.11(19) $Å^3$
Z	2
Density (calculated)	1.221 Mg/m^3
Absorption coefficient	1.987 mm^{-1}
F(000)	1237
Crystal size	0.35 x 0.18 x 0.12 mm^3
Theta range for data collection	3.22 to 67.72°.
Index ranges	-16<=h<=16, -18<=k<=18, 0<=l<=20
Reflections collected	26139
Independent reflections	10875 [R(int) = 0.0229]
Completeness to theta = 67.72°	98.5 %
Absorption correction	Semi-empirical from equivalents
Max. and min. transmission	0.7964 and 0.5430
Refinement method	Full-matrix least-squares on F^2

Data / restraints / parameters	10875 / 0 / 817
Goodness-of-fit on F^2	1.016
Final R indices [I>2sigma(I)]	R1 = 0.0905, wR2 = 0.2538
R indices (all data)	R1 = 0.0995, wR2 = 0.2645
Largest diff. peak and hole	1.471 and -0.568 e.Å^{-3}

Crystal data and structure refinement for raj16o

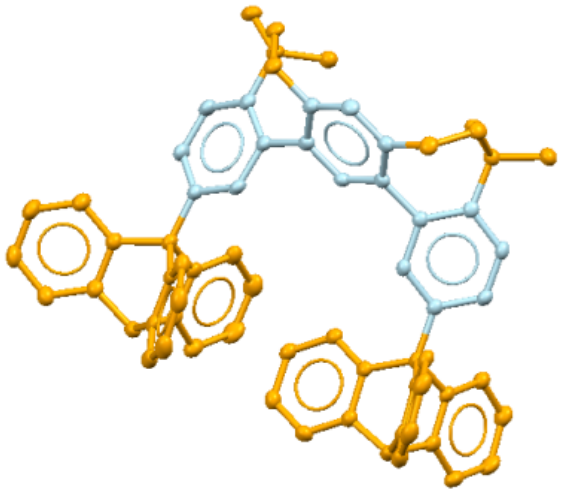

Identification code	raj16o
Empirical formula	C71.20 H60.40 Cl6.40
Formula weight	1142.88
Temperature	100(2) K
Wavelength	1.54178 Å
Crystal system	Triclinic
Space group	P -1
Unit cell dimensions	a = 12.4249(3) Å α= 66.8950(10)°. b = 15.9191(4) Å β= 70.4340(10)°. c = 17.4828(4) Å γ = 76.2170(10)°.
Volume	2974.09(12) Å^3
Z	2
Density (calculated)	1.276 Mg/m^3
Absorption coefficient	3.119 mm^{-1}
F(000)	1193

Crystal size	0.32 x 0.12 x 0.09 mm^3
Theta range for data collection	3.04 to 67.74°.
Index ranges	-13<=h<=14, -16<=k<=18, 0<=l<=20
Reflections collected	24320
Independent reflections	10073 [R(int) = 0.0268]
Completeness to theta = 67.74°	98.5 %
Absorption correction	Semi-empirical from equivalents
Max. and min. transmission	0.7666 and 0.4352
Refinement method	Full-matrix least-squares on F^2
Data / restraints / parameters	10073 / 9 / 738
Goodness-of-fit on F^2	1.001
Final R indices [I>2sigma(I)]	R1 = 0.0777, wR2 = 0.2001
R indices (all data)	R1 = 0.0820, wR2 = 0.2040
Largest diff. peak and hole	1.926 and -0.885 e.$Å^{-3}$

CHAPTER 3
EFFECT OF THE ANNULATION OF *M*-TERPHENYL PLATFORM TOWARDS THE FUNCTIONALITY OF THE TWEEZERS: DESIGN AND SYNTHESIS OF TWEEZERS WITH MULTIPLE PINCERS

Introduction

In the previous chapter we delineated the usage a common doubly-annulated *m*-terphenyl platform for the preparation of a variety of molecular tweezers with different pincers (see Figure 3.1A). We also confirmed that this new class of conformationally-adaptable tweezers binds a variety of electron-poor guests via electron donor-acceptor (EDA) or charge-transfer (CT) interactions (see Figure 3.1B). It was also demonstrated in a proof of concept experiments that these tweezers can undergo ready self-assembly when prompted by one-electron oxidation (see Figure 3.1C).

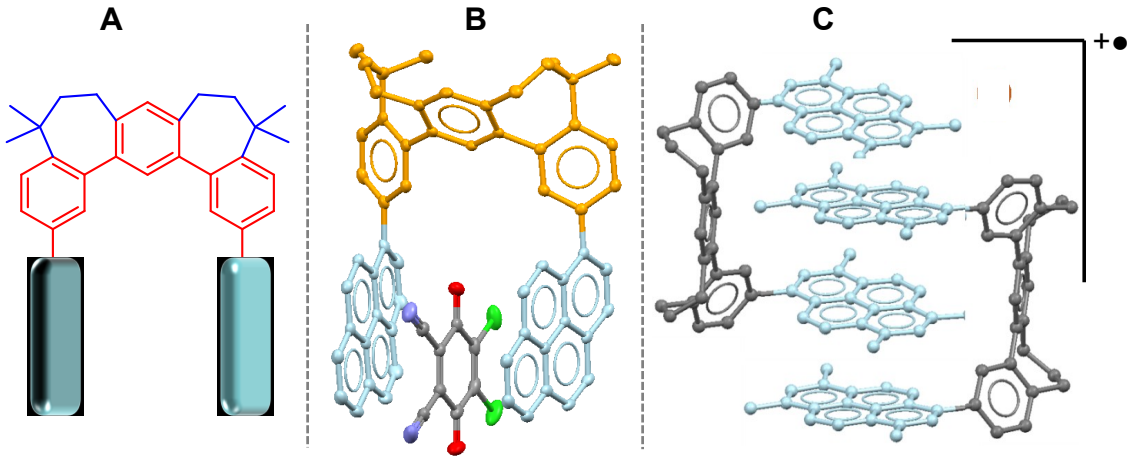

Figure 3.1 A. A doubly annulated *m*-terphenyl platform for tweezer synthesis. B. Molecular structure of an EDA complex of a representative tweezer with DDQ as a guest, obtained by X-ray crystallography. C. A calculated structure of a self-assembled tweezer dimer cation radical where charge is delocalized onto four cofacially stacked pyrenyl moieties.

As stated in the introduction, our ultimate goal for seeking out a new class of easily synthesized tweezers (see Figure 3.1) was largely driven by the fact that tweezer-like scaffolds hold potential for the preparation of self-assembled wire-like structures in which aromatic pincers are cofacially stacked (e.g. see Figure 3.1C). In order to prepare long wire-like self-assemblies, one would require the tweezers with multiple pincers; and preferably with the comb-like arrangement of the pincers on tweezer platform. The tweezer platform described in the previous chapter (i.e. the doubly annulated *m*-terphenyl platform) will only allow us to construct zig-zag structures as exemplified in the Figures 3.2 and 3.3.

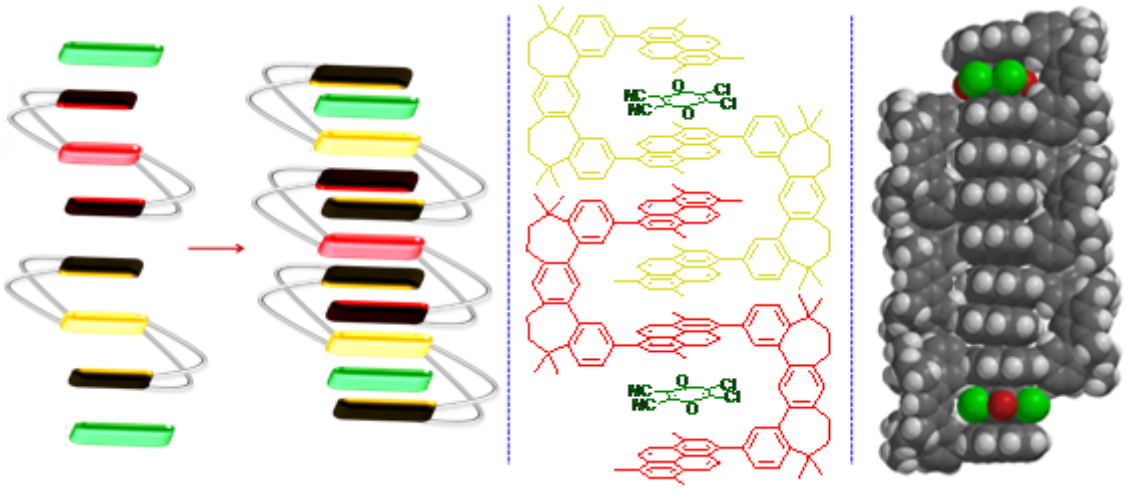

Figure 3.2 **Left:** A cartoon representation of an EDA assembly from a three-pincer tweezer and a pair of electron-poor guest molecules. **Middle:** Showing the actual chemical structures of the proposed three-pincer tweezer from a doubly-annulated tweezer platform and electron-poor guest molecules to produce the EDA assembly shown in the left by cartoon diagram. **Right:** An AM1 minimized structure of an EDA assembly consisting three molecules of the proposed three-pincer tweezer and a pair of chloranil molecules as electron-poor guests.

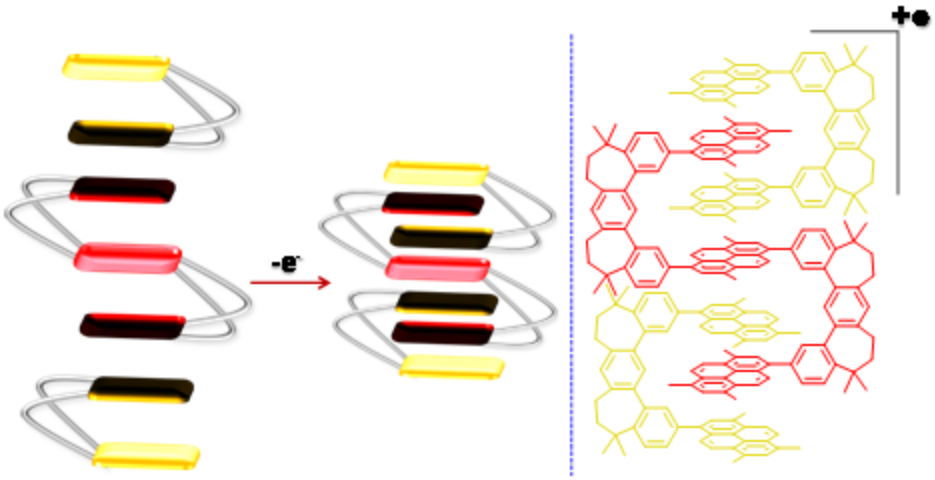

Figure 3.3 A cartoon (left) and actual chemical structure representation of the proposed self-assembly of a three pincer tweezer with a pair two pincer tweezer molecules when prompted by 1-electron oxidation.

In order to construct large comb-like multi-pincer molecules, one would require a new tweezer platform as shown in the Figure 3.4 below.

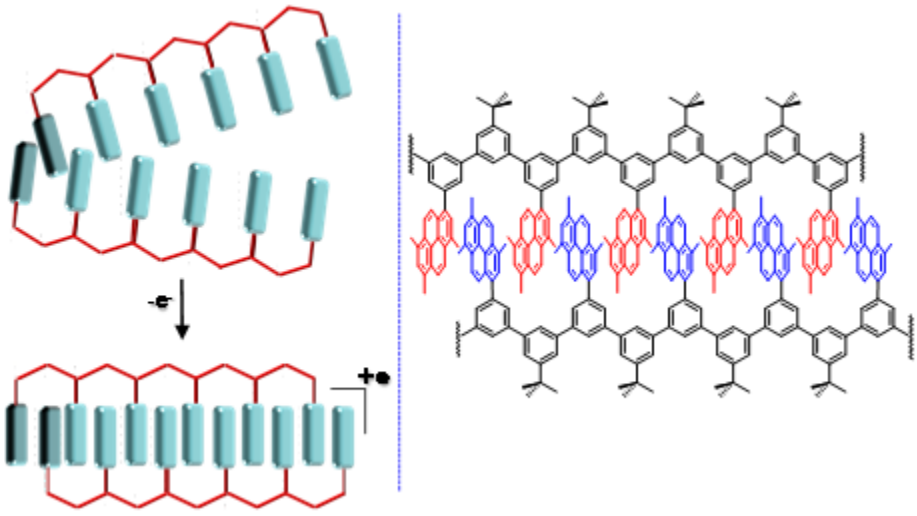

Figure 3.4 A cartoon (left) and actual chemical structure representation of the proposed self-assembly of comb-like poly-pincer molecules when prompted by 1-electron oxidation.

In order to test the viability of the preparation of wire-like self-assemblies from comb-like poly-pincer molecules, it is necessary to first establish if a simple tweezer derived from a non-annulated *m*-terphenyl framework, with added degrees of rotational freedom, will possess any tweezer-like functionality, e.g. Scheme 3.1.

Scheme 3.1 Showing the different conformations of a simple tweezer derived from a non-annulated *m*-terphenyl platform.

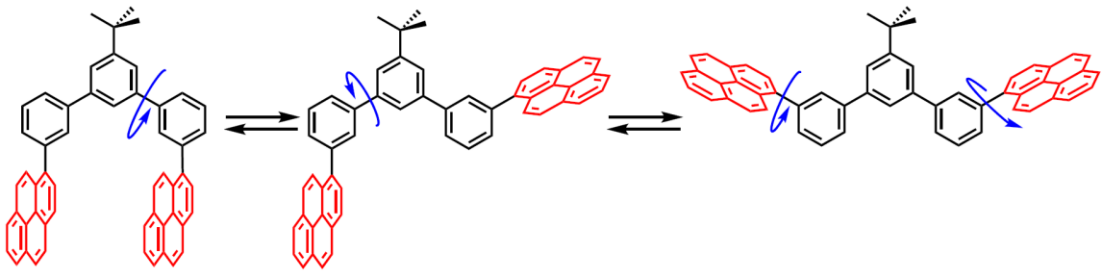

In order to address this question, we undertake the synthesis of two new tweezer platforms where one of them is completely rigid with appropriate provision for solubility by employing 9,9-dihexylfluorenyl moieties (Figure 3.5, left) and the other one is a simple *m*-terphenyl derivative containing *tert*-butyl as a solubilizing group (Figure 3.5, right).

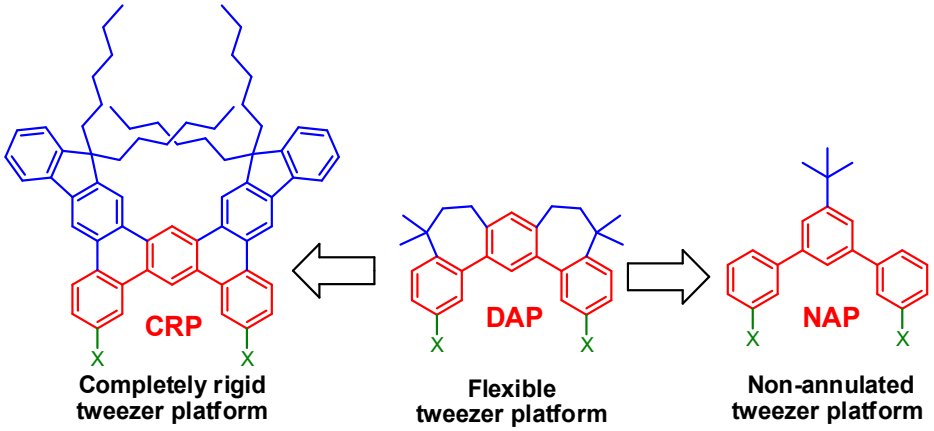

Figure 3.5 Proposed rigid (left) and non-annulated (right) tweezer platforms.

Accordingly in this chapter we will describe the successful synthesis of tweezers derived from completely rigid (**CRP**) and non-annulated platforms (**NAP**) and compare their functionality with tweezers derived from doubly-annulated platform (**DAP**) by EDA complexation studies. For example, a comparison of the binding efficiencies of DDQ to the tweezers derived from **DAP**, **CRP** and **NAP** platforms, containing pyrenyl pincers, will show that rigidification of the tweezer platform does not contribute in any significant way to the functionality of the **CRP** tweezer when compared to **DAP** tweezer. Furthermore, this comparison will also demonstrate that simple conformationally-mobile **NAP** tweezers retain some tweezer-like functionality toward binding the electron poor guests; interestingly, however, the one of the reversibly oxidized **NAP** tweezer undergoes ready self-association, with comparable efficiency to that of **DAP** tweezer, when prompted by 1-electron oxidation.

Based on these findings, we are actively pursuing the usages of both **DAP** and **NAP** platforms for the preparation of zig-zag and comb-like polypincer molecules for

self-assembled molecular wires (see Figures 3.2-3.4) as well as the molecules for 2-dimensional self-assemblies (vide infra). The preliminary details of these continuing efforts will also be described.

Result and Discussions

Synthesis of a pyrenyl tweezer from a completely rigid platform (CRP-Py).

As shown in Scheme 3.2 (below), the synthesis of the completely rigid tweezer platform (**CRP**) included the two important design criteria, i.e. an easy attachment of the pincers in one synthetic step and the ready solubility of the resulting tweezers.

Scheme 3.2 Synthesis of a pyrenyl tweezer from a completely rigid platform (CRP-Py).

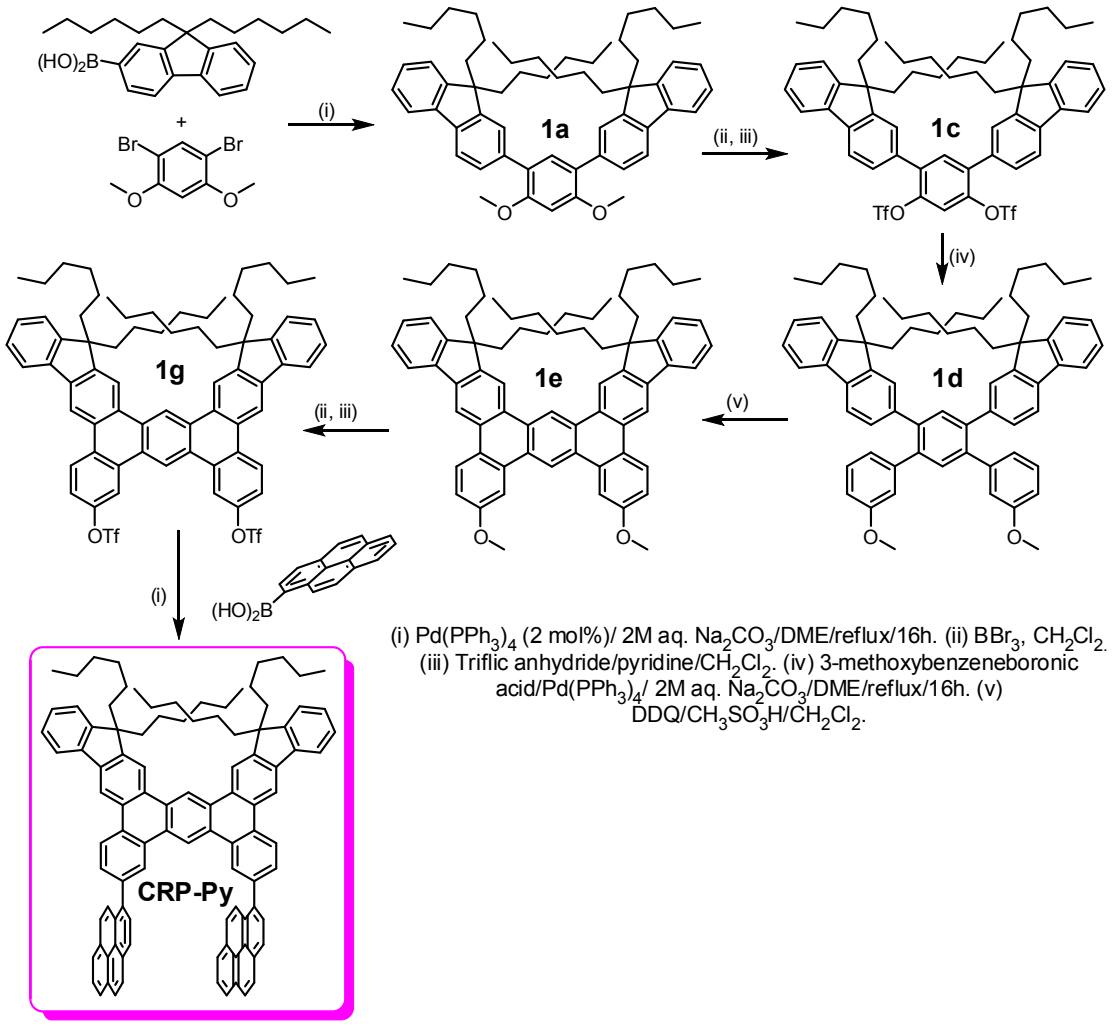

In order to include the sufficient solubility provision in the **CRP** tweezers, pair of doubly hexylated fluorenes was incorporated into the **CRP** platform. Thus, a standard Suzuki coupling reaction of 9,9-dihexylfluoreneboronic acid, generated in situ from the corresponding 9,9-dihexyl-2-bromofluorene, *n*-BuLi and $B(OMe)_3$ in THF, with 1,5-dibromo-2,4-dimethoxybenzene in the presence of a Pd(0) catalyst yielded **1a** in excellent yield. The conversion of the methoxy substituents to the corresponding

trifluoromethanesulfonates (i.e **1a** to **1c**) can be easily carried by a simple two-step transformation, i.e. a demethylation reaction using BBr_3 followed by reaction with triflic anhydride in a mixture of pyridine and dichloromethane. A standard Suzuki coupling[1] of **1c** with 3-methoxybenzoboronic acid in the presence of a Pd(0) catalyst afforded the desired **1d** in good yield. The oxidative cyclodehydrogenation of **1d** to **1e** using $FeCl_3$ as an oxidant afforded a complex mixture of products. However, the transformation of **1d** to **1e** can be successfully performed using a recently developed oxidant systems (i.e. DDQ in a mixture of methanesulfonic acid and dichloromethane) for the oxidative cyclodehydrogenation reactions.[2] A two-step conversion of the methoxy substituents of **1e** to the corresponding trifluoromethanesulfonates (i.e **1g**) afforded the CRP platform for the preparation of tweezers with a completely rigid platform. Indeed, a standard Suzuki coupling of 1g with 1-pyreneboronic acid in presence of Pd(0) catalyst afforded **CRP-Py** in excellent yield.

It is noted the tweezer **CRP-Py** derived from a completely rigid platform is completely soluble in common organic solvents and its structure was established by $^1H/^{13}C$ NMR spectroscopy and further confirmed by mass spectrometry.

Synthesis of a non-annulated *m*-terphenyl platform (NAP) and the NAP-based tweezers.

The synthesis of the simple non-annulated *m*-terphenyl platform (**NAP**), containing *tert*-butyl as a solubilizing group, was easily accomplished i.e. Scheme 3.3.

Scheme 3.3 Synthesis of a non-annulated *m*-terphenyl platform (NAP) and the NAP-based tweezers.

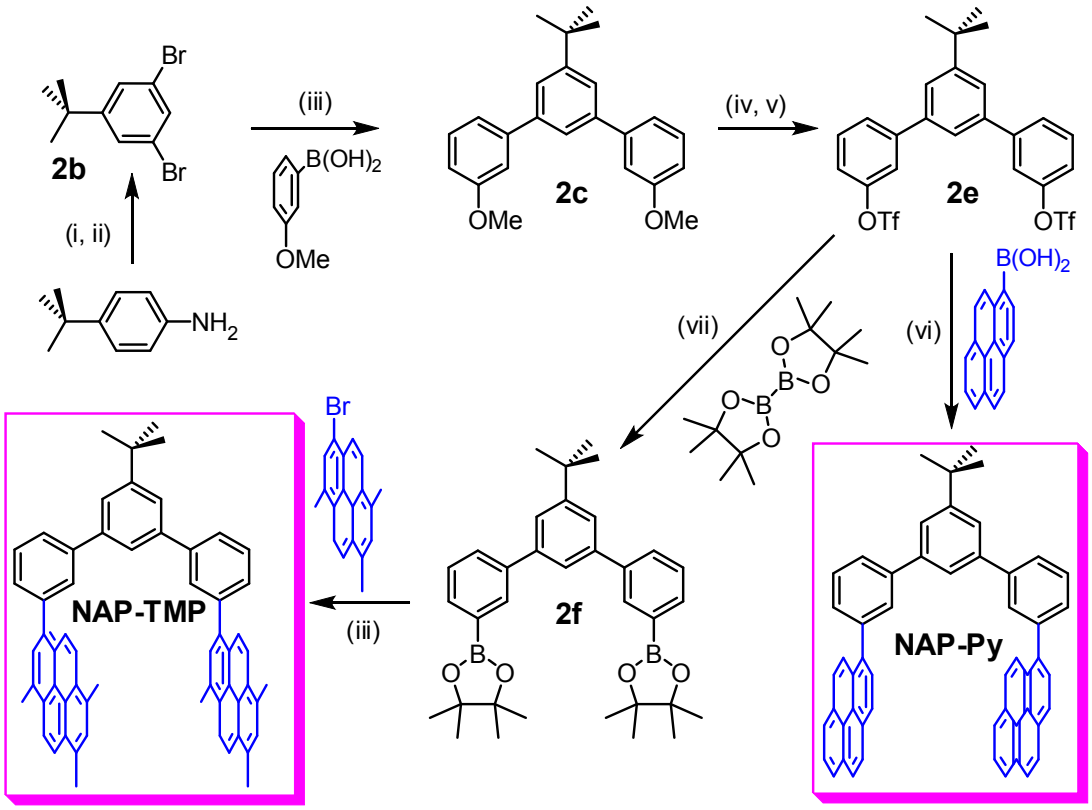

(i) Br_2/CH_2Cl_2-methanol (1:1). (ii) $NaNO_2/H_2SO_4$/ethanol/benzene. (iii) $Pd(PPh_3)_4$ (2 mol%)/2M aq. Na_2CO_3/DME/reflux. (iv) BBr_3/CH_2Cl_2. (v) Triflic anhydride/ pyridine/ CH_2Cl_2. (vi) $Pd(PPh_3)_4$ (2 mol%)/ 2M aq. Na_2CO_3/toluene/reflux. (vii) $PdCl_2(dppf)/Et_3N$/dioxane/reflux.

Thus, a solution of the commercially available 4-*tert*-butylaniline in a 1:1 mixture of dichloromethane and methanol (1:1) was treated dropwise with a solution of Br_2 in dichloromethane and the resulting mixture was stirred for 2 h. A standard aqueous workup afforded the diboromoaniline **2a** in nearly quantitative yield. The diboromoaniline **2a**, without additional purification, was further reacted with $NaNO_2$ and H_2SO_4 to furnish deaminated **2b** in good yield. A standard Suzuki coupling of 3-methoxybenzoboronic acid with **2b** in presence of Pd(0) catalyst afforded terphenyl **2c** in excellent yield. The conversion of methoxy substituents in **2c** to the corresponding

trifluoromethanesulfonates in **2e** was easily accomplished by a facile demethylation reaction using BBr_3 followed by reaction with triflic anhydride in a mixture of pyridine and dichloromethane. The non-annulated tweezer platform (**NAP**) was easily transformed into tweezer **NAP-Py** by its reaction with 1-pyreneboronic acid using reaction conditions employed for the standard Suzuki coupling.

Synthesis of a **NAP**-based tweezer containing reversibly-oxidized trimethylpyrene pincers (i.e. **NAP-TMP**) was accomplished by first transforming the ditriflete **2e** to the corresponding diboronic ester[3] **2f**, using bis(pinacoloto)diboron in the presence of triethylamine and $PdCl_2$(dppf) as a catalyst, followed by its reaction with bromotrimethylpyrene[4] under standard conditions employed for the Suzuki reaction to afford good yield of **NAP-TMP** (see Scheme 3.3).

The molecular structures of soluble **NAP** platform and **NAP-Py** and **NAP-TMP** tweezers were established by $^1H/^{13}C$ NMR spectroscopy and further confirmed by mass spectrometry.

Comparison of the binding efficiencies of DDQ as electron-poor guest to tweezers built on different platforms with a pair of pyrenyl pincers.

In the chapter 2, we described the EDA complexation studies of the doubly annulated tweezer **DAP-Py** (referred to as **T-Py** in Chapter 2) with different acceptors. These studies revealed that **DAP-Py** binds a variety of electron-poor guests with higher efficiency (e.g. **DAP-Py** with DDQ, K_{DA} = 415 M^{-1} and $\varepsilon_{899\ nm}$ ~70 M^{-1} $cm^{-}1$) than the corresponding model compound (e.g. **Ph-Py** with DDQ, K_{DA} = 23 M^{-1} and $\varepsilon_{909\ nm}$ ~147 M^{-1} cm^{-1}). Accordingly, herein the binding efficiencies of a completely rigid tweezer

CRP-Py and a non-annulated tweezer **NAP-Py** are compared with the doubly-annulated tweezer **DAP-Py** with the DDQ as a common electron acceptor as follows.

For example, the quantitative analysis of the binding of DDQ with all tweezers in solution was carried out by spectrophotometric analyses (see Figure 3.6) and the absorbance data were treated according to the Benesi-Hildebrand procedure[5]. The Benesi-Hildebrand plots of [**DDQ**]/Absorbance$_{CT}$ versus the reciprocal donor concentration (1/[**D**]) are compiled in Figure 3.6. The comparison of the values of association constants (K), extinction coefficient (ε_{CT}), and the "effective absorbance" ($K_{DA}\varepsilon_{CT}$) of the EDA complexes of all three tweezers (**CRP-Py**, **DAP-Py**, **NAP-Py**) are shown in Figure 3.6.

Comparison of both association constants (K) and "effective absorbance" ($K_{DA}\varepsilon_{CT}$) of various EDA complexes in Figure 3.6 clearly indicates that both completely rigid **CRP-Py** and semi-flexible doubly-annulated **DAP-Py** tweezers (K_{DA} = 415 and 401 M^{-1}, respectively) have very similar binding constants, whereas the non-annulated tweezer **NAP-Py** binds DDQ relatively poorly (K_{DA} = 73 M^{-1}) but retains some tweezer functionality and therefore can serve as a platform for the preparation of comb-like polypincer tweezers (vide infra).

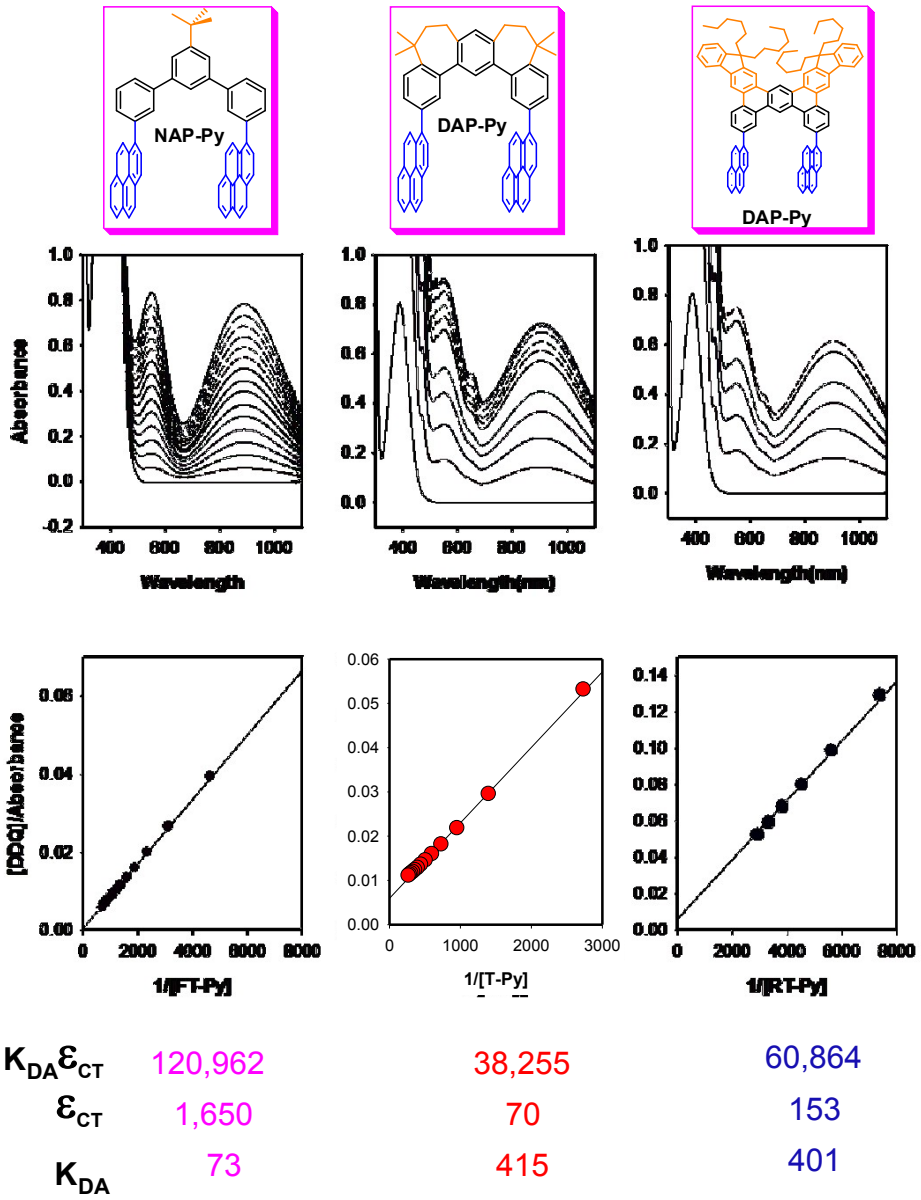

$K_{DA}\varepsilon_{CT}$	120,962	38,255	60,864
ε_{CT}	1,650	70	153
K_{DA}	73	415	401

Figure 3.6 Comparison of the binding effeciencies of DDQ to the tweezers **CRP-Py, DAP-Py, NAP-Py**.

Comparison of the efficiency of electron-transfer prompted self-assembly of non-annulated (NAP_TMP) and doubly-annulated (DAP-TMP) tweezers.

In the previous chapter we described the efficient electron-transfer prompted self-assembly of a doubly annulated tweezer containing trimethylpyrenes as pincers (i.e. **DAP-TMP**) by comparison with a model tetramethylpyrene donor. It was shown, by spectral titration, that a self-assembly between **DAP-TMP**$^{+\bullet}$ and neutral **DAP-TMP** was

complete at their equimolar concentration, while the completion of the dimerization process between **TMP**$^{+\bullet}$ and neutral **TMP** required its concentration to be 30 times larger i.e. eqs 1 and 2.

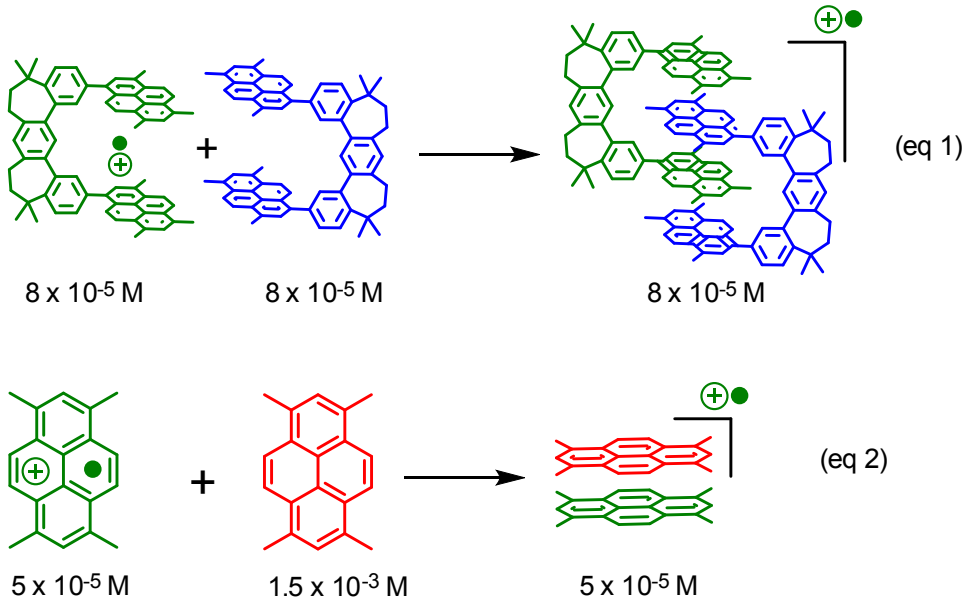

The effective dimerization of **DAP-TMP**$^{+\bullet}$ and neutral **DAP-TMP** was attributed to efficient charge delocalization amongst four cofacially arrayed TMP moieties. As such this conclusion was further supported by a significant red shift of the inter-valence transition in dimeric (**DAP-TMP**)$_2^{+\bullet}$ when compared to the model (**TMP**)$_2^{+\bullet}$ in which a single charge is delocalized only over two cofacially arrayed pyrenyl moieties.

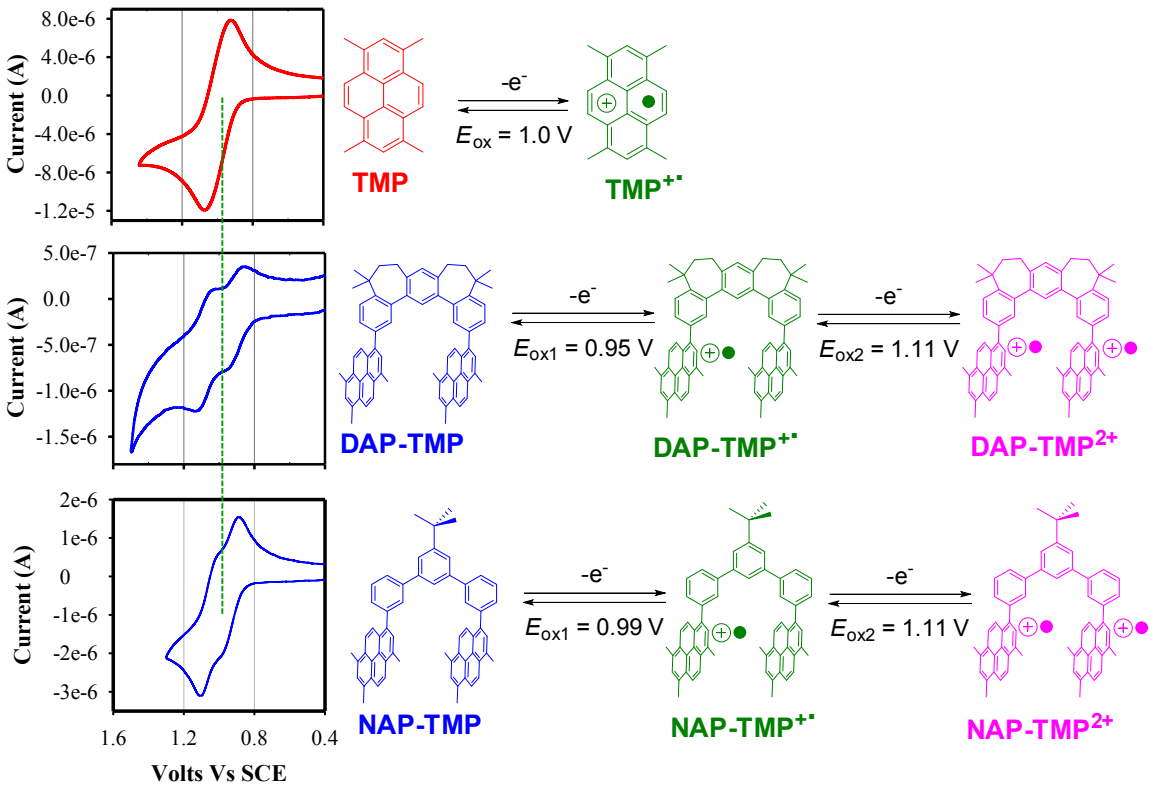

Figure 3.7 Comparison of the cyclic voltammograms of the 2 mM solution of the tweezers **DAP-Py** and **NAP-Py** and model **TMP** in dichloromethane containing 0.1 M *n*-Bu_4NPF_6 as the supporting electrolyte at a scan rate of v = 100 mV s^{-1} at 22 ^oC.

Accordingly, non-annulated tweezer **NAP-TMP** was subjected to the electrochemical oxidation at platinum electrode as a 2 mM solution in dichloromethane containing 0.1 M *n*-Bu_4NPF_6 as a supporting electrolyte. The cyclic voltammogram of **NAP-TMP** meets the all reversibility criteria (as discussed in the previous chapter) and is compared with the cyclic voltammograms of **DAP-TMP** as well as model **TMP** (see Figure 3.7).

The observation of two reversible oxidation waves in the CV of **NAP-TMP** similar to those observed in the CV of **DAP-TMP** (Figure 3.7) at the potentials of 0.99

and 1.11 V versus SCE (ΔE = 0.12 V vs. SCE) suggest that after removal of first electron from **NAP-TMP**, its cation radical must exist largely in the tweezer-like conformation, i.e. structure on the left in Scheme below.

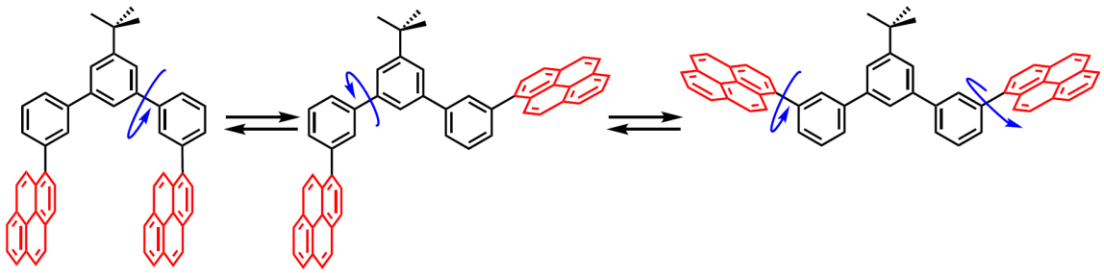

As such the cyclic votammetric observation that **NAP-TMP** cation radical exists largely in tweezer-like conformation is further supported by similar efficiency of both **NAP-TMP** and **DAP-TMP** cation radicals with their neutral counterparts as shown in Figure 3.8. It is noted that partial self-assembly between **NAP-TMP** cation radical and neutral is more or less complete upon addition of 1.0 equivalent (or equimolar) of neutral **NAP-TMP** tweezer and suggests that formation of $(\mathbf{NAP\text{-}TMP})_2^{+\bullet}$ cation radical is as efficient as the formation of $(\mathbf{DAP\text{-}TMP})_2^{+\bullet}$ cation radical (see Figure 3.8). The effective dimerization of $\mathbf{NAP\text{-}TMP}^{+\bullet}$ and neutral **NAP-TMP** was further inferred by the observation of similarly red-shift inter-valence transition as that observed in the dimeric $(\mathbf{DAP\text{-}TMP})_2^{+\bullet}$ (see Figure 3.8).

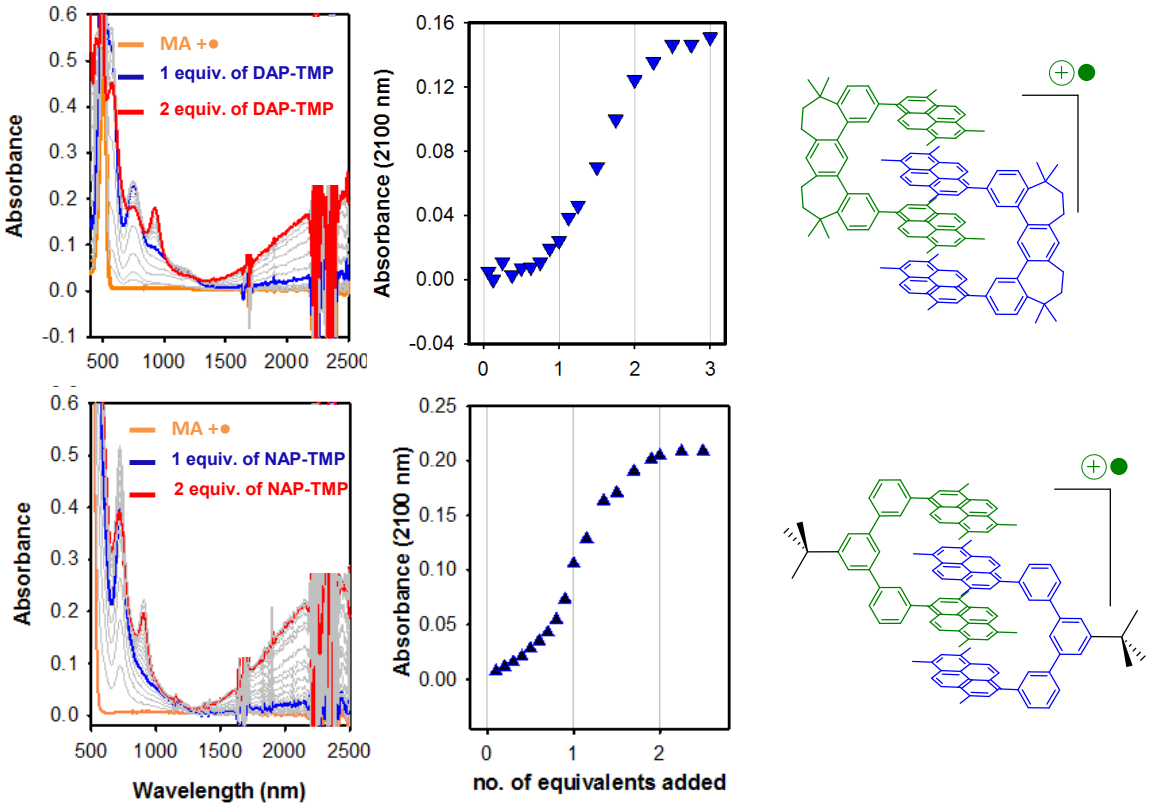

Figure 3.8 **Top: (right)** Spectral changes upon the reduction of 0.8 x10^{-4} M $MA^{+\bullet}$[6] by an incremental addition of a concentrated solution of **DAP-TMP** and **(left)** a plot of increase of absorbance of dimeric **$(DAP\text{-}TMP)_2^{+\bullet}$** against the equivalents of added neutral **DAP-TMP**. **Bottom: (right)** Spectral changes upon the reduction of 1.6 x10^{-4} M $MA^{+\bullet}$ by an incremental addition of a concentrated solution of **NAP-TMP** and **(left)** a plot of increase of absorbance of dimeric **$(NAP\text{-}TMP)_2^{+\bullet}$** against the equivalents of added neutral **NAP-TMP.**

Thus, the efficient self-assembly of **NAP-TMP**, prompted by 1-electron oxidation is further summarized by the cartoon representation in Scheme 3.3.

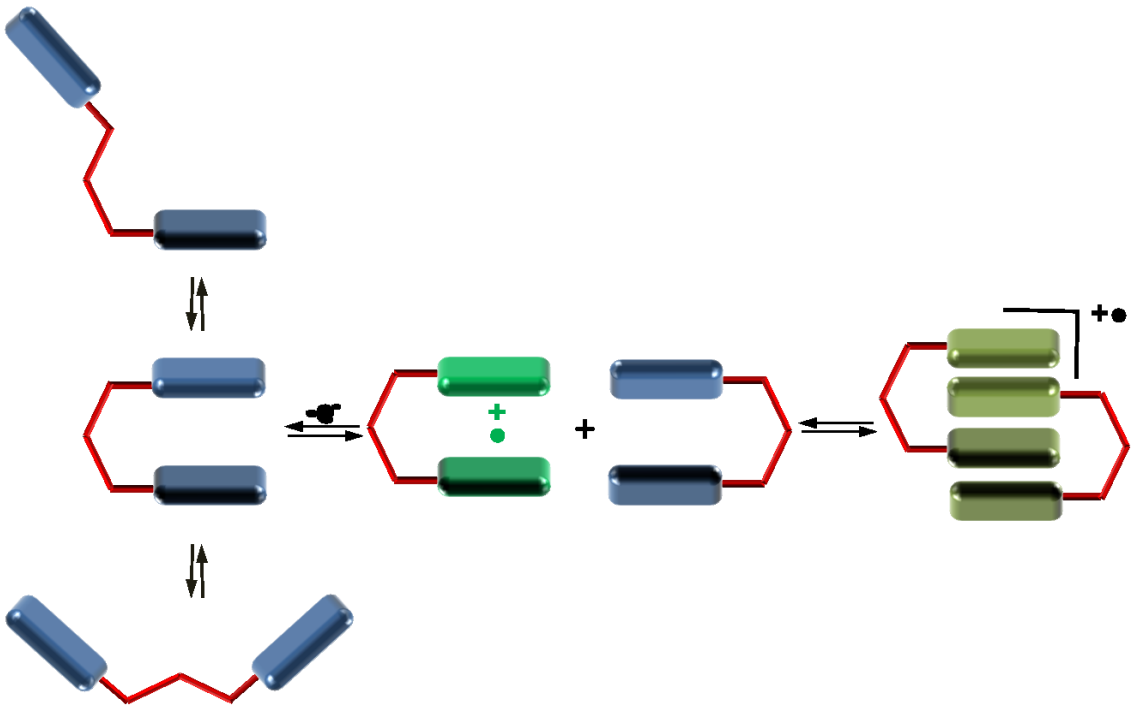

Figure 3.9 Cartoon diagram of the dimer cation radical formation of **NAP-TMP** with $CRET^{+\bullet}SbCl_6$.

Summary. A successful synthesis of the tweezers derived from completely rigid (**CRP**) and non-annulated platforms (**NAP**) and comparison of their functionality with tweezers derived from doubly-annulated platform (**DAP**) by EDA complexation studies established that rigidification of the tweezer platform does not contribute in any significant way to the functionality of the tweezers. Moreover, a comparative study of electron transfer prompted self-assembly of the **NAP-TMP** and **DAP-TMP** tweezers established that they both undergo ready self-association with comparable efficiency.

Experimental section

General Experimental Methods and Materials. All reactions were performed under argon atmosphere unless otherwise noted. All commercial reagents were used without further purification unless otherwise noted. Dichloromethane (Aldrich) was repeatedly stirred with fresh aliquots of concentrated sulfuric acid (~10 % by volume) until the acid layer remained colorless. After separation it was washed successively with water, aqueous sodium bicarbonate, water, and aqueous sodium chloride and dried over anhydrous calcium chloride. The dichloromethane was distilled twice from P_2O_5 under an argon atmosphere and stored in a Schlenk flask equipped with a Teflon valve fitted with Viton O-rings. The hexanes and toluene were distilled from P_2O_5 under an argon atmosphere and then refluxed over calcium hydride (~12 h). After distillation from CaH_2, the solvents were stored in Schlenk flasks under an argon atmosphere. Tetrahydrofuran (THF) was dried initially by distilling over lithium aluminum hydride under an argon atmosphere. The THF was further refluxed over metallic sodium in the presence of benzophenone until a persistent blue color was obtained and then it was distilled under an argon atmosphere and stored in a Schlenk flask equipped with a Teflon valve fitted with Viton O-rings. NMR spectra were recorded on Varian 300 and 400 MHz NMR spectrometers. GC-MS spectra were obtained on a Fisons 8000 trio instrument at an ionization potential of 70 eV.

Cyclic Voltammetry (CV). The CV cell was of an air-tight design with high vacuum Teflon valves and Viton O-ring seals to allow an inert atmosphere to be maintained without contamination by grease. The working electrode consisted of an adjustable

platinum disk embedded in a glass seal to allow periodic polishing (with a fine emery cloth) without changing the surface area (~1 mm2) significantly. The reference SCE electrode (saturated calomel electrode) and its salt bridge were separated from the catholyte by a sintered glass frit. The counter electrode consisted of platinum gauze that was separated from the working electrode by ~3 mm. The CV measurements were carried out in a solution of 0.2 M supporting electrolyte (tetra-*n*-butylammonium hexafluorophosphate, TBAH) and 2-5 x 10^{-3} M substrate in dry dichloromethane under an argon atmosphere. All the cyclic voltammograms were recorded at a sweep rate of 200 mV sec^{-1}, unless otherwise specified and were IR compensated. The oxidation potentials ($E_{1/2}$) were referenced to SCE, which was calibrated with added (equimolar) ferrocene ($E_{1/2}$ = 0.450 V *vs*. SCE). The $E_{1/2}$ values were calculated by taking the average of anodic and cathodic peak potentials in the reversible cyclic voltammograms.

Synthesis of Compounds:

Preparation of 1a:

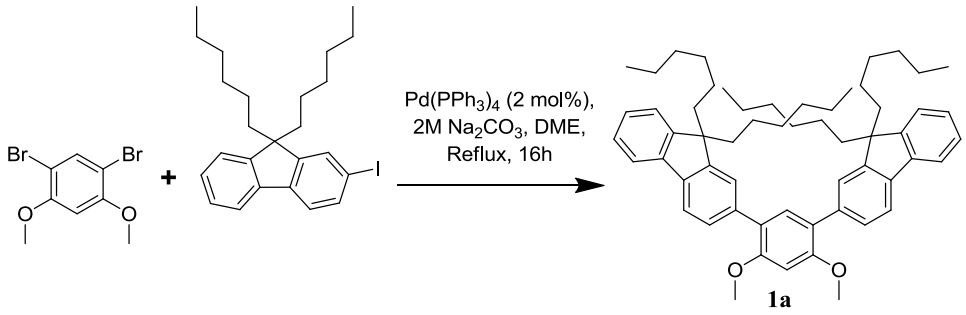

In a Schlenk flask under an argon atmosphere iodofluorene (11.2 g, 24.33 mmol) was dissolved in dry THF (40 mL). The solution was cooled to -78 ^{o}C using acetone and dry ice bath. n-BuLi was added dropwise making sure that temperature will not raise above -

70 ^{o}C. The solution was stirred at -78 ^{o}C .After an hour trimethyl borate (8.15 mL, 73 mmol) was added dropwise to the solution and stirred overnight allowing it to come to the room temperature. Next day the solution of 1,5-dibromo-2,4-dimethoxybenzene (2.4 g, 8.11 mmol) in toluene (40 mL) and ethanol (40 mL) was added in the reaction mixture. In another oven dried Schlenk flask a solution of anhydrous sodium carbonate (5.0 g) in water (20 mL) was prepared under an argon atmosphere and the flask was evacuated and refilled with argon (3x). To the reaction mixture, $Pd(PPh_3)_4$ (50 mg) and the salt solution were added sequentially under a strict argon atmosphere followed by evacuation and refilling the flask with argon (3x) after each addition. The flask was covered with aluminum foil and the solution was allowed to reflux overnight. The resulting solution was cooled to room temperature, quenched with water (50 mL) and extracted with dichloromethane (3 x 50 mL). The organic layer was dried over anhydrous magnesium sulfate, evaporated and dried under vacuum. The product thus formed was purified by column chromatography using a hexanes/ethyl acetate mixture as the eluent. Yield (4.5 g, 40%) ^{1}H NMR ($CDCl_3$) δ : 7.73 (4H, t, J = 6.79 Hz), 7.58 (2H, s), 7.56 (1H, d, J = 1.53 Hz), 7.54 (1H, d, J = 1.53 Hz), 7.50 (1H, s), 7.33 (6H, m), 6.73 (1H, s), 3.90 (6H, s), 1.98 (8H, m), 1.10 (24H, m), 0.77 (20H, t, J =7.18 Hz). ^{13}C NMR ($CDCl_3$) δ: 14.22, 22.82, 24.08, 30.02, 31.75, 40.53, 55.18, 56.35, 119.43, 119.80, 123.05, 124.33, 124.52, 126.88, 126.94, 128.16, 132.93, 136.99, 139.76, 141.23, 150.54, 151.32, 157.05.

Preparation of 1b:

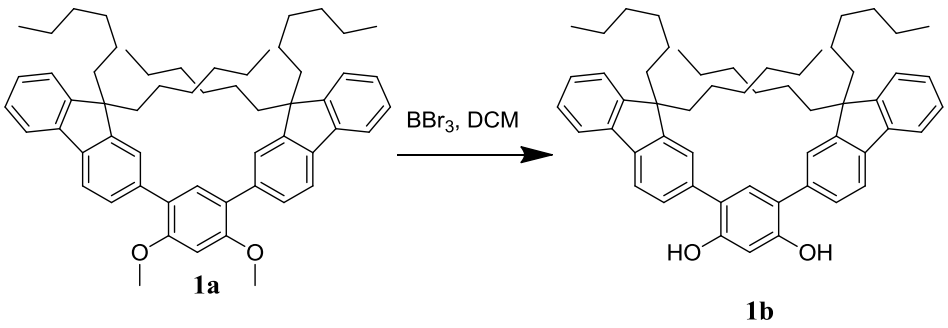

1a **1b**

The solution of diether **1a** (4.5 g, 5.60 mmol) in DCM (50 mL) was cooled to -10 ^{o}C under argon atmosphere using ice-acetone bath. The solution of BBr_3 (3.2 mL, 33.61 mmol) in DCM (10 mL) was added to the above cooled solution drop wise over a period of 30 min. The mixture was gradually warmed to room temperature and stirred for 2 hrs. The reaction was quenched with water (50 mL) and extracted with dichloromethane (3 x 20 mL). The organic layer was dried over anhydrous magnesium sulfate, evaporated and dried under vacuum**.** The product **1b** formed (4.0 g, 92.1%) was immediately subjected to the next step without any further purification.

Preparation of 1c:

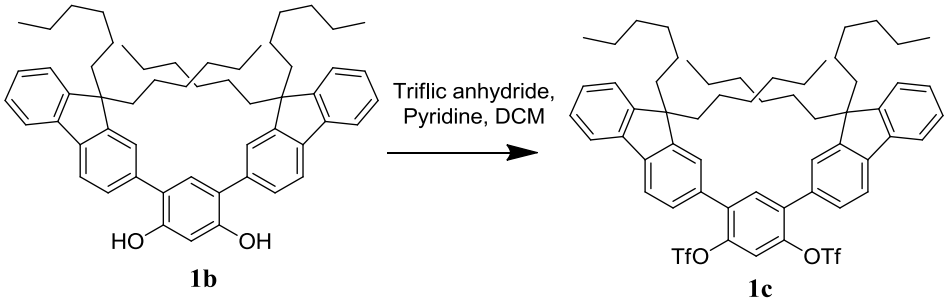

1b **1c**

In a Schlenk flask under an argon atmosphere **1b** (4 g, 5.16 mmol) and pyridine (1.3 mL, 15.48 mmol) were dissolved in dry DCM (50 mL). Cool the solution to -10 ^{o}C with ice-acetone bath. Triflic anhydride (2.02 mL, 12.38 mmol) in of DCM (10 mL) in a dropping funnel was added to the above cooled solution over a period of 10 min. The reaction mixture was stirred for 6 hrs at 0 ^{o}C. Then it was concentrated on the rotary evaporator. The residual brown oil was diluted with ethyl acetate. Washed with 5% HCl followed by sat. NaCl and sodium bicarbonate. The organic layer was dried over anhydrous magnesium sulfate, evaporated and dried under vacuum**.** The product formed was purified by Column chromatography using a hexanes/ethyl acetate mixture as the eluent. Yield (4.6 g, 86.7%). m.p. 128-130 ^{o}C. ^{1}H NMR ($CDCl_3$) δ : 7.82 (2H, d, *J* = 8.15 Hz), 7.75 (2H, m), 7.72(1H, s), 7.49 (4H, d, *J* = 3.33 Hz), 7.47 (1H, d, *J* = 1.49 Hz), 7.38 (4H, d, *J* = 3.33 Hz), 7.36 (2H, s), 2.01 (8H, t, *J* = 8.15 Hz), 1.08 (24H, m), 0.75 (12H, t, *J* = 6.65 Hz), 0.65 (8H, m). ^{13}C NMR ($CDCl_3$) δ: 14.16, 22.75, 23.90, 29.88, 31.70, 40.61, 55.61, 120.20, 120.21, 120.34, 123.18, 124.04, 127.11, 127.93, 128.39, 132.78, 134.76, 136.95, 140.34, 142.34, 145.37, 151.31, 151.64.

Preparation of 1d:

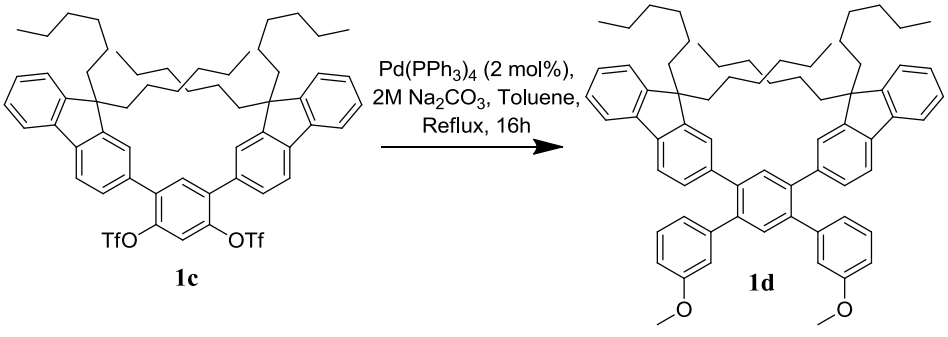

Ditriflate compound **1c** (3.2 g, 3.08 mmol) and 3-methoxybenzoboronic acid (1.41 g, 9.24 mmol) were dissolved in anhydrous toluene (40 mL) in an oven dried Schlenk flask under an argon atmosphere and the flask was evacuated and refilled with argon (3x). In another oven dried Schlenk flask a solution of anhydrous sodium carbonate (5.0 g) in water (20 mL) was prepared under an argon atmosphere and the flask was also evacuated and refilled with argon (3x). To the toluene solution, $Pd(PPh_3)_4$ (50 mg) and the salt solution were added sequentially under a strict argon atmosphere followed by evacuation and refilling the flask with argon (3x) after each addition. The flask was covered with aluminum foil and the solution was allowed to reflux overnight. The resulting solution was cooled to room temperature, quenched with water (50 mL) and extracted with dichloromethane (3 x 50 mL). The organic layer was dried over anhydrous magnesium sulfate, evaporated and dried under vacuum. The product was further purified by column chromatography using a hexanes/ethyl mixture as the eluent to give the pure product **1d** (2.72 g, 92.5%) m.p. 156-158 ^{o}C. ^{1}H NMR ($CDCl_3$) δ : 7.86 (5H, m), 7.60(1H, s), 7.41(2H, dd, *J* = 7.85,1.57 Hz), 7.29 (6H, m), 7.14 (2H, d, *J* = 7.85 Hz), 7.11 (2H, d, *J* = 1.57 Hz), 6.88 (2H, d, *J* = 7.85 Hz), 6.85 (2H, s), 6.74 (2H, dd, *J* = 7.85,2.35 Hz), 1.75 (8H, m), 1.12 (12H, m), 0.77 (12H, t, *J* = 7.29 Hz), 0.51 (8H, m). ^{13}C NMR ($CDCl_3$) δ:14.30, 22.94, 23.89, 30.01, 31.75, 40.58, 55.12, 55.30, 113.16, 115.24, 119.65, 119.90, 122.63, 123.09, 125.09, 126.92, 127.17, 128.47, 129.17, 133.16, 133.18, 139.77, 139.95, 139.96, 140.53, 141.01, 142.78, 150.62, 151.16, 159.41.

Preparation of 1e:

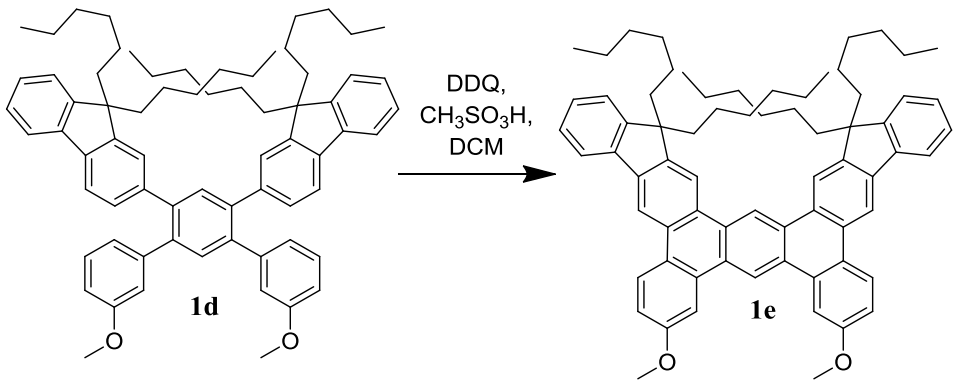

In a Schlenk flask under an argon atmosphere, compound **1d** (0.3 g, 0.31 mmol) was dissolved in DCM (18 mL) and the solution was cooled to 0 ^{o}C. To the above solution DDQ (0.14 g, 0.63 mmol) and methane sulfonic acid (2 mL) were added. The solution was stirred for 30min at 0 ^{o}C, saturated $NaHCO_3$ was added and the product was extracted with DCM. The product was further purified by column chromatography using a hexanes/ethyl acetate mixture as the eluent to give the pure product **1e** (0.160 g, 54%) m.p. 108-110 ^{o}C. ^{1}H NMR ($CDCl_3$) δ: 9.97(1H, s), 9.62(1H, s), 8.87 (4H, d, J = 3.35 Hz), 8.70 (2H, d, J = 9.26 Hz), 8.22 (2H, d, J = 2.56 Hz), 7.99 (2H, dd, J = 5.94 Hz, 1.74 Hz), 7.48 (6H, m), 7.31 (2H, dd, J = 8.97 Hz, 2.56 Hz), 4.04 (6H, s), 2.27 (8H, m), 1.15 (24H, m), 0.90 (8H, m), 0.75 (12H, t, J = 6.25 Hz). ^{13}C NMR ($CDCl_3$) δ : 14.16, 22.77, 24.20, 30.04, 31.72, 41.27, 55.33, 55.78, 107.03, 113.80, 115.32, 117.35, 120.36, 123.32, 124.80, 125.42, 127.27, 127.96, 128.35, 128.59, 129.97, 130.02, 131.47, 140.92, 141.47, 149.40, 151.72, 159.09.

Preparation of 1f:

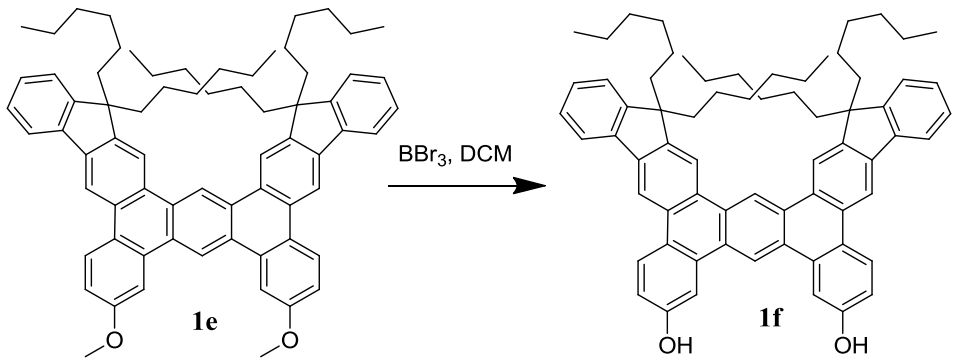

A solution of diether **1e** (0.64 g, 0.67 mmol) in DCM (15 mL) was cooled to -10 ^{o}C under an argon atmosphere using ice-acetone bath. A solution of BBr_3 (0.4 mL, 4.03 mmol) in DCM (10 mL) was added to the above cooled solution dropwise over a period of 30 min. The mixture was gradually warmed to room temperature and stirred for 2 hrs. The reaction was quenched with water (50 mL) and extracted with dichloromethane (3 x 20 mL). The organic layer was dried over anhydrous magnesium sulfate, evaporated and dried under vacuum**.** The product formed **1f** (0.62 g, 99%) was immediately subjected to the next step without any further purification. ^{1}H NMR ($CDCl_3$) δ: 9.91 (1H, s), 9.61 (1H, s), 8.82 (4H, d, J = 3.35 Hz), 8.65 (2H, d, J = 9.26 Hz), 8.31 (2H, s), 7.94 (2H, d, J = 5.94 Hz), 7.45 (6H, m), 7.24 (2H, s), 2.23 (8H, m), 1.09 (24H, m), 0.85 (8H, m), 0.71 (12H, t, J = 6.25 Hz).

Preparation of 1g:

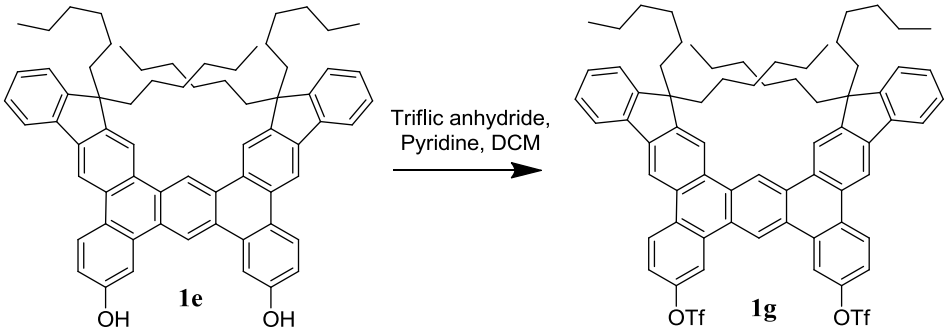

In a Schlenk flask under an argon atmosphere **1e** (0.62 g, 0.67 mmol) and pyridine (0.4 mL, 2.01 mmol) were dissolved in dry DCM (30 mL). The solution was cooled to -10 ^{o}C with ice-acetone bath. Triflic anhydride (0.3 mL, 1.61 mmol) in DCM (10 mL) in a dropping funnel was added to the above cooled solution over a period of 10 min. The reaction mixture was stirred for 6 hrs at 0 ^{o}C and then concentrated the reaction mixture on rotary evaporator. The residual brown oil was diluted with ethyl acetate. Washed with 5% HCl followed by sat. NaCl and sodium bicarbonate. The organic layer was dried over anhydrous magnesium sulfate, evaporated and dried under vacuum**.** The product **1g** formed (0.65 g, 82.2%) was purified by Column chromatography using a hexanes/ethyl acetate mixture as the eluent. m.p. 164-166 ^{o}C. ^{1}H NMR ($CDCl_3$) δ : 10.01 (1H, s), 9.59 (1H, s), 8.91 (6H, dd, *J* = 8.91 Hz), 8.74 (2H, d, *J* = 2.25 Hz), 8.02 (2H, d, *J* = 7.52 Hz), 7.68 (2H, dd, *J* = 8.84 Hz, 2.44 Hz), 7.49 (6H, m), 2.26 (8H, m), 1.13 (24H, m), 0.843 (8H, m), 0.73 (12H, t, *J* = 6.96 Hz). ^{13}C NMR ($CDCl_3$) δ : 22.73, 24.17, 29.97, 31.69, 41.19, 55.58, 114.62, 115.88, 117.58, 118.38, 118.53, 120.57, 120.82, 123.43, 126.34, 127.49, 127.59, 128.54, 128.92, 129.38, 130.71, 130.73, 131.48, 140.29, 142.30, 149.05, 151.21, 151.62.

Preparation of CRP-Py:

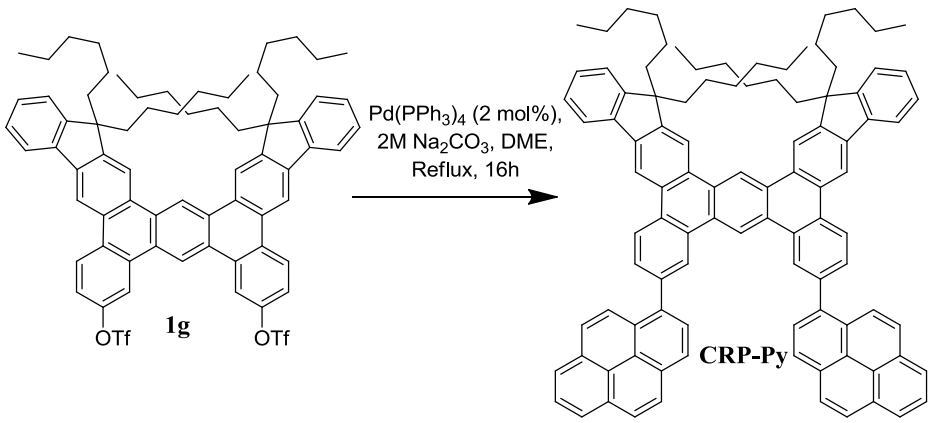

Ditriflate compound **1g** (0.350 g, 0.3 mmol) and pyrene-1-boronic acid (0.39 g, 1.2 mmol) were dissolved in anhydrous toluene (15 mL) in an oven dried Schlenk flask under an argon atmosphere and the flask was evacuated and refilled with argon (3x). In another oven dried Schlenk flask a solution of anhydrous sodium carbonate (2.5 g) in water (10 mL) was prepared under an argon atmosphere and the flask was also evacuated and refilled with argon (3x). To the toluene solution, $Pd(PPh_3)_4$ (50 mg) and the salt solution were added sequentially under a strict argon atmosphere followed by evacuation and refilling the flask with argon (3x) after each addition. The flask was covered with aluminum foil and the solution was allowed to reflux overnight. The resulting solution was cooled to room temperature, quenched with water (50 mL) and extracted with dichloromethane (3 x 20 mL). The organic layer was dried over anhydrous magnesium sulfate, evaporated and dried under vacuum. The product was further purified by column chromatography using a hexanes/ethyl acetate mixture as the eluent to give the pure product **CRP-Py** (0.25 g, 65%) m.p. 220-240 ^{o}C. ^{1}H NMR ($CDCl_3$) δ: 8.92 (2H, m), 8.75 (2H, m), 8.63 (2H, m), 8.34 (5H, m), 8.16 (3H, s), 7.60 (10H, m), 7.35 (4H, m), 6.96

(10H, m), 2.51 (8H, t), 1.56 (8H, broad), 1.37 (24H, broad), 0.87 (12H, broad). ^{13}C NMR ($CDCl_3$) δ :14.32, 23.10, 24.88, 30.77, 32.22, 41.72, 55.23, 113.58, 117.19, 120.50, 123.25, 123.60, 123.89, 123.90, 124.03, 124.06, 124.30, 125.14, 125.84, 125.84, 125.86, 126.09, 126.30, 126.32, 126.33, 126.74, 126.74, 127.42, 127.66, 127.67, 127.68, 127.87, 128.59, 128.62, 129.09, 129.61, 130.05, 130.93, 137.12, 139.01, 140.50, 141.22, 151.76, 151.77.

Preparation of 2a:

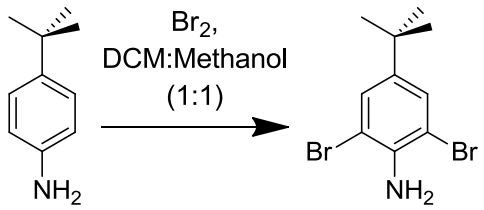

2a

To a stirred solution of *p*-tert-butyl aniline (4.0 g, 26.84 mmol) in 1:1 mixture of DCM: methanol (50:50 mL) was added a solution of bromine (10.73 g, 67.11 mmol) in mixture of DCM: methanol (10:10 mL). The reaction mixture was stirred for 2 hrs. After 2 hrs solvent was evaporated, washed with 20% NaOH and extracted with ether. The solution was dried over anhydrous $MgSO_4$ and solvent was evaporated to give the product **2a** as a purple oil (8.24 g, 99%).^{1}H NMR ($CDCl_3$) δ: 7.37 (2H, s), 4.40 (2H, s), 1.25 (9H, s). ^{13}C NMR ($CDCl_3$) δ: 31.47, 34.31, 108.94, 129.08, 139.67, 143.25.

Preparation of 2b:

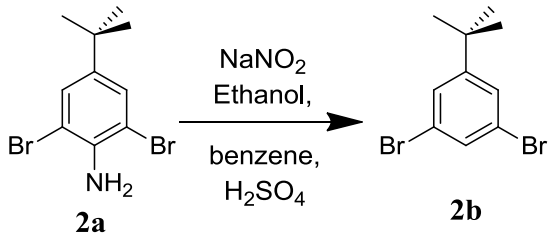

2a **2b**

To a stirred solution of 2,6-Dibromo-4-tert-butylaniline (8.24 g, 26.84 mmol) in a mixture of ethanol (50 mL) and benzene (17 mL) concentrated H_2SO_4 (4.5 mL) and $NaNO_2$ were added and the mixture was refluxed for 3 hrs. The solution was cooled to the room temperature, quenched with water and extracted with ether. The organic layer was dried over anhydrous $MgSO_4$. Evaporation of solvent afforded crude brown product which upon passing through column with hexane afforded slightly yellow oily product **2b** (6.0 g, 76.6%). ^{1}H NMR ($CDCl_3$) δ: 7.48 (1H, t, J = 1.74 Hz), 7.43 (2H, d, J = 1.74 Hz), 1.29 (9H, s). ^{13}C NMR ($CDCl_3$) δ: 31.20, 35.21, 122.94, 127.72, 131.31, 155.35.

Preparation of 2c:

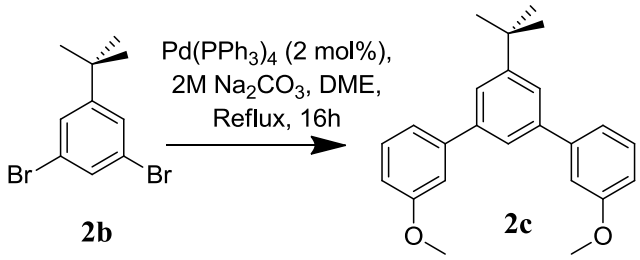

2b **2c**

1,3-dibromo-5-tert-butylbenzene compound **2b** (3.0 g, 10.27 mmol) and the 3-methoxybenzoboronic acid (4.68 g, 30.82 mmol) were dissolved in anhydrous 1,2-dimethoxyethane (DME) (60 mL) in an oven dried Schlenk flask under an argon atmosphere and the flask was evacuated and refilled with argon (3x). In another oven

dried Schlenk flask a solution of anhydrous sodium carbonate (5.0 g) in water (20 mL) was prepared under an argon atmosphere and the flask was also evacuated and refilled with argon (3x). To the DME solution, $Pd(PPh_3)_4$ (50 mg) and the salt solution were added sequentially under a strict argon atmosphere followed by evacuation and refilling the flask with argon (3x) after each addition. The flask was covered with aluminum foil and the solution was allowed to reflux overnight. The resulting solution was cooled to room temperature, quenched with water (50 mL) and extracted with dichloromethane (3 x 50 mL). The organic layer was dried over anhydrous magnesium sulfate, evaporated and dried under vacuum. The product was purified by column chromatography using a hexanes/ethyl acetate mixture to afford the pure product **2e** (3.0 g, 84.50%); ^{1}H NMR ($CDCl_3$) δ: 7.59 (3H, s), 7.39 (2H, t, *J* = 7.95 Hz), 7.25 (1H, t, *J* = 1.22 Hz), 7.22 (1H, t, *J* = 1.22 Hz), 7.18 (2H, t, *J* = 1.68 Hz), 6.92 (2H, dd, *J* = 8.19 Hz, 2.59 Hz), 3.88 (6H, s), 1.42 (9H, s). ^{13}C NMR ($CDCl_3$) δ :31.64, 35.13, 55.41, 112.64, 113.47, 119.83, 120.08, 123.81, 129.93, 141.61, 143.46, 152.24, 160.09.

Preparation of 2d:

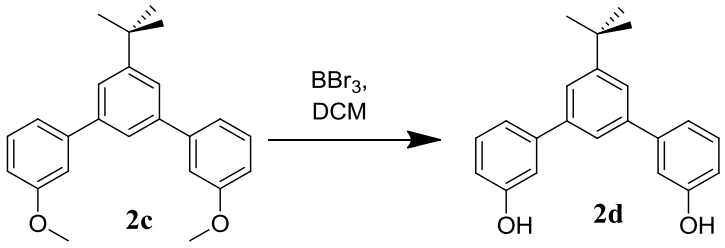

A solution of diether **2c** (3 g, 8.66 mmol) in DCM (70 mL) was cooled to -10 ^{o}C under argon atmosphere using an ice-acetone bath. The solution of BBr_3 (5.40 mL, 57.13 mmol) in DCM (10 mL) was added to the above cooled solution dropwise over a period of 30

min. The mixture was gradually warmed to room temperature and stirred for 2 hrs. The reaction was quenched with water (50 mL) and extracted with dichloromethane (3 x 20 mL). The organic layer was dried over anhydrous magnesium sulfate, evaporated and dried under vacuum**.** The product **2d** formed (2.75 g, 99%) was immediately subjected to the next step without any further purification. ^{1}H NMR ($CDCl_3$) δ : 7.57 (3H, s), 7.33 (2H, t, *J* = 7.80 Hz), 7.23 (1H, t, *J* = 1.03 Hz), 7.20 (1H, t, *J* = 1.03 Hz), 7.12 (2H, t, *J* = 1.76 Hz), 6.84 (2H, dd, *J* = 7.99, 2.52 Hz), 4.93 (2H, Broad s), 1.41 (9H, s).

Preparation of 2e:

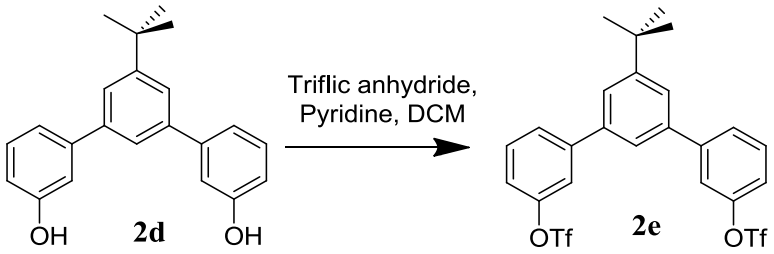

In a Schlenk flask under an argon atmosphere **2d** (2.75 g, 8.63 mmol) and pyridine (2.08 mL, 25.89 mmol) were dissolved in dry DCM (100 mL). The solution was cooled to -10 ^{o}C with an ice-acetone bath. Triflic anhydride (3.53 mL, 21.59 mmol) in DCM (10 mL) in a dropping funnel was added to the above cooled solution over 10 min under Ar. The reaction mixture was stirred for 6 hrs at 0 ^{o}C and then concentrated on rotary evaporator. the residual brown oil was diluted with ethyl acetate, washed with 5% HCl followed by sat. NaCl and sodium bicarbonate solution. The organic layer was dried over anhydrous magnesium sulfate, evaporated and dried under vacuum**.** The product **2e** formed (4.52 g, 90.0%) was purified by Column chromatography. ^{1}H NMR ($CDCl_3$) δ: 7.65 (2H, d, *J* = 7.96 Hz), 7.59 (2H, t, *J* = 1.7 Hz), 7.55 (1H, s), 7.51 (3H, m), 7.29 (2H,

d, *J* = 7.96 Hz), 1.44 (9H, s). ^{13}C NMR ($CDCl_3$) δ: 31.57, 35.28, 120.27, 120.48, 123.78, 124.64, 127.59, 130.81, 140.08, 144.34, 150.21, 153.27.

Preparation of NAP-Py:

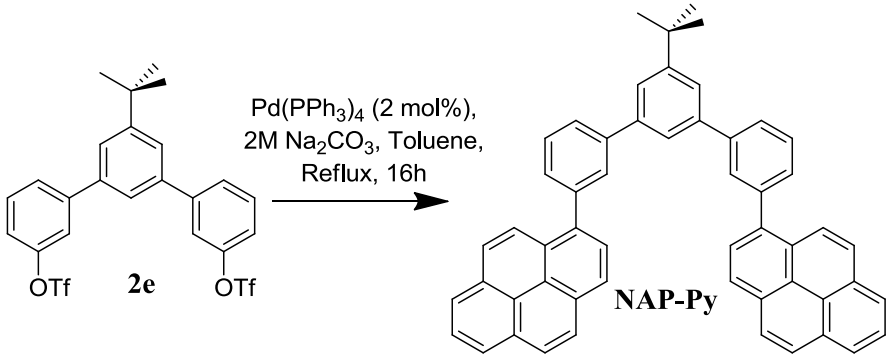

Ditriflate compound **2e** (0.5 g, 0.85 mmol) and1-pyreneboronicacid (3 equiv,0.63 g, 2.57 mmol) were dissolved in anhydrous toluene (40 mL) in an oven dried Schlenk flask under an argon atmosphere and the flask was evacuated and refilled with argon (3x). In another oven dried Schlenk flask a solution of anhydrous sodium carbonate (2.5 g) in water (10 mL) was prepared under an argon atmosphere and the flask was also evacuated and refilled with argon (3x). To the above toluene reaction mixture, $Pd(PPh_3)_4$ (50 mg) and the salt solution were added sequentially under a strict argon atmosphere followed by evacuation and refilling the flask with argon (3x) after each addition. The flask was covered with aluminum foil and the solution was allowed to reflux overnight. The resulting solution was cooled to room temperature, quenched with water (50 mL) and extracted with dichloromethane (3 x 20 mL). The organic layer was dried over anhydrous magnesium sulfate, evaporated and dried under vacuum. The product was further purified by column chromatography using a hexanes/ethyl acetate mixture to give the pure product **NAP-Py** (0.3 g, 50%) m.p. 158-160 ^{o}C. ^{1}H NMR ($CDCl_3$) δ: 8.23 (6H, m), 8.14

(2H, d, *J* =7.579 Hz), 8.10 (4H, s), 8.05 (4H, m), 7.98 (4H, m), 7.85 (1H, s), 7.80 (2H, m), 7.75 (2H, d, *J* = 4.726 Hz), 7.65 (4H, m), 1.45 (9H, s). ^{13}C NMR ($CDCl_3$) δ: 31.73, 35.28, 123.96, 124.13, 124.87, 125.08, 125.10, 125.16, 125.34, 125.50, 126.22, 126.54, 127.61, 127.69, 127.79, 127.83, 128.78, 129.02, 129.77, 129.84, 130.88, 131.17, 131.68, 137.80, 141.72, 141.95, 142.05, 152.64.

Preparation of 2f:

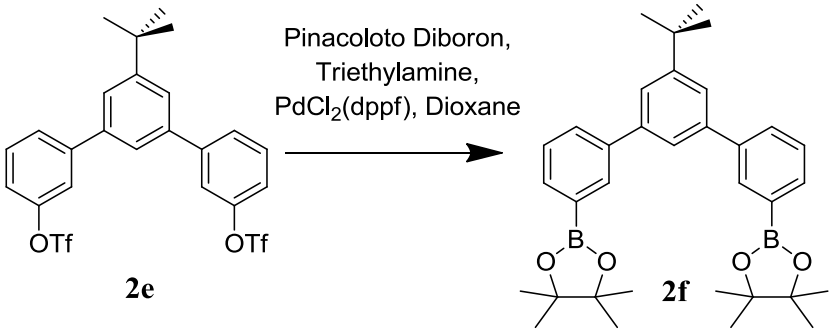

2e **2f**

To the oven dried Schlenk flask under an argon atmosphere the mixture of $PdCl_2$(dppf) (50 mg), ditriflate **2e** (1.0 g, 1.71 mmol) and triethyl amine (0.72 mL, 5.14 mmol) in dioxane (50 mL), was added bis(pinacoloto)diboarne (1.30 g, 5.14 mmol). The reaction mixture was heated to reflux overnight, which gives monoboronic ester .It was subjected back to the same reaction procedure to give diboronic ester. Water was slowly added to quench the reaction mixture and it was extracted with DCM. The crude product was subjected to column chromatography to offord pure product **2f** (0.5 g, 46%). ^{1}H NMR ($CDCl_3$) δ: 8.09 (2H, s), 7.84 (2H, dt, *J* = 7.34, 1.15 Hz), 7.76 (2H, dt, *J* = 7.68, 1.62 Hz), 7.67 (1H, t, *J* = 1.62 Hz), 7.60 (2H, d, *J* = 1.62 Hz), 7.49 (2H, t, *J* = 7.58 Hz), 1.45 (9H, s), 1.38 (24H, s). ^{13}C NMR ($CDCl_3$) δ : 25.67, 31.75, 35.19, 84.06, 123.68, 124.16, 128.32, 130.65, 133.85, 133.92, 141.49, 141.73, 152.04.

Preparation of NAP-TMP:

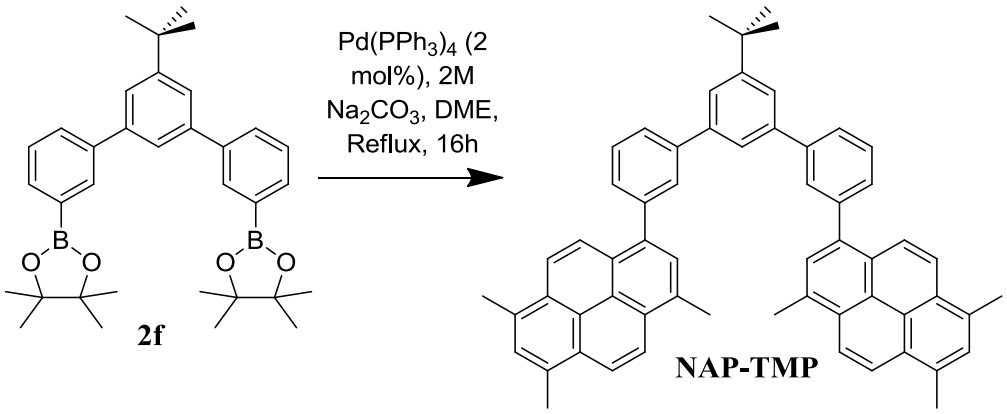

Diboronic ester **2f** (0.3 g, 055 mmol) and the trimethylbromopyrene (0.54 g, 1.67 mmol) were dissolved in anhydrous 1,2-dimethoxyethane (DME) (30 mL) in an oven dried Schlenk flask under an argon atmosphere and the flask was evacuated and refilled with argon (3x). In another oven dried Schlenk flask a solution of anhydrous sodium carbonate (2.5 g) in water (10 mL) was prepared under an argon atmosphere and the flask was also evacuated and refilled with argon (3x). To the above DME solution, $Pd(PPh_3)_4$ (50 mg) and the salt solution were added sequentially under a strict argon atmosphere followed by evacuation and refilling the flask with argon (3x) after each addition. The flask was covered with aluminum foil and the solution was allowed to reflux overnight. The resulting solution was cooled to room temperature, quenched with water (50 mL) and extracted with dichloromethane (3 x 20 mL). The organic layer was dried over anhydrous magnesium sulfate, evaporated and dried under vacuum. The crude product was purified by column chromatography using a hexanes/ethyl acetate mixture to give the pure product **NAP-TMP** (0.06 g, 14%) m.p. 318-320 ^{o}C. ^{1}H NMR ($CDCl_3$) δ: 8.26 (2H, d, *J* = 9.50 Hz), 8.22 (2H, d, *J* = 9.50 Hz), 8.15 (2H, d, *J* = 9.50 Hz), 8.06 (2H, d, *J* = 9.50 Hz

), 7.90 (4H, d, J = 6.64 Hz), 7.82 (1H, t, J = 1.66 Hz), 7.74 (6H, m), 7.62 (6H, m), 2.99 (6H, s), 2.96 (6H, s), 2.89 (6H, s), 1.42 (9H, s). ^{13}C NMR ($CDCl_3$) δ :19.99, 20.04, 20.18, 31.32, 35.27, 122.50, 123.12, 123.73, 123.93, 124.12, 124.28, 125.70, 125.75, 126.38, 127.45, 128.01, 128.09, 128.88, 129.08, 129.75, 129.77, 129.84, 130.42, 131.49, 131.70, 131.83, 136.91, 141.70, 142.02, 142.24, 152.55.

^{1}H NMR spectrum of 1,5-dibromo-2,4-dimethoxybenzene

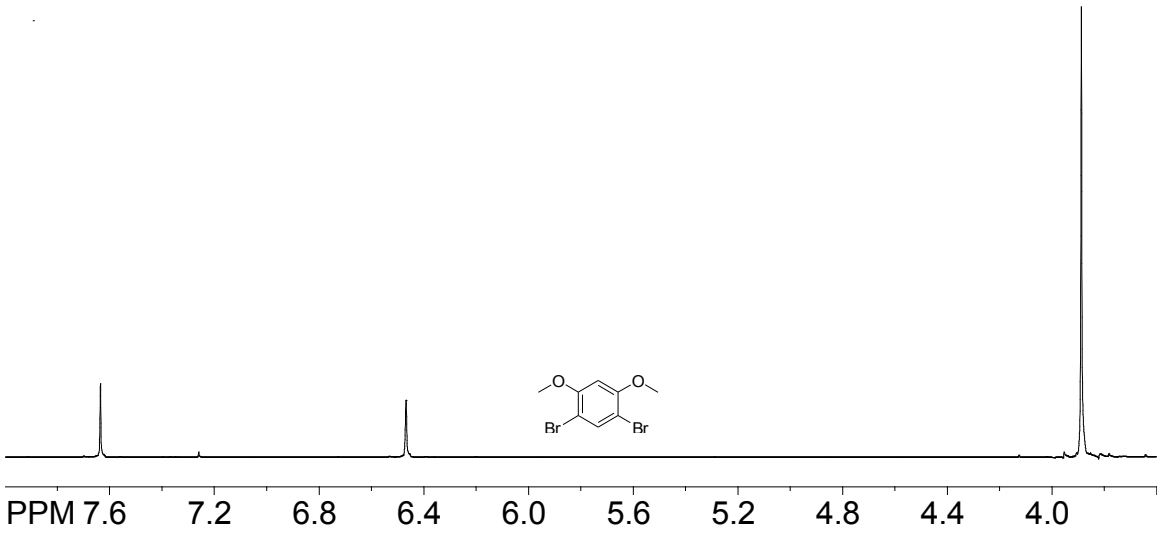

^{13}C NMR spectrum of 1,5-dibromo-2,4-dimethoxybenzene

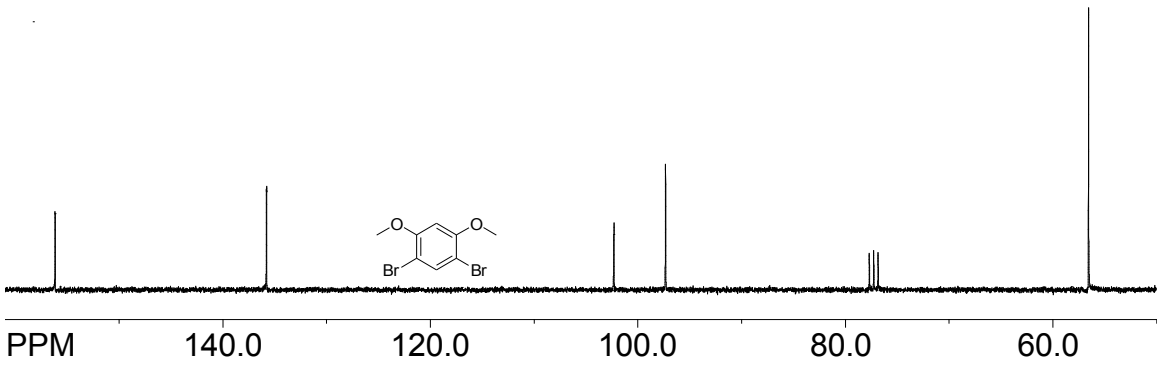

^{1}H NMR spectrum of 1a

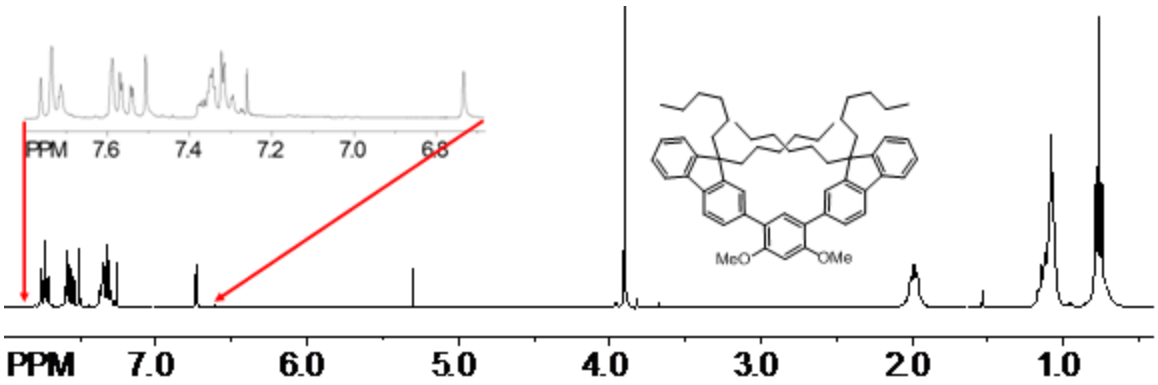

^{13}C NMR spectrum of 1a

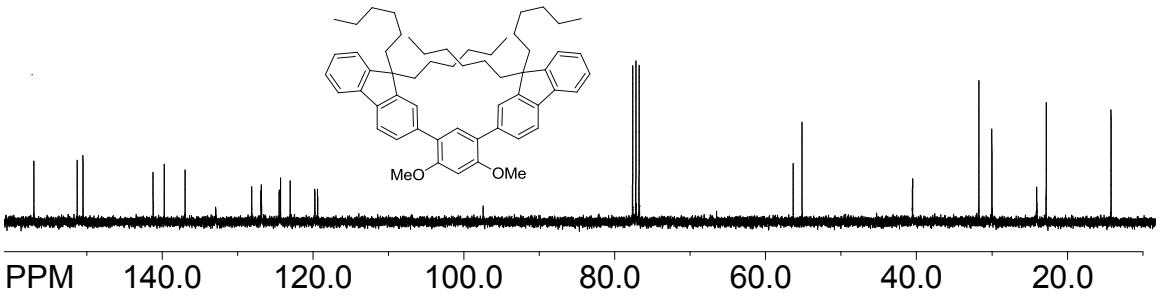

^{1}H NMR spectrum of 1b

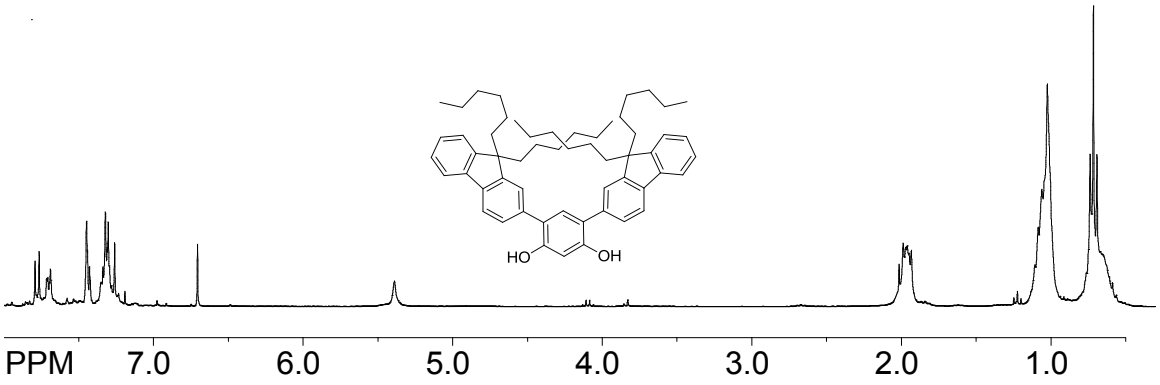

^{1}H NMR spectrum of 1c

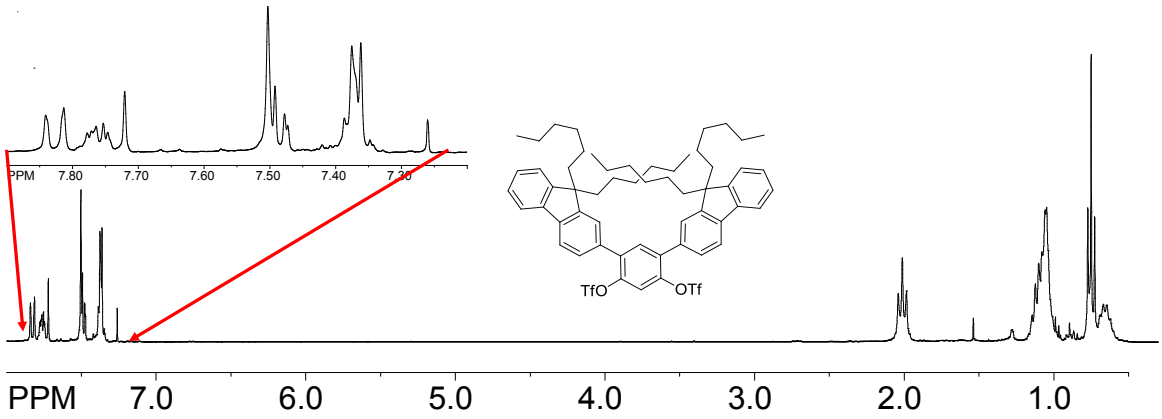

^{13}C NMR spectrum of 1c

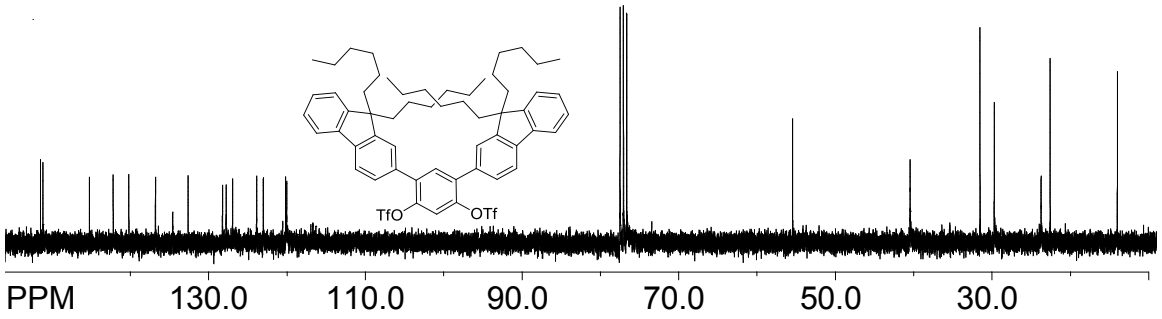

^{1}H NMR spectrum of 1d

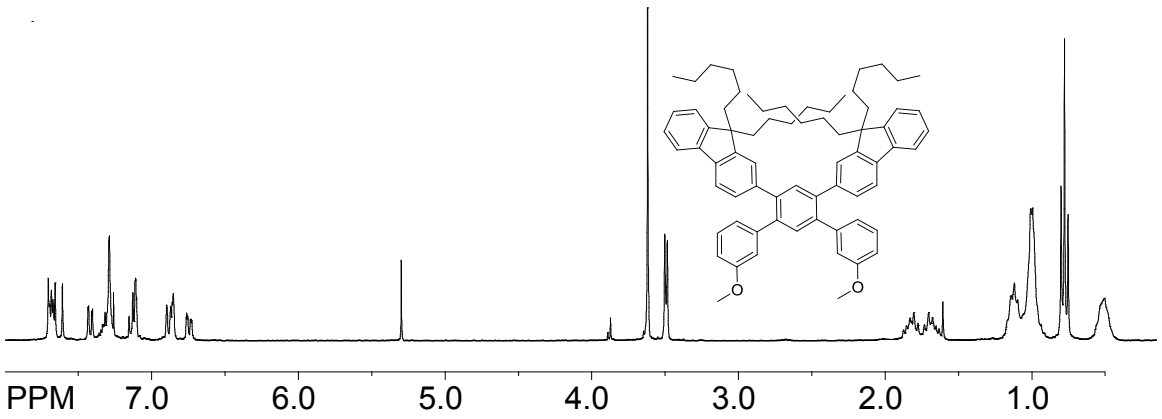

^{13}C NMR spectrum of 1d

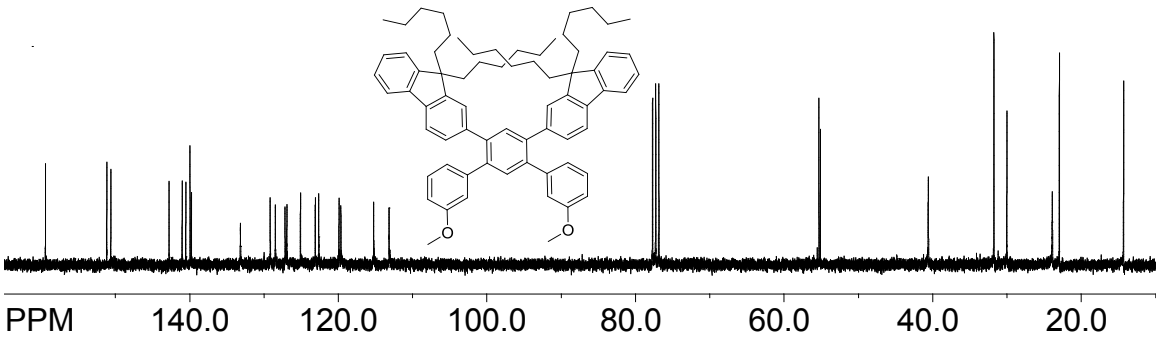

^{1}H NMR spectrum of 1e

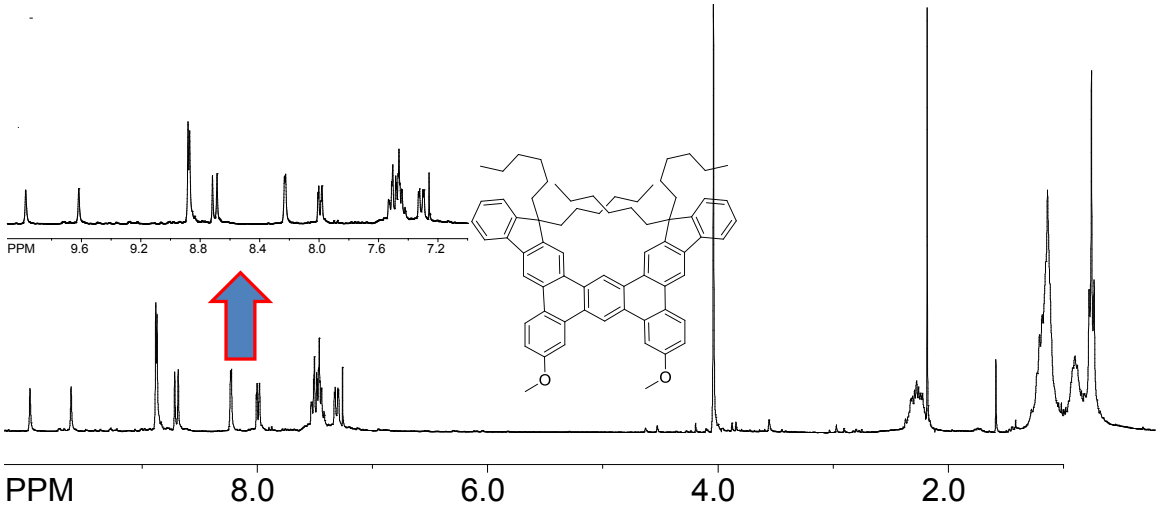

^{13}C NMR spectrum of 1e

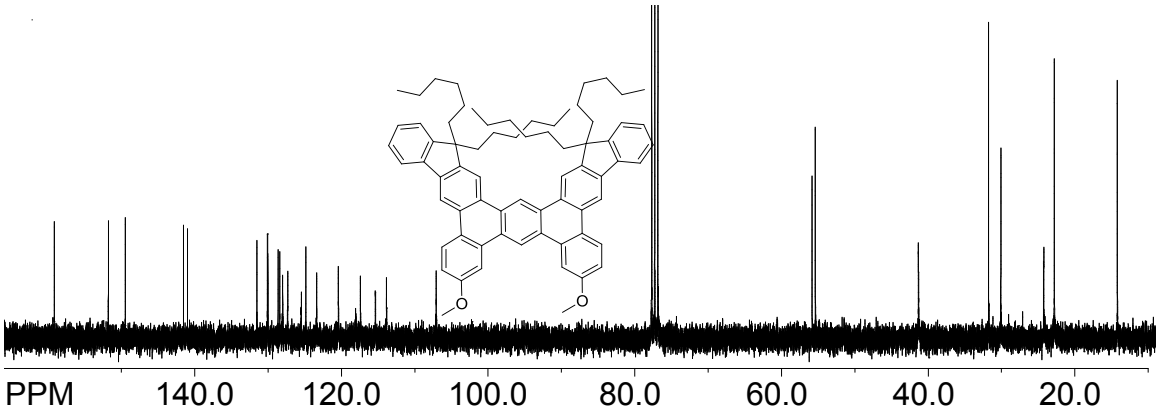

^{1}H NMR spectrum of 1f

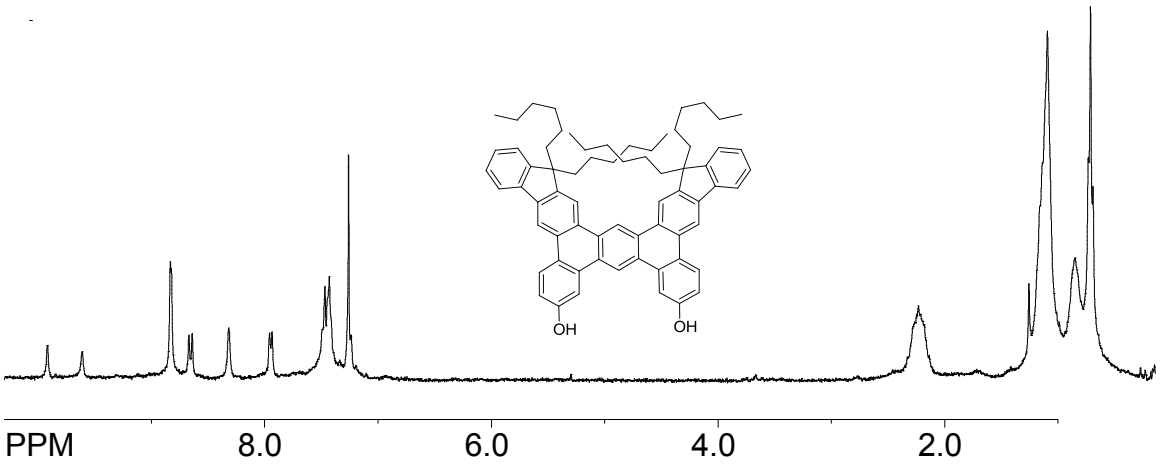

^{1}H NMR spectrum of 1g

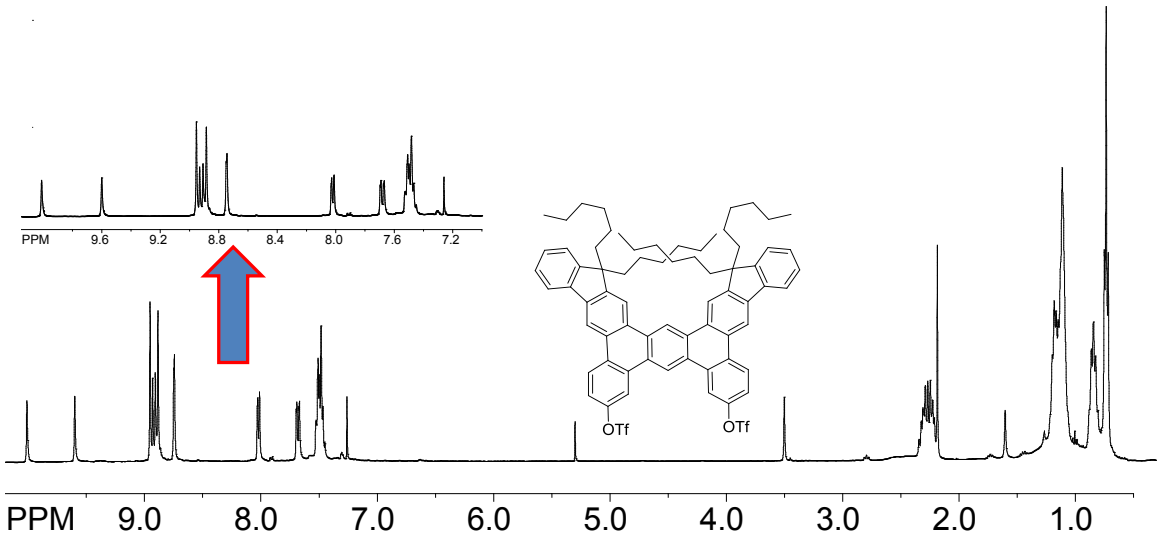

^{13}C NMR spectrum of 1g

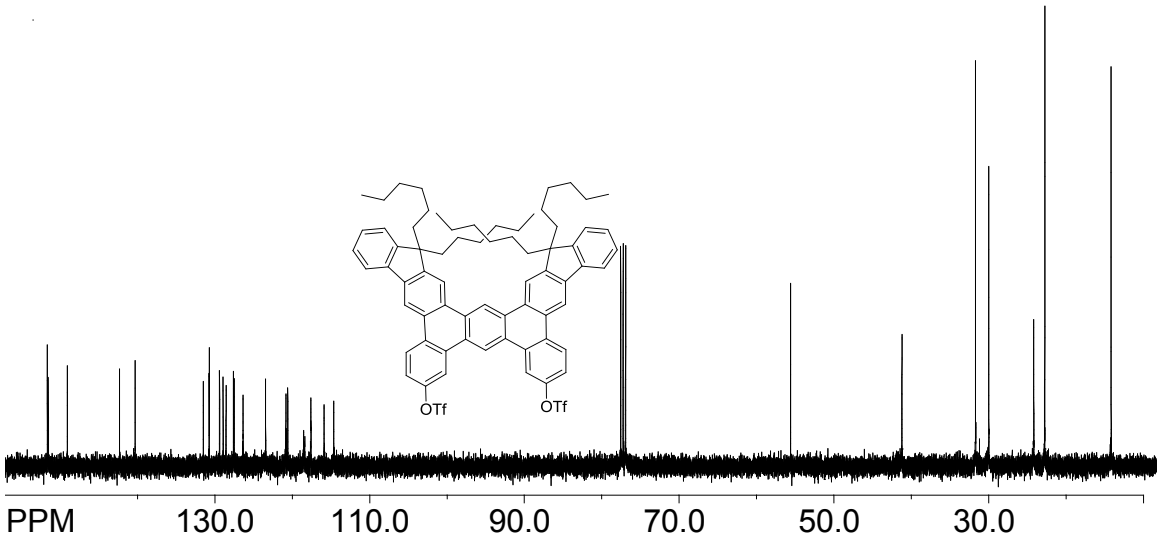

^{1}H NMR spectrum of CRP-Py

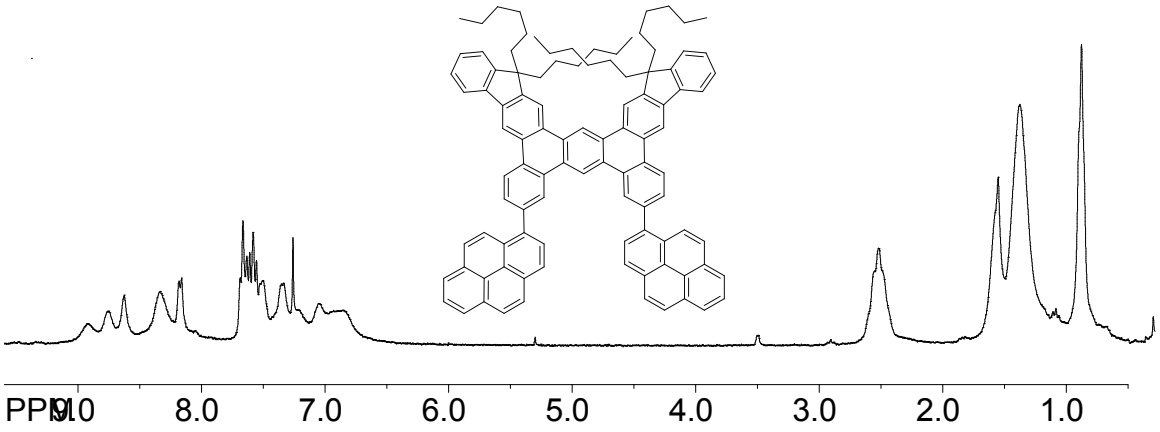

^{13}C NMR spectrum of CRP-Py

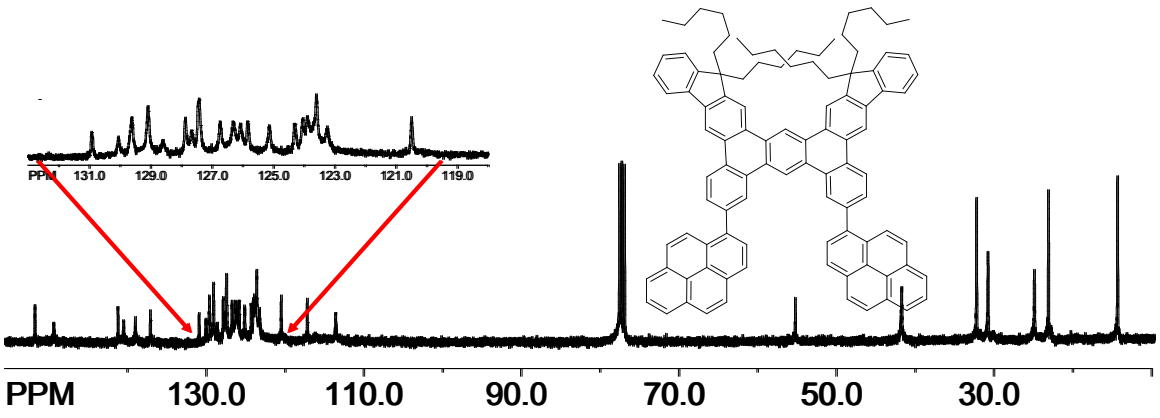

^{1}H NMR spectrum of 2a

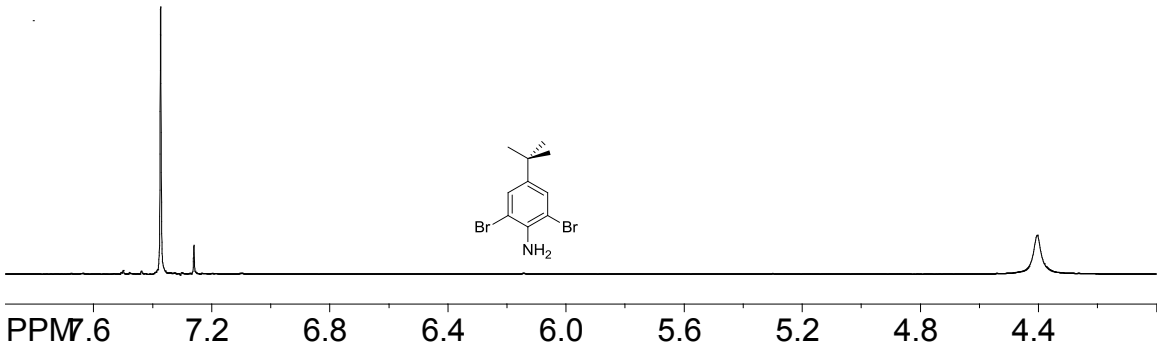

^{13}C NMR spectrum of 2a

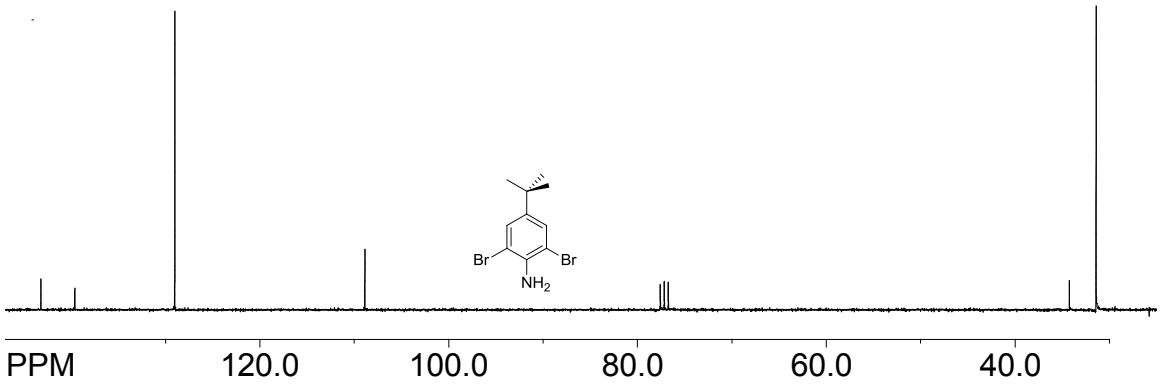

^{1}H NMR spectrum of 2b

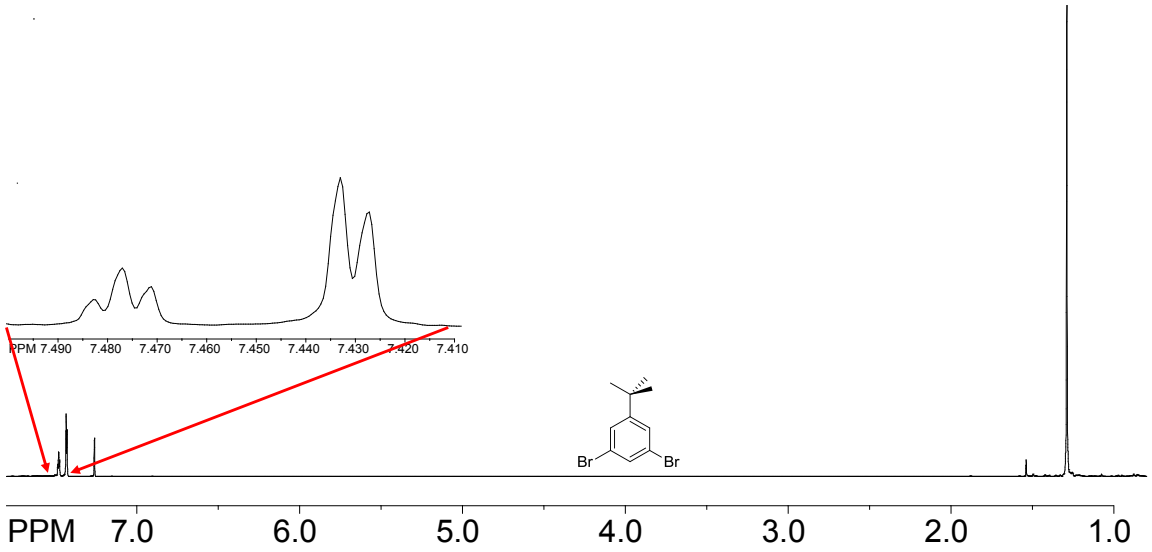

^{13}C NMR spectrum of 2b

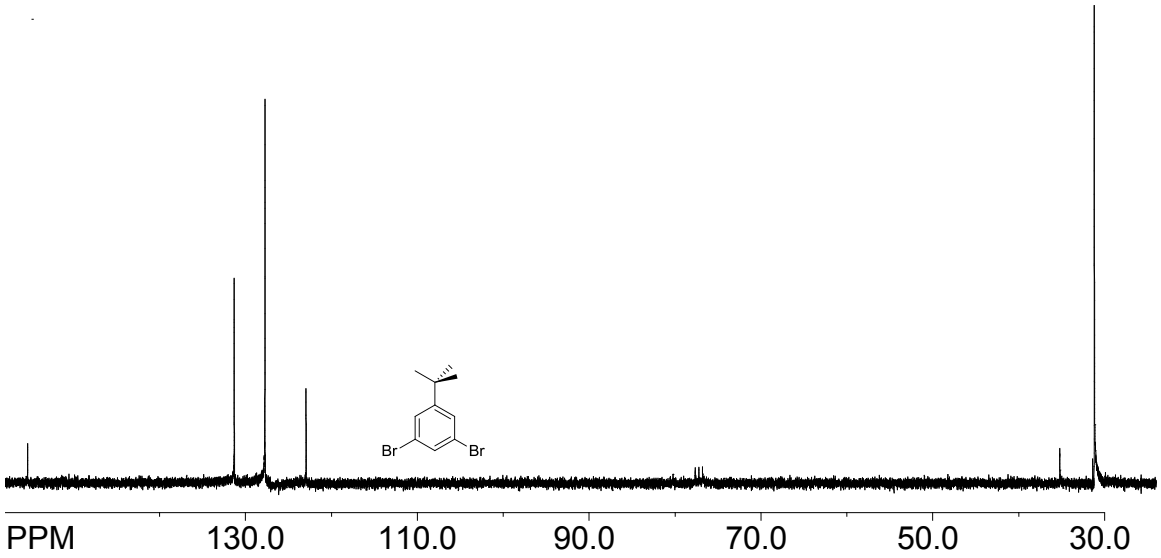

^{1}H NMR spectrum of 2c

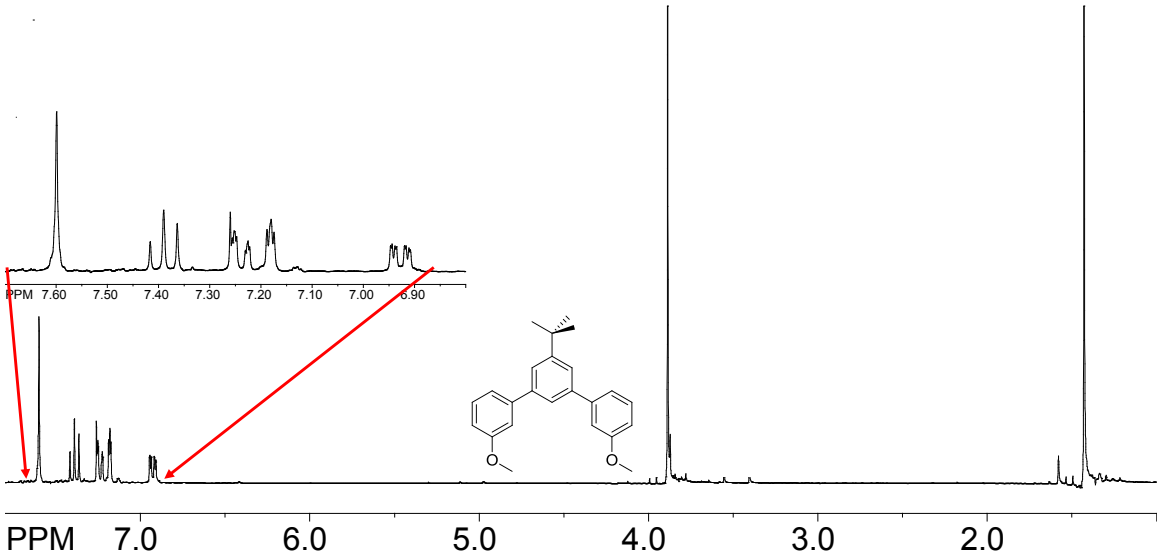

^{13}C NMR spectrum of 2c

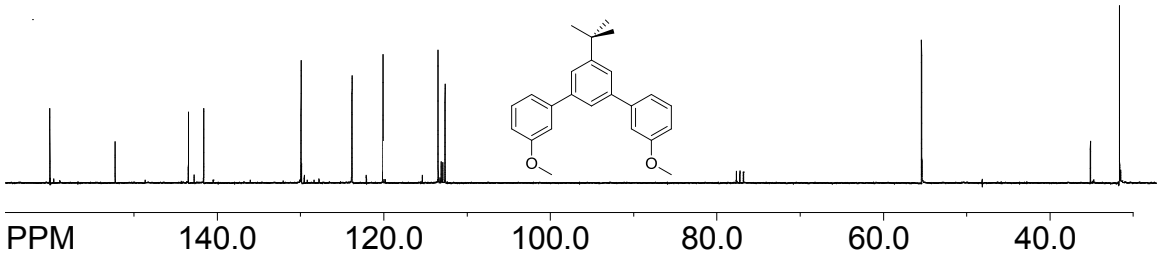

^{1}H NMR spectrum of 2d

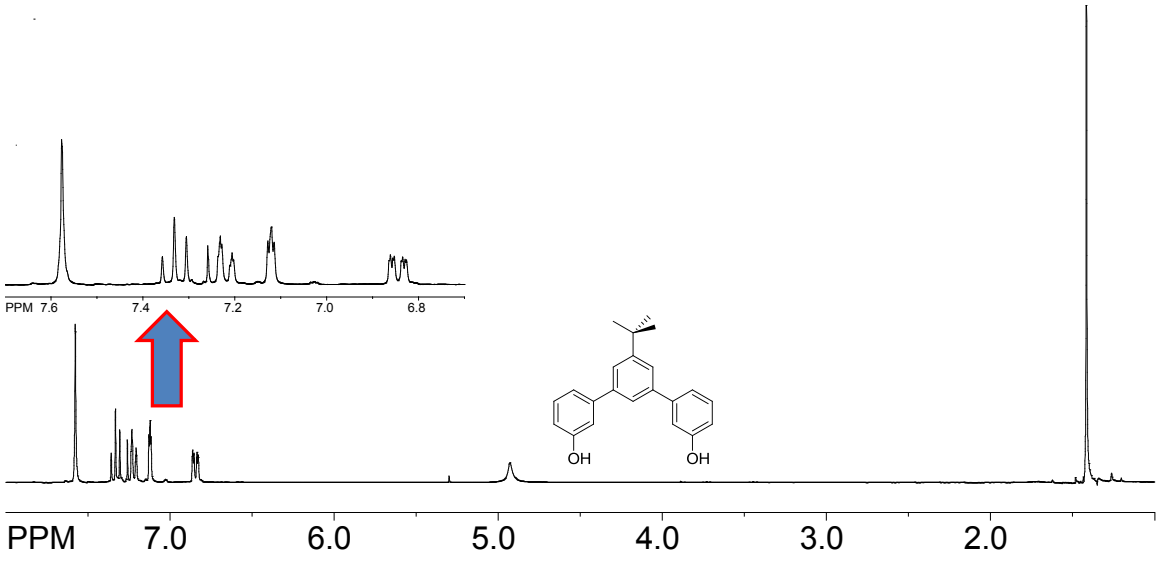

^{1}H NMR spectrum of 2d

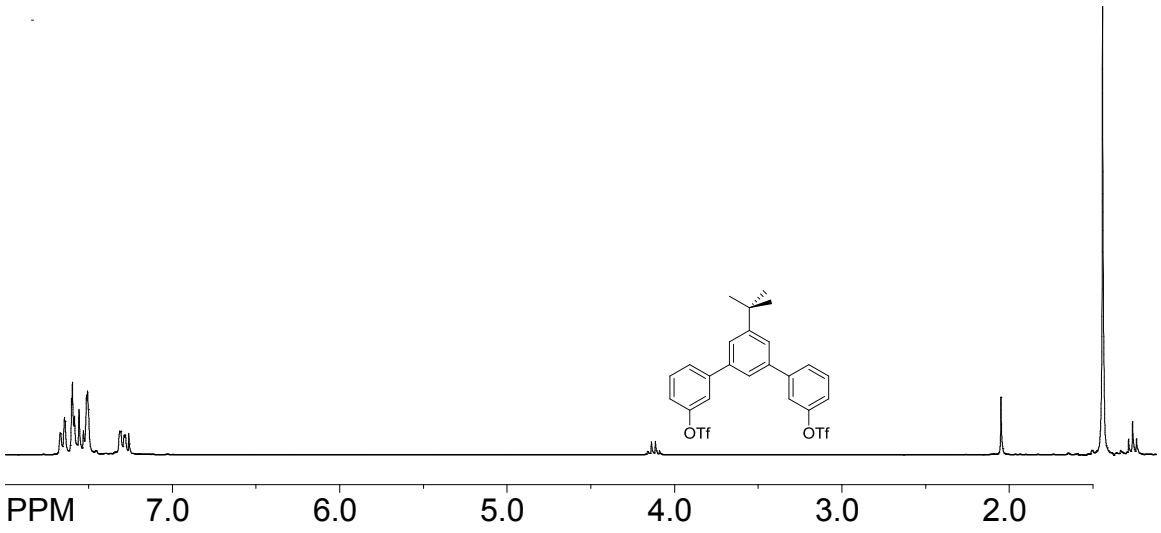

^{13}C NMR spectrum of 2d

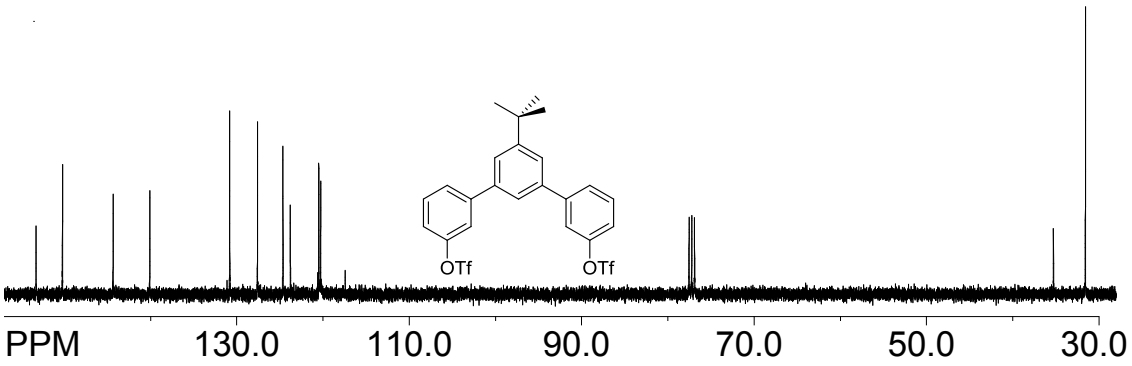

^{1}H NMR spectrum of NAP-Py

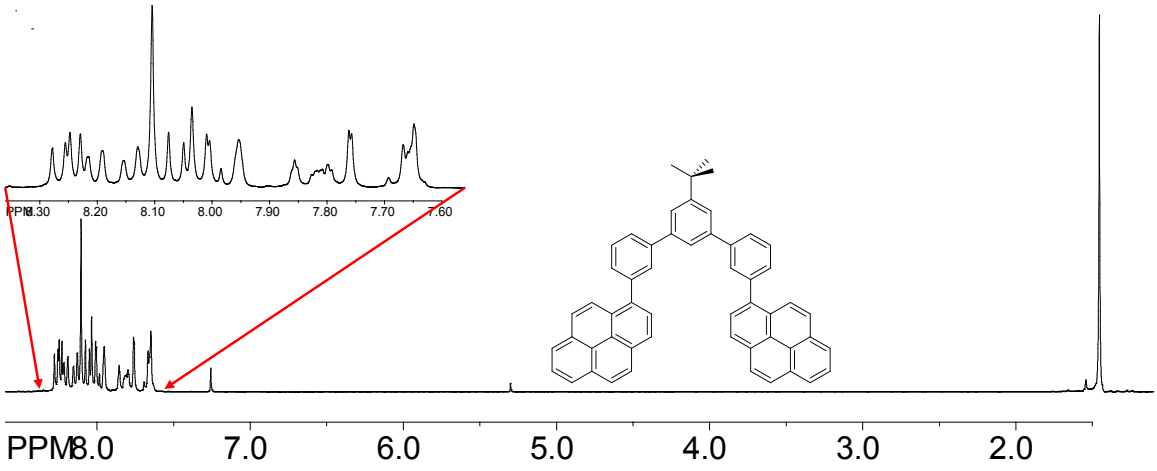

^{13}C NMR spectrum of NAP-Py

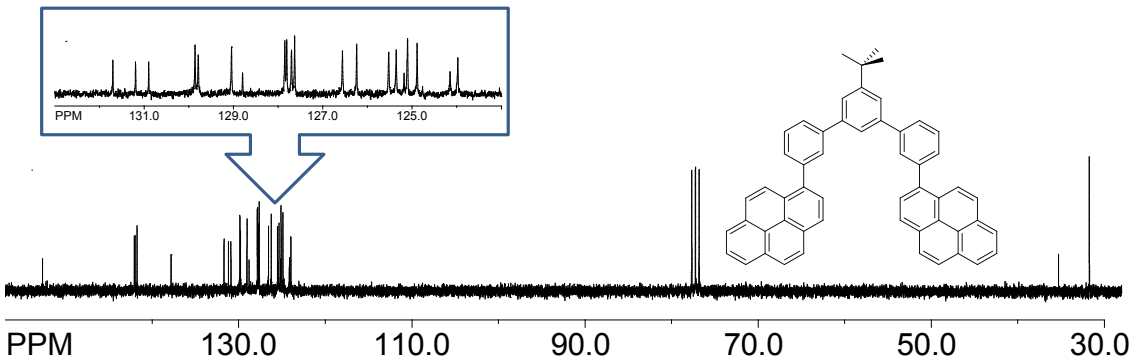

^{1}H NMR spectrum of 2f

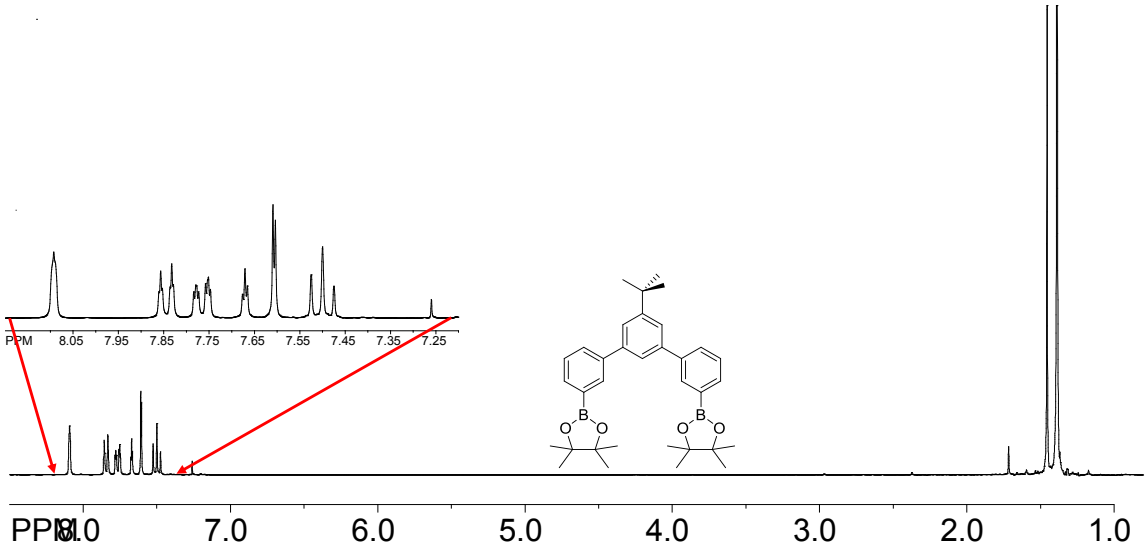

^{13}C NMR spectrum of 2f

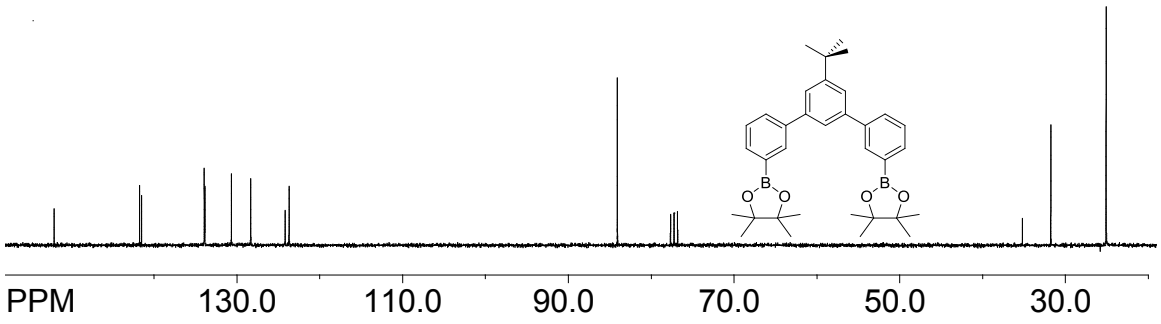

^{1}H NMR spectrum of NAP-TMP

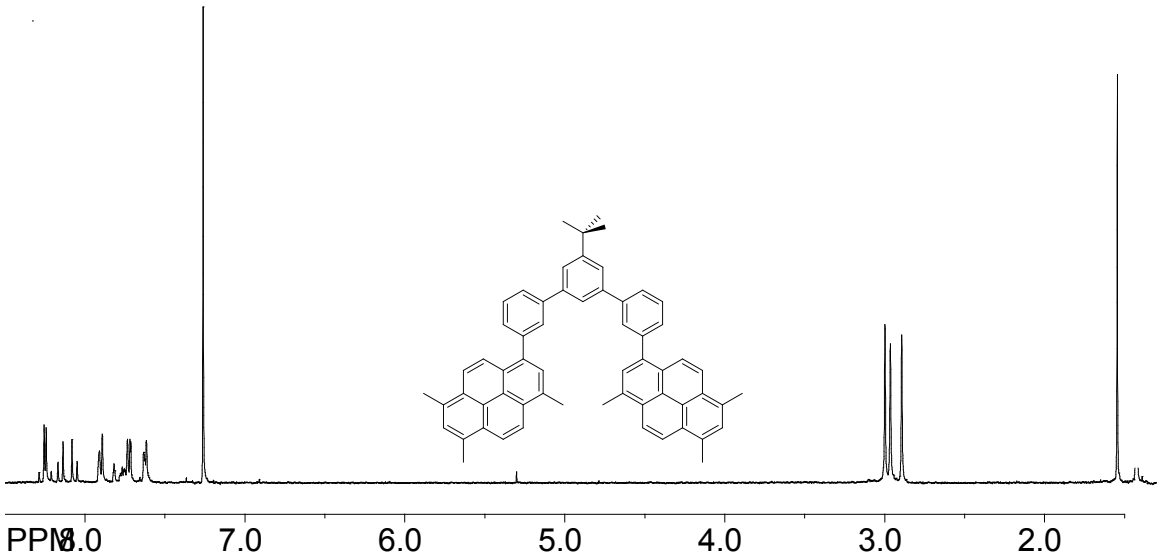

^{13}C NMR spectrum of NAP-TMP

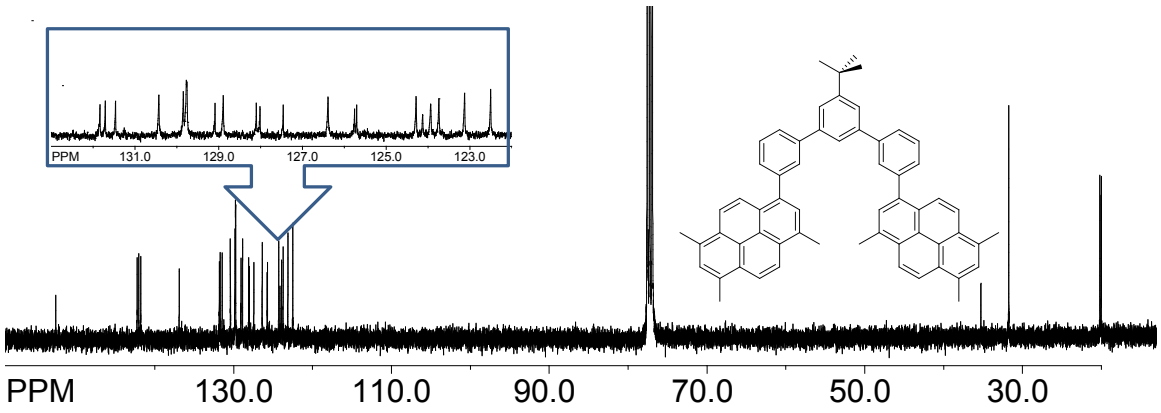

Crystal data and structure refinement for raj16z

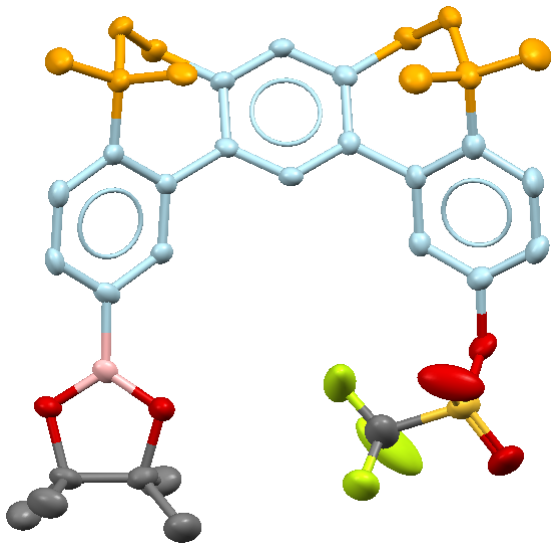

Identification code	raj16z
Empirical formula	C35 H40 B F3 O5 S
Formula weight	640.54
Temperature	100(2) K
Wavelength	1.54178 Å

Crystal system	Monoclinic	
Space group	P c	
Unit cell dimensions	a = 12.1333(3) Å	α= 90°.
	b = 12.1624(3) Å	β= 111.9230(10)°.
	c = 12.0399(3) Å	γ = 90°.
Volume	1648.25(7) $Å^3$	
Z	2	
Density (calculated)	1.291 Mg/m^3	
Absorption coefficient	1.359 mm^{-1}	
F(000)	676	
Crystal size	0.28 x 0.23 x 0.10 mm^3	
Theta range for data collection	3.63 to 67.59°.	
Index ranges	-14<=h<=14, 0<=k<=14, -14<=l<=14	
Reflections collected	13525	
Independent reflections	4994 [R(int) = 0.0187]	
Completeness to theta = 67.59°	98.9 %	
Absorption correction	Semi-empirical from equivalents	
Max. and min. transmission	0.8761 and 0.7022	
Refinement method	Full-matrix least-squares on F^2	
Data / restraints / parameters	4994 / 2 / 415	
Goodness-of-fit on F^2	1.040	
Final R indices [I>2sigma(I)]	R1 = 0.0541, wR2 = 0.1442	
R indices (all data)	R1 = 0.0544, wR2 = 0.1445	
Absolute structure parameter	0.56(3)	
Largest diff. peak and hole	0.501 and -0.373 $e.Å^{-3}$	

CHAPTER 4
DIRECT OBSERVATION OF ELECTRON-TRANSFER INDUCED CONFORMATIONAL TRANSFORMATION (MOLECULAR ACTUATION) IN A BICHROMOPHORIC ELECTRON DONOR

Introduction

A variety of functional materials such as synthetic foldamers,[1] molecular muscles,[2] molecular switches,[3] and functional molecular rotaxanes[4] exhibit structural or conformational changes when triggered by external stimuli such as heat, light, pH-changes, metal ion binding, electron transfer, etc. Electro-mechanical molecular actuators[5] are another class of such functional molecules in which a conformational change is caused by an electrochemical (redox) trigger. The conformational motions induced by electrochemical triggers are tantamount to the conversion of electrical energy into mechanical energy; and such molecules are expected to be potentially useful building blocks for the functional molecular muscles.[2]

We have recently shown[6] that a conformationally-mobile bichromophoric electron donor (tetramethoxydibenzobicyclo[4.4.1.]undecane, **1**) exists in rapidly interchanging mirror image (extended) conformations in the neutral state. This was demonstrated by variable-temperature NMR spectroscopy,[7] and by spectral analysis of the electron donor-acceptor complexes of **1** in comparison with the cofacially-locked model compound **2** and a monochromophoric donor **3** with tetracyanobenzene as an electron acceptor.[8]

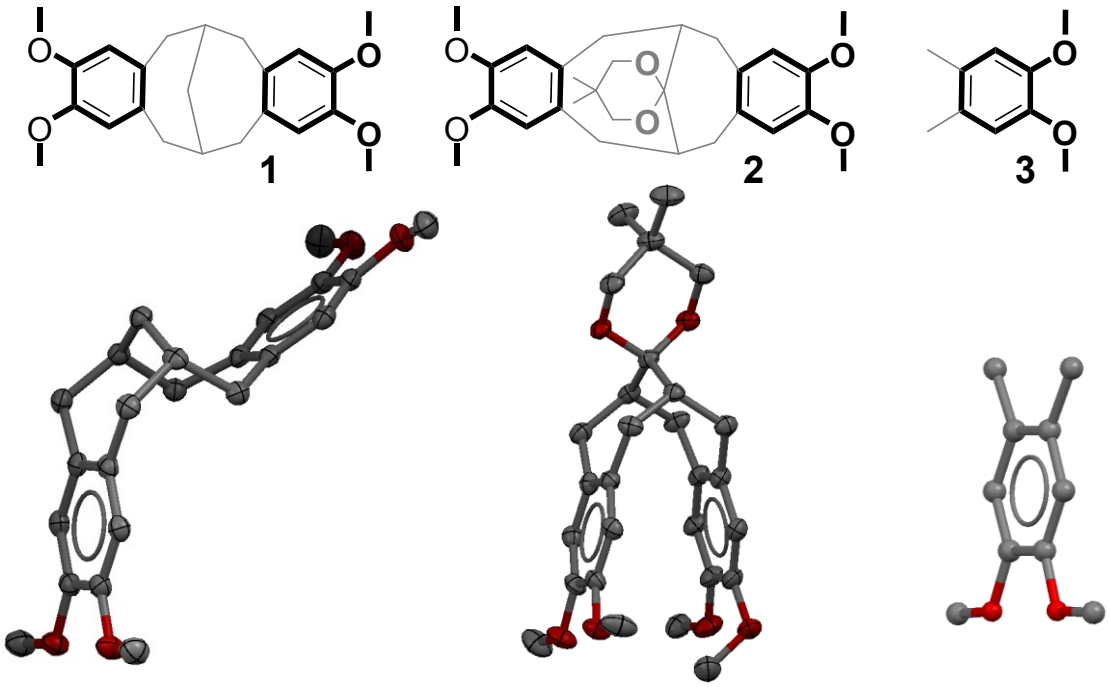

Figure 4.1 The molecules utilized in this study and their structures obtained either by X-ray crystallography (i.e. 1 and 2) or by DFT calculations (i.e. 3).

Interestingly, however, the one-electron oxidation of **1** to its cation radical leads to a rapid transformation of its extended conformation (**E-1**) into a folded π-stacked structure (**F-1**), i.e. eq 1.

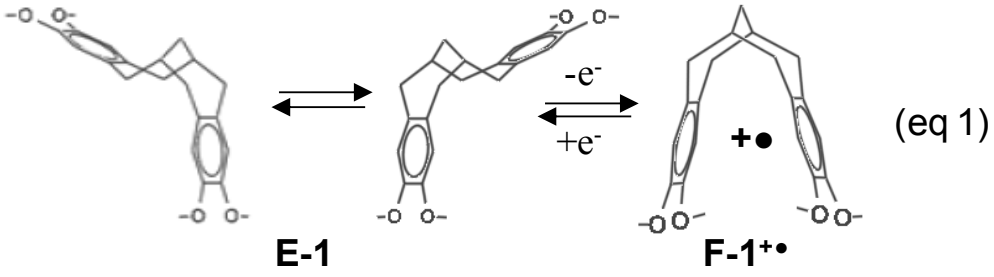

(eq 1)

The redox-triggered clam-like mechanical motion in **1** (eq 1) was delineated with the aid of electrochemical analysis, optical spectroscopy, and by X-ray crystallography of the cofacially-locked cationic conformation (see Figure 4.2).[6]

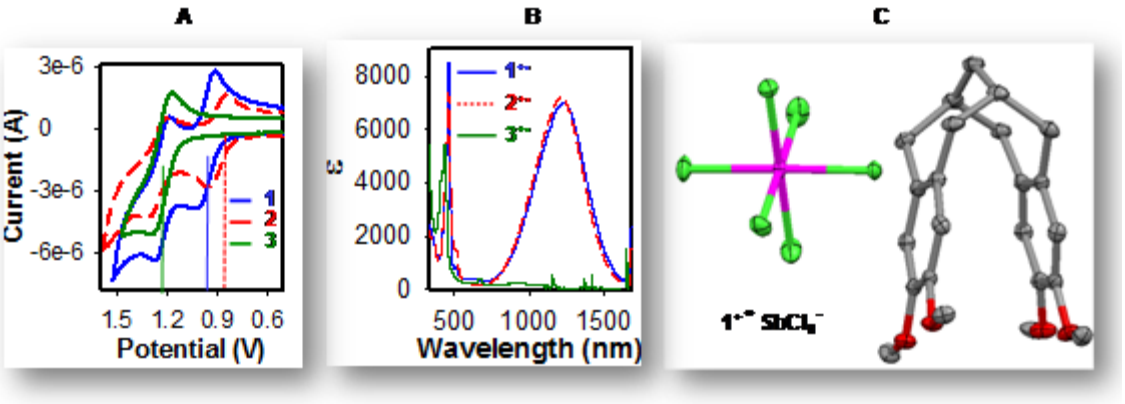

Figure 4.2 (**A**) The Cyclic voltammograms of 1-3 (1 mM) in CH_2Cl_2, containing 0.2 M *n*-Bu_4NPF_6, were measured at a v = 200 mV s^{-1} at 22 °C. (**B**) Overlay of the absorption spectra of $1^{+\bullet}$ (λ_{max} = 466, 1224 nm; ε_{1220} = 6,990 M^{-1} cm^{-1}), $2^{+\bullet}$ (λ_{max} = 464, 1218 nm; ε_{1220} = 7,170 M^{-1} cm^{-1}, and model $3^{+\bullet}$ (λ_{max} = 442 nm; ε_{442} = 5,400 M^{-1} cm^{-1}) in CH_2Cl_2 at 22 °C. (C) The crystal structure of $1^{+\bullet}$ $SbCl_6^-$ showing the cofacial π-stacked arrangement of the veratrole moieties.

Firstly, the electrochemical analysis of **1** together with the model compound **2**, in which the two veratrole moieties are cofacially locked, showed their first reversible oxidation waves at the potentials of 0.96 and 0.87 V vs. SCE, respectively, whereas the monochromophoric model donor **3** showed its reversible oxidation wave at a potential of 1.22 V vs. SCE (Figure 4.2A).[9] The observation of similar and relatively lower E_{ox1} values for both **1** and **2** as compared to monochromophoric **3** suggested that the cationic charge in both **1** and **2** is stabilized by a similar cofacial conformation. Secondly, the

observation of a highly characteristic charge-resonance transition at ~1200 nm in both $\mathbf{1}^{+\bullet}$ and $\mathbf{2}^{+\bullet}$, and its singular absence in the monochromophoric $\mathbf{3}^{+\bullet}$ (Figure 4.2B), further suggested that $\mathbf{1}^{+\bullet}$ adapts a cofacial conformation similar to that of cofacially-locked $\mathbf{2}^{+\bullet}$. Finally, the definitive X-ray crystallographic evidence for the transformation of the extended cation radical $\mathbf{E\text{-}1}^{+\bullet}$ into the cofacially folded $\mathbf{F\text{-}1}^{+\bullet}$ in eq 1 was provided by its isolation and characterization by X-ray crystallography (Figure 4.2C).

Variable temperature NMR spectroscopy is often employed for the conformational analysis of neutral organic molecules.[10] Unfortunately, the conformational transformation of cationic $\mathbf{1}^{+\bullet}$ could not be studied by dynamic NMR spectroscopy owing to the paramagnetic nature of cation radicals produced by one electron oxidation of neutral molecules. However, the distinct spectroscopic signatures of both the extended $\mathbf{E\text{-}1}^{+\bullet}$ (which is expected to be spectroscopically similar to the model $\mathbf{1}^{+\bullet}$) and π- stacked $\mathbf{F\text{-}1}^{+\bullet}$ (which showed characteristic charge-resonance transition at ~1200 nm in both $\mathbf{1}^{+\bullet}$ and $\mathbf{2}^{+\bullet}$) should allow the direct monitoring of redox-induced conformational transformation in eq 1 by time-resolved laser flash photolysis technique. Indeed, herein we will describe the generation of cation radicals of **1-3**, using photoexcited chloranil as an oxidant, and delineation that extended $\mathbf{E\text{-}1}^{+\bullet}$ undergoes a conformational transformation to the π- stacked folded $\mathbf{F\text{-}1}^{+\bullet}$ on a micro-second time scale which is relatively faster than electrochemical events described in Figure 4.2A. Moreover, the time-resolved studies of the conformational transformation of **1** will be further corroborated by theoretical calculations which show, in agreement with experiment, that the π- stacked conformer is stabilized upon ionization.

Results and Discussion

In order to probe the time-dependent conformational transformation of the cation radical of electron donors **1**, it was generated based on time-resolved absorption measurements upon diffusional electron-transfer quenching of photoexcited chloranil triplet as an oxidant (E_{red} = 2.2 V vs. SCE)[12] using laser-flash photolysis as follows.

Thus, the transient spectra in the UV-vis region obtained 100-ns after laser excitation (10 ns) of chloranil (5 mM) in the presence of conformationally-mobile **1** (10 mM) in 1:1 dichloromethane-acetonitrile mixture showed an absorption band at λ_{max} ~ 460 nm with a shoulder at ~420 nm, characteristic of a chloranil radical anion.[13] Note that the local absorption band of the veratrole cation radicals only absorb at ~460 nm[14] and thus lie within the envelop of chloranil anion radical spectrum. It is further noted that the transient absorption spectra of donors **1-3** in the UV-vis region, obtained by quenching of the photoexcited chloranil triplet, were characteristically similar with their absorption band buried in the envelope of chloranil anion radical.

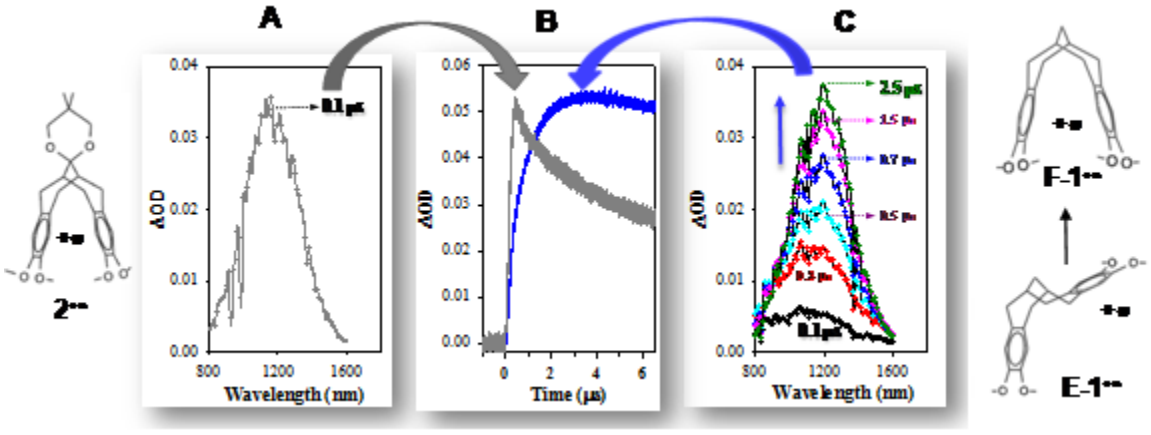

Figure 4.3 Transient NIR absorption spectra of cation radicals of 1 (spectra C) and 2 (spectrum A) from laser flash photolysis of 0.005 M

solution of chloranil and 0.01 M of 1 or 2 in a 1:1 acetonitrile-dichloromethane mixture following the 10-ns laser excitation at 355 nm. (**B**) Kinetic traces of the formation/decay of cation radicals of 1 (blue trace) and 2 (grey trace) at 22 ^{o}C.

Interestingly, however, as shown in Figure 4.3, the transient spectra in the NIR region obtained 100-ns after laser excitation (10 ns) of chloranil (5 mM) in the presence of conformationally-mobile **1** (10 mM) in 1:1 dichloromethane-acetonitrile mixture showed a weak absorption band centered at ε_{max} ~1200 nm (Figure 4.3C). Furthermore, Figure 4.3C shows that the NIR transition at ~1200 nm intensified as a function of time and acquired the maximum intensity in ~2-3 microseconds. In contrast, the transient spectrum of the cation radical of conformationally-locked **2** in Figure 4.3A, generated under identical conditions, was formed instantaneously within the laser pulse and attained the maximum intensity in only ~100 ns. It is further emphasized that the cation radical of monochromophoric model donor **3**, generated similarly, lacked any absorption in the near-IR region. The fully-evolved NIR transients at ~1200 nm in Figure 4.3C and 4.3A for $\mathbf{1}^{+\bullet}$ and $\mathbf{2}^{+\bullet}$, respectively, were characteristically similar to the near IR transitions observed in the steady-state spectrum of $\mathbf{1}^{+\bullet}$ and $\mathbf{2}^{+\bullet}$ (compare Figures 4.2B and 4.3A and 4.3C).

Figure 4.3B compares the kinetic traces for the formation/decay of cation radicals $\mathbf{1}^{+\bullet}$ and $\mathbf{2}^{+\bullet}$ at 1200 nm as a function of time. As expected, the transient at 1200 nm for the cation radical of conformationally-locked **2** was formed faster than the response function of our germanium detector (i.e. ~150 ns). In contrast, the transient at 1200 nm for the cation radical of conformationally-mobile **1** grew-in up to ~2-3 μs and a reconvolution fit[15] of the blue trace in Figure 4.3 showed that growth of the transient for

$\mathbf{1}^{+\bullet}$ occurred with a time constant of τ_{rise} ~0.9 μs and is schematically summarized in Scheme 4.1.

Scheme 4.1 Schematic depiction of the redox-induced conformational transformation of **1**.

The observed time constant of ~1 μs for growth of the NIR transient (at ~1200 nm) for the cofacially-locked conformation of $\mathbf{1}^{+\bullet}$ is somewhat slow and may arise from the fact that conformational transformation of extended $\mathbf{E\text{-}1}^{+\bullet}$ to folded $\mathbf{F\text{-}1}^{+\bullet}$ requires a demanding simultaneous inversion at a pair of benzylic methylenes (indicated by orange carbons), i.e. eq 2.

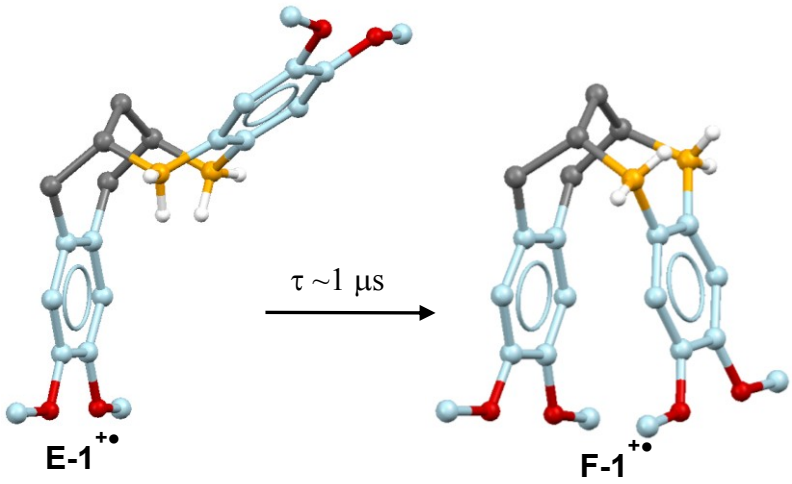

The observed differences in the decay kinetics of $\mathbf{1}^{+\bullet}$ and $\mathbf{2}^{+\bullet}$, via back electron transfer to chloranil anion radical, in Figure 4.3B with rather disparate time constants of τ_{decay} ~ 53 and ~9 μs, for $\mathbf{1}^{+\bullet}$ and $\mathbf{2}^{+\bullet}$, respectively, are rather intriguing. We tentatively suggest that the large conformational reordering in the cation radical of conformationally-mobile $\mathbf{1}^{+\bullet}$ may lead to a highly perturbed and well-separated ion radical pair and therefore results into a slow back electron transfer between $\mathbf{1}^{+\bullet}$ and chloranil anion radical.[16]

In order to obtain the energetics of the observed conformational transformation of extended $\mathbf{E\text{-}1}^{+\bullet}$ to folded $\mathbf{F\text{-}1}^{+\bullet}$, we performed DFT calculations at B3LYP/6-31G* level, summarized in Figure 4.4.

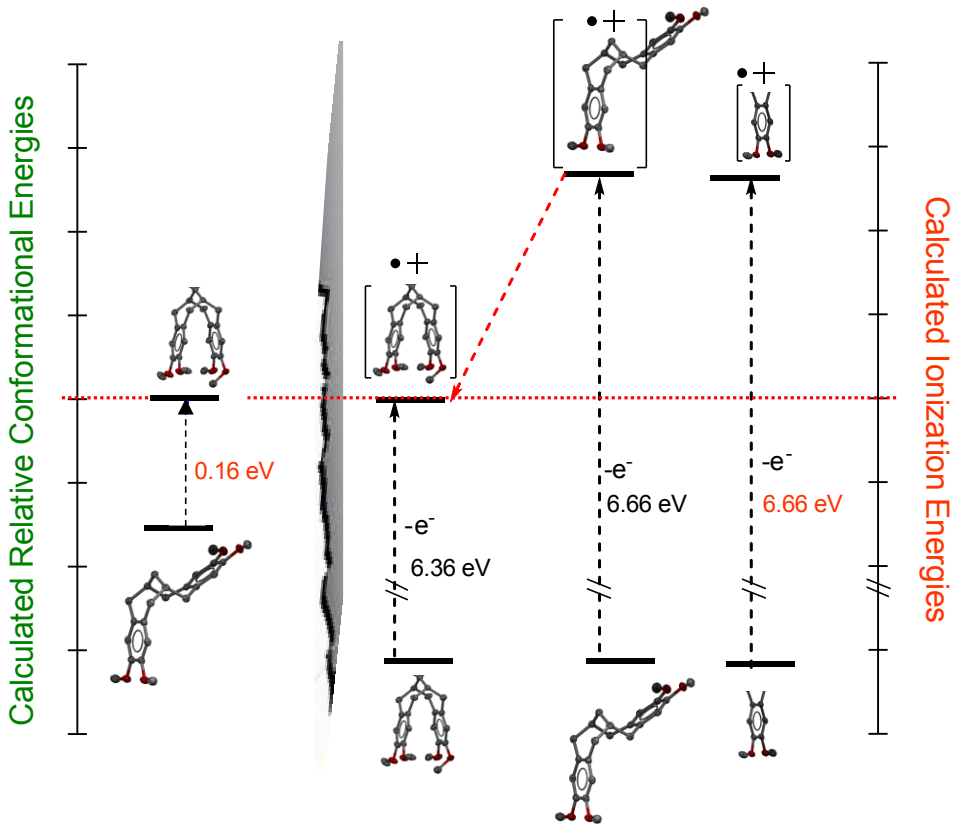

Figure 4.4 Comparison of the relative conformational energies, obtained by DFT calculations at B3LYP/6-31G* level, of the extended and folded conformers of **1** in both in neutral and cationic forms and the ionization energies of the extended and folded conformers of **1** and monochromophoric model donor **3**. Note that the ionization energy of the extended **1** was presumed to be same as the model monochromophoric **3**.

On the left-hand side of Figure 4.4 is shown the relative (gas-phase) conformational energies of the neutral extended and folded conformers of **1**. As expected, the extended neutral conformer lies lower in energy, by 0.16 eV. This trend is reversed for the extended and folded cation radicals of **1**. From the (gas-phase) DFT calculations, the folded conformer lies ~0.2 eV lower in energy, reflecting a relative stabilization of the folded conformer by ~0.4 eV upon ionization. However, this number is slightly misleading, because the calculations show that the charge is delocalized over both aryl groups in the extended conformer. A potentially better estimate of the stabilization of the folded conformer upon ionization is obtained by using the ionization energy of the model monochromophoric **3** as an estimate for the extended conformer **1** where the charge is localized only on one ring (Figure 4.4), which gives a slightly higher number for the stabilization of the folded cation radical of ~0.3 eV. In any case, the calculations show that, consistent with experiment, the folded conformer is the global minimum for the cation radical, and is stabilized relative to the extended conformer by ~0.4-0.5 eV upon ionization. Calculations of the solvation energy for neutral and ionized **1** using the SM8 model show little variation in solvation energy for the folded and extended structures; we therefore conclude that the incorporation of solvation effects will not change the picture presented in Figure 4.4.

Conclusions

The one-electron oxidation of tetramethoxydibenzobicyclo[4.4.1]undecane (**1**) prompts it to undergo a clam-like electromechanical actuation into a cofacially π-stacked conformer as established by (i) electrochemical analysis, (ii) by the observation of the intense charge-resonance transition in the near IR region in its cation radical spectrum, and (iii) by X-ray crystallographic characterization of the isolated cation radical salt ($\mathbf{1}^{+\bullet}$ $SbCl_6^-$). Generation of the cation radical of conformationally-mobile **1**, with the aid of laser flash photolysis, allows us to delineate that extended $\mathbf{1}^{+\bullet}$ undergoes a conformational transformation to π- stacked folded $\mathbf{1}^{+\bullet}$ on micro-second time scale ($\tau \sim 1$ μs). Furthermore, somewhat slow conformation transformation of $\mathbf{1}^{+\bullet}$ is attributed to a demanding simultaneous inversion at a pair of benzylic methylenes.

Experimental and Theoretical Methods

Materials. Syntheses of tetramethoxydibenzobicyclo[4.4.1]undecane (**1**), cofacially-locked (model) bichromophoric **2**, and a monochromophoric model donor, i.e. 3,4-dimethyl-1,2-dimethoxybenzene (**3**) were accomplished according to the procedures described previously.[6] Chloranil was purchased from Aldrich and was recrystallized from a mixture of dichloromethane and hexanes. Dichloromethane (Aldrich) was purified by repeatedly stirring with fresh aliquots of conc. sulfuric acid (~10 % by volume) until the acid layer remained colorless. After separation it was washed successively with water, aqueous sodium bicarbonate, water, and saturated aqueous sodium chloride and dried over anhydrous calcium chloride. The dichloromethane was distilled twice from P_2O_5 under an argon atmosphere and stored in a Schlenk flask

equipped with a Teflon valve fitted with Viton O-rings. The acetonitrile was distilled from P_2O_5 under an argon atmosphere and then refluxed over calcium hydride (~12 h). After distillation from CaH_2, it was stored in Schlenk flasks under an argon atmosphere.

Cyclic Voltammetry (CV). The CV cell was of an air-tight design with high vacuum Teflon valves and Viton O-ring seals to allow an inert atmosphere to be maintained without contamination by grease. The working electrode consisted of an adjustable platinum disk embedded in a glass seal to allow periodic polishing (with a fine emery cloth) without changing the surface area (~1 mm^2) significantly. The reference SCE electrode (saturated calomel electrode) and its salt bridge were separated from the catholyte by a sintered glass frit. The counter electrode consisted of platinum gauze that was separated from the working electrode by ~3 mm. The CV measurements were carried out in a solution of 0.2 M supporting electrolyte (tetra-*n*-butylammonium hexafluorophosphate, TBAH) and the substrate in dry dichloromethane under an argon atmosphere. All the cyclic voltammograms were recorded at a sweep rate of 200 mV sec^{-1}, unless otherwise specified, and were IR compensated. The oxidation potentials (*E1/2*) were referenced to SCE, which was calibrated with added (equimolar) ferrocene (*E1/*2 = 0.450 V *vs*. SCE). The *E1/2* values were calculated by taking the average of anodic and cathodic peak potentials in the reversible cyclic voltammograms.

Laser-Flash Photolysis. The laser photolysis experiments were carried out with the third harmonic (355 nm) output of a Q switched Nd:YAG laser (10-ns fwhm, ~10 mJ) using a turnkey spectrometer (LP900 from Edinburgh Instruments) equipped with a liquid-nitrogen cooled germanium detector.

Computational Methods. Calculations for the relevant neutral and cation radicals were performed using Density Functional Theory with a Pople basis set (B3LYP/6-31G*) via the PC Spartan 08 program suite. For all structures frequency calculations were performed to verify the existence of a minimum energy stationary point. The solvation energy of each species was calculated using the SM8 model,[11] with dichloromethane as solvent.

CHAPTER 5
TRIPTYCENE-BASED SCAFFOLD FOR LONG-RANGE CHARGE TRANSPORT ASSEMBLIES/MATERIALS

Introduction

As discussed in Chapter 1, the three cofacially juxtaposed phenelyne rings in triptycene are electronically coupled, where single hole is completely delocalized onto three benzenoid rings (Figure 5.1),[1] and these molecules produce solid state assemblies which may hold potential for long range charge transport.

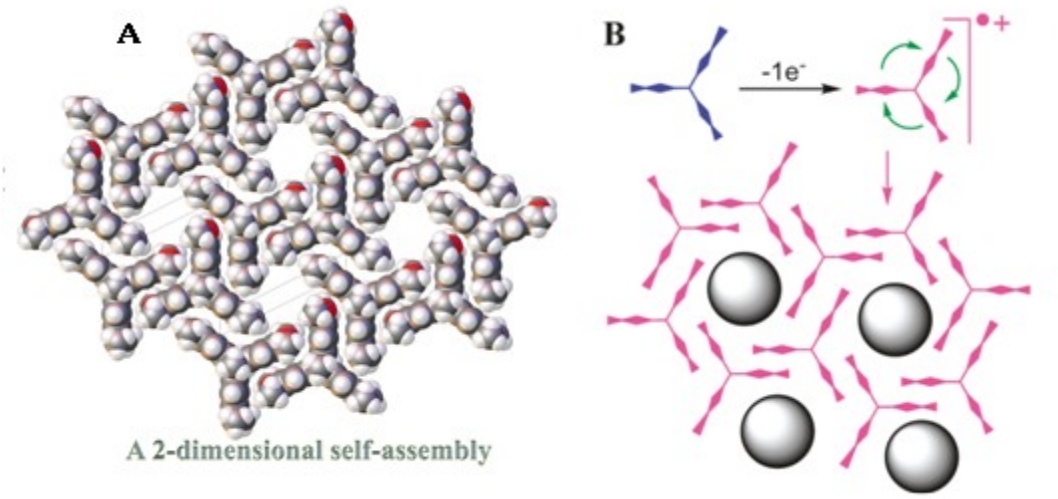

Figure 5.1 (A) Ultimate 2D electronically coupled solid-state assembly of hexamethoxytriptycene cation radical ($SbCl_6^-$) as determined by X-ray crystallography. (B) A cartoon diagrams showing the same 2D assembly of hexamethoxytriptycene cation radicals with holes (shown by shaded black spheres) for counteranions in which a single charge is deloc-alized on all electronically coupled chromophores. Note that the holes in 2D assemblies, shown by shaded black spheres, may allow the incorporation of counteranions and other guest molecules.[1]

Accordingly, we considered the preparation of new triptycene-based molecules which may be better suited for producing molecular assemblies for long-range charge transport. It is noted that triptycene itself contains two identical reactive sites on each benzenoid ring for possible attachment of function groups, i.e. Figure 5.2, structure A. It was envisioned that by transforming the benzenoid rings of the triptycene core into fluorene moieties will lead to a molecule which is amenable for controlled growth, i.e. Figure 5.2, structure B. Furthermore, a ready incorporation of alkyl groups onto the reactive methylene carbon of fluorene moieties in fluorenotriptycene (structure B) provides provision for enhanced solubility, i.e. Figure 5.2, structure B.

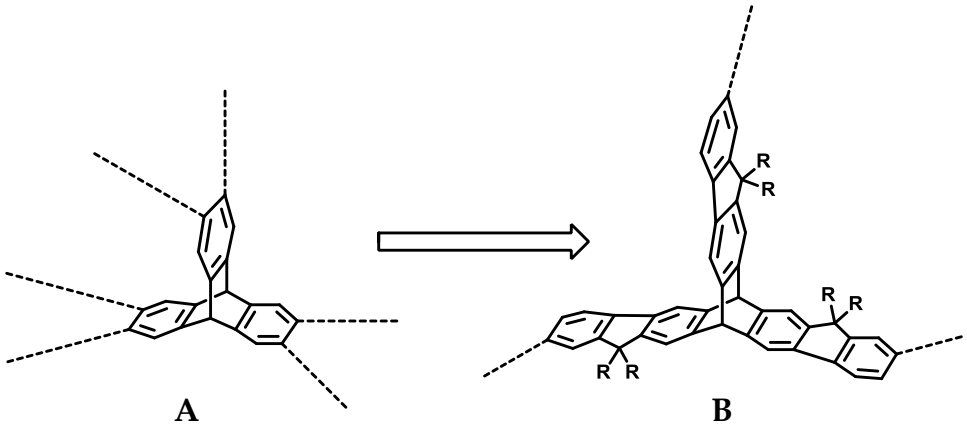

Figure 5.2 (A) Showing two reactive sites on each phenylene of parent triptycene core. (B) Showing that incorporation of fluorene moieties onto triptycene core limits it to only one reactive site per branch.

Accordingly, in this chapter we will describe a successful synthetic strategy for the preparation of fluorenotriptycene (**1**) and its annulated derivative **TF3** (**3**) and a tribromo derivative **4a**, i.e. Scheme 5.1. We will also demonstrate with the aid electrochemistry and electronic spectroscopy that a single cationic charge in fluorenotriptycene cation radical delocalizes onto all three fluorene moieties. By making

use of the tribromo derivative **4a** of fluorenotriptycene, a series of derivatives will be synthesized in order to assess their feasibility for potential applications in photovoltaic devices. The details of these findings are described herein.

Results and discussion

Synthesis of fluorenotriptycene and its annulated and tribromo derivatives. According to Scheme 5.1, the synthesis of annulated **TF3** begins with the synthesis of triptycene which was prepared in large scales (~20-30 g) following a literature procedure.[2] Bromination of triptycene was then carried out using neat bromine and pinch of iodine as catalyst, which produces hexabromotriptycene in excellent yield. Boronic acid of commercially available o-bromotoluene was made by standard lithiation using n-BuLi followed by reaction with tri-isopropylborate. This boronic acid was then coupled with hexabromotriptycene to give **1a** and **1s** via Suzuki coupling followed by cyclization in a one pot.[3] This reaction was carried out in DMA, using K_2CO_3 as base while palladium (II) acetate, tricyclohexylphosphine and trimethylacetic acid as catalyst at 140-150 ^oC. Two isomers were obtained after the coupling which is syn and anti. Column chromatography was performed in order to separate these isomers but it was found that we could separate only some anti-product otherwise rest of the product eluted as a mixture of syn and anti. The mixture of **1a** and **1s** was then subjected to hexylation which was carried out in dry THF using t-BuOK and 1-bromohexane to give **2a** and **2s**. The yield of this reaction was found to be very low. Hexylated syn **2a** and anti **2s** isomers were the separated by column chromatography using hexane as elutant. Separated syn and anti-isomer were then subjected to annulation to give **3a (anti TF3)** and **3s (syn**

TF3). Annulation was carried out in DCE by using 2, 5-Dichloro-2, 5-dimethylhexane and $AlCl_3$, and heating reaction mixture to 60-80 ^oC.

Scheme 5.1 Synthesis of annulated TF3.

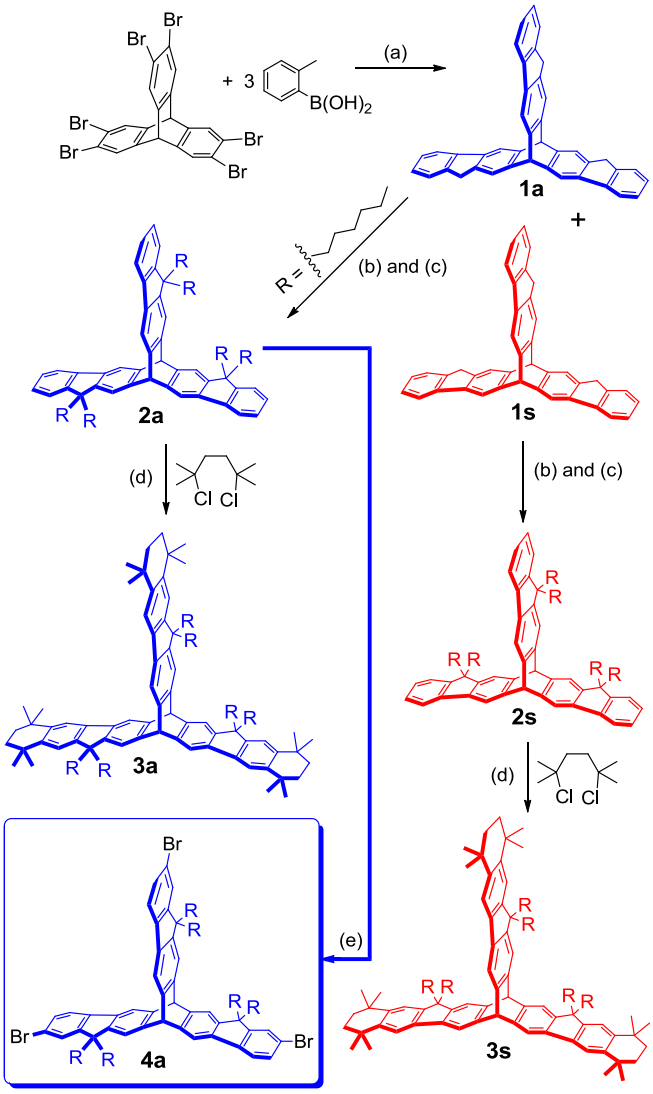

(a) $Pd(OAc)_2$ (1 mol%)/PCy3 (2 mol%)/trimethylacetic acid-DMA (1:3)/140-150 ^oC, 5h. (b) *t*-BuOK/1-bromohexane/ THF/22 ^oC. (c) Column purification on silica gel using hexane-ethylacetate (9:1) mixture. (d) $AlCl_3$, dichloroethane/60-80 ^oC/3 h. (e) Br_2/CH_2Cl_2.

In order to compare the properties of these TF3 molecules, we also prepared the model compound which is doubly annulated fluorene (DAF). According to scheme 5.2 commercially available fluorene was subjected to the hexylation reaction using 1-

bromohexane and t-BuOK in THF. After purification from column chromatography the hexylated fluorene was subjected for the annulation which was carried out in DCE by using 2, 5-dichloro-2, 5-dimethylhexane and $AlCl_3$, and heating reaction mixture to 60-80 ^oC for 2-3 hrs. The product thus formed was purified by passing through short pad of silica gel to afford a 62% yield.

Scheme 5.2 Synthesis of annulated fluorene(DAF)

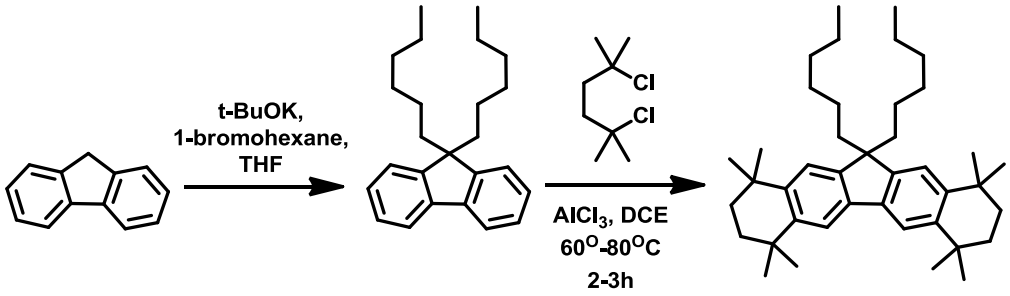

Explanation for the formation of syn and anti-isomer in 1:3 ratio.

Hexabromotriptycene upon reacting with methyl boronic acid forms two isomer which are syn and anti. As shown in the Scheme 5.3,

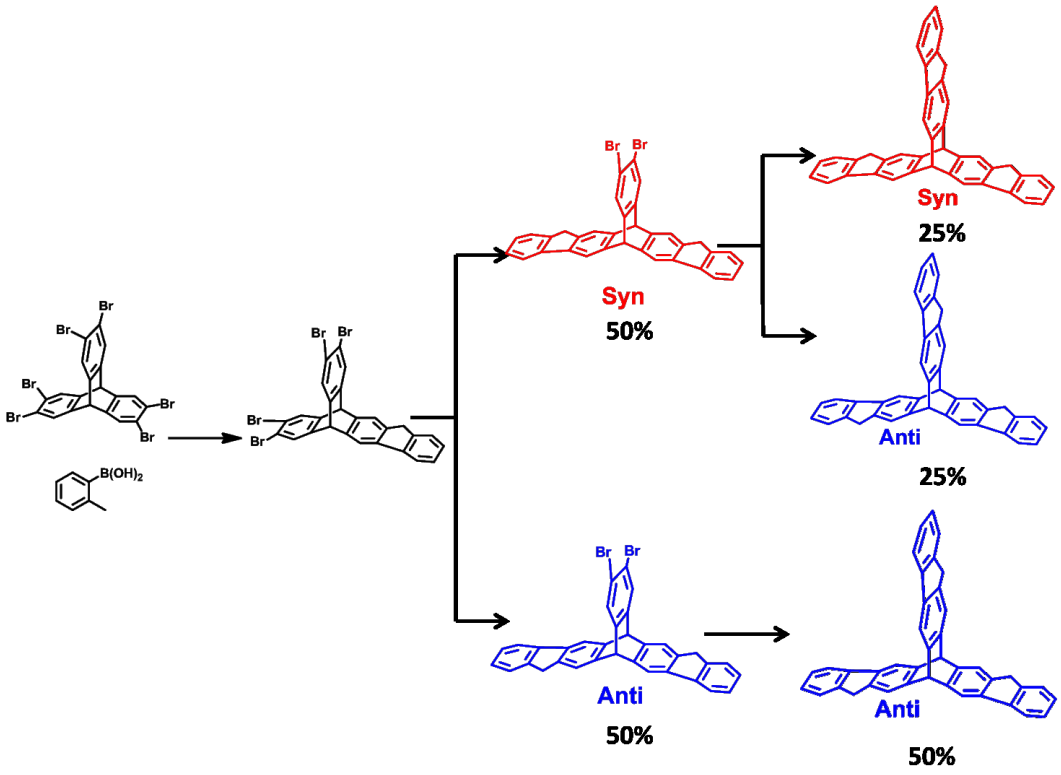

Scheme 5.3 Formation of syn and anti-isomer in 25:75 ratios.

We can clearly conclude that upon attaching first group there are no conformational isomers formed in the reaction while upon coupling 2nd group there are two isomers formed, syn and anti. Possibility of formation of syn and anti is 1:1. But in coupling of last group anti-isomer can form only anti-product while syn product can form both syn and anti in 1:1 ratio. So in the whole reaction process possibility of forming anti is approximately 75% while that of syn is only 25% and that is why very low yields of syn were observed in synthesis.

Comparison of optoelectronic properties of syn and anti-isomer of TF3 and model compound

The electron donor strength of both **syn-TF3** and **anti-TF3** were evaluated by electrochemical oxidation at a platinum electrode as a 2 x 10^{-3} M solution in dichloromethane containing 0.2 M *n*-Bu_4NPF_6 as the supporting electrolyte. The cyclic voltammograms of **syn-TF3** and **anti-TF3** showed three reversible oxidation waves (Figure 5.3), which consistently met the reversibility criteria at various scan rates of 50-500 mV/s, as they all showed cathodic/anodic peak current ratios of i_a/i_c=1.0 (theoretical). The reversible oxidation potentials of both isomers were calibrated with ferrocene as internal standard (E_{ox} = 0.45 V vs SCE) and were found to be 1.18 and 1.43 and 1.68 V vs. SCE corresponding to the formation of monocation,dication and trication respectively.

Electrochemical properties of diannulated fluorene **DAF** (model compound) were studied and compared with properties of **anti TF3**. Quantitative evaluation of CV peaks and peak currents with added ferrocene (as an internal standard, E_{ox} = 0.45V vs. SCE) revealed that the first wave in reversible cyclic volatmmograms of **DAF** and **TF3** corresponds to the production of mono cation radical (by transfer of one electron) at E_{ox1} = 1.34 and 1.18 (V vs. SCE), respectively. Comparison of first oxidation potential of DAF and TF3 showed that with increased number of fluorene groups which are electronically coupled E_{ox1} values decreases as shown in Figure 5.4.

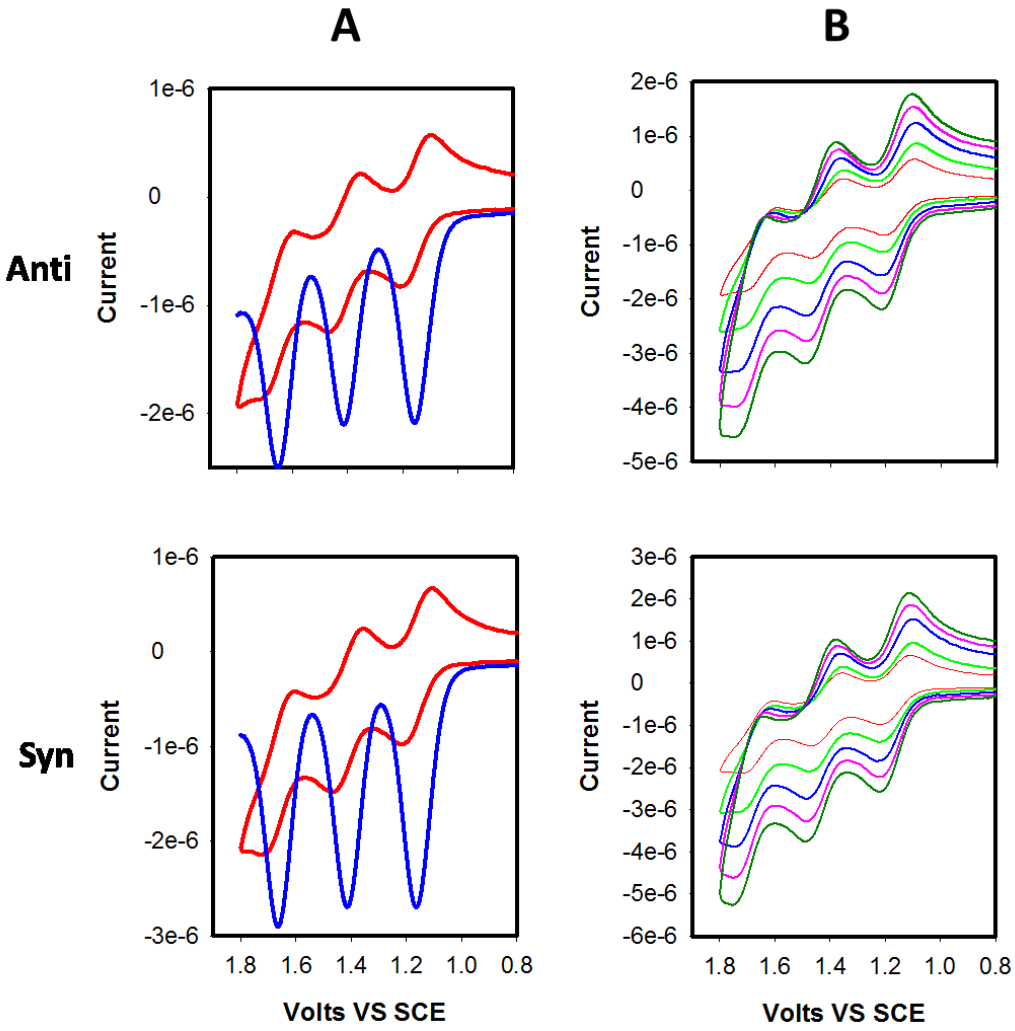

Figure 5.3 **(A)** Cyclic voltammograms of 0.5 x 10^{-3} M syn (Top) and anti (Bottom) in CH_2Cl_2 containing 0.2 M *n*-Bu_4NPF_6 at a scan rate of 200 mV/s and **(B)** cyclic voltammograms of syn (Top) and anti (Bottom) at scan rates of 50-400 mV/s at 22 °C.

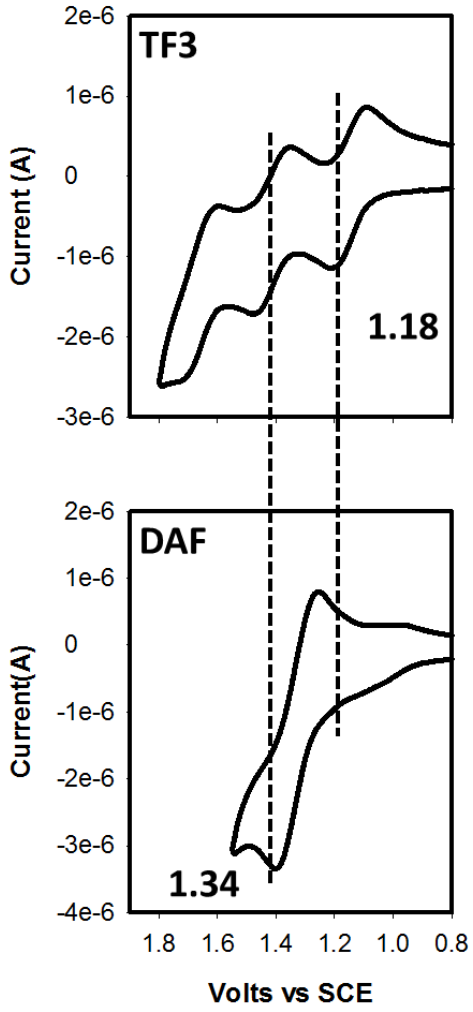

Figure 5.4 Cyclic voltamograms of **TF3** and **DAF** in CH_2Cl_2 containing 0.2M *n*-Bu_4NPF_4 at a scan rate of 100mV s^{-1} at $22^{O}C$.

Decrease in first oxiadation potential indicates that charge is more stabilized in TF3 and it was further conformed by cation radical titration.

The electrochemical reversibility of syn and anti and their relatively low oxidation potential permits its ready oxidation to the corresponding cation radical using naphthyl cation radical (**NAP**$^{+\bullet}$ $SbCl_6^-$; E_{red} = 1.34 V vs. SCE).

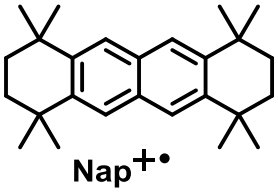

$Nap^{+\bullet}$

E^{o}_{red} = 1.34V vs. SCE

Thus Figure 5.5(A) shows the spectral changes attendant upon the reduction **NAP**$^{+\bullet}$ $SbCl_6^-$ (λmax = 672nm) by incremental addition of **Syn TF3** and **Anti TF3** to their cation radical in dichloromethane at 22^{O}C. The presence of well-defined isosbestic points at λmax = 672nm and 2350nm (**Syn TF3**) and 2450nm (**Anti TF3**) in Figure 5.5(A) established the uncluttered character of the electron transfer.

Furthermore the **plots B** of the depletion of **NAP**$^{+\bullet}$ and formation of **TF3**$^{+\bullet}$ against increments of added neutral TF3 establish that **NAP**$^{+\bullet}$ was completely consumed after the addition of one equivalent of neutral **TF3**; the resulting absorption spectrum of TF3$^{+\bullet}$ remained unchanged upon further addition of neutral **TF3**.

Comparing the cation radical spectra of both **Syn TF3** and **Anti TF3** it was found that Figure 5.5(C). Furthermore, the molar absorptivity of both Syn TF3 and anti TF3 were found to be similar as shown in Figure 5.5(C).

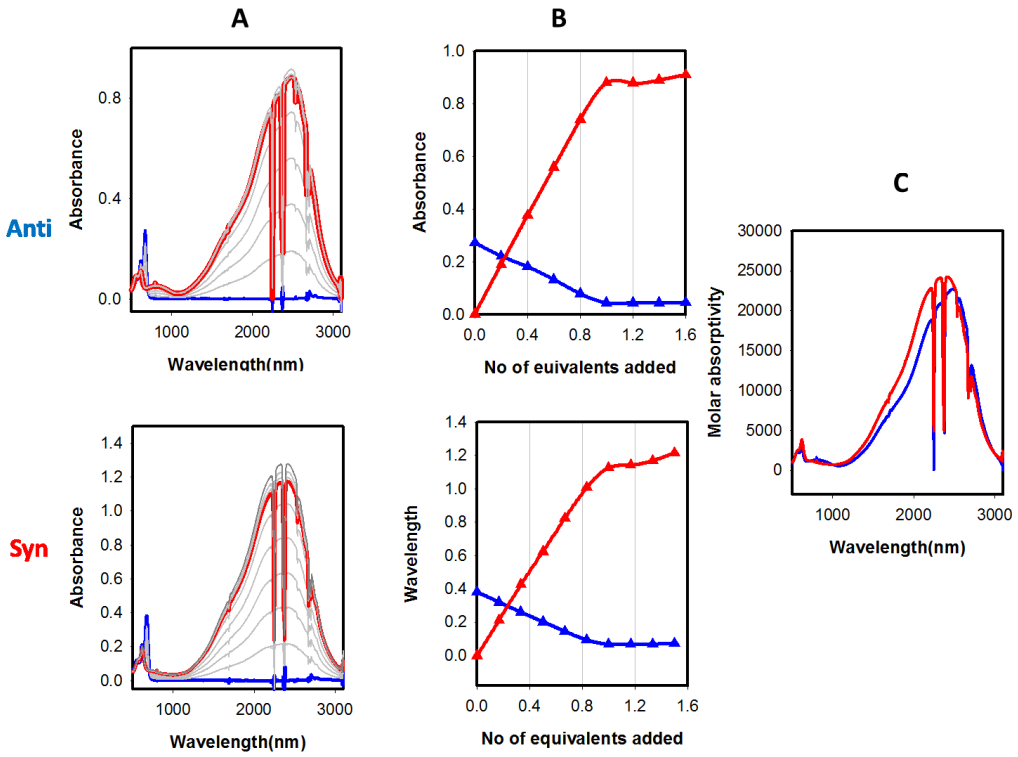

Figure 5.5 **(A)** Spectral changes observed upon the reduction of 0.877 x 10^{-4} (**anti** and) 1.22 x 10^{-4}(**syn**) M **NAP**$^{+\bullet}$**(**blue line) by an incremental addition of **anti TF3** and **syn TF3** to its cation radical(red line). **(B)**A plot of change in absorbance of **TF3**$^{+\bullet}$ and **NAP**$^{+\bullet}$ against equivalent of TF3 added in CH_2Cl_2 at 22 ^{o}C. **(C)** Comparison of molar absorptivity of **anti TF3**$^{+\bullet}$ (red) and **syn TF3**$^{+\bullet}$ (blue).

Cation radical titration of model compound was performed with naphthalene **NAP**$^{+\bullet}$ $SbCl_6^-$ (E_{red} = 1.34 V vs. SCE).

Thus Figure 5.6(A) shows the spectral changes attendant upon the reduction **NAP**$^{+\bullet}$ $SbCl_6^-$ (λmax = 672nm) by incremental addition of **DAF** to its cation radical in dichloromethane at 22 ^{o}C. The presence of well-defined isosbestic points at λmax = 672nm and 713nm in Figure 5.6 established the uncluttered character of the electron transfer. Furthermore the plots B of the depletion of **NAP**$^{+\bullet}$ and formation of **DAF**$^{+\bullet}$ against increments of added neutral **DAF** establish that **NAP**$^{+\bullet}$ was completely consumed

after the addition of one equivalent of **DAF**; the resulting absorption spectrum of **DAF**$^{+\bullet}$ remained unchanged upon further addition of neutral **DAF**.

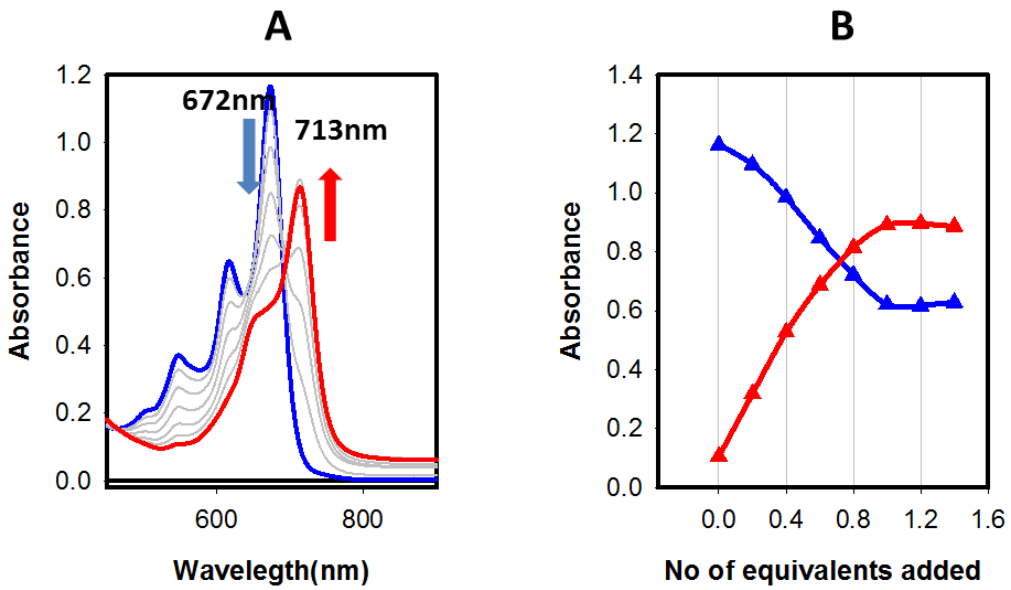

Figure 5.6 **(A)** Spectral changes observed upon the reduction of 1.737 x 10^{-4}M **NAP**$^{+\bullet}$ (blue line) by incremental addition of **DAF** to its cation radical (red line). **(B)** A plot of change in absorbance of **DAF**$^{+\bullet}$ (at 713nm) and **NAP**$^{+\bullet}$ (at 672nm) against equivalent of added **DAF** in CH_2Cl_2 at 22 ^{o}C.

The large NIR transition in **TF3**$^{+\bullet}$ was observed which was expected due to the delocalization of charge over three fluorene moieties while for **DAF**$^{+\bullet}$ local band at 713nm was observed. Figure 5.7 indicates the comparison of molar absorptivity of DAF$^{+\bullet}$ and **TF3**$^{+\bullet}$. Molar absorptivity was fond to increase almost 3 times as compared to **DAF**$^{+\bullet}$ which is another evidence of charge migration in TF3 molecule.

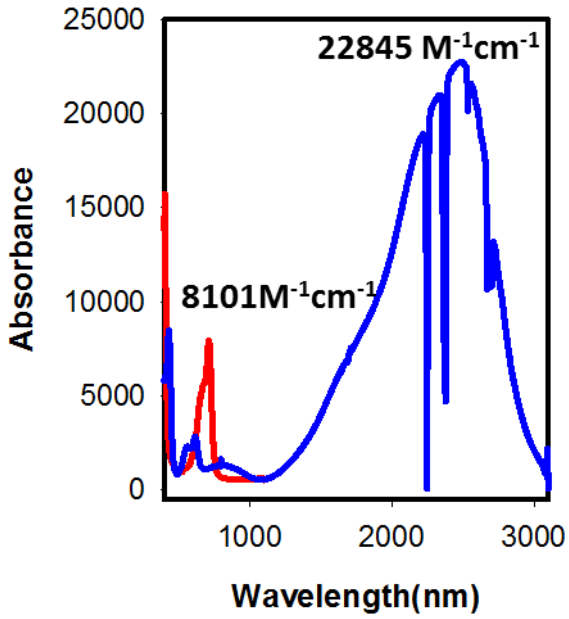

Figure 5.7 The comparison of molar absorptivity of **DAF**$^{+\bullet}$ and **TF3**$^{+\bullet}$.

The optical properties of neutral TF3 were evaluated with the aid of UV-Vis and emission spectroscopy as follows. The electronic absorption spectra of both Syn and anti-isomer, in dichloromethane, were recorded under identical concentration and temperature (22 ^{o}C) and are compiled in Figure 5.8. Both Syn and Anti isomers showed characteristic absorption band at 330nm and molar extinction coefficients of both isomers were found to be 24363$M^{-1}cm^{-1}$ and 22845$M^{-1}cm^{-1}$ respectively.

The emission spectra were recorded under conditions of constant concentration and temperature (22 ^{o}C). Expectedly both isomers showed emission at 340nm.

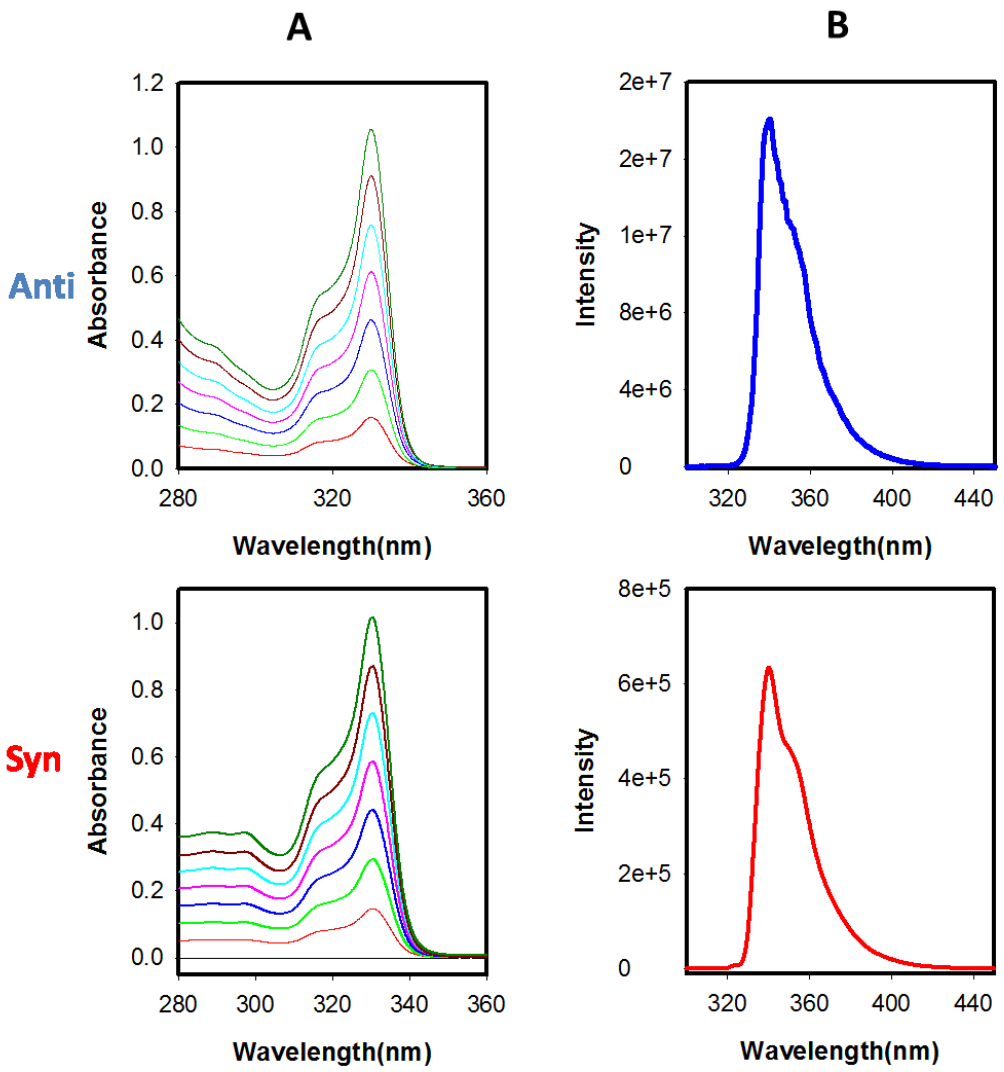

Figure 5.8 **(A)** Absorption spectra for **anti TF3** and **syn TF3**. **(B)** Emission spectra for **anti TF3** and **syn TF3**.

Similar studies were carried out for model compound DAF. For DAF maximum absorption peak at 317nm and maximum emission peak at 325nm were observed while maximum absorption peak at 330nm and maximum emission peak at 340nm were observed for TF3. The large red shifts for absorption and emission from DAF to TF3 is consistent with electrochemical evidence of electronic delocalization (Figure 5.9).

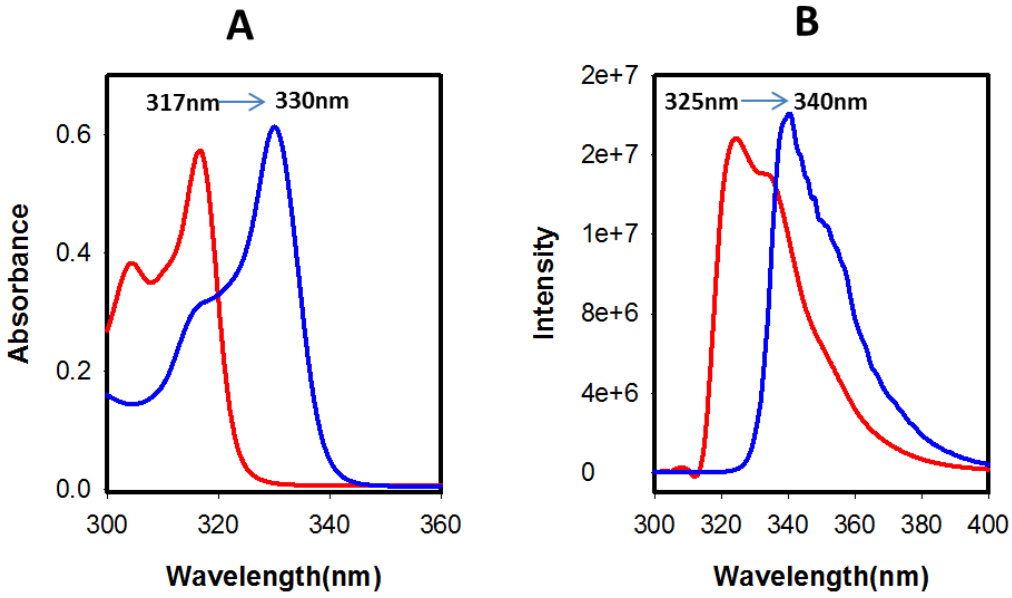

Figure 5.9 **(A)** Comparison of absorption of **DAF**$^{+\bullet}$ (Red line) and **TF3**$^{+\bullet}$ (blue line). **(B)** Comparison of emission spectra of **DAF**$^{+\bullet}$ (Red line) and **TF3**$^{+\bullet}$ (blue line).

TF3 derivatives for self-assembled charge transport materials

Since optoelectronic properties of both syn-TF3 and anti TF3 were found to be same and also the 75% formation of anti TF3 in the reaction lead us for the utilization of anti TF3 for further investigation on these molecules. As explained in Scheme 5.1 anti TF3 can be easily brominated using NBS in acetonitrile and using catalytic amount of Ammonium nitrate. This tribromo derivative of anti TF3 was subjected to Suzuki coupling with various aryl boronic acids (Scheme 5.4) to give TF3 derivatives which can be used in self-assembled charge transport materials.

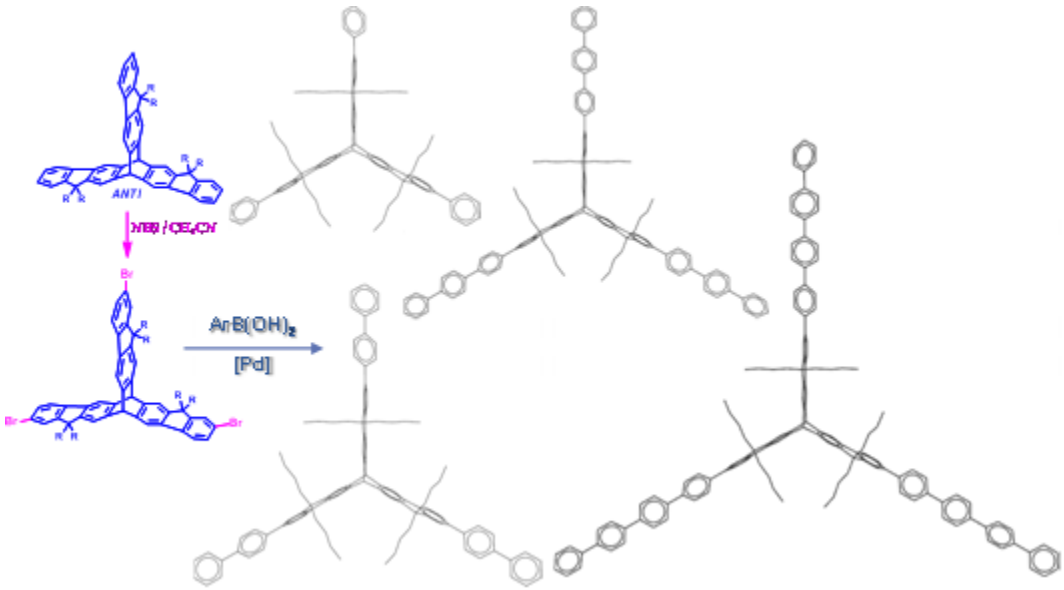

Scheme 5.4 Formation of various TF3 derivatives which can be used in self assembled charge transport materials.

Derivatives with phenyl, biphenyl and terphenyl are prepared and their characterization is given in experimental section. These molecules are expected to show non-covalent self-assemblies (Figure 5.10 (A)) while controlled covalent assemblies can also be achieved by synthetic route (Figure 5.10 (B)).

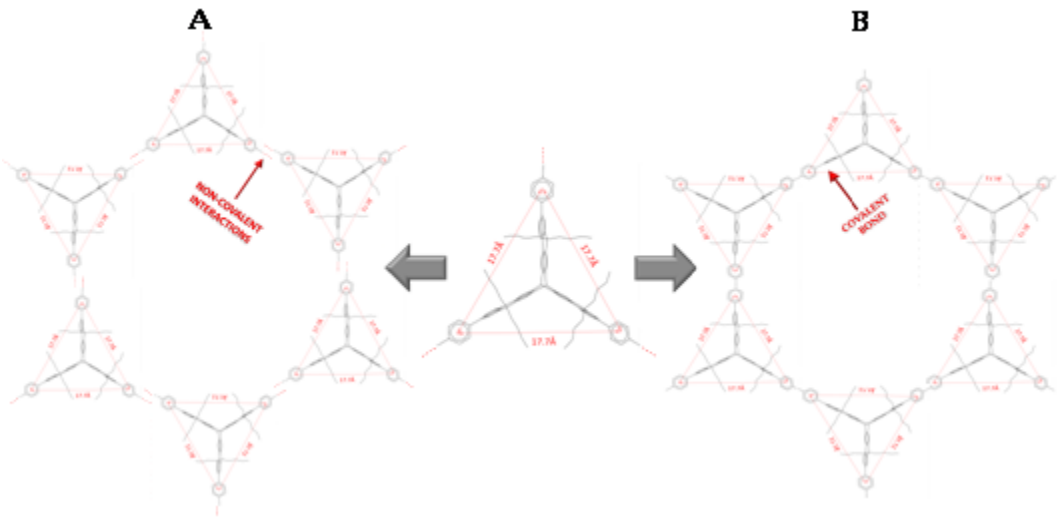

Figure 5.10 **(A)** Non-covalent assembly of TF3 derivatives **(B)** Covalent assembly of TF3 derivative.

Conclusions

We have successfully demonstrated the synthesis of the triptycene based TF3 molecule and separation of syn and anti-isomer thus formed in the reaction. These molecules were found to show the electronic coupling between interacting aryl moieties was shown by electrochemical oxidation as well as charge resonance transitions in UV-Vis-NIR absorption spectra. These molecules can also be further expanded by attaching larger and longer chromophores to it. This triptycene scaffold and its derivatives are expected to form two-dimensional self-assemblies which are potentially useful as long-range charge-transport materials in modern photovoltaic devices.

Experimental section

General Experimental Methods and Materials. All reactions were performed under argon atmosphere unless otherwise noted. All commercial reagents were used without further purification unless otherwise noted. Dichloromethane (Aldrich) was repeatedly stirred with fresh aliquots of concentrated sulfuric acid (~10 % by volume) until the acid layer remained colorless. After separation it was washed successively with water, aqueous sodium bicarbonate, water, and aqueous sodium chloride and dried over anhydrous calcium chloride. The dichloromethane was distilled twice from P_2O_5 under an argon atmosphere and stored in a Schlenk flask equipped with a Teflon valve fitted with Viton O-rings. The hexanes and toluene were distilled from P_2O_5 under an argon atmosphere and then refluxed over calcium hydride (~12 h). After distillation from CaH_2, the solvents were stored in Schlenk flasks under an argon atmosphere. Tetrahydrofuran (THF) was dried initially by distilling over lithium aluminum hydride under an argon atmosphere. The THF was further refluxed over metallic sodium in the presence of benzophenone until a persistent blue color was obtained and then it was distilled under an argon atmosphere and stored in a Schlenk flask equipped with a Teflon valve fitted with Viton O-rings. NMR spectra were recorded on Varian 300 and 400 MHz NMR spectrometers. GC-MS spectra were obtained on a Fisons 8000 trio instrument at an ionization potential of 70 eV.

Cyclic Voltammetry (CV). The CV cell was of an air-tight design with high vacuum Teflon valves and Viton O-ring seals to allow an inert atmosphere to be maintained without contamination by grease. The working electrode consisted of an adjustable

platinum disk embedded in a glass seal to allow periodic polishing (with a fine emery cloth) without changing the surface area (~1 mm2) significantly. The reference SCE electrode (saturated calomel electrode) and its salt bridge were separated from the catholyte by a sintered glass frit. The counter electrode consisted of platinum gauze that was separated from the working electrode by ~3 mm. The CV measurements were carried out in a solution of 0.2 M supporting electrolyte (tetra-*n*-butylammonium hexafluorophosphate, TBAH) and 2-5 x 10^{-3} M substrate in dry dichloromethane under an argon atmosphere. All the cyclic voltammograms were recorded at a sweep rate of 200 mV sec^{-1}, unless otherwise specified and were IR compensated. The oxidation potentials ($E_{1/2}$) were referenced to SCE, which was calibrated with added (equimolar) ferrocene ($E_{1/2}$ = 0.450 V *vs*. SCE). The $E_{1/2}$ values were calculated by taking the average of anodic and cathodic peak potentials in the reversible cyclic voltammograms.

Preparation of various intermediates

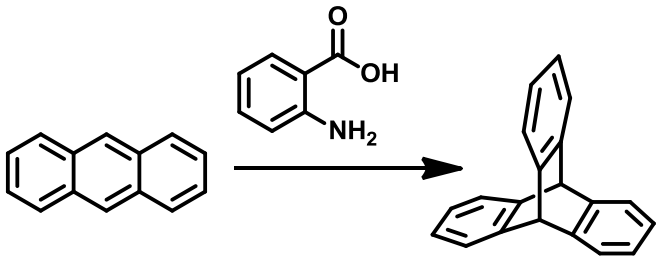

Triptycene : In 125mL round bottomed flask, mounted in a heating mental and fitted with short reflux condenser, 2g of anthracene , 2mL of isoamyl nitrite and 20mL of 1,2-dimethoxyethane were placed. A filter paper moistened with 1, 2-dimethoxyethane and inserted in stem funnel. 2.6g of anthranilic acid was placed in filter paper and funnel was rested on top of condenser. Reaction mixture was brought to gentle boil. 20mL of 1, 2-

dimethoxyethane was measured in graduated cylinder and added to the anthranilic acid slowly using capillary dropping tube, to slowly leach the acid into reaction flask. Leaching of acid was done in no less than 20min. using 10mL of 1, 2-dimethoxyethane. Second 2.6g portion of anthranilic acid was added to the funnel. Heating source was removed and another portion of isoamyl nitrite (2mL) was added. Heat was resumed and added anthranilic acid was leached to another 20min. reaction mixture was refluxed for 10 min. 10mL of 95% ethanol and a solution of sodium hydroxide (3g in 40mL water) was added to reaction mixture to produce suspension which was then cooled thoroughly in ice. Precipitate thus formed was filtered through Buchner funnel and washed with ice cold mixture of 4:1 methanol-water. 1g of maleic anhydride and 20mL of triethylene glycol dimethyl ether was added to the above precipitate and the mixture was heated to reflux for 5min. Then it was cooled down to 100^0C and 10mL of 95% ethanol and a solution of sodium hydroxide (3g in 40mL water) were added to reaction mixture to produce suspension which was then cooled thoroughly in ice. Precipitate thus formed was filtered through Buchner funnel and washed with ice cold mixture of 4:1 methanol-water. (1.5g, 52%) M.P. 255 ^{o}C, ^{1}H NMR ($CDCl_3$) δ: 5.43(2H, s), 6.96-7.01(4H, m), 7.36-7.41(4H, m). ^{13}C NMR ($CDCl_3$) δ: 54.25, 123.80, 125.33, 145.45.

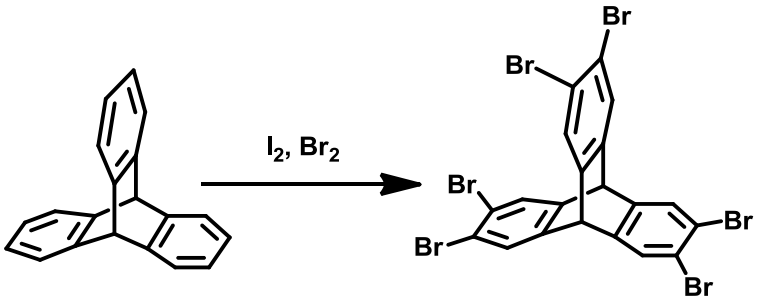

Hexabromotriptycene: To an ice cold mixture of bromine (2mL, 0.39mmol) and iodine (10mg, 0.04mmol) was added triptycene (508mg, 2mmol) in small portions over a period of an hour. The reaction vessel was shielded from light and the reaction was continued for 6hrs in an ice cold bath followed by 18hrs stirring at room temperature.Excess bromine was removed by treating the reaction mixture with ethanol at -78 ^{o}C. Product was purified by recrystallization with DCM and methanol (1.3g, 92.85 %). M.P. >350 ^{o}C, ^{1}H NMR ($CDCl_3$) δ: 5.23(s, 2H), 7.02(s, 6H). ^{13}C NMR ($CDCl_3$) δ: 51.24, 121.90, 129.25, 144.06.

Synthesis of **1s** and **1a**

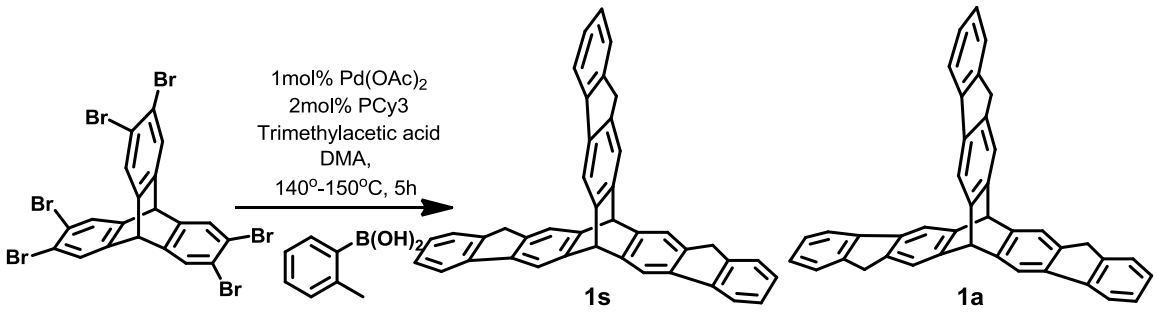

DMA (60mL) was added to the flask containing hexambromotriptycene(7.8g, 10.71mmol) ,2-methylphenylboronic acid(4.81g, 35.37mmol), K_2CO_3 (26.64g, 192.78mmols), Palladium(II) acetate (1.071mmols), tricyclohexylphosphine (2.142mmol), and trimethylacetic acid(3.281g, 32.13mmol). After the reaction mixture had been stirred at 140–150 ^{o}C for 5 h, the mixture was cooled down to room temperature. The reaction mixture was quenched by adding water. The mixture was extracted with CH_2Cl_2. The organic layer was washed with brine. After removal of the solvents the crude reaction mixture was purified by column chromatography on silica gel

with hexanes as the eluent to afford the desired mixture of syn and anti-product (4.0g, 71%), ^{1}H NMR ($CDCl_3$) δ: 3.63(12H, s), 5.42(1H, s), 5.48(1H, s), 5.54(1H, s), 5.60(1H, s), 7.10(6H, t, J=7.88Hz), 7.21(6H, t, J= 7.38Hz), 7.33(6H, d, J=7.38Hz), 7.46-7.51(6H, m), 7.60(6H, d, J=7.63Hz), 7.71-7.77(6H, m).

Synthesis of **2s** and **2a**

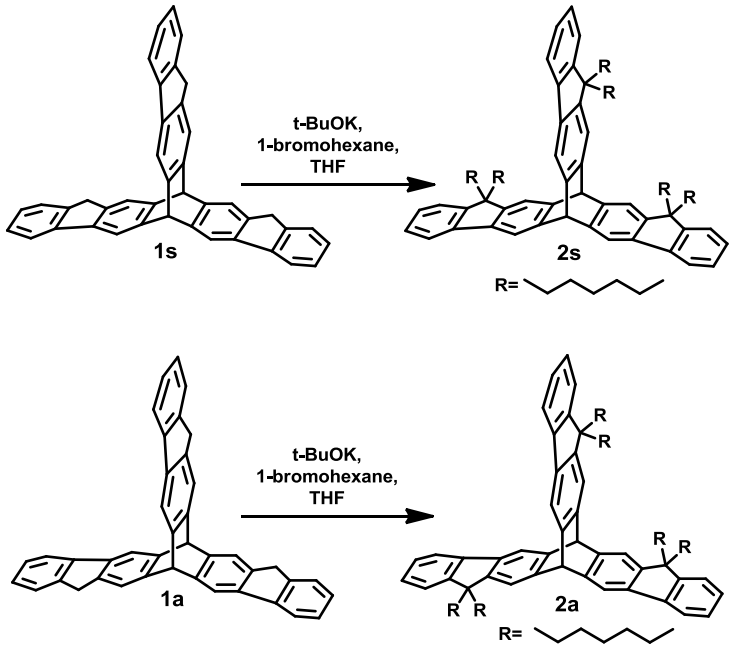

In schlenk under Ar mixture of **1a** and **1s** (0.3g, 0.578mmol) was dissolved in THF (20mL) and t-BuOK(0.648g, 5.78mmol) was added to it. Dark red colored reaction mixture was stirred for half an hour and then 1-bromohexane (0.954g, 5.78mmol) was added drop wise and reaction mixture was stirred at room temperature overnight. It was then quenched by addition of 5%HCl. The mixture was extracted with CH_2Cl_2. The organic layer was washed with brine. After removal of the solvents the crude reaction mixture containing both syn and anti-isomers was purified by column chromatography.

Syn and anti-isomers were separated by column chromatography using only hexane as elutant (0.3g, 50%)

Anti: M.P. >170 ^{o}C ^{1}H NMR ($CDCl_3$) δ: 0.45-0.73(30H, m), 0.84-1.08(36H, m), 1.80-1.96(12H, m), 5.51(1H, s), 5.55(1H, s), 7.15-7.29(9H, m), 7.34-7.37(3H, m), 7.59-7.65(3H, m), 7.74(3H, s). ^{13}C NMR ($CDCl_3$) δ: 14.13, 14.18, 22.71, 23.83, 23.83, 29.81, 29.82, 31.51, 31.52, 40.12, 40.25, 40.55, 54.87, 54.89, 55.28, 55.43, 115.28, 118.42, 118.54, 119.16, 119.21, 122.89, 123.06, 126.39, 126.75, 137.79, 137.91, 141.37, 141.41, 144.68, 144.83, 145.43, 145.52, 148.26, 148.38, 151.36, 151.45.

Syn: ^{1}H NMR ($CDCl_3$) δ: 0.44-0.60(12H, m), 0.68(18H, t, J=7.13Hz), 0.83-1.08(36H, m), 1.79-1.98(12H, m), 5.50(1H, s), 5.63(1H, s), 7.15-7.30(9H, m), 7.37(3H, m), 7.61(3H, d, J=7.86Hz), 7.76(3H, s). ^{13}C NMR ($CDCl_3$) δ: 14.16, 22.71, 23.77, 29.82, 31.52, 40.46, 54.93, 55.08, 55.53, 115.35, 118.39, 119.26, 122.73, 126.40, 126.79, 138.11, 141.45, 144.74, 145.36, 148.20, 151.26.

Synthesis of **3a**

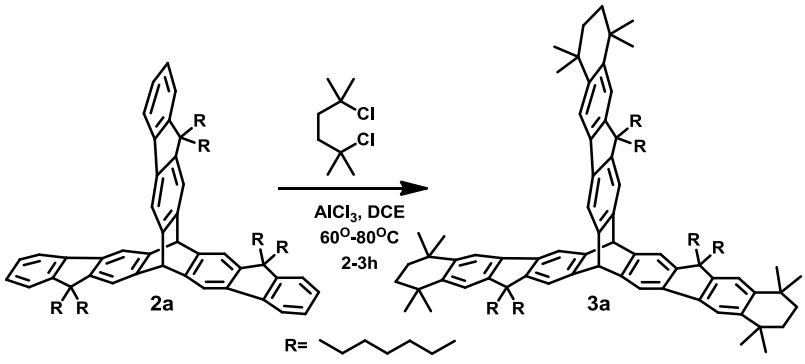

Anhydrous AlCl3 (~10mg) was added portion wise to the solution of **2a** (0.16mg, 0.195mmol) in DCE (20mL). Reaction mixture was then cooled to -0 ^{o}C. Solution of 2,

5-Dichloro-2, 5-dimethylhexane (0.143g, 0.78mmol) in DCE (5mL) was added to above mixture drop wise. Reaction mixture was then heated to 60 -80 ^{o}C overnight. Reaction mixture was cooled to room temperature and then poured in the mixture of ice and HCl. Stirred for 10min and then extracted with DCM. Organic layer was washed with water and then dried over anhydrous $MgSO_4$. It is then evaporated to afford crude product which was further purified by column chromatography using only hexane as elutant (0.150g, 71%). M.P. >104 ^{o}C

^{1}H NMR ($CDCl_3$) δ: 0.56-0.79(30H, m), 1.02-1.14(36H, m), 1.28-1.40(36H, m), 1.72(12H, s), 1.80-1.94(12H, m), 5.51(1H, s), 5.55(1H, s), 7.18(2H, s), 7.20(1H, s), 7.34(2H, s), 7.35(1H, s), 7.56(2H, s), 7.59(1H, s), 7.75(2H, s), 7.77(1H, s). ^{13}C NMR ($CDCl_3$) δ: 14.19, 22.65, 22.73, 23.78, 2397, 29.72, 29.85, 29.86, 29.96, 31.45, 31.55, 31.56, 32.35, 32.43, 34.62, 34.63, 34.72, 34.74, 35.54, 35.57, 39.91, 40.11, 40.45, 54.38, 54.41, 55.42, 55.50, 114.79, 114.86, 116.62, 116.71, 118.40, 118.54, 120.81, 121.05, 137.89, 138.05, 138.63, 138.67, 143.01, 143.03, 143.09, 144.67, 144.87, 144.89, 145.09, 148.35, 148.43, 148.47, 148.60.

Synthesis of **3s**

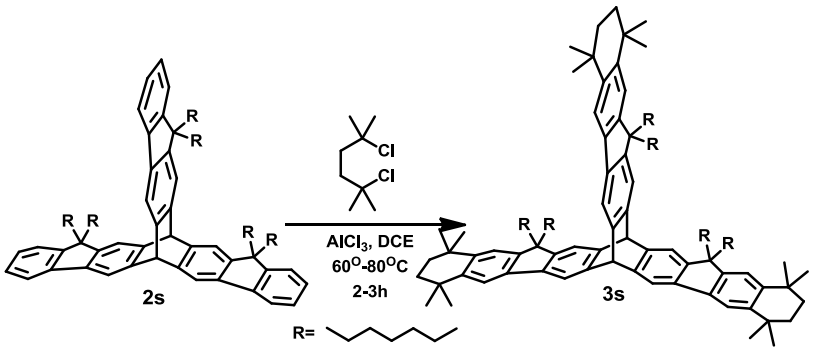

Anhydrous AlCl3 (~10mg) was added portion wise to the solution of **2s** (0.07mg, 0.068mmol) in DCE(10mL). Reaction mixture was then cooled to -0 ^{o}C. Solution of 2,5-Dichloro-2,5-dimethylhexane(0.045g, 0.25mmol) in DCE(5mL) was added to above mixture drop wise. Reaction mixture was then heated to 60-80 ^{o}C overnight. Reaction mixture was cooled to room temperature and then poured in the mixture of ice and HCl. Stirred for 10min and then extracted with DCM. Organic layer was washed with water and then dried over anhydrous $MgSO_4$. It is then evaporated to afford crude product which was further purified by column chromatography using only hexane as elutant (0.04g, 43%). M.P. >160 ^{o}C

^{1}H NMR ($CDCl_3$) δ: 0.52-0.64(12H, m), 0.70(18H, t, J= 7.20Hz), 0.91-1.08(36H, m), 1.27(18H, s), 1.32(18H, s), 1.68(12H, s), 1.76-1.88(12H, m), 5.43(1H, s), 5.56(1H, s), 7.12(3H, s), 7.31(3H, s), 7.50(3H, s), 7.70(3H, s). ^{13}C NMR ($CDCl_3$) δ: 14.16, 22.64, 23.80, 29.73, 31.46, 32.37, 32.41, 34.61, 34.71, 35.52, 35.53, 40.23, 54.43, 55.26, 55.51, 114.78, 116.80, 118.35, 120.62, 138.26, 138.69, 142.99, 144.73, 144.89, 148.21, 148.38.

Synthesis of **4a**

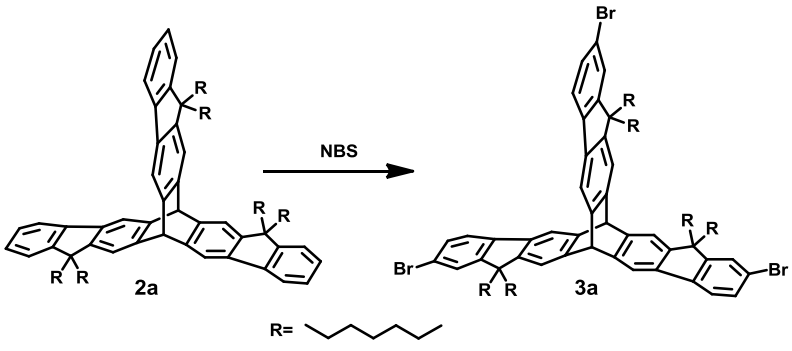

To a solution of **3a** (0.1g, 0.097 mmol) in acetonitrile (25 mL) was added *N*-bromosuccinimide (0.052 g, 0.293 mmol) and NH_4NO_3 (~10 mg, 0.0097 mmol). The

mixture was stirred overnight at room temperature and thereafter filtered and washed with water (10 mL × 3) and methanol (10 mL × 2) to yield the crude product which was used as such in the next step. Yield (0.12g, 97.5 %).

Anti: ^{1}H NMR ($CDCl_3$) δ: 0.44-0.76(30H, m), 0.89-1.10(36H, m), 1.80-1.97(12H, m), 5.53(1H, s), 5.57(1H, s), 7.36(3H, s), 7.38-7.43(6H, m), 7.46-7.52(3H, m), 7.72(3H, s).

^{13}C NMR ($CDCl_3$) δ: 14.08, 14.14, 22.64, 22.67, 23.72, 29.67, 29.75, 31.45, 39.93, 40.06, 40.37, 53.62, 55.10, 55.27, 115.40, 115.42, 118.48, 118.57, 120.44, 120.55, 126.20, 126.32, 129.95, 136.94, 137.02, 140.30, 140.33, 144.61, 144.77, 145.57, 145.65, 148.11, 148.21, 153.59, 153.65.

Synthesis of **Hexylated fluorene**

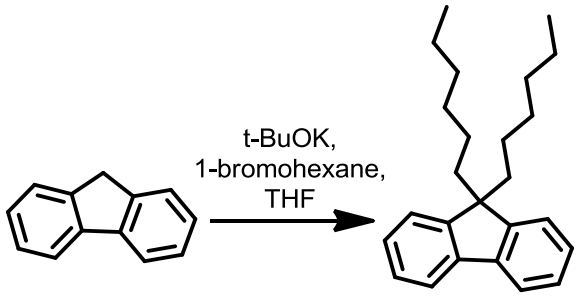

In schlenk under Ar commercially available fluorene (0.3g, 0.578mmol) was dissolved in THF (20mL) and t-BuOK(0.648g, 5.78mmol) was added to it. Dark red colored reaction mixture was stirred for half an hour and then 1-bromohexane (0.954g, 5.78mmol) was added drop wise and reaction mixture was stirred at room temperature overnight. It was then quenched by addition of 5%HCl. The mixture was extracted with CH_2Cl_2. The organic layer was washed with brine. After removal of the solvents the crude reaction mixture containing both syn and anti-isomers was purified by column chromatography.

Syn and anti-isomers were separated by column chromatography using only hexane as elutant (0.3g, 50%) ^{1}H NMR ($CDCl_3$) δ: 0.51-0.68(4H, m), 0.74(6H, t, J= 6.98Hz), 0.92-1.16(12H, m), 1.87-2.02(4H, m), 7.2-7.4(6H, m), 7.69(2H, d, J=6.65Hz). ^{13}C NMR ($CDCl_3$) δ: 14.22, 22.79, 23.91, 29.94, 31.71, 40.62, 55.19, 119.82, 123.01, 126.82, 127.17, 141.29, 150.86.

Synthesis of **Doubly Annulated Fluorene**

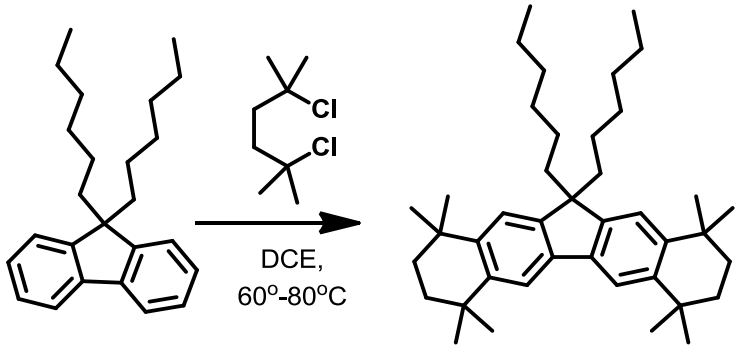

Anhydrous AlCl3 (~50mg) was added portion wise to the solution of hehylated fluorene (1.0g, 2.98mmol) in DCE(40mL). Reaction mixture was then cooled to -0 ^{o}C. Solution of 2,5-Dichloro-2,5-dimethylhexane(1.20g, 6.57mmol) in DCE(10mL) was added to above mixture drop wise. Reaction mixture was then heated to 60-80 ^{o}C overnight. Reaction mixture was cooled to room temperature and then poured in the mixture of ice and HCl. Stirred for 10min and then extracted with DCM. Organic layer was washed with water and then dried over anhydrous $MgSO_4$. It is then evaporated to afford crude product which was further purified by column chromatography using only hexane as elutant (1.03g, 62.4%). ^{1}H NMR ($CDCl_3$) δ: 0.68-0.97(10H, m), 1.00-1.17(12H, m), 1.30(12H, s), 1.36(12H, s), 1.71(8H, s), 1.79-1.86(4H, m), 7.18(2H, s), 7.54(2H, s). ^{13}C NMR

($CDCl_3$) δ: 14.23, 22.69, 24.06, 29.82, 31.58, 32.44, 32.46, 34.68, 34.77, 35.54, 35.64, 40.17, 54.17, 116.81, 120.97, 138.60, 143.03, 143.29, 148.34.

Synthesis of **4-Bromo-p-terphenyl**

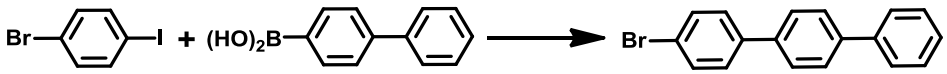

1-Bromo-4-iodobenzene (5.0 g, 17.67 mmol) and 4-Biphenylboronic acid acid (3.32 g, 16.79 mmol) were dissolved in anhydrous 1,2-dimethoxyethane (DME) (60 mL) in an oven dried Schlenk flask under an argon atmosphere and the flask was evacuated and filled with argon (3x). In another oven dried Schlenk flask a solution of anhydrous sodium carbonate (5 g) in water (20 mL) was prepared under an argon atmosphere and the flask was also evacuated and filled with argon (3x). To the DME solution, $Pd(PPh_3)_4$ (50 mg) and the salt solution were added sequentially under a strict argon atmosphere followed by evacuation and filling the flask with argon (3x) after each addition. The flask was covered with foil and the solution was allowed to reflux overnight. The resulting solution was cooled to room temperature, quenched with water (50 mL) and extracted with dichloromethane (3 x 20mL). The organic layer was dried over anhydrous magnesium sulfate, evaporated and dried under vacuum. Purified by column chromatography using a hexanes/ethyl mixture to give the pure product (4.5 g, 82.41%); ^{1}H NMR ($CDCl_3$) δ: 7.37(1H, t, J=7.34Hz), 7.44-7.53(4H, m), 7.56-7.60(2H, m), 7.62-7.70(6H, m). ^{13}C NMR ($CDCl_3$) δ: 121.81, 127.25, 127.50, 127.69, 127.84, 128.82, 129.07, 132.13, 139.05, 139.80, 140.71.

Synthesis of **Terphenyl-4-boronic ester**

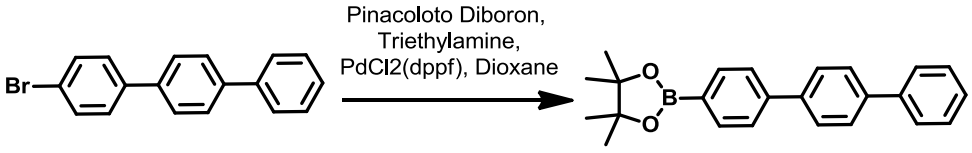

To a Schlenk flask under argon atmosphere, a mixture of 4-Bromo-p-terphenyl (2.0 g, 5.96 mmol) and $PdCl_2$ (100 mg) were added to a solution of 1, 4-dioxane (60 mL) and KOAc (1.46g, 14.9 mmol). The mixture was stirred and then Bis(Pinacoloto)Diboron (3.03 g, 11.93 mmol) was added. The reaction mixture was heated to reflux overnight. Reaction was quenched with water and extracted with DCM. Organic lay was washed with water and then dried over $MgSO_4$. Solvent was evaporated with rotavap to give crude product which was then passed through short pad of $MgSO_4$ using hexane as solvent to give pure product (1.5g, 70.75%).

^{1}H NMR ($CDCl_3$) δ: 1.37(12H, s), 7.36(1H, t, J=7.34Hz), 7.46(2H, t, J=7.92Hz), 7.62-7.74(8H, m), 7.91(2H, d, J=8.11Hz). ^{13}C NMR ($CDCl_3$) δ: 25.01, 67.21, 83.95, 126.43, 127.18, 127.51, 127.63, 127.70, 128.95, 135.44, 139.97, 140.55, 140.77, 143.43.

Synthesis of **Terphenyl derivative of TF3**

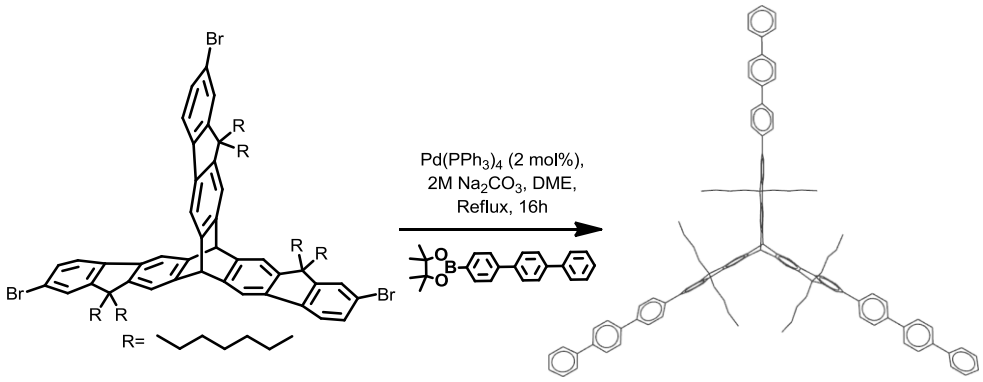

4a (0.2 g, 0.16 mmol) and terphenyl-4-boronic ester (0.228 g, 0.64 mmol) were dissolved in anhydrous 1,2-dimethoxyethane (DME) (30 mL) in an oven dried Schlenk flask under an argon atmosphere and the flask was evacuated and filled with argon (3x). In another oven dried Schlenk flask a solution of anhydrous sodium carbonate (2.5 g) in water (10 mL) was prepared under an argon atmosphere and the flask was also evacuated and filled with argon (3x). To the DME solution, $Pd(PPh_3)_4$ (50 mg) and the salt solution were added sequentially under a strict argon atmosphere followed by evacuation and filling the flask with argon (3x) after each addition. The flask was covered with foil and the solution was allowed to reflux overnight. The resulting solution was cooled to room temperature, quenched with water (50 mL) and extracted with dichloromethane (3 x 20mL). The organic layer was dried over anhydrous magnesium sulfate, evaporated and dried under vacuum. Purified by column chromatography using a hexanes/ethyl mixture to give the pure product (0.126 g, 50%); ^{1}H NMR ($CDCl_3$) δ: 0.56-0.74(30H, m), 0.91-1.08(36H, m), 1.87-2.01(12H, m), 5.57(1H, s), 5.62(1H, s), 7.36(3H, t, J=7.37Hz), 7.40-7.43(3H, m), 7.47(6H, t, J=7.82Hz), 7.53-7.62(6H, m), 7.63-7.69(8H, m), 7.70-7.76(25H, m), 7.81(3H, s). ^{13}C NMR ($CDCl_3$) δ: 14.15, 14.19, 22.72, 23.90, 29.81, 31.51, 31.53, 40.19, 40.29, 40.31, 40.59, 40.60, 55.06, 55.08, 55.31, 55.45, 115.44, 118.55, 118.67, 119.56, 121.44, 121.61, 125.91, 125.94, 127.26, 127.56, 127.72, 127.77, 129.04, 137.49, 137.62, 138.80, 138.83, 139.43, 139.46, 139.87, 140.35, 140.36, 140.91, 140.96, 140.98, 144.76, 144.90, 145.50, 145.58, 148.70, 148.82, 152.15, 152.24.

Synthesis of **Biphenyl derivative of TF3**

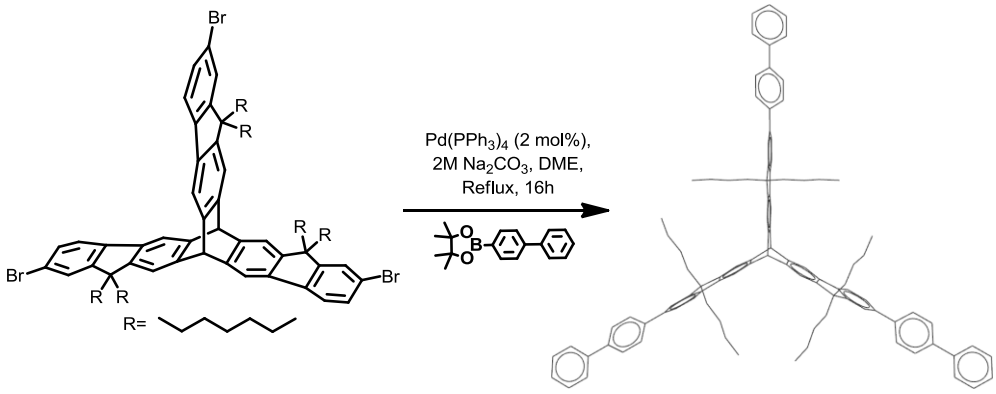

4a (0.2 g, 0.16 mmol) and biphenyl-4-boronic acid (0.126 g, 0.64 mmol) were dissolved in anhydrous 1,2-dimethoxyethane (DME) (30 mL) in an oven dried Schlenk flask under an argon atmosphere and the flask was evacuated and filled with argon (3x). In another oven dried Schlenk flask a solution of anhydrous sodium carbonate (2.5 g) in water (10 mL) was prepared under an argon atmosphere and the flask was also evacuated and filled with argon (3x). To the DME solution, $Pd(PPh_3)_4$ (50 mg) and the salt solution were added sequentially under a strict argon atmosphere followed by evacuation and filling the flask with argon (3x) after each addition. The flask was covered with foil and the solution was allowed to reflux overnight. The resulting solution was cooled to room temperature, quenched with water (50 mL) and extracted with dichloromethane (3 x 20mL). The organic layer was dried over anhydrous magnesium sulfate, evaporated and dried under vacuum. Purified by column chromatography using a hexanes/ethyl mixture to give the pure product (0.10 g, 42%); ^{1}H NMR ($CDCl_3$) δ: 0.55-0.75(30H, m), 0.92-1.08(36H, m), 1.87-2.02(12H, m), 5.57(1H, s), 5.62(1H, s), 7.36(3H, t, J=7.55Hz), 7.41(3H, d, J=4.22Hz), 7.46(6H, t, J=7.77Hz), 7.52-7.61(6H, m), 7.63-7.75(20H, m), 7.80(3H, s).

^{13}C NMR ($CDCl_3$) δ: 14.14, 22.71, 23.87, 29.87, 31.51, 40.17, 40.27, 40.61, 55.07, 55.31, 55.44, 115.42, 118.53, 119.54, 121.45, 125.93, 127.24, 127.51, 127.66, 129.02, 137.62, 138.82, 139.99, 140.87, 140.89, 140.99, 144.89, 145.57, 148.68, 148.81, 152.13, 152.22.

^{1}H NMR spectrum of hexambromotriptycene

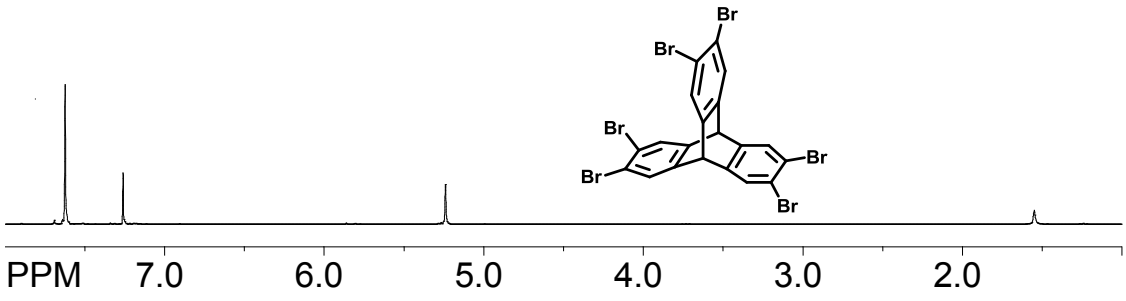

^{13}C NMR spectrum of hexambromotriptycene

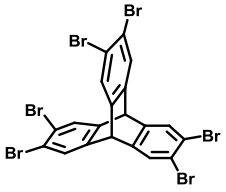

^{1}H NMR spectrum of 2-methylphenyl boronic acid

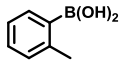

^{13}C NMR spectrum of 2-methylphenyl boronic acid

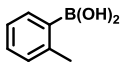

^{1}H NMR spectrum of mixture of 1a and 1s

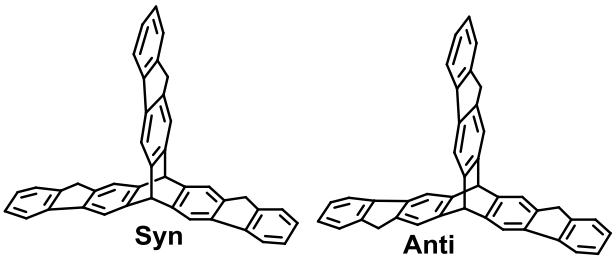

^{1}H NMR spectrum of 2s

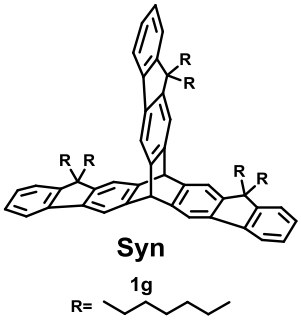

^{13}C NMR spectrum of 2s

^{1}H NMR spectrum of 2a

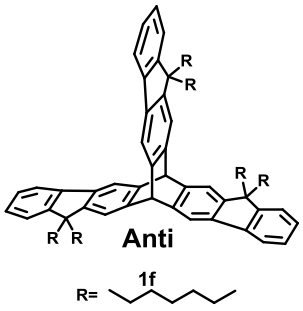

^{13}C NMR spectrum of 2a

^{1}H NMR spectrum of 3a

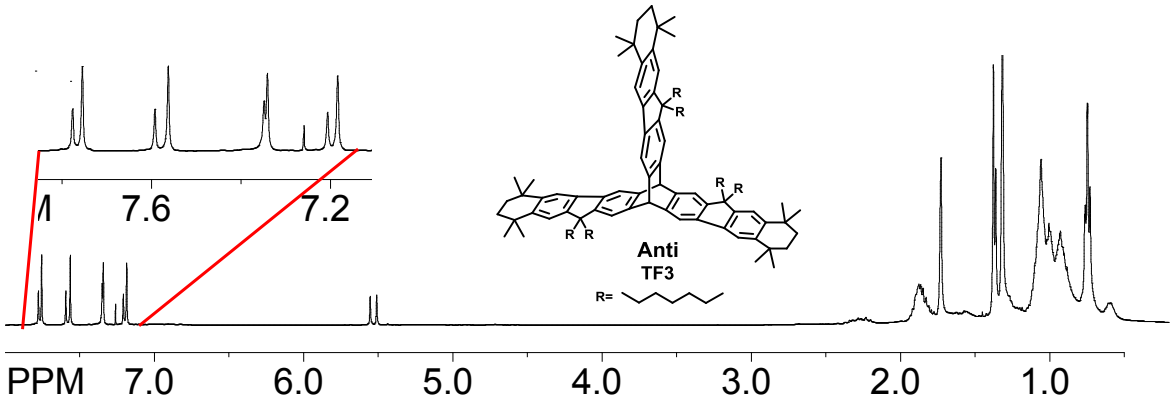

^{13}C NMR spectrum of 3a

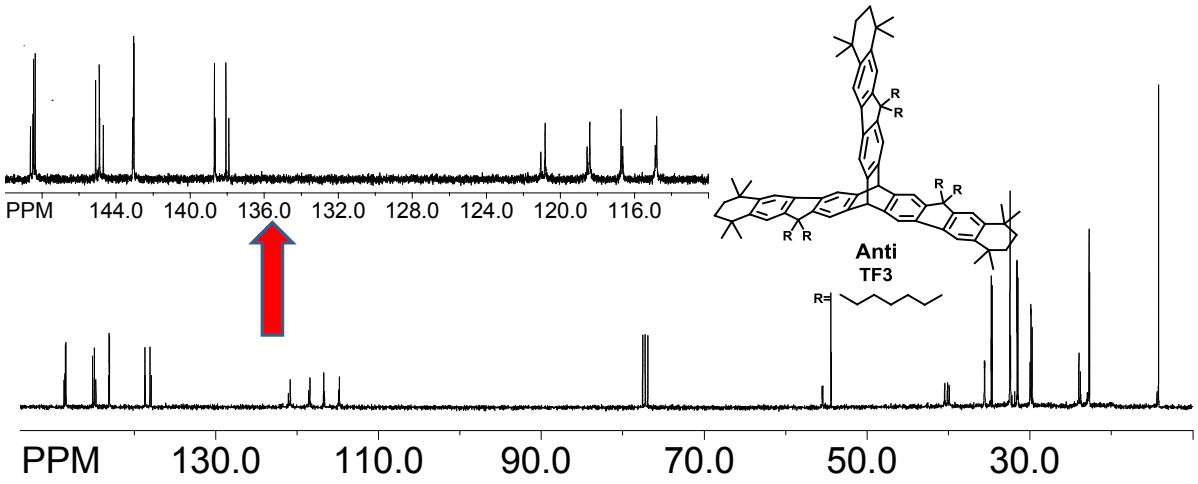

^{1}H NMR spectrum of 3s

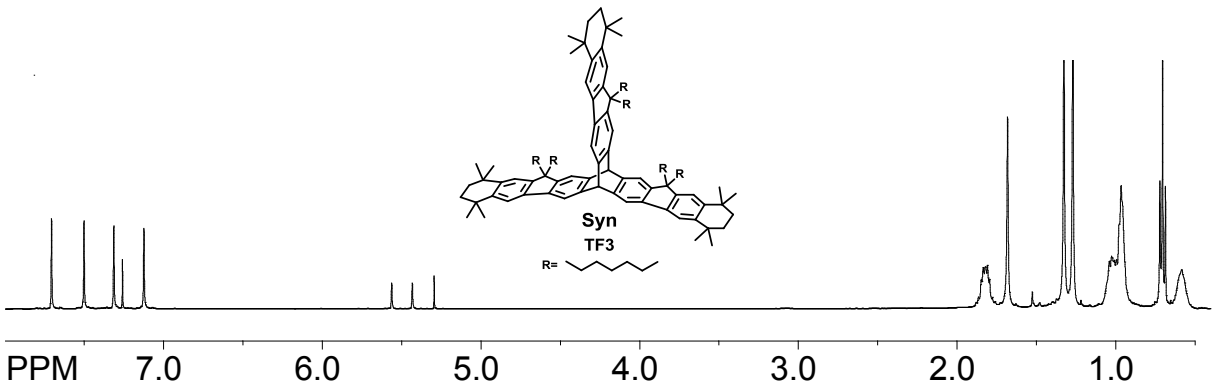

^{13}C NMR spectrum of 3s

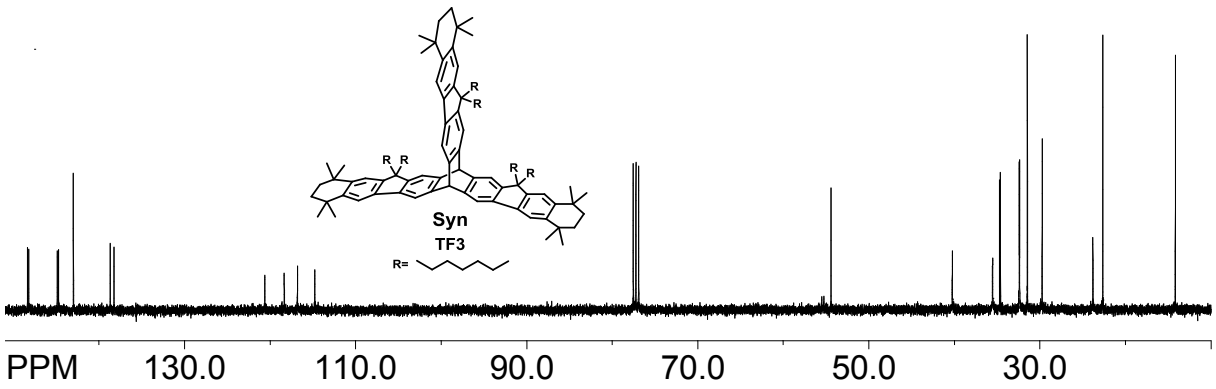

^{1}H NMR spectrum of 9, 9-dihexyl fluorene

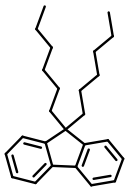

^{13}C NMR spectrum of 9, 9-dihexyl fluorene

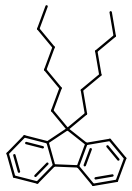

^{1}H NMR spectrum of DAF

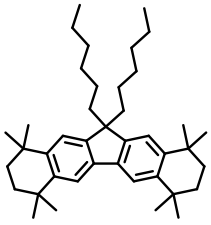

^{13}C NMR spectrum of DAF

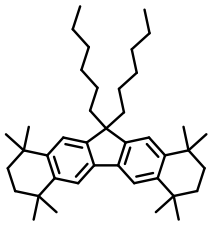

^{1}H NMR spectrum of 4-Bromo-p-terphenyl

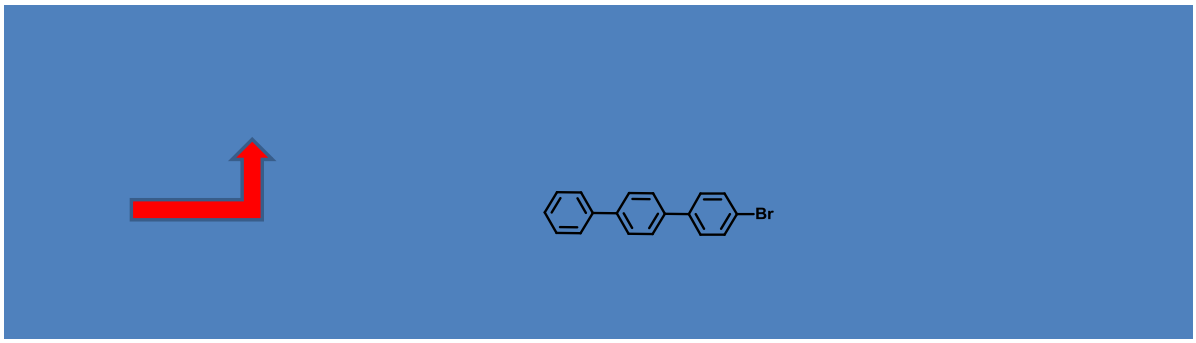

^{13}C NMR spectrum of 4-Bromo-p-terphenyl

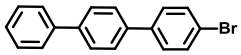

^{1}H NMR spectrum of Terphenyl-4-boronic ester

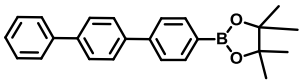

^{13}C NMR spectrum of Terphenyl-4-boronic ester

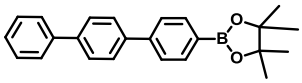

^{1}H NMR spectrum of terphenyl derivative of TF3

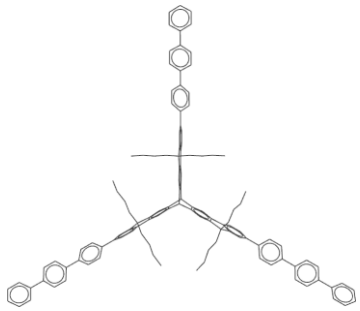

^{13}C NMR spectrum of terphenyl derivative of TF3

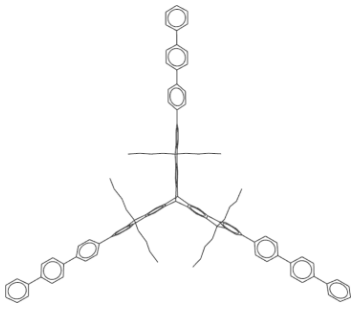

^{1}H NMR spectrum of biphenyl derivative of TF3

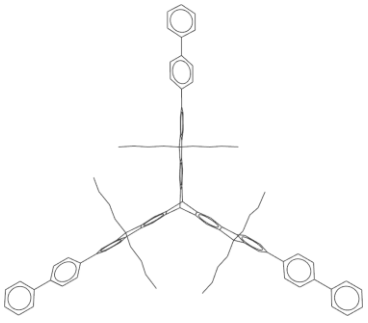

^{13}C NMR spectrum of terphenyl derivative of TF3

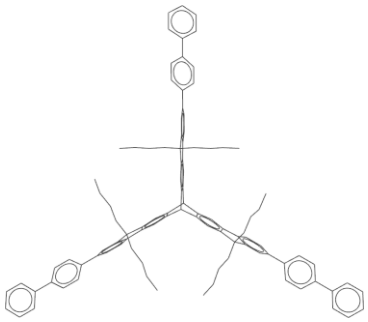

BIBLIOGRAPHY

(Chapter 1)

1. Weiss, E. A.; Tauber, M. J.; Kelley, R. F.; Ahrens, M. J.; Ratner, M. A.; Wasielewski, M. R. *J. Am. Chem. Soc.* **2005**, 127, 11842.

2. Berresheim, A. J.; Muller, M.; Mullen, K. *Chem. Rev.* **1999**, 99, 1747.

3. Zade, S. S.; Bendikov, M. *Org. Lett*. **2006**, 8, 5243.

4. Roncali, J. Chem. Rev. **1992**, 92, 711.

5. Inganaes, O.; Berggren, M.; Andersson, M. R.; Gustafsson, G.; Hjertberg, T.; Wennerstroem, O.; Dyreklev, P.; Granstroem, *M. Synth. Met*. **1995**, 71, 2121.

6. Handbook of Oligo- and Polythiophenes; Fichou, D., Ed.; Wiley-VCH: Weinheim, Germany, **1999**.

7. Bauerle, P.; Mitschke, U.; Gruner, G.; Rimmel, G. *Pure Appl. Chem*. **1999**, 71, 2153.

8. Davis, W. B.; Svec, W. A.; Ratner, M. A.; Wasielewski, M. R. *Nature* **1998**, 396, 60.

9. Van Hutten, P. F.; Krasnikov, V. V.; Hadziioannou, G. *Acc. Chem. Res*. **1999**, 32, 257.

10. Scherf, U.; List, E. J. W. *Adv. Mater*. **2002**, 14, 477.

11. Li, Z. H.; Wong, M. S.; Tao, Y.; Lu, *J. Chem.—Eur. J*. **2005**, 11, 3285.

12. Goldsmith, R. H.; Sinks, L. E.; Kelley, R. F.; Betzen, L. J.; Liu, W.; Wiess, E. A.; Ratner, M. A.; Wasielewski, M. R. *Proc. Natl. Acad. Sci. U.S.A*. **2005**, 102, 3540.

13. Perepichka, I. I.; Perepichka, I. F.; Bryce, M. R.; Palsson, L.-O. *Chem. Commun*. **2005**, 3397.

14. Morisaki, Y.; Chujo, Y. *Macromolecules* **2004**, 37, 4099.

15. Zyss, J.; Ledoux, I.; Volkov, S.; Chernyak, V.; Mukamel, S.; Bartholomew, G. P.; Bazan, G. C. *J. Am. Chem. Soc*. **2000**, 122, 11956.

16. Bartholomew, G. P.; Bazan, G. C. *Acc. Chem. Res*. **2001**, 34, 30.

17. Bartholomew, G. P.; Bazan, G. C. *J. Am. Chem. Soc*. **2002**, 124, 5183.

18. Rathore, R.; Abdelwahed, S. H.; Guzei, I. A. *J. Am. Chem. Soc*. **2003**, 125, 8712.

19. Rathore, R.; Abdelwahed, S. H.; Kiesewetter, M. K.; Reiter, R. C.; Stevenson, C. D. *J. Phys. Chem. B* **2006**, 110, 1536.

20. Vura-Weis, J.; Abdelwahed, S. H.; Shukla, R.; Rathore, R.; Ratner, M. A.; Wasielewski, M. R. *Science* **2010**, 328, 1547.

21. Qi, H.; Chang, J.; Abdelwahed, S. H.; Thakur, K.; Rathore, R.; Bard, A. J. *J. Am. Chem. Soc.* **2012**, *134*, 16265.

22. Navale, T. S.; Thakur, K.; Vyas, V. S.; Wadumethrige, S. H.; Shukla, R.; Lindeman, S. V.; Rathore, R. *Langmuir* **2012**, *28*, 71.

23. Chen, C.-W.; Whitlock, H. W., Jr. *J. Am. Chem. Soc.* **1978**, *100,* 4921.

24. Klärner F. G.; Kahlert, B. *Acc. Chem. Res.* **2003**, *36*, 919–932.

25. (a) Chen, W.; Turro, C.; Friedman, L. A.; Barton, J. K.; Turro, N. J. *J. Phys Chem B* **1997**, *101*, 6995.

(b) Krotz, A. H.; Hudson, B. P.; Barton J. K. *J. Am. Chem. Soc.* **1993**, *115* , 12577–12578.

26. www.platinummetalsreview.com

27. Biron, E.; Voyer, N. *Org. Biomol. Chem.* **2008**, *6*, 2507.

28. (a) Zimmerman, S. C.; VanZyl, C. M. *J. Am. Chem. Soc.* **1987**, *109*, 7894.

(b) Zimmerman, S. C.; Vanzyl, C. M.; Hamilton, G. S. *J. Am. Chem. Soc.* **1989**, 111, 1373.

(c) Zimmerman, S. C.; Zeng, Z. J.; Wu, W. M.; Reichert, D. E. *J. Am. Chem. Soc.* **1991**, *113*, 183.

(d) Zimmerman, S. C.; Wu, W. M.; Zeng, Z. J. *J. Am. Chem. Soc.* **1991**, *113*, 196.

(e) Zimmerman, S. C. *Top. Curr. Chem*. **1993**, *165*, 71.

29. (a) Kurebayashi, H.; Haino, T.; Usui, S.; Fukazawa, Y. *Tetrahedron* **2001,** *57*, 8667.

(b) Kurebayashi, H.; Sakaguchi, H.; Okajima, T.; Haino, T.; Usui, S.; Fukazawa, Y. *Tetrahedron Lett* **1999**, *40*, 5545.

(c) Kurebayashi, H.; Sakaguchi, H.; Okajima, T.; Haino, T.; Usui, S.; Fukazawa, Y. *Tetrahedron Lett* **1999**, *40*, 5545.

30. (a) Harmata, M.; Murray, T, *J. Org. Chem.* **1989**, *54*, 3761.

(b) Harmata, M.; Barnes, C. L.; Karra, S. R.; Elahmad, S. *J. Am. Chem. Soc.* **1994**, *116*, 8392.

(c) Harmata, M.; Barnes, C. L. *J. Am. Chem. Soc.* **1990**, *112*, 5655.

31. (a) Valík, M.; Čejka, J.; Havlík, M.; Král, V.; Dolenský, B. *Chem. Commun.* **2007**, 3835.

(b) Pardo, C.; Sesmilo, E.; Gutiérrez-Puebla, E.; Monge, A.; Elguero, J.; Fruchier, A. *J. Org. Chem.* **2001**, *66*, 1607.

(c)Havlík, M.; Kr l, V.; Kapl nek, R.; Dolensk , B. *Org. lett.* **2008**, *10*, 4767.

32. Sygula, A.; Fronczek, F. R.; Sygula, R.; Rabideau, P. W.; Olmstead, M. M. *J. Am. Chem. Soc.* **2007**, *129*, 3842.

33. Wu, Z.; Shao, X.; Li, C.; Hou, J.; Wang, K.; Jiang, X.; Li, Z. *J. Am. Chem. Soc.* **2005**, *127*, 17460.

(Chapter 2)

1. Chen, C.-W.; Whitlock, H. W., Jr. *J. Am. Chem. Soc.* **1978**, *100,* 4921.

2. Klärner F. G.; Kahlert, B. *Acc. Chem. Res.* **2003**, *36*, 919–932.

3. (a) Petitjean, A.; Khoury, R. G.; Kyritsakas, N.; Lehn, J. M. *J. Am. Chem. Soc.* **2004**, *126*, 6637–6647.

(b) Yamaguchi, S.; Swager, T. M. *J. Am. Chem. Soc.* **2001**, *123,* 12087- 12088.

4. (a) Zimmerman, S. C.; VanZyl, C. M. *J. Am. Chem. Soc.* **1987**, *109*, 7894.

(b) Zimmerman, S. C.; Vanzyl, C. M.; Hamilton, G. S. *J. Am. Chem. Soc.* **1989**, *111*, 1373.

(c) Zimmerman, S. C.; Zeng, Z. J.; Wu, W. M.; Reichert, D. E. *J. Am. Chem. Soc.* **1991**, *113*, 183.
(d) Zimmerman, S. C.; Wu, W. M.; Zeng, Z. J. *J. Am. Chem. Soc.* **1991**, *113*, 196.

(e) Zimmerman, S. C. *Top. Curr. Chem*. **1993**, *165*, 71.

5. Patoux, C.; Coudret, C.; Launay J. P.; Joachim, C.; Gourdon, A. *Inorg. Chem.* **1997**, *36,* 5037-5049.

6. (a) Suzuki, A. *Chem. Commun.* **2005**, 4759-4763.

(b) Hassan, J.; Sevignon, M.; Gozzi, C.; Schulz, E.; Lemaire, M. *Chem. Rev.* **2002**, *102*, 1359-1469 and references therein.

7. Sonogashira, K. in *Comprehensive Organic Synthesis*; Trost, B. M., Fleming, I., Eds.; Pergamon: Oxford, **1991**; Vol. 3, 521-548.

8. James E., Jr.; Boyd, D. R.; Berchtold, G. A. *J. Org. Chem.* **1981**, *46*, 1817- 1820.

9. Goossen, L. J.; Rodriguez, N.; Linder, C. *J. Am. Chem. Soc.* **2008**, *130*, 15248-15249.

10. Chebny, V. J.; Gwengo, C.; Gardinier, J. R.; Rathore, R. *Tetrahedron. Lett.* **2008**, *49*, 4869.

12 We thank professor James R. Gardinier for giving us a sample of *pentakis*(4- *tert*-butylphenyl)-4-bromophenylbenzene. Also see: Sadhukhan, S. K.; Viala, C.; Gourdon, A. *NanoScience Group*, CEMES-CNRS, Toulouse, Fr. Synthesis, **2003**, *10*, 1521-1525**.**

13. Zhai, L. Y.; Shukla, R.; Rathore, R. *Org. Lett.* **2009**, *11*, 3474.

14. Miura, M.; Koike, T.; Ishihara, T.; Hirayama, F.; Sakamoto, S.; Okada, M.; Ohta, M.; Tsukamoto, S. *Synthetic Communications*, **2006**, *36*, 3809-3820.

15. Banerjee, M.; Vyas, V. S.; Lindeman, S. V.; Rathore, R. *Chem.Comm.* **2008**, 1889.

16. Heng, W. Y.; Hu, J.; Yip, J. H. K. *Organometallics*, **2007**, *26*, 6760-6768.

17. Maeda, H.; Maeda, T.; Mizuno, K.; Fujimoto, K.; Shimizu, H.; Inouye, M. *Chem. Eur. J.* **2006**, *12*, 824-831.

18. Cooper, T.; Novak, A.; Humphreys, L. D.; Woodward, S. *Adv. Synth. Catal*. **2006**, *348*, 686-690.

19. Tanemura, K.; Suzuki, T.; Nishida, Y.; Satsumabayashi, K.; Horaguchi, T. *Org. Lett*. **2003**, *32*, 932-933.

20. Rathore, R.; Lindeman, S. V.; Kochi, J. K. *J. Am. Chem. Soc.* **1997**, *119*, 9393.

21. (a) Benesi, H. A.; Hildebrand, J. J. *J. Am. Chem. Soc*. **1949**, *71*, 2703.

(b) Person, W. B. *J. Am. Chem. Soc.* **1965**, *87*, 167.

(c) Foster, R. *Molecular Complexes*; Crane, Russak & Co.: New York, **1974**; Vol. 2.

22. (a) Mulliken, R. S. *J. Am. Chem. Soc.* **1952**, *74*, 811.

(b) Mulliken, R. S.; Person, W. B. *Molecular Complexes. A Lecture and Reprint Volume*; Wiley: New York 1969.

(c) Foster, R. *Organic Charge-Transfer Complexes*; Academic: New York, 1969.

(d) Briegleb, G. *Elektronen - Donator-Acceptor Komplexe*; Springer: Berlin, 1961.

23. Shukla, R.; Lindeman, S. V.; Rathore, R. *Chem. Comm.* **2007**, 3717 and references cited therein.

24. (a) Rathore, R.; Le Maguères, P.; Kochi, J. K. *J. Org. Chem*. **2000**, *65*, 6826.

(b) Rathore, R; Kumar, A. S.; Lindeman, S. V.; Kochi, J. K. *J. Org. Chem.* **1998**, *63*, 5847.

(c) Badger, B.; Brocklehurst, B. *Trans. Faraday Soc*. **1969**, *65*, 2576, 2582, 2588.

(d) Davies, A. G.; Ng, K. M. *J. Chem. Soc. Perkin Trans. 2* **1998**, 2599.

25. (a) Rathore, R.; Abdelwahed, S. H.; Guzei, I. A. *J. Am. Chem. Soc.* **2003**, *125*, 8712.

(b) Chebny, V. J.; Shukla, R.; Rathore, R. *J. Phys. Chem. A* **2006**, *110*, 13003 and references cited therein.

26. Rathore, R.; Burns, C.; Deselnicu, M. I.; Denmark, S. E.; Bui, T. *Org. Synth*. **2005**, *82*, 1.

27. Kelly, T. R.; Sestelo, J. P. *Structure and Bonding (Berlin, Germany.)* **2001**, *99*, 19-53.

28. Kelly, T. R. *Acc. Chem. Res*. **2001**, *34*, 514-522.

(Chapter 3)

1. (a) Suzuki, A. *Chem. Commun.* **2005**, 4759-4763.

(b) Hassan, J.; Sevignon, M.; Gozzi, C.; Schulz, E.; Lemaire, M. *Chem. Rev.* **2002**, *102*, 1359-1469 and references therein.

2. Zhai, L. Y.; Shukla, R.; Rathore, R. *Org. Lett.* **2009**, *11*, 3474.

3. Miura, M.; Koike, T.; Ishihara, T.; Hirayama, F.; Sakamoto, S.; Okada, M.; Ohta, M.; Tsukamoto, S. *Synthetic Communications*, **2006**, *36*, 3809-3820.

4. (a) Maeda, H.; Maeda, T.; Mizuno, K.; Fujimoto, K.; Shimizu, H.; Inouye, M. *Chem. Eur. J.* **2006**, *12*, 824-831.

   (b) Cooper, T.; Novak, A.; Humphreys, L. D.; Woodward, S. *Adv. Synth. Catal*. **2006**, *348*, 686-690.

   (c) Tanemura, K.; Suzuki, T.; Nishida, Y.; Satsumabayashi, K.; Horaguchi, T. *Org. Lett*. **2003**, *32*, 932-933.

5. (a) Benesi, H. A.; Hildebrand, J. J. *J. Am. Chem. Soc*. **1949**, *71*, 2703.

   (b) Person, W. B. *J. Am. Chem. Soc.* **1965**, *87*, 167.

   (c) Foster, R. *Molecular Complexes*; Crane, Russak & Co.: New York, **1974**; Vol. 2.

6. Rathore, R.; Burns, C.; Deselnicu, M. I.; Denmark, S. E.; Bui, T. *Org. Synth*. **2005**, *82*, 1.

(Chapter 4)

1. Hill, D. J.; Mio, M. J.; Prince, R. B.; Hughes, T. S.; Moore, J. S. *Chem. Rev.* **2001**, *101*, 3893. (b) Chebny, V. J.; Rathore, R. *J. Am. Chem. Soc.* **2007**, *129*, 8458 and references therein.

2. (a) Marsella, M. J.; Reid, R. J. Macromolecules 1999, 32, 5982. (b) Tseng, H.-R.; Vignon, S. A.; Stoddart, J. F. Polymer Preprints 2003, 44, 377.

3. (a) *Molecular Switches,* Feringa, B. L., Ed.; Wiley-VCH: Weinheim, Germany, 2001. (b) Feringa, B. L. *J. Org. Chem.* **2007**, *72*, 6635. (c) Rathore, R.; Magueres, P. L.; Lindeman, S. V.; Kochi, J. K. *Angew. Chem. Int. Ed.* **2000**, *39*, 809. (d) McQuade, T. D.; Pullen, A. E.; Swager, T. M. *Chem. Rev.* **2000**, *100*, 2537 and references cited therein.

4. (a) Kaifer, A. E.; Stoddart, J. F. *Nature* **1994**, *369*, 133. (b) Grossel, M. C. *Nanomaterials Chem.* **2007**, 319. (c) Saha, S.; Stoddart, J. F. *Functional Org. Mat.* **2007**, 295.

5. (a) Baughman, R. H. *Synth. Met.* **1996**, *78*, 339. (b) Song, C.; Swager, T. M. *Org. Lett.* **2008**, *10*, 3575 and references cited therein.

6. Chebny, V. J.; Shukla, R.; Lindeman, S. V.; Rathore, R. *Org. Lett.* **2009**, *11*, 2080.

7. The activation energy for the interchange into two isoenergetic (non-cofacial) neutral conformers of **1** in eq 1 was estimated to be E_a = 10.2 kcal mol^{-1} K^{-1} by line-shape

analysis of the signals in the variable temperature ^{1}H NMR spectra. Also see: Mataka, S.; Shigaki, K.; Sawada, T.; Mitoma, Y.; Taniguchi, M.; Thiemann, T.; Ohga, K.; Egashira, N. *Angew. Chem. Int. Ed.* **1998**, *37*, 2352. Also see: Mataka, S.; Takahashi, K.; Hirota, T.; Takuma, K.; Kobayashi, H.; Tashiro, M.; Imada, K.; Kuniyoshi, M. *J. Org. Chem.* **1986**, *51*, 4618.

8. (a) Singer, L. A.; Cram, D. J. *J. Am. Chem. Soc.* **1963**, *85*, 1080. (b) Taniguchi, M.; Mataka, S.; Thiemann, T.; Sawada, T.; Mimura, K.; Mitoma, Y. *Bull. Chem. Soc. Jpn.* **1998**, *71*, 2661. (c) Rathore, R.; Lindeman, S. V.; Kochi, J. K. *J. Am. Chem. Soc*. **1997**, *119*, 9343 and references therein.

9. The observed difference (~90 mV) in the first oxidation potentials of conformationally-mobile **1** when compared to the rigid □-stacked **2** can be attributed to the energy required for the transformation of the extended conformation **E-1** into the cofacially stacked **F-1** conformation.

10. Bovey, F. A., "*Nuclear Magnetic Resonance Spectroscopy*," Academic Press, New York, 1969, Chapter VII.

11. Marenich A. V.; Olson R. M.; Kelly C. P.; Cramer C. J.; Truhlar D. G. *J. Chem. Theory Comput.* **2007**, *3*, 2011.

12. (a) Rathore, R.; Hubig, S. M.; Kochi, J. K. *J. Am. Chem. Soc.* **1997**, *119*, 11468. (b) Hübig, S. M.; Rathore, R.; Kochi, J. K. *J. Am. Chem. Soc.* **1999**, *121*, 617.

13. Rathore, R.; Chebny, V. J.; Kopatz, E. J.; Guzei, I. A. *Angew. Chem. Int. Ed.* **2005**, *44*, 2771.

14. Shida, T., Electronic Absorption Spectra of Radical Ions; Elsevier: Amsterdam, 1988.

15. The kinetic traces were fit using a D$A(t) = \sum_{i=1}^{5}[A_1\ exp(-t/t_i)]+A_5$ function convoluted with the instrument response function.

(Chapter 5)

1. Navale, T. S.; Thakur, K.; Vyas, V. S.; Wadumethrige, S. H.; Shukla, R.; Lindeman, S. V.; Rathore, R. *Langmuir* **2012**, *28*, 71.

2. Lin, C. *Chin. J. Polym. Sci.* **2010**, *28*, 69.

3. Liu, T. P.; Xing, C. H.; Hu, Q. S. *Angew. Chem. Int. Ed.* **2010**, *49*, 2909.